The University of Nottingham
UNITED KINGDOM · CHINA · MALAYSIA

Children's Brain Tumour Research Centre

An investigation of druggable prognostic markers in paediatric ependymoma

Durgagauri H. Sabnis
B.Pharm., MSc. Oncology

Thesis submitted to the University of Nottingham for the degree of Doctor of Philosophy

February, 2016

This thesis is dedicated to all the children and their families whose lives have been affected by brain tumours

Abstract I

Conference abstracts and publications III

Acknowledgments IV

Table of contents V

List of figures X

List of tables XIV

Abbreviations XV

ABSTRACT

Background: Paediatric ependymomas are the second most common malignant brain tumours in children. Tumour recurrence, chemoresistance and invasion of surrounding critical structures are the hallmarks of ependymomas. These features are consistent with the cancer stem cell (CSC) hypothesis which states that tumours harbour a sub-population of stem-like cells which underlie therapeutic resistance. This study investigates the role of the radial glial stem cell marker BLBP, the multidrug transporter ABCB1, and the DNA repair enzyme MGMT in therapy failure in ependymomas with particular emphasis on the role of CSCs.

Material and Methods: Database analyses were performed to assess the expression of the aforementioned markers in patients from 3 publicly available gene expression datasets. Furthermore, samples from 2 European paediatric ependymoma trial cohorts were screened for ABCB1, BLBP and MGMT expression by immunohistochemistry to elucidate their prognostic value. The expression of these markers was also determined in a panel of 5 ependymoma derived cell lines by QRT-PCR or western blotting analysis. Roles in chemoresistance (clonogenic & cytotoxicity assays) and tumour invasion (wound healing & 3D invasion assay) were then investigated.

Results: Poor survival in the chemotherapy-led paediatric ependymoma CNS9204 trial was significantly associated with ABCB1 ($P=0.007$) and BLBP ($P=0.03$) expression whilst MGMT ($P<0.001$) and BLBP ($P=0.002$) expression predicted poor survival in the radiotherapy-led CNS9904 trial cohort. ABCB1 and BLBP expression was consistent with the CSC hypothesis whilst MGMT was expressed in both CSCs as well as the tumour bulk. Inhibition of ABCB1 and BLBP, with the phosphodiesterase-5 inhibitor vardenafil and PPAR-ϒ antagonist GW9662 respectively, potentiated response to chemotherapy and also inhibited the ability of ependymoma cell lines to migrate and invade. Finally, whilst each of the

tested cell lines were resistant to the alkylating agent temozolomide, they were sensitive to the novel N3-propargyl analogue of temozolomide.

Conclusion: ABCB1, BLBP and MGMT were not only markers of robust prognostic value but they also contributed functionally to the aggressive behaviour of ependymoma. Inhibition of ABCB1 and BLBP by vardenafil and GW9662 may represent effective approaches to overcome chemoresistance and invasion in ependymoma patients. The N3-propargyl analogue of temozolomide could also represent a novel treatment option for MGMT expressing ependymoma patients.

- **Conference abstracts**

- Functional analysis of Radial Glial Stem Cell Marker BLBP, which associates with poor prognosis in paediatric ependymomas.
  D. H.Sabnis, L. Storer, L. Simmonds, S. Blackburn, J. Lowe, R. Grundy, I. Kerr, B. Coyle
  NEURO-ONCOLOGY 16(SUPPL 8), 24-24. NOVEMBER 2014

- Functional analysis of multi-drug resistance transporter ABCB1 which correlates with poor prognosis in paediatric ependymoma
  D. H.Sabnis, L.C.D. Storer, J.-P. Kilday, J. Lowe, R.G. Grundy, I. Kerr, B. Coyle
  NEURO-ONCOLOGY 17(SUPPL 8):VIII16.5-VIII17 · NOVEMBER 2015

- Druggable prognostic markers in paediatric ependymoma; is BLBP the solution?
  D.H. Sabnis, L.C.D. Storer, L. Simmonds, S. Blackburn, J.-P. Kilday, J. Lowe, G.R. Grundy, I. Kerr, B. Coyle
  NEURO-ONCOLOGY 17(SUPPL 8):VIII19.5-VIII19 · NOVEMBER 2015

  MGMT expression, promoter methylation and circumvention in ependymomas
  D. H. Sabnis, R.G. Grundy, I. Kerr, T. Bradshaw, B. Coyle
  NEURO-ONCOLOGY 17(SUPPL 8): VIII13.3-VIII13 · NOVEMBER 2015
  0115

- **Publications**

- ABCB1 in children's brain tumours
  Coyle, B., M. Kessler, D. H. Sabnis and Ian D. Kerr; Biochemical Society Transactions 43(5): 1018- 1022. (2015)

  <u>Manuscripts in preparation to be submitted to the Acta Neuropathalogica journal</u>

- Multidrug transporter ABCB1: its role in prognosis, chemoresistance and metastasis of ependymoma
  Sabnis, D.H., Storer, L., Lowe, J., Kilday, J.P., Grundy, R., Kerr, I., Coyle, B.

- Druggable prognostic markers in ependymomas, is BLBP the solution?
  Sabnis, D.H., Storer, L., Simmonds, L., Blackburn, S., Lowe, J., Kilday J.P., Grundy, R., Kerr, I., Coyle, B.

- MGMT expression, promoter methylation and circumvention in ependymoma
  Sabnis, D.H., Bradshaw, T., Rogers, H., Kerr, I., Coyle, B.

ACKNOWLEDGEMENTS



I would like to begin by paying my regards to my late aaji and aajoba (grandparents) who inspired me to take on this path of pursuing a PhD and have had a tremendous impact on my life. I would also like to thank my fantastic aai-baba (parents); for putting up with my (numerous!) eccentricities, letting me dream and supporting me.

I would like to then acknowledge my amazing supervisors. Thank you Beth; you have been the 'coolest' supervisor ever. I can't possibly thank you enough for being so supportive and for having confidence in my abilities. I aspire to be like you one day! And to Ian, thank you so much for all your help and guidance. I am very grateful for your constructive criticism on all my presentations, the brilliant attention to detail and most importantly, for teaching me how to be succinct and precise. I would also like to thank Dr. Victoria Sedman for her brilliant advice and support throughout my PhD. I would also like to acknowledge my teachers, Patankar Sir, Nadkarni Sir, Vaishali ma'am, Vrushali ma'am and Raheja ma'am for helping me build a strong foundation in various subjects.

I would then like to thank my family in Nottingham. Thank you Tanvi, Fede, Brina, Aishah, Shosho, Jasper, James, Josh, Laura, Sameerah, Melinda and Mehreen; for being there whenever I needed you.

I would also like to pay my regards to the brilliant CBTRC team. Thank you Lisa and Becky; for being so helpful and caring throughout my tenure at the CBTRC. Thank you Hazel for being such a great friend and colleague. I appreciate all the help and advice.

Finally, I would like to thank my family: my pillars of strength, my amazing brother Hrishi and even better sister-in law Sukanya, my acting-parents in the UK Hemantdada and Kishoritai, my favourite niece in the whole wide world, Kaavya, my fantastic uncle and aunts: Vasantkaka-Vidyaatya, Milindmama-Ujjumami, Mandarmama-Shubahamami and finally, the first friends you have in life, my cousins; Madhuritai-Anirudh, Yashu-Aditi, Dhanu, Aniket, Pallavi and Apoorva.

Contents

CHAPTER 1. Introduction 1
1.1 Paediatric brain tumours 1
1.2 Ependymomas 3
1.2.1 Symptoms 4
1.2.2 Diagnosis 4
1.2.3 Genetics, tumour heterogeneity and prognostic markers 6
1.2.4 Treatment of ependymomas 13
1.3 Cancer stem cells in ependymoma 19
1.4 Multi-drug resistance in CSCs and ABCB1 22
1.5 Radial glial cells and BLBP 26
1.6 DNA damage, repair and MGMT 32
1.7 Aims and hypothesis 37
CHAPTER 2. Materials and methods 38
2.1 Public gene expression data analysis 38
2.2 Paediatric ependymoma trial cohorts 38
2.2.1 Statistical analysis 40
2.3 Cell culture and cell based assays 40
2.3.1 Origin of cell lines and cell culture 40
2.3.2 Recovering cells from liquid nitrogen 41
2.3.3 Harvesting and sub-culturing monolayer cells 41
2.3.4 Snap freezing of cell pellets 42
2.3.5 Preparation of cell line stocks 42
2.3.6 Neurosphere culture 42
2.4 Viability assays 43
2.4.1 Clonogenic assay 43
2.4.2 MTT assay 45
2.4.3 Neurosphere alamar blue assay 47
2.5 Wound healing assay 48
2.6 Invasion assay 49
2.7 Immunohistochemistry (IHC) 51
2.8 Western blotting 53

2.8.1 Protein lysate preparation 53
2.8.2 Protein quantification and sample preparation 53
2.8.3 Gel electrophoresis 54
2.8.4 Transfer of proteins onto a membrane 56
2.8.5 Antibody treatment: 56
2.8.6 Enhanced chemiluminescence (ECL) detection: 56
2.9 RNA extraction 57
2.9.1 DNase treatment 58
2.10 cDNA synthesis 58
2.11 Reverse transcriptase-polymerase chain reaction (RT-PCR) . 61
2.11.1 PCR product analysis by agarose gel electrophoresis 62
2.12 Quantitative reverse transcriptase-PCR (QRT-PCR) 62
2.12.1 Primer efficiency estimation 63
2.12.2 Quantitative reverse transcriptase PCR for ABCB1 and BLBP66
2.12.3 Quantification of target gene amplification 67
CHAPTER 3. Characterisation of ependymoma cell lines 68
3.1 Introduction 68
3.2 Results 68
3.2.1 Doubling times of all cell lines 68
3.2.2 All ependymoma cell lines used in this study were of human origin……69
3.2.3 ABCB1, BLBP and MGMT protein expression in the original patient tumours and the orthotopic tumour from which the EPN1 cell line was derived. 71
3.2.4 C11orf95-RELA gene fusion was expressed in 3 out of 5 ST ependymoma derived cell lines. 73
3.3 Summary 76
CHAPTER 4. Multidrug transporter ABCB1: Its role in prognosis, drug-resistance and metastasis of ependymoma.....77
4.1 Introduction 77
4.2 Results 79
4.2.1 Higher ABCB1 gene expression was observed in paediatric in comparison to adult ependymomas. 79
4.2.2 ABCB1 gene expression was the highest in ST ependymoma.81

4.2.3 ABCB1 protein expression was independently associated with reduced survival in the chemotherapy–led CNS9204 trial. 83

4.2.4 ABCB1 expression could not predict survival in the radiotherapy-led CNS9904 trial.....86

4.2.5 ABCB1 was expressed in 4 out of 5 paediatric ependymoma derived cell lines…… 87

4.2.6 ABCB1 expression was enriched in stem cell enriched neurospheres. 88

4.2.7 ABCB1 inhibition potentiated response to chemotherapy in the ABCB1^{lo} BXD1425EPN cell line in a stem cell relevant clonogenic assay..89

4.2.8 ABCB1 inhibition potentiated response to chemotherapy in the ABCB1^{lo} BXD-1425EPN cell line by the MTT assay. 91

4.2.9 ABCB1 inhibition could not potentiate response to chemotherapy in the ABCB1^{hi} DKFZ-EP1 cell line by the MTT assay. 92

4.2.10 ABCB1 inhibition reduced migration in the ependymoma cell lines. 94

4.2.11 ABCB1 inhibition reduced invasion in the ABCB1^{lo} BXD-1425EPN cell line…… 96

4.2.12 ABCB1^{hi} DKFZ-EP1 cell line did not invade in Cultrex ^{TM} BME.98

4.3 Summary 99

CHAPTER 5. Functional analysis of radial glial stem cell marker BLBP, which correlates with poor prognosis in ependymoma 100

5.1 Introduction..... 100

5.2 Results..... 102

5.2.1 BLBP gene expression did not correlate with age in ependymomas. 102

5.2.2 BLBP gene expression was higher in SP and ST ependymomas in comparison to PF ependymomas. 103

5.2.3 BLBP expression correlated with expression of other brain tumour relevant CSC markers; CD133 and SOX2. 106

5.2.4 BLBP protein expression correlated with prognosis in the chemotherapy-led CNS9204 trial. 109

5.2.5 BLBP expression predicted poor prognosis in the radiotherapy-led CNS9904 trial. 112

5.2.6 BLBP was expressed in all paediatric ependymoma cell lines.113

5.2.7 BLBP expression was elevated in DKFZ-EP1NS neurospheres.115

5.2.8 DHA had a differential effect on proliferation in ependymoma cell lines…… 116

5.2.9 DHA induced cytotoxicity in ependymoma stem cells. 117

5.2.10 Effect of DHA on response to chemotherapy 118

5.2.11 DHA inhibited the migratory capacity of ependymoma cells. .121

5.2.12 DHA inhibited invasion in BLBP^{lo} BXD-1425EPN cell line. 123

5.2.13 PPAR-γ and δ antagonists inhibited BLBP expression in ependymoma cell lines…… 125

5.2.14 The PPAR-γ antagonist GW9662 had a weak but statistically significant anti-proliferative effect on ependymoma cell lines. 127

5.2.15 The dual PPAR-(γ/δ) antagonist FH535 and PPAR-γ antagonist GW9662 inhibited viability of ependymoma stem cells. 129

5.2.16 Effect of BLBP inhibition on response to chemotherapy 131

5.2.17 PPAR antagonists reduced the migratory capacity of ependymoma cells…….....134

5.2.18 PPAR antagonists attenuated invasion in BLBP^{lo} BXD-1425EPN cell line…… 136

5.3 Summary 138

CHAPTER 6. Expression, promoter methylation and circumvention of MGMT in ependymoma 141

6.1 Introduction 141

6.2 Results 144

6.2.1 MGMT expression was higher in paediatric ependymoma patients in comparison to adults. 144

6.2.2 MGMT gene expression was marginally higher in PF tumours in comparison to ST and SP ependymomas.....145

6.2.3 Paediatric ependymomas had low levels of MGMT promoter methylation……. 147

6.2.4 MGMT promoter methylation correlated with a favourable prognosis in adults with PF ependymoma. 149

6.2.5 MGMT expression predicted poor prognosis in the chemotherapy-led CNS9204 trial by univariate analysis.....152

6.2.6 MGMT expression predicted poor prognosis in the radiotherapy-led CNS9904 trial.....155

6.2.7 MGMT, MLH1 and MSH6 expression across ependymoma derived cell lines and stem cell enriched neurospheres.....157

6.2.8 All ependymoma derived cell lines exhibited resistance to TMZ.159

6.2.9 Ependymoma cell lines were sensitive to the MGMT circumventing N3-propargyl analogue of TMZ. 161

6.2.10 Resistance to TMZ and sensitivity to the N3-propargyl analogue was maintained in ependymoma stem cells.....162

6.3 Summary 164

CHAPTER 7. Discussion and future work 166

7.1 Introduction 166

7.2 ABCB1; drug efflux and much more – Chapter 4 166

7.3 BLBP; not just a stem cell marker – Chapter 5 175

7.4 MGMT; an unexplored avenue in ependymoma treatment- Chapter 6.……184

7.5 Conclusion 188

7.6 Future work 189

7.6.1 General 189

7.6.2 ABCB1 190

7.6.3 BLBP.....190

7.6.4 MGMT 191

APPENDICES…….193

Appendix A1 solution for western blotting analysis 193

Appendix A2 preparation of lower resolving gel..... 193

Appendix A3 preparation of upper stacking gel 194

Appendix A4 Protein expression of the C11orf95-RELA fusion in ependymoma cell lines by western blotting analysis ……..…194

REFERENCES……...195

LIST OF FIGURES

Figure 1.1 Location of the tentorium cerebelli 2
Figure 1.2 MRI image of a posterior fossa ependymoma..... 3
Figure 1.3 Histological appearance of paediatric ependymoma 5
Figure 1.4 Classification of ependymoma into 9 subgroups on the basis of methylation profiles 12
Figure 1.5 Cancer Stem Cell (CSC) Hypothesis 19
Figure 1.6 Asymmetric cell division of normal stem cells and the origin of cancer stem cells 20
Figure 1.7 Organisation of ABC transporters. 23
Figure 1.8 Symmetric and asymmetric division of RG..... 28
Figure 1.9 PPAR antagonists inhibit transcription and function of BLBP P. 31
Figure 2.1 BXD-1425EPN spheroid invading through the basement membrane extract (BME) in a 3D invasion assay. 50
Figure 2.2 Amplification curve for ABCB1 gene generated by the CFX-96 real time system..... 65
Figure 2.3 Melt curves for ABCB1..... 65
Figure 2.4 Scatter plot of the mean Ct values for the ABCB1 primers at serially diluted concentrations of DNA template..... 66
Figure 3.1 Doubling time of ependymoma cell lines..... 69
Figure 3.2 Alignment *β*-actin gene sequence for all cell lines with the human, rat and mouse sequences..... 70
Figure 3.3 ABCB1, BLBP and MGMT expression in patient tumours and the orthotopic ependymoma from which the EPN1 cell line was derived..... 72
Figure 3.4 Expression of C11orf95-RELA fusion gene in ependymoma cell lines 74
Figure 3.5 Break-points of the C11orf95-RELA fusion gene sequences in ependymoma cell lines 75
Figure 4.1 Chemical structure of vardenafil..... 78
Figure 4.2 ABCB1 gene expression in ependymoma patients across 3 trial ependymoma cohorts. 80

Figure 4.3 ABCB1 expression was the highest in supratentorial ependymoma 82
Figure 4.4 Membranous expression of ABCB1 was associated with poor survival in the chemotherapy-led CNS9204 cohort 84
Figure 4.5 ABCB1 could not predict survival in the radiotherapy-led CNS9904 trial 86
Figure 4.6 ABCB1 was expressed in 4 out of 5 ependymoma cell lines ... 87
Figure 4.7 ABCB1 gene expression was maintained at recurrence in the Hoffman dataset 88
Figure 4.8 ABCB1 was enriched in neurospheres derived from the DKFZ-EP1 cell line 89
Figure 4.9 ABCB1 inhibition potentiated response to chemotherapy in $ABCB1^{lo}$ ependymoma cell line 90
Figure 4.10 ABCB1 inhibition potentiated response to chemotherapy in $ABCB1^{lo}$ BXD-1425EPN cell line by the MTT assay 92
Figure 4.11 Chemoresistance in $ABCB1^{hi}$ DKFZ-EP1 cell line) 93
Figure 4.12 ABCB1 inhibition diminished migration in ependymoma cell lines 95
Figure 4.13 ABCB1 inhibition reduced invasion in the BXD-1425EPN cell line 97
Figure 4.14 Spheroids formed from the DKFZ-EP1 cell line remained circumscribed in a 3D invasion assay 98
Figure 5.1 BLBP expression was maintained in ependymoma patients across all age groups 103
Figure 5.2 BLBP gene expression was significantly higher in SP and ST ependymomas in comparison to PF ependymomas 105
Figure 5.3 BLBP expression significantly correlated with expression of other brain tumour relevant CSC markers 108
Figure 5.4 BLBP expression correlates with poor prognosis in the chemotherapy-led CNS9204 trial 110
Figure 5.5 BLBP expression correlated with reduced OS in the radiotherapy-led CNS9904 trial 112
Figure 5.6 BLBP was expressed in all ependymoma cell lines 114

Figure 5.7 BLBP gene expression was maintained at recurrence in the Hoffman dataset 115
Figure 5.8 Elevation in BLBP expression in stem cell enriched neurospheres derived from the DKFZ-EP1 cell line 116
Figure 5.9 DHA had a differential effect on proliferation on ependymoma cell lines 117
Figure 5.10 DHA inhibited colony formation in the $BLBP^{lo}$ BXD-1425EPN cell line at high concentrations in a stem cell relevant clonogenic assay. 118
Figure 5.11 DHA had a differential effect on response to chemotherapy in the $BLBP^{lo}$ BXD-1425EPN cell line 119
Figure 5.12 DHA enhanced the cytotoxic effect of etoposide in the $BLBP^{lo}$ BXD-1425EPN cell line in a clonogenic assay 120
Figure 5.13 DHA diminished migration in ependymoma cell lines 122
Figure 5.14 DHA inhibits invasion of the $BLBP^{lo}$ BXD-1425EPN cell line.124
Figure 5.15 PPAR antagonists inhibited BLBP expression in ependymoma cell lines 126
Figure 5.16 The PPAR-γ antagonist GW9662 inhibited proliferation in ependymoma cell lines 128
Figure 5.17 Dual PPAR- (γ/δ) antagonist FH535 and PPAR-γ antagonist GW9662 induced toxicity in ependymoma stem cells 130
Figure 5.18 BLBP inhibition by PPAR-γ antagonist GW9662 could not potentiate response to chemotherapy 132
Figure 5.19 The PPAR-γ antagonist GW9662 potentiated response to chemotherapy in the $BLBP^{lo}$ BXD-1425EPN cell line in a clonogenic assay 133
Figure 5.20 PPAR antagonists decreased migration in ependymoma cell lines 135
Figure 5.21 PPAR antagonists inhibited invasion in $BLBP^{lo}$ BXD-1425EPN cell line 137
Figure 6.1 MGMT expression was higher in paediatric ependymoma patients in comparison to adults. 145
Figure 6.2 MGMT gene expression was marginally higher in PF tumours in comparison to ST and SP ependymomas 146

Figure 6.3 Low MGMT promoter methylation levels in ependymoma 149
Figure 6.4 Paediatric ependymomas showed low levels of MGMT promoter methylation which was associated with poor prognosis 151
Figure 6.5 Nuclear expression of MGMT correlated with reduced survival in the chemotherapy-led CNS9204 trial 153
Figure 6.6 Nuclear expression of MGMT correlated with reduced survival in the radiotherapy-led CNS9904 trial. 155
Figure 6.7 Protein expression of MGMT and MMR pathway enzymes (MLH1 and MSH6) in ependymoma cell lines and stem cell enriched neurospheres 158
Figure 6.8 Ependymoma cell lines were TMZ resistant 160
Figure 6.9 MGMT circumventing N3-propargyl analogue of TMZ induced cytotoxicity in ependymoma cell lines 161
Figure 6.10 BXD-1425EPN cell line exhibited resistance to TMZ and sensitivity to the N3-propargyl analogue of TMZ in a stem cell relevant clonogenic assay I 163
Figure 6.11 Stem cell enriched DKFZ-EP1NS are TMZ resistant but sensitive to the N3-propargyl analogue 163
Figure 7.1 Similarity in the invasion patterns of the BXD-1425EPN orthotopic tumour and spheroid in BME 174
Figure 7.2 Heterogeneity in invasion behaviour of the BXD-1425EPN cell line in the BME 190
Figure 7.3 Elevation in BLBP expression after exposure to radiotherapy in the $BLBP^{lo}$ BXD-1425EPB cell line 191
A4 Protein expression of the C11orf95-RELA fusion in ependymoma cell lines by western blotting analysis 194

LIST OF TABLES

Table 2.1 Clinicopathological characteristics of paediatric ependymoma patient samples from each of the two European trial cohorts, UKCCLG 1992 04 (CNS9204) and SIOP Ependymoma I (CNS9904)..... 39
Table 2.2 Clinicopathological details of paediatric ependymoma cell lines.40
Table 2.3 Drug concentrations employed in the clonogenic assay to treat the BXD-1425EPN cell line..... 44
Table 2.4 Drug concentrations employed in the MTT assay..... 46
Table 2.5 List of antibodies used for IHC..... 52
Table 2.6 List of antibodies used in Western blotting 55
Table 2.7 Reagents used in the first step of cDNA synthesis..... 58
Table 2.8 List of primers used in RT-PCR and QRT-PCR..... 60
Table 2.9 RT-PCR master-mix recipe..... 61
Table 2.10 QRT PCR master-mix..... 63
Table 2.11 QRT- PCR program..... 64
Table 4.1 Multivariate analysis of ABCB1 expression in the chemotherapy-led CNS9204 trial..... 85
Table 5.1 Multivariate survival analyses of BLBP expression in the chemotherapy-led CNS9204 trial..... 111
Table 6.1 Multivariate analysis of MGMT expression in the CNS9204 trial 154
Table 6.2 Multivariate analysis of MGMT expression in the CNS9904 trial 156

ABBREVIATIONS

AA - arachidonic acid

ABCB1- ATP binding cassette B1

AML – acute myeloid leukemia

APS - ammonium persulphate

BBB - blood brain barrier

BME - basement membrane extract

BLBP - brain lipid binding protein

BSA - bovine serum albumin

CGH- comparative genomic hybridization

CCLG - Children's Cancer and Leukaemia Group

cDNA - complementary DNA

CIMP – CpG island methylator phenotype

CNS - central nervous system

CT- computed tomography

Ct - cycle threshold

CSC - Cancer Stem Cells

DAB - 3,3'diaminobenzidine

DEPC H_2O - diethylpyrocarbonate treated water

DHA - docosahexanoic acid

DHFR – dihydrofolate reductase

dNTP - deoxyribonucleotide triphosphate

DTT - dithiothreitol

EDTA - ethylene-diamine-tetra-acetic acid

EFS - event free survival

EMA - epithelial membrane antigen

EphB2 - Ephrin type-B receptor 2

FA- fatty acid

FBS - foetal bovine serum

FISH - Fluorescence in situ hybridisation

GAPDH - glyceraldehyde 3-phosphate dehydrogenase

GTR - Gross total resection

H&E – haematoxylin & eosin

HBSS - Hanks Balanced Salt Solution

HRP - horseradish peroxidase

HSC – human stem cells

IMS - industrial methylated spirits

kDa - Kilodaltons

mRNA - messenger ribonucleic acid

NGS - normal goat serum

MGMT - O6-methyl guanine methyl transferase

MLH1 - MutL homolog 1

MMR - mismatch repair

MRI - Magnetic Resonance Induction

MSH6 - MutS homolog 6

OS - overall survival

PARP- Poly (ADP-ribose) polymerase

PBT – proton beam therapy

PBS (-T) - phosphate buffered saline (with tween)

PCR - polymerase chain reaction

PF – posterior fossa

PFA - paraformaldehyde

PPAR - peroxisome proliferator activated receptor

RG- radial glia

RNA - ribonucleic acid

RPMI - Roswell Park Memorial Institute medium

SDS - sodium dodecyl sulphate

SEM - standard error of the mean

SIOP - The International Society of Paediatric Oncology

SPSS - statistical programming for social sciences

SP – spinal

ST – supratentorial

SVZ – subventricular zone

TAE buffer - tris-acetate-EDTA buffer

Taq - Thermus aquaticus

Temed – tetramethylethylenediamine

TMZ- temozolomide

TBS(-T) - tris buffered saline (with tween)

TMA - tissue microarray

VPL - verapamil

Vdfl - vardenafil

CHAPTER 1. INTRODUCTION

1.1 Paediatric brain tumours

Brain tumours are the most common solid neoplasms in children. They are almost as prevalent as acute lymphoblastic leukemia and are more likely to cause death (Tumours/Childhood and http://www.ccrg.ox.ac.uk. , Duffner, Cohen et al. 1986, Johnson, Cullen et al. 2014). The most common brain tumours in children are astrocytomas which account for 52% of patients followed by medulloblastomas and ependymomas which account for 21% and 9% of cases respectively (Baldwin and Preston-Martin 2004, Ostrom, Gittleman et al. 2014). The predominant risk factors for development of brain tumours are genetic disorders such as Li-\fraumeni syndrome, Neurofibromatosis type 2 (NF2) as well as environmental factors such as exposure to ionizing radiation (Khatua, Sadighi et al. 2012).

The tentorium as well as the location of supratentorial and infratentorial regions are highlighted in Figure 1.1. Most supratentorial brain tumours predominate in infants and late adolescents whilst infratentorial sites are generally more common throughout childhood and account for 50% cases (Pollack, Gerszten et al. 1995). The mode of presentation of brain tumours depends on the age of the child as well as the location of the tumour. Brain tumours are notorious for their protean manifestations which could include progressively worsening bouts of headache, nausea, and/ or vomiting with or without focal neurological deficits. Symptoms generally progress slowly with benign tumours, such as low-grade gliomas, and more rapidly with aggressive lesions, such as anaplastic ependymomas (Pollack 1999). Histological grade still remains the standard method used to predict the biological nature of brain tumours. The World Health Organisation (WHO) classifies brain tumours on the basis of histological features using light microscopy. Grade I tumours have low proliferative potential and gross surgical resection is generally enough to treat these tumours. Although Grade II tumours have low proliferative potential, they are generally

infiltrative and can develop into tumours of a higher grade. Grade III tumours display anaplastic histological features such as nuclear atypia, high mitotic index and require post-operative chemotherapy or radiotherapy in order to improve prognosis. Grade IV tumours are the most aggressive. They show histological features such as high mitotic index, necrosis and are associated with an immensely poor prognosis (Rorke 1985).

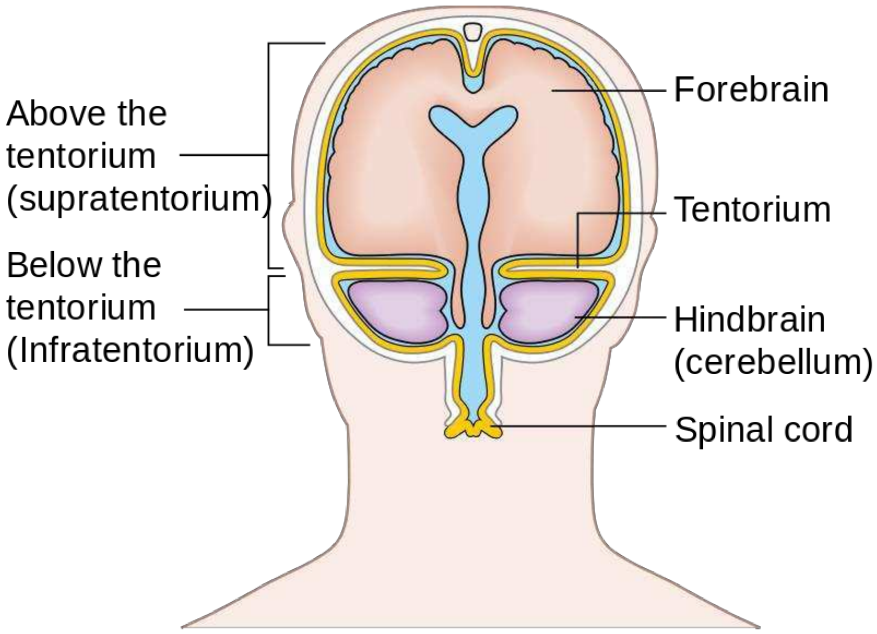


Figure 1.1 Location of the tentorium cerebelli The tentorium cerebelli is an extension of dura mater which separates the cerebellum (infratentorial region) from the inferior portion of the occipital lobes (supratentorial region). (Figure adapted from http://msk-anatomy.blogspot.co.uk/2013/04/the-tentorium.html)

Depending on patient age and histology, paediatric brain tumours are generally treated with surgery combined with adjuvant chemotherapy and/or radiotherapy (Northcott, Pfister et al. 2015). In recent years, survival rates in patients have improved due to multimodal approaches to treatment combined with advances in neuroimaging and surgical techniques.

Current chemotherapeutic options available to patients with brain tumours fail to be efficacious. Hence, in addition to generating a sub-optimal therapeutic effect, they also induce non-specific side effects. Therefore, continued research in understanding the cell of tumour origin as well as

underlying therapeutic resistance mechanisms is essential to facilitate discovery of novel biologically relevant therapeutic approaches to improve the currently achieved clinical outcome in children.

1.2 Ependymomas

Ependymomas are the 2nd most common malignant brain tumours in children accounting for 6-12% cases (Ostrom, Gittleman et al. 2014). They are so called due to the resemblance they share with the cerebrospinal fluid (CSF) secreting ependymal cells and can arise along the entire neuroaxis consisting of the hemispheres, hindbrain as well as the spinal cord (Louis, Ohgaki et al. 2007). In children, almost 90% of ependymomas are intracranial; two-thirds of them arising infratentorially from the posterior fossa (PF) (as shown in Figure 1.2) and the remaining one-third from the supratentorial (ST) compartment. Spinal (SP) ependymomas predominantly occur in adults (Kilday, Rahman et al. 2009).

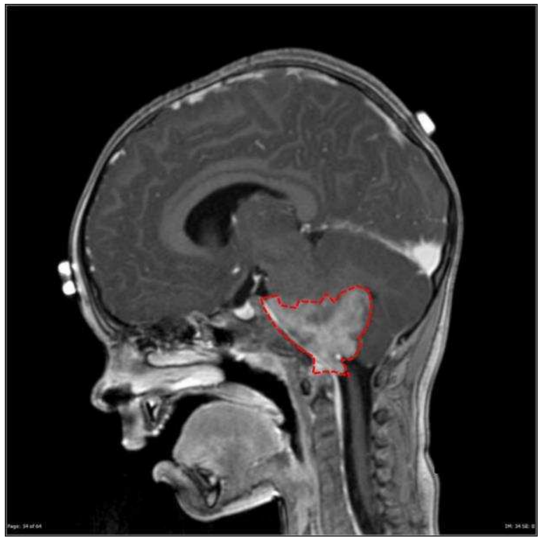


Figure 1.2 MRI image of a posterior fossa ependymoma Sagittal view of a classic paediatric posterior fossa tumour (demarcated by a dotted red line) located in the fourth ventricle, emanating from the foramen of Luschka and invading the brainstem. (Image obtained and modified from http://radiopaedia.org/articles/ependymoma).

Currently 40% of ependymoma cases remain incurable and the 5-year survival in infant patients stands at a dismal 40-52% (Gajjar, Pfister et al. 2014, Gatta, Botta et al. 2014). Challenges such as heterogeneous clinical behaviour of ependymomas arising from different locations,

contradictory studies regarding the prognostic value of the histopathological grading system and insufficient patient recruitment in trials to test new treatment options have hampered the ability to stratify patients into clinically relevant groups (Kilday, Rahman et al. 2009, Ellison, Kocak et al. 2011, Pajtler, Witt et al. 2015).

With surgical resection being the only favourable clinicopathological prognostic factor and their highly chemoresistant nature, there is a paucity of treatment options available to ependymoma patients (Bouffet, Perilongo et al. 1998, Merchant, Li et al. 2009). Due to their aggressive and clinically unpredictable behaviour, a better understanding of the underlying tumour propagating molecular mechanisms in ependymoma is essential for the development of novel prognostic markers and targeted treatments.

In this study, the aim was to investigate the role of cancer stem cells as a contributor to the cellular and phenotypic heterogeneity of ependymoma, in order to identify novel and translationally relevant druggable prognostic markers.

1.2.1 Symptoms

Clinical symptoms of ependymomas are dependent on the location of the tumour. Involvement of the posterior fossa may give rise to visual disturbances, cerebellar ataxia, dizziness and paresis. Supratentorial tumours may be associated with seizures and focal neurological deficits. Spinal ependymomas present with motor and sensory disabilities (Duncan 1995, Louis, Ohgaki et al. 2007).

1.2.2 Diagnosis

There is a standard protocol followed to diagnose ependymomas or brain tumours which in general consists of the following steps:

1. Physical examination of patients to assess neurological functions including reflexes, muscle strength, eye and mouth movement, co-ordination and alertness (Chowdhary, Green et al. 2006).

2. Imaging of the tumour by means of CT (computed tomography) or MRI (magnetic resonance imaging) scans is employed for preliminary diagnosis, although the latter is preferred due to the lack of radiation and added detail to images (Chowdhary, Green et al. 2006). Other advanced imaging techniques such as magnetic resonance spectroscopy and diffusion-weighted imaging are currently used in paediatric neuro-oncology. These have shown promise in identifying PF ependymomas due to their particularly low N-acetylaspartate levels (Zacharoulis and Moreno 2009). Ependymomas rarely spread; however, doctors may decide to do a spinal scan (myelogram) to investigate the metastatic status of the tumour (Zacharoulis, Ji et al. 2008) as well as a lumbar puncture to check the dissemination of tumour cells in the cerebrospinal fluid (CSF) (Laberge 2002).

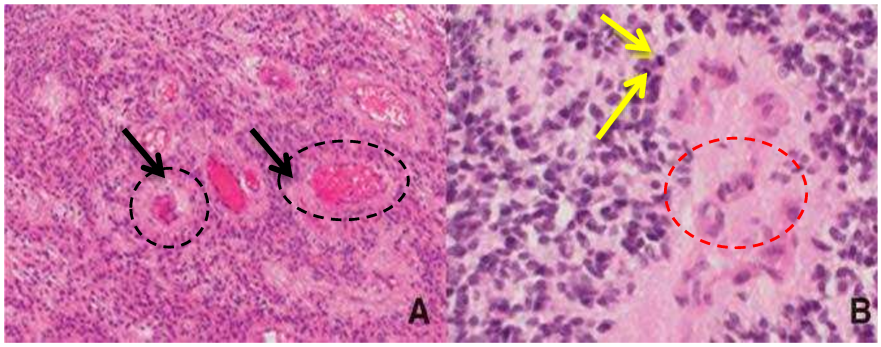


Figure 1.3 Histological appearance of paediatric ependymoma **A.**Classical (grade II) ependymoma with perivascular pseudorosettes (black arrows). **B.** Anaplastic (grade III) ependymoma with high mitotic activity (yellow arrows) and vascular proliferation (bottom right-red dotted line demarcation) in the same section. [Magnifications were X10 and X40 respectively.] Figure adapted from (Kilday, Rahman et al. 2009)

3. Tumour biopsy is obtained by surgical means to confirm the histopathology of the tumour and to grade it (Grill, Le Deley et al. 2001, Ellison, Kocak et al. 2011, Wright and Gajjar 2012, Cage, Clark et al. 2013). Ependymomas are classified into 3 groups based on histopathological criteria: Grade I (myxopapillary); Grade II, classical ependymoma (Figure 1.3 A) which is further subdivided into 4 subtypes (cellular, papillary, clear-cell, and tanycytic); and Grade III (anaplastic) ependymoma (Figure 1.3 B).

There are very few studies so far reporting tumour grade as a robust predictor of biological behaviour of ependymoma owing to the tremendous variability in terms of clinical outcome both across and within pathological grades (Schiffer, Chio et al. 1991, Carter, Nicholson et al. 2002, Merchant, Zhu et al. 2002, Massimino, Gandola et al. 2004, Kilday, Rahman et al. 2009, Ellison, Kocak et al. 2011, Wright and Gajjar 2012). Meta-analysis of prognostic values of various histological factors led to reclassification of Grade II and Grade III tumours based on parameters such as cell density, nodularity, mitotic activity, and angiogenesis. Unfortunately, this set of criteria was only significantly associated with survival exclusively in older children (Kilday, Rahman et al. 2009).

There is therefore a need to develop novel prognostic markers to predict the biological behaviour of the tumour and to stratify paediatric ependymoma patients into clinically relevant groups (discussed in detail in section 1.2.3).

1.2.3 Genetics, tumour heterogeneity and prognostic markers

A lot of interest in understanding the molecular biology of ependymoma has burgeoned from their rather complex and heterogeneous clinical behaviour.

Before the advent of complex genomic analysis, karyotypic studies were employed to study the molecular biology of ependymoma. Meta-analysis of 21 such studies by Kilday et al. showed that 89.2% of cases of intracranial ependymoma showed aberrant karyotypes with abnormalities in chromosome 22 and long arm of chromosome 1 reported in 30% and 20% cases respectively (Kilday, Rahman et al. 2009). However, these analyses also showed that there were no genomic aberrations restricted to paediatric ependymomas and the frequency of these abnormalities was consistent between adult and paediatric cases. Since paediatric ependymoma are distinct in terms of location from adult ependymoma; 90% paediatric ependymomas occur intracranially whilst the majority of ependymomas in adulthood are spinal in origin (Zacharoulis and Moreno 2009); higher

resolution analyses were essential to discover distinct anomalies in paediatric patients.

Metaphase Comparative Genomic Hybridization (CGH) has been a common technique for the molecular analysis of ependymoma (Granzow, Popp et al. 2001, Carter, Nicholson et al. 2002, Dyer, Prebble et al. 2002). This procedure involves the simultaneous hybridization of genomic tumour and constitutional DNA, each labelled with different fluorescent markers, to normal target metaphase chromosomes. Differences in fluorescent intensities between the two markers along the length of each chromosome can subsequently help identify aberrant genomic regions.

One such CGH study by Dyer et al. made the first attempt at using genomic profiling to subdivide ependymoma patients into clinically relevant groups (Dyer, Prebble et al. 2002). In this study, 42 primary and 11 recurrent ependymomas were screened to classify patients into 3 subgroups: numerical group (more than 13 chromosomal imbalances), structural group (0-5 complete/partial chromosomal imbalances) and balanced group (no chromosomal loss or gains). Patients in the numerical group showed a genomic profile similar to adult SP ependymomas consistent with a good prognosis. The structural group mainly consisted of recurrent tumours with an aggressive phenotype and hence, the worst prognosis. Gain of the long arm of chromosome 1 was seen in 26% of these tumours and has been reported as a common feature of paediatric ependymoma arising from the PF by a number of other studies (discussed in detail below). All of patients under 3 years of age showed a balanced genotype. 1q gain was reported in these patients at recurrence suggesting that the pathway of progression of balanced tumours may be similar to structural ones (Kramer, Parmiter et al. 1998, Carter, Nicholson et al. 2002). These results were in agreement with an array CGH study by Modena et al. which reported that younger patients had tumours with significantly smaller and more complex genomic imbalances in comparison to adult ependymomas (Modena, Lualdi et al. 2006).

Meta-analysis of 13 such CGH studies by Kilday et al. showed that the mean number chromosomal aberrations in children was 3.8 per tumour in contrast to 7.5 per tumour in adult patients (Kilday, Rahman et al. 2009). All these findings taken together indicated that either a small number of potent mutated oncogenes/ tumour suppressor genes regulating cell differentiation/ self-renewal or an aberrant epigenetic phenomenon affecting expression profiles of genes were responsible for imparting a balanced genomic profile associated with a very aggressive tumour phenotype in paediatric ependymoma. High resolution genotyping studies looking at single nucleotide polymorphisms or global methylation profiling were therefore necessary to gain a better understanding of the various factors underlying the pathogenesis of ependymoma in younger children.

Gain of chromosome 1q is a common aberration in cancer (Struski, Doco-Fenzy et al. 2002) and has been reported to have an incidence of >20% in ependymomas especially those arising from the PF compartment (Dyer, Prebble et al. 2002). There have been a number of CGH and serial analysis of gene expression studies carried out to look at candidate genes on chromosome 1q and their prognostic role in paediatric ependymomas. The gain of the entire q arm has been associated with poor prognosis in ependymomas (Dyer, Prebble et al. 2002), with the region specific amplicon 1q21.1 to 1q32.1 being correlated with recurrence in ependymomas (Mendrzyk, Korshunov et al. 2006). DUSP12 which is a candidate oncogene in ependymomas has been traced to a frequently gained 'hotspot' 1q23.3 (Suarez-Merino, Hubank et al. 2005, Mendrzyk, Korshunov et al. 2006). Rand et al. validated candidates on 1q chromosome in patient samples using immunohistochemistry in order to identify a potential clinicopathological role. Members of the S100 family were differentially expressed in clinical relevant subgroups (S100A6 expression correlated with ST tumours and S100A4 in patients under 3 years of age) in intracranial paediatric ependymomas (Rand, Prebble et al. 2008). Furthermore, copy number gain of 1q25 was associated with poor survival in two independent intracranial paediatric ependymoma cohorts (Mendrzyk, Korshunov et al. 2006, Kilday, Mitra et al. 2012). Taken together, these data

strongly implicate gain of 1q and possible oncogenes in this region in the progression and pathogenesis of poor outcome in paediatric intracranial ependymomas. It also highlights the need to investigate and validate the functional role of various genes encoded on 1q in the pathogenesis of paediatric ependymoma in greater detail.

In order to devise a robust and clinically relevant system of classifying ependymomas, several groups have recently carried out unbiased clustering of gene expression array data to identify subgroups. Johnson et al. clustered ependymomas on the basis of site-specific copy number alternations to define 9 subgroups (A-I; A-D mainly consisted of ST tumours; E, F represented SP tumours and G-I consisted of PF tumours) (Johnson, Wright et al. 2010). However, this classification did not provide any insight into the biological behaviour of the tumour. A similar approach was taken by Witt et al. who were, however also able to classify ependymomas from the posterior fossa compartment into clinically relevant, PFA and PFB groups. The PFA group mainly consisted of younger patients who had lateral tumours with a balanced genome, exhibited metastases at recurrence and were more likely to recur/die in comparison to the patients belonging to the PFB group. PFA patients were identified by the higher expression of NELL2 (Neural Epidermal Growth Factor Like-2) whilst PFB patients expressed LAMA2 (Laminin2). In parallel studies by Wani et al. and Hoffman et al., PF ependymomas were classified in two clinical relevant groups (similar to classification by Witt et al.), identified on the basis of expression of a 10 gene prognostic signature and immunoactive phenotype respectively (Wani, Armstrong et al. 2012, Hoffman, Donson et al. 2014). Although the aforementioned studies made a noteworthy contribution towards classifying ependymomas into clinically relevant groups, the utility of an expression array is restricted to identification of limited number of genes, probes for which were present on it. In contrast, as far as ST tumours were concerned, a more modern approach was taken by Pietsch et al. and Parker et al. who carried out RNA sequencing analyses to identify a novel fusion mRNA gene, expressed in two-thirds of ST tumours. This gene was a fusion between C11orf95, a gene with unknown function, and v-rel

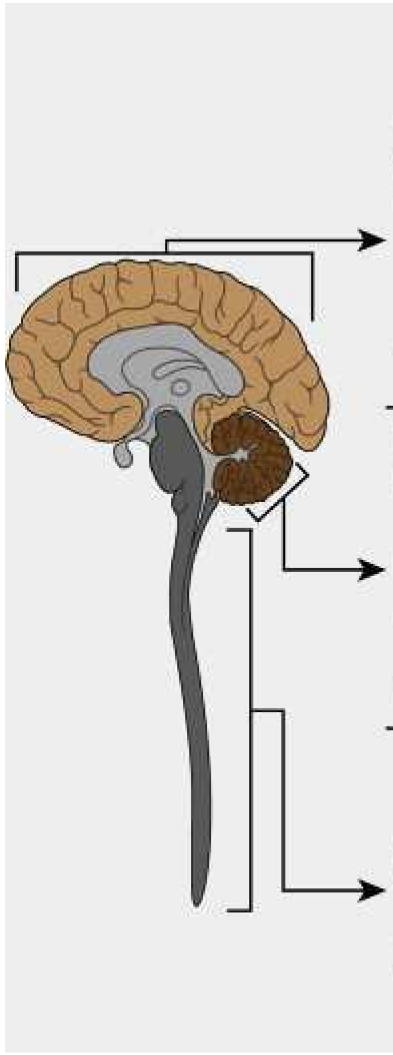
avian reticuloendotheliosis viral oncogene homolog A (RELA) encoding the RELA p65 subunit of the central NF-κB complex in a large number of ST ependymomas. Since the C11orf95–RELA fusion represented a unique mechanism leading to pathological activation of NF-κB signalling in ST ependymomas; targeting this pathway was proposed as a useful strategy for treatment of these neoplasms (Parker, Mohankumar et al. 2014, Pietsch, Wohlers et al. 2014). All these studies highlighted the need to collate and validate these results in a large ependymoma cohort consisting of tumours belonging to different locations.

As mentioned above, since ependymomas were regarded as genomically bland or balanced (Parker, Mohankumar et al. 2014), various studies investigated the status of an epigenetic phenomenon such as promoter hyper-methylation of various genes to subgroup patients. A follow up study by Witt et al. looked at the methylation profiles of PF tumours and reported that PFA ependymomas exhibit a CpG island methylator phenotype (CIMP positive) with a lot of genes silenced by CpG methylation while low levels of methylation were reported in PFB (CIMP negative) ependymomas (Mack, Witt et al. 2014). A recent study by Pajtler et al. validated data from the various subgrouping studies mentioned above by carrying out DNA methylation profiling on a large dataset of 500 paediatric ependymoma patients to define 9 molecular subgroups in ependymoma (Pajtler, Witt et al. 2015). Using unsupervised hierarchical clustering, they showed that tumours in each CNS compartment (SP, PF and ST) comprised 3 subgroups (as shown in Figure 1.4). SP ependymomas were classified into benign subependymoma (SP-SE), myxopapillary (SP-MPE), and anaplastic ependymoma (SP-EPN) with neurofibromatosis type 2 gene (NF2) mutations or deletions. PF ependymomas were categorised into subependymoma (PF-SE) and previously described subtypes A and B (Archer and Pomeroy, 2011; Witt et al., 2011), addressed in this study as PF-EPN-A and PF-EPN-B. PF-EPN-A (PFA) represented the largest element of the ependymoma subgroups comprising nearly 50% of all cases with a stable genome, CIMP-positive status and a remarkably poor outcome. Finally, ST ependymomas were divided into benign

subependymoma (ST-SE) and two subgroups characterized by molecular fusions. The largest supratentorial subgroup, ST-EPN-RELA, was characterized by expression of the previously described C11orf95-RelA fusion transcripts while other group, ST-EPN-YAP1 (Yes-associated protein 1) was primarily characterised by the uncharacterised YAP1-MAMLD1 fusions. It is not clear how the YAP1- MAMLD1 fusion drives tumour growth, although MAMLD1 (mastermind like domain containing-1) and MAML2 (mastermind like transcriptional coactivator 2), both members of the Mastermind gene family, are known co-activators of NOTCH which has been shown to be upregulated in ST ependymomas (Taylor, Poppleton et al. 2005).

In spite of providing a robust method classification based on methylation profiling; only a few subgroups in this study were identified by markers which can be targeted therapeutically. Additionally, carrying out methylation array profiling as part of routine diagnostic analysis, is not only expensive but also labour intensive. Similar to the NPI+ (Nottingham Prognostic Index Plus) consisting of an array of histopathological, clinical as well as molecular markers used to stratify breast cancer patients (Rakha, Soria et al. 2014); a panel of targetable markers needs to be defined in ependymoma patients belonging to each of the groups which could help identify and effectively treat high risk patients.

There have been a number of studies investigating potential prognostic markers in intracranial ependymomas such as Nestin, a marker for neural stem and progenitor cells (Milde, Hielscher et al. 2012); EZH2 (Enhancer of zeste homolog 2) (Li, Dunham et al. 2015), responsible for chromatin remodelling through histone methylation and Tenascin-C, involved in central nervous system neurogenesis (Gupta, Sharma et al. 2014). Evi-1 was deemed to be a marker of poor prognosis in tumours specifically arising from the PF (Koos, Bender et al. 2011). From these findings, it can be inferred that there has been some progress in the development of prognostic factors which can help effectively stratify patients on the basis of clinical outcome.



	Molecular subgroup	Age group	Gender distribution	Prognosis	Genetics	Histopathology
Supratentorial (ST-)	SE	adults	m > f	good	balanced	subependymoma (WHO I)
	EPN-YAP1	children	m < f	good	focal aberrations Chr. 11; *YAP1*-fusion	(anaplastic) ependymoma (WHO II/III)
	EPN-RELA	children and adults	m > f	poor	aberrations Chr. 11; chromothripsis; *RELA*-fusion	(anaplastic) ependymoma (WHO II/III)
Posterior Fossa (PF-)	SE	adults	m > f	good	balanced	subependymoma (WHO I)
	EPN-A	children	m > f	poor	balanced	(anaplastic) ependymoma (WHO II/III)
	EPN-B	children and adults	m < f	good	CIN	(anaplastic) ependymoma (WHO II/III)
Spine (SP-)	SE	adults	m = f	good	6q deletion	subependymoma (WHO I)
	MPE	predominantly adults	m = f	good	CIN	myxopapillary ependymoma (WHO I)
	EPN	predominantly adults	m > f	good	CIN; *NF2* mutation	(anaplastic) ependymoma (WHO II/III)

Figure 1.4 Classification of ependymoma into 9 subgroups on the basis of methylation profiles Pajtler et al. classified ependymoma in to 3 primary groups on the basis of their location (SP, PF, ST ependymomas); further classifying each of these groups on the basis of their methylation profiles into 3 subgroups as shown in figure above, identified by their molecular signatures. The figure also provides the summary of age groups (adults / children), gender, patient outcome, genetic signatures and tumour grade for ependymomas belonging to each subgroup. Image adapted from (Pajtler, Pfister et al. 2015). (CIN-chromosomal instability)

However, there have been very few studies which have identified druggable prognostic markers in ependymoma. One such study investigated the oncogenic role of PI3-Kinase pathway in ependymoma pathogenesis and poor clinical outcome. Furthermore, it also demonstrated that targeting the PI3-Kinase pathway by small molecule inhibitors would represent a novel treatment option available to those patients expressing it (Rogers, Mayne et al. 2013). All these studies highlight the need to continue performing active research in order to identify novel druggable markers in ependymomas and furthermore to validate the expression of these markers in the various subgroups defined by Pajter el al. (Pajtler, Witt et al. 2015).

In our study, the aim was to investigate the gene expression, prognostic value and in vitro inhibition / circumvention of 3 prognostic makers in paediatric ependymoma. However, validating the expression of these markers in various subgroups identified by Pajtler et al. was beyond the scope of this project.

1.2.4 Treatment of ependymomas

1.2.4.1 Surgery

Ependymoma is considered a surgical disease (Kilday, Rahman et al. 2009). Contemporary "standard" therapy for children and adults with ependymoma consists of gross total resection (GTR) followed by focal irradiation and adjuvant chemotherapy (Wright and Gajjar 2012). GTR is a consistent favourable prognostic factor in ependymomas and is curative in patients with Grade I myxopapillary ependymoma as well as a subset of patients with ST ependymomas. However, 29% patients suffer from surgical complications such as mutism and pseudobulbar palsy. Furthermore, improving surgical outcome has been difficult in patients who have unresectable anaplastic ependymomas invading surrounding critical structures and macroscopic metastases (Wright and Gajjar 2012).

However, in recent times novel MRI - and CT - guided stereotactic neurosurgical techniques as well as advances in neuroanesthesia and postoperative intensive care, have contributed to marked improvements in

surgical outcome (Chowdhary, Green et al. 2006, Kano, Yang et al. 2010, Wright and Gajjar 2012).

1.2.4.2 Radiotherapy

Adjuvant radiotherapy (RT) is administered to target residual microscopic disease in patients and has provided cure rates of >70% in patients with aggressive PF ependymomas (Merchant, Li et al. 2009). However, owing to the long term neurological deficits as a result of exposure to normal tissues, it has generally been avoided in patients under 3 years of age (Ellison, Kocak et al. 2011, Tai, Grundy et al. 2011, Sung, Lim do et al. 2012).

The standard radiation dose to treat localized ependymoma is 54–59.4 Gy for localised disease whilst in 5-10% patients with disseminated disease at diagnosis, a craniospinal irradiation (CSI) dose of 36 Gy is recommended (Chowdhary, Green et al. 2006, Ellison, Kocak et al. 2011). A number of regimens which employed a hyper-fractionated dose of 54 Gy to treat patients with PF tumours have not been shown to provide any survival benefit to patients over standard regimens (Massimino, Gandola et al. 2004, Combs, Thilmann et al. 2006). However, methods such as three dimensional conformal irradiation or Intensity Modulated Radiotherapy (IMRT) which protect critical structures from unnecessary radiation have been shown to improve long term survival in patients along with reduction of the common cognitive deficits in PF ependymomas (Wright and Gajjar 2012).

Proton beam therapy (PBT) as adjuvant treatment, has gained interest over the past few years due to its ability to limit damage to surrounding normal tissues and minimal exit dose (Hoffman and Yock 2009). A number studies predicted its superior potential in treating brain tumours in terms of protection from radiogenic second cancers and out-of-field adverse effects (Lee, Bilton et al. 2005, Merchant, Hua et al. 2008, Armoogum and Thorp 2015). A study by McDonald et al. which employed PBT as adjuvant treatment post GTR to treat intracranial paediatric ependymoma reported Progression Free Survival (PFS), and Overall

Survival (OS) rates of 80% and 89% respectively at a 26 month follow-up after receiving treatment (MacDonald, Safai et al. 2008). Long term follow ups are however essential to confirm its therapeutic efficacy over other conventional radiotherapy employing photons or charged particles to target tumours.

1.2.4.3 Chemotherapy

Chemotherapy has been utilised to reduced tumour burden or delay radiotherapy in patients; though its use has not been proven to have a significant association with improved outcome in patients (Bouffet and Foreman 1999, Chowdhary, Green et al. 2006). There are a number of ongoing trials in paediatric ependymoma patients trying to incorporate post-operative multimodal chemotherapeutic regimens including drugs such as vincristine, carboplatin, cyclophosphamide, etoposide, and cisplatin along with radiation therapy in order to improve progression free survival in patients [Clinical trial identifier number- NCT01096368, NCT00027846 and NCT02265770 (www.clinicaltrials.gov , Wright and Gajjar 2012)]. None of these regimens have shown any conclusive evidence of benefit.

Drugs which are being investigated in this study have been discussed in more detail below.

1.2.4.3.1 Etoposide

Etoposide is a semisynthetic derivative of podophyllotoxin which causes DNA double strand breaks by interaction with DNA-topoisomerase II which is responsible for making transient DNA double- strand breaks allowing the cell to manipulate the DNA topology (Hande 1998). It has been employed as part of adjuvant treatment regimens to treat paediatric ependymoma patients in a number of studies, all of which have reported the lack of survival benefit associated with it (Bouffet and Foreman 1999, Zacharoulis, Levy et al. 2007, Zacharoulis, Ashley et al. 2010).

Etoposide forms a ternary complex with DNA and the topoisomerase II enzyme which prevents re-ligation of the DNA strands. This lethality is further potentiated when the replication machinery or

helicases attempt to traverse the covalently bound topoisomerase-DNA complexes; thus, converting the DNA transient double-strand breaks into permanent double-stranded fractures which are no longer held together by proteinaceous bridges. These catastrophic events present at sufficient concentration lead to chromosomal aberrations triggering a series of signalling cascades which ultimately culminate in cell death by apoptosis (Hande 1998, Baldwin and Osheroff 2005).

Principal mechanisms of resistance to etoposide include efflux by ABC transporters (including ABCB1), overproduction of the topoisomerase II enzyme or alteration in the etoposide binding site of the enzyme (Goodman, Gilman et al. 1980). Other mechanisms of resistance might include the lengthening of the cell cycle, since there is a high level of topoisomerase II enzyme required during the G2 and S Phase. Upregulation of the DNA repair mechanisms might also promote resistance to etoposide (Hande 1998, Baldwin and Osheroff 2005).

1.2.4.3.2 Methotrexate

Methotrexate (MTX), also known as amethopterin or α-methopterin, is a folate antagonist which inhibits the dihydrofolate reductase (DHFR); critical for the production of reduced folate factors, which are essential for DNA and RNA synthesis (Grosflam and Weinblatt 1991). MTX is a global immunosuppressive agent and is also used in the treatment of rheumatoid arthritis (Segal, Yaron et al. 1990) . Similar to etoposide, there are a number of trials employing MTX as a part of adjuvant regimens to treat ependymoma [Clinical trial identifier number-NCT00287924, NCT02265770, NCT00602667 (www.clinicaltrials.gov)].

There are a several mechanisms of resistance as far as MTX is concerned; reduced transport of MTX into the cell, efflux of the drug by drug exporters such as ABCB1, ABCC1 and ABCG2, overexpression of the DHFR gene in the cells and finally, an alteration in the MTX binding site of DHFR (Mikkelsen, Thorn et al. 2011).

1.2.4.3.3 Vincristine

Vincristine is a chemotherapeutic drug derived from Madagascar periwinkle plant, Catharanthus roseus. It targets tumour cells by selectively binding to tubulin, to prevent its polymerisation into microtubules leading to cell cycle arrest during metaphase (Jordan 2002). Vincristine is very widely used against childhood cancer and is part of the treatment regimens for ALL (acute lymphoblastic leukaemia), neuroblastoma, Wilms tumour, Ewing's sarcoma, rhabdomyosarcoma, Hodgkin's disease, non-Hodgkin's lymphoma and retinoblastoma, as well as brain tumours (Goodman, Gilman et al. 1980). The primary mechanism of resistance to vincristine is through efflux by ABCB1 (Endicott and Ling 1989). Other mechanisms include efflux by other drug transporters such as ABCC1 and ABCG2 as well as β-tubulin polymorphism which prevents it from binding to the drug (Goodman, Gilman et al. 1980).

1.2.4.3.4 Temozolomide

Temozolomide (TMZ) is an imidazotetrazine DNA alkylating agent (Newlands, Blackledge et al. 1992). It is rapidly absorbed and undergoes spontaneous breakdown in plasma at pH>7 to eventually form the highly reactive methyldiazonium cation. This methyldiazonium cation methylates DNA purine residues, preferentially N7-guanine (N7-MeG, 70%) (Tisdale 1987, Denny, Wheelhouse et al. 1994) as well as N3- adenine (N3-MeA, 9%) and O6-guanine (O6-MeG, 6%) (Tisdale 1987).

Brain tumours possess a more alkaline pH compared with surrounding healthy tissue, a situation which favours prodrug activation preferentially within tumour tissue (Rottenberg, Ginos et al. 1984). Thus, TMZ is used commonly with RT to treat brain tumours; with relatively good therapeutic benefit reported in GBM and recurrent medulloblastoma patients (O'Reilly, Newlands et al. 1993, Stupp, Mason et al. 2005, Wang, Hsu et al. 2009, Padovani, Andre et al. 2011, Akyüz, Demir et al. 2012, Aguilera, Mazewski et al. 2013). Although it has been used as a part of adjuvant chemotherapeutic regimens to treat ependymomas; there has been considerable controversy surrounding its therapeutic efficacy

(Chamberlain and Johnston 2009, Khoo, Kishima et al. 2013, Lombardi, Pambuku et al. 2013).

O6-MeG lesions represent just 6% of TMZ-induced DNA adducts, however, they are highly mutagenic, carcinogenic and cytotoxic (Wedge, Porteous et al. 1996). These lesions are repaired by O6- methyl guanine-DNA methyltransferase (MGMT), overexpression of which leads to resistance to the drug. Unrepaired O6-MeG mispairs with thymine, leading to activation of DNA mismatch repair (MMR) (Margison and Santibáñez-Koref 2002). MMR exclusively recognises and removes mispaired thymine, only to reinsert thymine opposite unrepaired O6-MeG. Therefore, futile cycles of thymine excision and reinsertion lead to persistent DNA strand breaks resulting in cell cycle arrest and apoptosis (D'Atri, Tentori et al. 1998, Cejka, Stojic et al. 2003). N3-adenine (less toxic) and N7-guanine (highly toxic) methylation on the other hand are rapidly repaired by Base Excision Repair (BER) that is facilitated by poly (ADP-ribose) polymerase-1(PARP-1) (Horton and Wilson 2007). TMZ's mechanism of action and cytotoxicity is therefore dependent on deficient MGMT & BER mechanisms and proficient MMR pathway.

Overexpression of MGMT as well as PARP-1 (involved in BER) has been shown to induce TMZ resistance (Zhang, Stevens et al. 2012) whilst dysfunctional MMR can induce mutagenicity in response to the drug (van Thuijl, Mazor et al. 2015). (Discussed in detail in section 1.7) It is therefore, essential to investigate optimal functioning of these aforementioned repair pathways prior to treatment, to ensure efficacious response to TMZ in ependymoma patients.

1.3 Cancer stem cells in ependymoma

The discovery of Cancer Stem Cells (CSCs) has radically transformed our outlook on carcinogenesis and response to treatment. The CSC hypothesis states that tumours harbour a sub-population of multi-potent stem-like cells resistant to treatment which recapitulates tumour growth, as depicted in Figure 1.5. In order to understand the role played by these treatment resistant CSCs in tumour pathogenesis and maintenance, it is essential to first elaborate on the biology of normal stem cells.

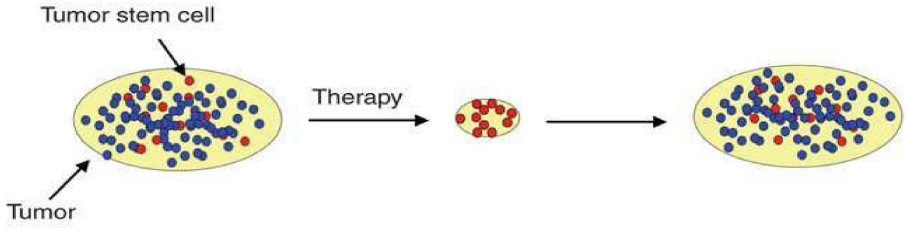


Figure 1.5 Cancer Stem Cell (CSC) Hypothesis The tumour contains CSCs (red) and malignant progeny (blue). After exposure to standard treatment, only CSCs survive and divide to repopulate the tumour with more CSCs and mature malignant cells. These mature cells also possess the ability to de-differentiate to form more CSCs. Image adapted from (Moitra, Lou et al. 2011).

Russian biologist Alexander Maximow came up with the concept of stem cells in relation to haemapoietic stem cells (HSCs) in 1920 [Reviewed by (Novik, Ionova et al. 2009, Moitra, Lou et al. 2011)]. Stem cells are defined as self-renewing multi-potent cells that possess multi-lineage differentiation [Reviewed by (Reya, Morrison et al. 2001)]. A healthy tissue has a pool of normal stem cells which undergoes asymmetric division to form more stem cells as well as progenitor cells which ultimately differentiate into specialised cells (depicted in Figure 1.6a). In the brain, the presence of neural stem cells was demonstrated by Lee et al. who isolated CD133 (prominin-1) expressing multipotent neural stem cells from murine post-natal cerebellum that were capable of forming self-renewing neurospheres as well as differentiating into astrocytes, oligodendrocytes and neurons in vitro (Lee, Kessler et al. 2005).

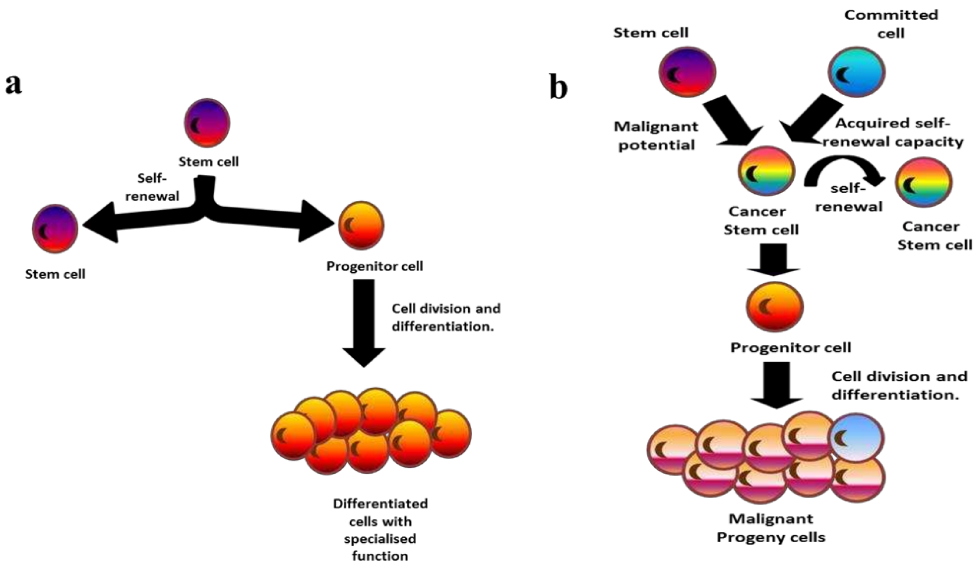


Figure 1.6 Asymmetric cell division of normal stem cells and the origin of cancer stem cells a. Asymmetric division of normal stem cells to self-renew to form another stem cell as well as a progenitor cell which further divides to form somatic cells with specialised function. **b.** Mutation in stem cells could lead to the dysregulation of this mechanism leading to malignant transformation; which also shows that a cancer stem cell could originate from a more differentiated cell. Image adapted from (Moitra, Lou et al. 2011)

The first conclusive evidence of CSCs was provided by Dick et al. in AML (acute myeloid leukaemia) in the year 1997. They demonstrated that a sub-population of CD34 (hematopoietic progenitor cell antigen) expressing leukaemic cells, which also lacked expression of CD38 (differentiation marker for white blood cells), was capable of inducing human AML in immune-deficient mice that histologically resembled the original patient malignancy (Bonnet and Dick 1997). There is a huge body of literature regarding the origin of CSCs. Calabrese et al. reported that for tumours containing a sub-population of cancer stem cells; there are at least two ways that the CSCs could have arisen (Figure 1.6 b). In the first, dysregulation of the process of asymmetric division as a result of oncogenic mutations may inactivate the constraints on normal stem cell expansion, resulting in CSCs that originated from normal stem cells. (Calabrese, Poppleton et al. 2007, O'Connor, Xiang et al. 2014). However, Friedmann-Morvinski et al. demonstrated that neurons and astrocytes could undergo de-differentiation by activation of oncogenes to induce gliomas in mice. In other words, most differentiated cells in the CNS upon defined genetic

alterations could generate CSCs (Friedmann-Morvinski, Bushong et al. 2012).

These CSCs have been identified in tumours by means of cell surface markers such as CD133 (Prominin1, a transmembrane protein) or CD34 as well as their ability to extrude dyes such as Rhodamine123 and Hoechst by expression of multidrug transporters such as ABCB1 and ABCG2 respectively (Dean, Fojo et al. 2005, Hadnagy, Gaboury et al. 2006, Bleau, Hambardzumyan et al. 2009). In addition to possessing normal stem cell-like properties such as self-renewal and differentiation; CSCs are additionally characterised by traits such as quiescence, multi-potency (differentiation to mature cells), ability to initiate tumour growth in immune-compromised mice and multidrug resistance (MDR-discussed in detail in Section 1.5) (Reya, Morrison et al. 2001, Graham, Jørgensen et al. 2002, Hirschmann-Jax, Foster et al. 2004, Clevers 2011, Ramaswamy, Remke et al. 2013). Singh at al. isolated CD133 expressing cells from a number of paediatric brain tumours such as astrocytoma, medulloblastoma, and glioblastoma. These cells were not only capable of forming self-renewing neurospheres but were also capable of forming tumours in immunodeficient (NOD-SCID) mice (Singh, Clarke et al. 2004).

In ependymomas, Taylor et al. showed that the gene expression profiles of human supratentorial and spinal ependymomas are shared by murine embryonic radial glia (RG) from the corresponding region in the CNS. RG are multi-potent stem cells capable of differentiating into ependymal cells, astrocytes and oligodendrocytes. Furthermore, these self-renewing RG-like CSCs isolated from ependymomas were also capable of initiating ependymomas in mice which histologically resembled the original patient tumour from which they were derived (Taylor, Poppleton et al. 2005, Poppleton and Gilbertson 2007). (Discussed in detail in the section 1.6)

Ependymomas are known to be chemoresistant (Bouffet and Foreman 1999, Atkinson, Shelat et al. 2011) and have a tendency to recur (Bouffet and Foreman 1999, Pollack 1999); it is believed that the same multi-drug resistance exhibited by CSCs in ependymomas might underlie

this behaviour (Discussed in Sections 1.5 and 1.6). This study aims to identify these CSCs in ependymoma as well as provide a clearer understanding of the chemoresistance mechanisms active in them.

1.4 Multi-drug resistance in CSCs and ABCB1

As mentioned in Section 1.4, multi-drug resistance (MDR) is a hallmark of CSCs. It has been widely studied in a number of cancers and has also been reported as a marker for poor prognosis in leukaemia, pancreatic cancer and brain tumours (Chou, Reyes-Mugica et al. 1995, Leighton Jr and Goldstein 1995, von Bossanyi, Diete et al. 1997, Jamroziak and Robak 2004).

Classical MDR is mainly mediated by 3 members of the ATP-binding cassette (ABC) transporters super-family (consisting of 49 proteins in humans); ABCB1 [also known as P-glycoprotein (Pgp)], ABCC1 [also known as multidrug resistance-associated protein (MRP1)] and ABCG2 [also known as breast cancer-resistance protein (BCRP) or mitoxantrone-resistance protein (MXR)]. Efflux by these transporters prevents accumulation of chemotherapy in cells; leading to a sub-optimal response (Kroetz, Pauli-Magnus et al. 2003). ABC multi-drug transporters extrude a wide array of substrates or toxic substances; thus having a protective function in the kidneys, liver, gastrointestinal tissue, brain, testis and placenta (Gottesman and Ambudkar 2001, Kowalsky, Nieminen et al. 2004, Sazakcs, Paterson et al. 2006).

ABCB1 actively exports structurally diverse hydrophobic compounds from the cell. It is a large transmembrane membrane protein of 170 kDa which is encoded by the MDR1 gene located on the chromosome 7q21 in humans (Chen, Chin et al. 1986). Intrinsically drug-resistant tumours such as colon, kidney, liver and pancreatic cancer have shown elevated MDR1 mRNA levels while some others including acute lymphocytic leukaemia, breast cancer, neuroblastoma, pheochromocytoma, and poorly differentiated lymphoma showed an increased level of MDR1 mRNA at relapse after chemotherapy (Goldstein, Galski et al. 1989). The consistent association of MDR1 expression with several intrinsically resistant cancers

as well as cancers with acquired drug resistance indicates that MDR1 contributes to chemoresistance in many human cancers.

A functional ABC transporter is composed of four domains: two transmembrane domains (TMDs) and two nucleotide-binding folds (NBFs) (Figure 1.7). The NBF, also known as the ATP-binding domain, hydrolyses ATP to provide energy to transport substrates across the membrane while the TMD is responsible for forming the substrate transport pathway across the membrane (Chen, Chin et al. 1986). Hypothetical models such as the flippase model and hydrophobic vacuum cleaner (HVC) model have been proposed to explain the substrate efflux function by ABCB1. In the vacuum cleaner model, several lipophilic molecules concentrated in the lipid bilayer bind to the transporters and are exported as a result. The flippase model on

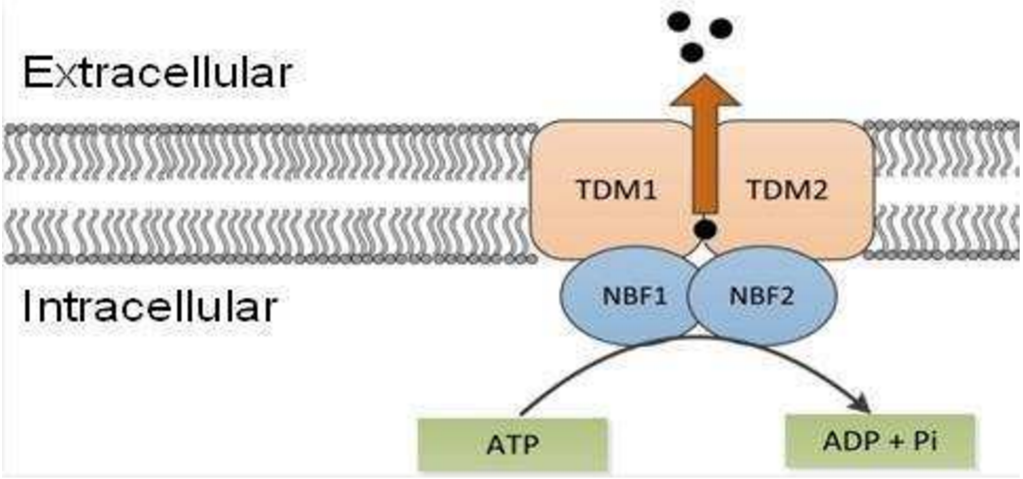


Figure 1.7 Organisation of ABC transporters Structure of a functional ABC transporter contains two TMDs and two NBFs. ABC transporters actively efflux substrates (black circles) by ATP hydrolysis to ADP. ABC, ATP-binding cassette; TMD, transmembrane domain; NBF, nucleotide-binding fold; ATP, adenosine triphosphate; ADP, adenosine diphosphate. This figure is adapted from (Moitra, Lou et al. 2011).

the other hand involves the transfer of the drug from the inner leaflet of the transporter to the outer leaflet (Eckford and Sharom 2006).

ABCB1 is normally expressed in the liver and the luminal membrane of the endothelial cells of the blood brain barrier so as to protect these cells from a range of toxic agents. ABCB1 can transport drugs with a wide array of chemical structures, ranging from 250 Da (cimetidine) to 1202 Da

(cyclosporin) (Pan, Dutt et al. 1994, Wu, Benet et al. 1995). Cancer cells expressing ABCB1 are resistant to a broad spectrum of anti-tumour drugs including anthracyclines (e.g. DOX), vinca alkaloids (e.g. vincristine), podophyllotoxins (e.g. etoposide) and taxanes (e.g. taxol), as a result of reduced intracellular drug concentrations which decreases the cytotoxicity induced by them.

ABCB1 expression has been correlated with MDR and hence, poor outcome in brain tumours including glioma (von Bossanyi, Diete et al. 1997) and medulloblastoma (Chou, Reyes-Mugica et al. 1995, Othman, Kimishi et al. 2014). Tumours are frequently heterogeneous with respect to ABCB1 expression and those cells with higher levels of ABCB1 are proposed to have a selective advantage during the progression of the disease (Krishna and Mayer 2000). Chemoresistance and heterogeneous clinical behaviour has been widely reported in ependymoma (Bouffet, Perilongo et al. 1998, Atkinson, Shelat et al. 2011). In this thesis, it is hypothesised that high ABCB1 expressing chemoresistant cells representing a subset of the tumour may confer a survival advantage over other tumour cells.

ABCB1 inhibition has been proposed to have a favourable effect on cancer treatment due to numerous benefits associated with it. ABCB1 inhibition could not only increase the efficacy of cytotoxic drugs but also reduce the dose related side effects associated with them (Filipski, Berland et al. 2014, Othman, Kimishi et al. 2014). Since ABCB1 is expressed in the blood brain barrier (BBB), its inhibition could also increase the delivery of the drug to the tumour site (Black, Yin et al. 2008). Inhibition of ABCB1 was shown to increase cytotoxicity of chemotherapeutic drugs in endothelial cells that overexpressed it, thus enhancing the therapeutic effect of the drugs (Mouthon, Fouchet et al. 2006). Finally, some reports also demonstrate inhibition of ABCB1 might increase apoptosis in cancer cells expressing ABCB1 in a manner not related to the drug efflux (Johnstone, Ruefli et al. 2000, Ruth and Roninson 2000, Tainton, Smyth et al. 2004).

Due to the abundant aforementioned advantages; several compounds belonging to a variety of chemical and pharmacological classes

have been studied and shown to inhibit the drug efflux by ABCB1, thereby, reversing cellular resistance to chemotherapy (Ford and Hait 1993, Wang, Monagle et al. 2004, Sazakcs, Paterson et al. 2006). So far 3 generations of ABCB1 transporter inhibitors have been widely studied.

First generation inhibitors consisted of drugs belonging to various pharmacological classes such as calcium channel blockers (verapamil, nifedipine, diltiazem), camodulin inhibitors (chlorpromazine, prochlorperzine), anti-malarials (quinine, quinidine) and immunosuppressants (cyclosporine A) (Krishna and Mayer 2000). These were however non-specific and also inhibited ABCG2 in addition to ABCB1 (Takara, Matsubara et al. 2012). Despite promising results in in vitro and in vivo experiments (Krishna and Mayer 2000); they failed to impart clinical benefit due to unacceptable side effects (Ozols, Cunnion et al. 1987, Daenen, van der Holt et al. 2004).

Most of the second generation inhibitors were analogues of the first generation such as dexverapamil (R-enantiomer of verapamil), emopamil, and valspodar (PSC-833, non-immunosuppressive analogue of CyA). Though very effective at lower concentrations compared to their analogues (Boesch, Muller et al. 1991, Alaoui-Jamali, Schecter et al. 1993, Krishna, De Jong et al. 1997), their therapeutic benefit was limited because of pharmacokinetic interactions (Goldman 2003, Kolitz, George et al. 2004).

The third generation ABCB1 inhibitors include laniquidar (R101933), zosuquidar (LY335979), elacridar (GF-120918) and tariquidar (XR9576). These modulators were developed using structure–activity relationships and combinatorial chemistry approaches targeted against specific MDR mechanisms (Dantzig, Shepard et al. 1996, Peck, Hewett et al. 2001, Guns, Denyssevych et al. 2002). Tariquidar is currently in clinical trials to treat solid tumours (including brain tumours) in children. There are however still toxicity issues associated with this generation (clinical trials identification number-NCT00020514, www.clinicaltrials.gov,).

In recent years, there has been a lot of interest in repurposing off-patent drugs to treat cancer. These drugs are normally used to treat several

other conditions such as diabetes or acne and clinicians already possess knowledge of their pharmacokinetic and toxicity profiles. Phosphodiesterase type 5 (PDE5) inhibitors have so far been widely used in the treatment of male erectile dysfunction (Boddi, Castellini et al. 2015). They inhibit cGMP hydrolysis by PDE5, increasing the intracellular levels of cGMP; triggering smooth muscle relaxation (Bischoff 2004). In a study by Ding et al. an ABCB1 over-expressing parental epidermoid carcinoma cell line; concomitant treatment with paclitaxel and PDE5 inhibitors vardenafil or sildenafil, potentiated the response to the chemotherapeutic drug. Notably, vardenafil was more effective and ABCB1 specific than sildenafil which also inhibited ABCG2 (Ding, Tiwari et al. 2011, Shi, Tiwari et al. 2011). In a recent study, vardenafil was shown to not only increase the BBB permeability but also enhance adriamycin and herceptin induced cytotoxicity in rodents bearing primary brain tumours (Black, Yin et al. 2008) and metastatic breast / lung cancers (Hu, Ljubimova et al. 2010) respectively. Vardenafil is routinely used to treat pulmonary hypertension in children (Jing, Yu et al. 2011) and is well tolerated, making it a good candidate for being repurposed to treat paediatric patients with brain tumours.

Drugs such as methotrexate, etoposide and vincristine which are routinely part of chemotherapeutic regimens to treat ependymoma are ABCB1 substrates. It is therefore fair to assume the possibility of ABCB1 playing a crucial role in MDR in ependymoma. In this study, the potential prognostic value of ABCB1 as well as its functional role in chemoresistance exhibited by ependymoma was investigated. Furthermore, in vitro analyses were carried out to establish the therapeutic efficacy of clinically relevant Vardenafil in ependymoma treatment.

1.5 Radial glial cells and BLBP

Taylor et al. showed that ependymomas tend to recapitulate the developmental signatures of anatomically restricted progenitor cells. Several members of Eph-EPHRIN and Notch signalling pathway involved in maintaining the stem cell population in the subventricular zone (SVZ) (Conover and Allen 2002) were expressed in ST ependymomas whilst SP

ependymomas expressed various members of the Homeobox (HOX) family involved in the antero-posterior development of the spinal cord (Dasen, Liu et al. 2003). This indicated that ependymomas either maintained or recapitulated anatomically restricted progenitor cells which normally expressed these developmentally relevant genes. Furthermore, they also showed distinct similarities between the expression profiles of RG from the developing mouse and ependymomas arising from the corresponding region in the human CNS; suggesting that transformed RG could be the stem cells of origin in ependymoma (Taylor, Poppleton et al. 2005).

Neuroepithelial cells are the earliest progenitors in the CNS and are the immediate precursors of RG. They express CD133, Nestin and the radial glial marker RC2. RG on the other hand express all the aforementioned proteins in addition to GLAST (Glutamate transporter)-an astroglial marker and BLBP (Brain Lipid Binding Protein) (Fishell and Kriegstein 2003, Gotz and Huttner 2005). When stem cell enriched neurospheres were isolated from ependymoma by Johnson et al. at a frequency of 0.34 to 0.74% per tumour sample; they also had $CD133^{+}$/$Nestin^{+}$/ $RC2^{+}$/$BLBP^{+}$ immunophenotype. In addition, they were capable of establishing orthotopic brain tumours in mice with expression profiles similar to the parent tumours (Johnson, Wright et al. 2010). Similar to CSCs described in section 1.4, these ependymoma derived transformed RG expressed surface markers such as CD133, formed self-renewing neurospheres and finally recapitulated orthotopic tumours in mice. These properties strongly indicated that RG were the CSCs in ependymoma.

Similar to normal stem cells described in section 1.4, RG undergo asymmetric division (depicted in Figure 1.8) to form a daughter stem cell and a differentiated cell. Dysregulation of this process through loss of adherin junctions which affect cell polarity, anomalous expression of Emx2 (Homeobox protein Emx2) or PAX6 (Paired box protein PAX6) which control asymmetric division of RG or aberrant signalling pathways such as Notch signalling in ST ependymomas culminate in tumorigenic transformation (Poppleton and Gilbertson 2007).

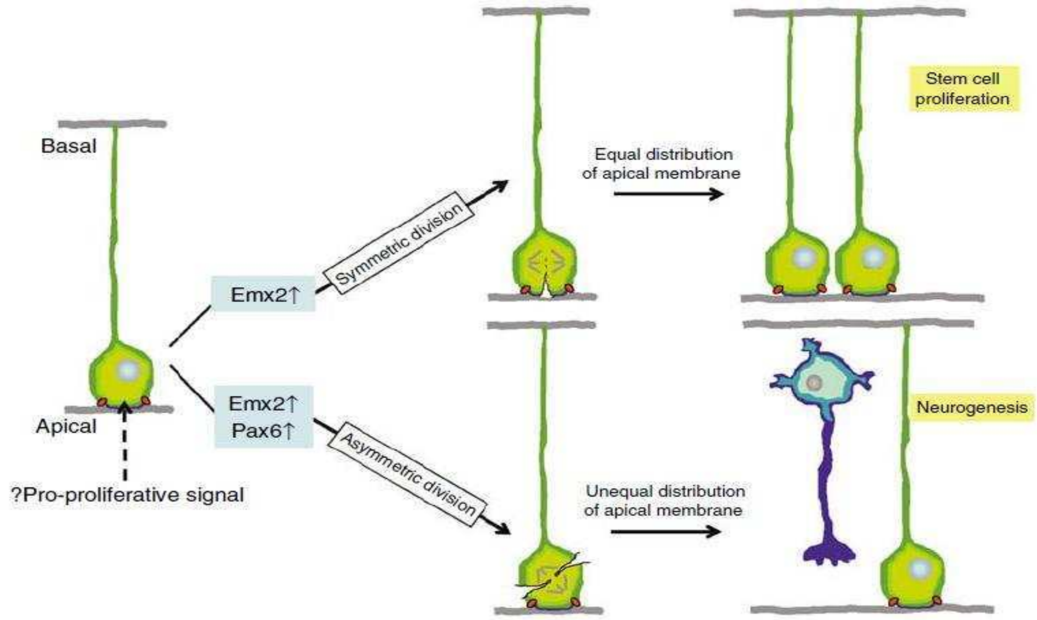


Figure 1.8 Symmetric and asymmetric division of RG RG undergo asymmetric division to form a differentiated daughter cell and another RG cell. Dysregulation of this process through increase in transcription factors such as Emx2, aberrant signalling pathways as well as loss of adherin junctions cause symmetric division of cell and tumorigenic transformation. Figure adapted from (Poppleton and Gilbertson 2007).

The fatty acid chaperone BLBP is expressed at high levels in RG during the embryonic period and is transcribed in response to Notch signalling which as mentioned before is highly expressed in supratentorial ependymoma (Anthony, Mason et al. 2005, Johnson, Wright et al. 2010). Furthermore, the expression of BLBP has been spatially and temporally correlated with neuronal differentiation in many parts of the rat CNS, including postnatal cerebellum, embryonic spinal cord, and cerebral cortex indicating its possible role in maintaining the RG population in all those locations (Koirala and Corfas 2010). Taken together, these studies highlight the need to study the possible role of BLBP in the maintenance and possibly the malignant transformation of RG which underlie ependymoma pathogenesis.

BLBP, also known as fatty acid binding protein 7 (BLBP) and brain fatty acid binding protein (B-FABP) is a member of the fatty acid binding protein family and maps to chromosome 6q23 (Anthony, Mason et al. 2005). It acts as a lipid chaperone and helps maintain intracellular lipid

balance. Docosahexaenoic (DHA), oleic, linoleic, and elaidic acid are its primary binding substrates (De Rosa, Pellegatta et al. 2012, Phuchareon, Overdevest et al. 2014).

Several studies have investigated the prognostic value of BLBP in cancer. BLBP expression has been associated with poor prognosis in renal cancer (Tolle, Krause et al. 2011), adenoid cystic carcinoma of the salivary glands (Phuchareon, Overdevest et al. 2014) and aggressive triple-negative breast cancer (Tang, Umemura et al. 2010). Furthermore, nuclear translocation of BLBP has been associated with epidermal growth factor receptor activation (Feng, Hatten et al. 1994) and glioblastomas which co-expressed BLBP and EGFR were shown to have a poor prognosis (Liang, Bollen et al. 2006). Taken together, these studies point out the strong prognostic potential of BLBP in stratifying cancer patients. Combined with evidence of it being marker of transformed RG, it is hypothesised in this study that BLBP could be useful tool in identifying high risk ependymoma patients.

BLBP expression has been shown to promote invasion and migration in glioma derived cell lines (De Rosa, Pellegatta et al. 2012) whilst its knockdown decreased proliferation and migration in renal carcinoma as well as melanoma cell lines (Slipicevic, Jørgensen et al. 2008, Tolle, Suhail et al. 2011). Goto et al. also reported that the BLBP antigen was detected in 56% of melanoma patients and could be a potential target for immunotherapy in this tumour type (Goto, Matsuzaki et al. 2006). All these studies highlight the possible functional role of BLBP in cancer maintenance and spread; but the exact mechanism by which it may be doing so still needs more research.

There is growing support for a global alteration in the metabolome of cancer cells that provides a growth and survival advantage that may be specific to various stages of tumour progression (Yoshida 2015). Cancer cells depend on energy inefficient mechanisms such as glycolysis in normoxic conditions (Warburg effect) instead of oxidative phosphorylation employed by normal cells to produce ATP (Manzi, Costantini et al. 2015). In

addition to formation of lactate, a proportion of pyruvate (produced as a result of glycolysis) also gets converted to fatty acids (FAs) via de novo synthesis employing enzymes such as fatty acid synthase and acetyl-coA carboxylase. These FAs are then used to produce energy via β-oxidation or production of phospholipids which are essential components of biological membranes (Wu, Daniels et al. 2014). Since BLBP chaperones these FAs intracellularly, it is plausible to believe that BLBP expression could give cancer cells a survival advantage and help them to thrive in the altered microenvironment. Lipids are the major components constituting up to 50% of the neural membrane in the brain. BLBP partners such as DHA (docosahexanoic acid), EPA (ecosapaentanoic acid), and AA (arachidonic acid) account for 20% of the brain's dry weight and are essential for membrane organisation, permeability, elasticity as well as formation of docosanoids and eicosanoids (Tapiero, Ba et al. 2002, Stillwell and Wassall 2003). They are taken up from the plasma by passive diffusion or via fatty acid translocases (CD36) and are intracellularly shuttled by BLBP (Chen, Green et al. 2008). These FAs shuttled by BLBP have also been proposed to be essential in modulating activity of PPAR transcription factors as depicted in Figure 1.9 (Mita, Beaulieu et al. 2010). PPARs are members of the nuclear receptor superfamily of transcription factors, known for their critical role in the development of different diseases, including obesity, cardiovascular disease, type-2 diabetes and cancer (Berger and Moller 2002). De Rosa et al. reported that the BLBP promoter had a PPRE (Peroxisome Proliferator Response Element); which indicated that in addition to other genes, PPARs (especially γ and δ subtypes) so transcribed BLBP. This finding was further supported by the observation that treatment of glioma cell lines by PPAR antagonists diminished expression of BLBP (De Rosa, Pellegatta et al. 2012). The nature of the FA translocated by BLBP has been shown to differentially modulate the gene expression by PPARs. Whilst the ω-3 FA DHA was shown to mitigate proliferation in gliomas and medulloblastomas by inhibition of genes such as p53, NF-κB and PI3-Kinase (Wang, Bhat et al. 2011); ω-6 FA AA was reported to promote cell migration in gliomas (Martin, Robbins et al. 1996). The genes inhibited/ activated by nuclear translocation of AA have not yet been

studied. This indicated that the equilibrium between ω-3 and ω-6 FAs was crucial in glioma pathogenesis and progression. Reports of 50% reduction in DHA levels and unchanged AA levels in malignant glioma samples in comparison to normal brain tissue (Martin, Robbins et al. 1996) suggest a shift in this ω-3 and ω-6 FA equilibrium, which could culminate in transcription of several oncogenic genes by PPARs. There are currently no metabolomics studies reporting altered FA levels in ependymoma. But, since RG are the cells of origin in both ependymomas and gliomas (Mita, Coles et al. 2007), it would be fair to assume that there may be an overlap in mechanisms which induce their transformation.

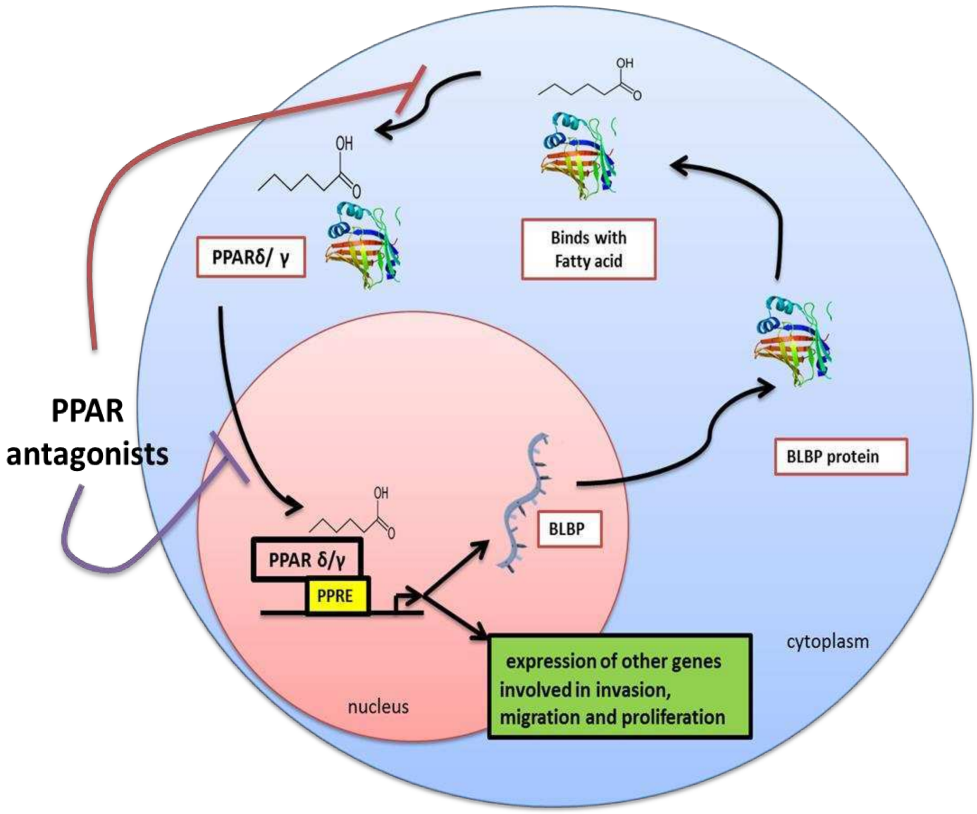


Figure 1.9 PPAR antagonists inhibit transcription and function of BLBP PPARs (γ and δ subtype) are transcription factors which are essential for regulating the transcription as well as function BLBP. The nuclear localization of the fatty acid chaperoned by BLBP is essential for transcription of genes by PPARs involved in proliferation and migration of cells. PPAR antagonists hence are predicted to block both the expression as well as the function of BLBP.

Taken together these findings imply that BLBP may be more than exclusively a marker of the ependymoma propagating transformed RG, since BLBP is an intracellular chaperone for FAs which not only provide

cells a metabolic survival advantage, but also promote migration/proliferation by modulation of transcription by PPARs. Therefore this study tests the hypothesis that BLBP expression and function could be important in ependymomas.

1.6 DNA damage, repair and MGMT

Human cells are exposed to mutagens on a regular basis; this exposure results in damage to DNA in the form of mutations. There are various intracellular repair mechanisms which are activated in response to DNA damage; these include recognition and signalling to denote the presence of damage, removal of damage, and subsequently, DNA repair. If the cell accumulates these mutations and loses the ability to repair them, then a series of signal transduction pathways are activated which either culminates into cellular apoptosis or unregulated cell growth. The latter causes malignant transformation. Therefore, the proper functioning of DNA repair mechanisms is essential for maintaining the integrity of the genome and for the normal functioning of an organism.

There are seven major DNA repair pathways: direct DNA repair, base excision repair (BER), nucleotide excision repair (NER), mismatch repair (MMR), homologous recombination (HR), non-homologous end joining (NHEJ) and trans-lesion synthesis (TLS) (Kuhn and Von Wartbung 1967, Radice, Bunn Jr et al. 1979, Kennedy and D'Andrea 2006). In general, BER, NER and MMR pathways are all involved in the repair of single DNA strand damage whilst the HR and NHEJ pathways repair DNA double strand breaks and crosslinks.

Alkylating agents such as temozolomide (TMZ) and lomustrine (BCNU)/ carmustine (CCNU) produce several adducts with DNA. As mentioned in section 1.2.4.3.4, the highly toxic O6-MeG lesions caused by TMZ are repaired directly by MGMT (Wedge, Porteous et al. 1996) while N7-MeG and N3-MeA are removed via the BER pathway (Dantzer, Schreiber et al. 1999).

MGMT, also called O6-alkylguanine DNA alkyltransferase (AGT), repairs alkylated bases like O6-alkylguanine by transferring the methyl group from the alkylated base to its cysteine side chain within the catalytic pocket (as shown in Figure 1.10), thereby restoring the DNA structure and inactivating MGMT (Pegg, Dolan et al. 1995, Xu-Welliver and Pegg 2002). It is a small protein (22 kDa) localised in the cytoplasm and nucleus, it can shuttle to the nucleus upon DNA alkylation (Lim and Li 1996). One MGMT molecule can repair only one alkyl adduct, therefore the cell's capacity for removing DNA O6-MeG adducts depends on the total number of MGMT molecules per cell and the rate at which the cell can re-synthesise MGMT (Gerson 2004).

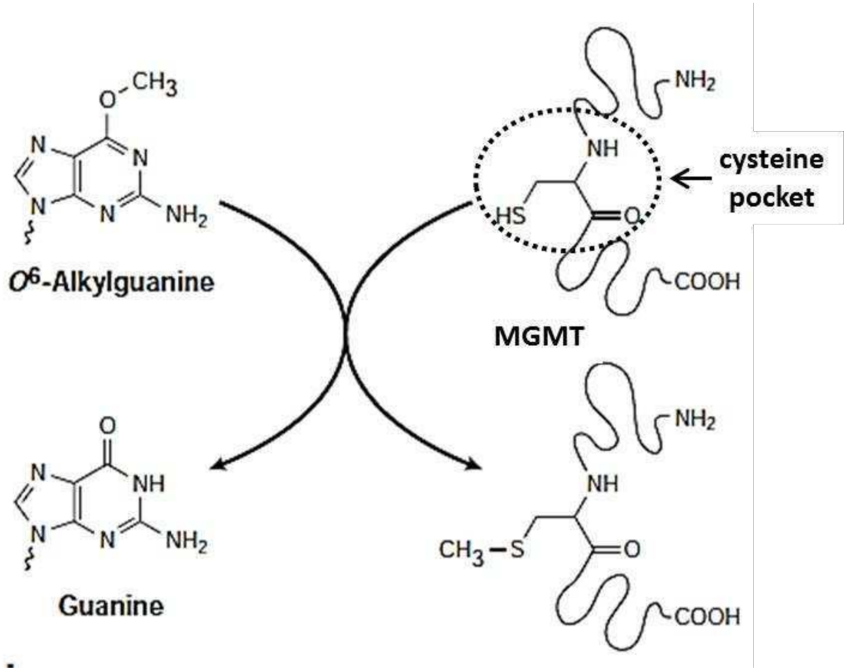


Figure 1.10 MGMT repair process MGMT scans double-stranded DNA for alkylation at the O6 position of guanine. Covalent transfer of the alkyl group (in this figure shown as a methyl, CH3, group) to the conserved active-site cysteine inactivates MGMT and restores the guanine to normal. Adapted from (Gerson 2004).

MGMT is of particular interest in cancer research because it has a role in the prevention, pathogenesis as well as treatment resistance witnessed in cancer.

MGMT serves as a DNA repair mechanism in normal tissues, protecting the genome from mutagenic lesions. O6-MeG is a tumorigenic lesion and MGMT is crucial in defending against neoplastic transformation. This has been confirmed in several in vivo experiments in animal models (Zagon and McLaughlin 1981, Jun, Ro et al. 1986, Nakatsuru, Matsukuma et al. 1993, Becker, Gregel et al. 2003). Therefore, individuals with no or low MGMT expression in brain tissue might be susceptible to brain tumour development (Silber, Blank et al. 1996). It has therefore been proposed that this protective property of MGMT can be harnessed through gene therapy to protect normal tissues from the toxic effects of chemotherapy (Gerson 2004).

MGMT expression in several cancers has been associated with poor response to alkylating agents and thus, dismal prognosis (Jiang, Dong et al. 2014, Ogura, Tsukamoto et al. 2015, Walter, van Brakel et al. 2015). MGMT has therefore emerged as a target for inhibition to potentiate the anticancer efficacy of alkylating agents. O6-benzyl guanine (O6-BG) and O6-(4-bromothenyl) guanine (lomeguatrib) are pseudosubstrates of MGMT which irreversibly inactivate MGMT by transferring the benzyl moiety or bromothenyl group to the active cysteine pocket respectively (Dolan, Moschel et al. 1990). Pre-clinical studies with these agents have shown a lot of promise due to their ability to potentiate response to chemotherapy (Wedge and Newlands 1996, Middleton, Kelly et al. 2000, Barvaux, Lorigan et al. 2004, Clemons, Kelly et al. 2005). O6-BG is currently employed in several clinical trials; however, due to its non-specific effect on normal tissues, a high level of chemotherapy induced haematological toxicity has been reported (Friedman, Pluda et al. 2000, Quinn, Pluda et al. 2002, Khan, Ranson et al. 2008, Tawbi, Villaruz et al. 2011). Therefore, there is a need to develop novel drug delivery methods which could enhance the specificity and tumour toxicity of these compounds. An alternative approach was recently proposed by Zhang et al., who demonstrated that some of the new

imidazotetrazine TMZ analogues could create toxic alkylated DNA lesions which cannot be recognised and repaired by MGMT. However, many of these analogues were prone to rapid activation following oral administration in nude mice; resulting in a sub-optimal tumour response (Zhang, Stevens et al. 2012). Therefore, similar to the aforementioned MGMT inhibitors, there is a need to develop novel delivery methods to improve the plasma stability and tumour toxicity induced by these agents.

MGMT has also been shown to be downregulated in many cancers, providing further insight into its role in malignant transformation and in intrinsic drug sensitivity of cancers. Loss of chromosome 10 (MGMT gene location) was found in 60% – 85% of glioma cases (Rolhion, Penault-Llorca et al. 1999) and MGMT promoter methylation was witnessed in 45% - 70% of high grade gliomas (Blanc, Wager et al. 2004, Stupp, Hegi et al. 2006). Hence, both are proposed to be common mechanisms of MGMT loss. Clinical evidence suggests that patients with MGMT promoter methylation respond better to alkylating agents such as carmustine or TMZ in combination with radiotherapy (Hegi, Diserens et al. 2005, Hegi, Liu et al. 2008). Thus, MGMT promoter methylation has been deemed as a marker of favourable outcome in patients treated with alkylating agents.

TMZ has been employed as a part of adjuvant regimen post-surgery as well as salvage therapy in ependymoma patients who fail respond to surgery and radiotherapy (Lombardi, Pambuku et al. 2013, Komori, Yanagisawa et al. 2016). However, similar to other chemotherapeutic drugs, there is a paucity of studies reporting any survival benefit from it (Chamberlain and Johnston 2009, Khoo, Kishima et al. 2013, Lombardi, Pambuku et al. 2013). Overexpression of MGMT in a small patient cohort of anaplastic recurrent ependymomas using immunohistochemistry reported by Buccoliero et al. could be an indication of its potential role in their chemo-resistant nature (Hegi, Diserens et al. 2005, Buccoliero, Castiglione et al. 2008). In ependymomas, there have been a few studies which have reported lack of MGMT promoter methylation (Michalowski, de Fraipont et al. 2006, Buccoliero, Castiglione et al. 2008); this is consistent with ependymoma patients showing poor response to TMZ. In contrast, a study

by Koos et al. reported that a subset of patients did in fact show low levels promoter methylation; with a negative trend in methylation status with an increase in grade. This result once again reiterated that MGMT expression might underlie the high level of chemoresistance in ependymomas (Koos, Peetz-Dienhart et al. 2010).

In conclusion, this study investigates the gene expression and promoter methylation of MGMT in large ependymoma patient cohorts and also elucidates the prognostic value of MGMT protein expression in stratifying ependymoma patients. Furthermore, it also examines the therapeutic efficacy of circumventing MGMT via a novel imidazotetrazine analogue of TMZ in in vitro models of ependymoma.

1.7 Aims and hypothesis

This study hypothesises that CSCs could be responsible for the chemoresistant and invasive behaviour of ependymomas. CSCs function through acquisition and accumulation of several resistance mechanisms which confer them with a survival advantage to thrive in the tumour microenvironment. This study investigates the expression and functional roles of multi-drug transporter ABCB1, radial glial stem cell marker BLBP and DNA repair enzyme, MGMT in poor prognosis of ependymoma with particular emphasis on the role of CSCs.

This thesis has the following aims:

- To investigate if the expression of ABCB1, BLBP and MGMT correlates with poor prognosis in 2 European paediatric ependymoma trial cohorts.
- To investigate if ABCB1 inhibition by PDE5 inhibitor vardenafil can overcome chemoresistance and invasion in in vitro models of ependymoma.
- To investigate if the BLBP partner DHA and BLBP inhibition by PPAR antagonists can help overcome chemoresistance and invasion in in vitro models of ependymoma.
- To assess the efficacy of the N3-propargyl analogue of TMZ in inducing toxicity in ependymomas, by circumventing MGMT induced resistance.

CHAPTER 2. MATERIALS AND METHODS

2.1 Public gene expression data analysis

Publicly available gene expression datasets accessible on the r2: Genomics Analysis and Visualisation Platform (http://r2.amc.nl) were downloaded and analysed in IBM SPSS Version 22. Four ependymoma datasets were used to carry out analyses: the Gilbertson dataset [Affymetrix U133 Plusv2 microarray, n=83, (Johnson, Wright et al. 2010)]; the Witt dataset [Heidelberg - Agilent two colour 4x44K Microarray, n=75, (Witt, Mack et al. 2011)]; the Mack dataset [Toronto - Affymetrix Exon 1.0ST Array, n=102, (Witt, Mack et al. 2011)] and Hoffman dataset (Affymetrix HG-U133 Plus 2 GeneChip microarray, n=14, (Hoffman, Donson et al. 2014)]. Whilst the Witt and the Mack datasets were published as part of the same study; they represent 2 independent cohorts of ependymoma patients from hospitals in Heidelberg and Toronto respectively.

2.2 Paediatric ependymoma trial cohorts

The tissue microarrays screened in this study comprised samples from two different paediatric intracranial ependymoma clinical trial cohorts where patients had received no previous neoadjuvant therapy (Table 2.1). The first UK CCLG 1992 04 (CNS9204) trial cohort consisted of patients aged less than 3 years at diagnosis who were treated with adjuvant chemotherapy (vincristine, carboplatin, methotrexate, cyclophosphamide, and cisplatin – 4 courses, 14 day intervals) following maximal resection. Radiotherapy was only given to these patients if progressive disease (relapse) was identified by neuro-imaging. Of the 89 patients included in this study 60 samples were available for tissue microarray analysis. The second cohort was from the SIOP Ependymoma I clinical trial (CNS9904) and consisted of patients aged over 3 and less than 21 years at diagnosis. Treatment for these patients involved either complete resection, followed by radiotherapy within 4 weeks or incomplete resection followed by further surgery then radiotherapy or radiotherapy combined with chemotherapy (vincristine, etoposide and cyclophosphamide). Of the 89 patients included

Table 2.1 Clinicopathological characteristics of paediatric ependymoma patient samples from each of the two European trial cohorts, UKCCLG 1992 04 (CNS9204) and SIOP Ependymoma I (CNS9904).

Variable		CNS9204 (n=60)	CNS9904 (n=47)	P value
Gender	Male	39 (65%)	20 (42.5%)	0.03
	Female	21 (35%)	27 (57.5%)	
Resection Status	Complete	28 (46.67%)	23 (48.93%)	0.84
	Incomplete	32 (53.33%)	24 (51.07%)	
Grade	WHO primary tumour Grade II	33 (55%)	28 (59.57%)	0.69
	WHO primary tumour Grade III	27 (45%)	19 (40.43%)	
Tumour Location	Posterior fossa (PF)	53 (88.33%)	28 (59.57%)	0.001
	Supratentorial (ST)	7 (11.67%)	19 (40.43%)	
Age	< 3 years	59 (98.33%)	2 (4.26%)	<0.001
	> 3 years	1 (1.67%)	45 (95.74%)	
Status	Dead	29 (48.33%)	19 (40.42%)	0.31
	Alive	31 (51.67%)	28 (59.57%)	
Event occurred (relapse/death)	Event	40 (66.67%)	26 (55.31%)	0.31
	No event	20 (33.99%)	21 (44.69%)	

in this study, 47 samples were available for tissue microarray analysis. The only significant differences between the trial cohorts, apart from age and axiomatic treatment, were tumour location (p=0.001) with the majority being infratentorial in the younger CNS9204 trial cohort, and sex (p=0.031) where there were almost double the incidence of males in the CNS9204 samples. Triplicate cores of 5 μm diameter were embedded in a tissue microarray paraffin block for each sample after review by a neuropathologist (Prof. Jim Lowe).

2.2.1 Statistical analysis

Univariate and multivariate survival analyses to assess the feasibility of the prognostic markers assessed in this study were performed using IBM SPSS Version 22.

2.3 Cell culture and cell based assays

2.3.1 Origin of cell lines and cell culture

Five paediatric ependymoma derived cell lines were used in this study. The clinicopathological details of the patients from whom these cell lines were derived are provided in Table 2.2.

Table 2.2 Clinicopathological details of paediatric ependymoma cell lines.

Cell line	Patient details	Diagnosis and WHO Grade
BXD-1425EPN (Baylor - Xenograft Derived) (Yu et al, 2010)	9 year old male	Recurrent anaplastic Ependymoma (Grade III)
EPN1 (Hussein et al, 2011)	22 year old male	Recurrent Ependymoma (Grade II)
EPN7 (Unpublished)	3.6 months old female	Anaplastic Ependymoma (Grade III)
EPN7R (Unpublished)	1.8 years old female	Recurrent Ependymoma (Grade II)
DKFZ-EP1 (Till et al, 2009)	18 year old female	Primary anaplastic Ependymoma (Grade III)

All tumours used to derive cell lines in this project were located in the supratentorial region of the brain. They were grown as monolayers in tumour media [15% Foetal Bovine Serum (FBS - GE Healthcare, Life Sciences) in Dulbecco's Modified Eagle Medium (DMEM, 1g/L glucose-Thermofisher)]. They were incubated in a standard humidified 5% CO_2-air incubator at 37 ˚C and sub-cultured when they reached 70-80 % confluency. All cell lines were tested routinely to ensure lack of mycoplasma infection by using the MycoAlert™ Mycoplasma detection kit (Lonza).

2.3.2 Recovering cells from liquid nitrogen

Cryovials containing cell suspensions were removed from liquid nitrogen storage and placed into a water bath at 37 ˚C for rapid thawing. The cell suspension was transferred into 5 ml pre-warmed tumour media in a 25 cm^2 tissue culture flask. The cells were incubated in a standard humidified 5% CO_2-air incubator at 37 ˚C. Media was changed after 24 hours (or when 50% of cells had attached to flask surface) to remove any dead cells.

2.3.3 Harvesting and sub-culturing monolayer cells

To maintain exponential growth of cells, cells were sub-cultured when they became 70-80% confluent. Tumour media was discarded and the adherent cells were washed with Hank's balanced salt solution (HBSS - GIBCO) 2-3 times. Cells were incubated at 37 ˚C with 3 ml of 1x trypsin-EDTA (Sigma) for 5 minutes until cells had detached. The cells were then distributed into different flasks depending upon their respective doubling times. The doubling time for each cell line was calculated using the equation given below obtained from http://www.doubling-time.com/compute.php

$$N_1 = N_0 * 2^{t/T}$$

$$T = t * Ln(2) / (Ln(N_1) - Ln(N_0))$$

N_0 the initial concentration of cells

N_1 the final concentration of cells

t the duration of culture

T the doubling time

Ln natural logarithm

2.3.4 Snap freezing of cell pellets

After harvesting cells as described in section 2.3.2, cell suspensions were centrifuged at 200 g for 5 minutes. The supernatant was discarded and the pellet was washed with 1 ml of phosphate buffered saline (PBS). The cell suspension was then transferred to a 1.5 ml eppendorf tube and centrifuged again at 200 g for 5 minutes. After discarding the supernatant, the eppendorf was dropped into a dewar flask containing liquid nitrogen (-210 ℃). Pellets were stored at - 80 ℃ for fu ture analysis.

2.3.5 Preparation of cell line stocks

Cells were harvested as described in section 2.3.3. They were then transferred to a 50 ml falcon tube and were centrifuged at 250 g for 5 minutes. The supernatant was then discarded and the cells were re-suspended in FBS containing 10 % DMSO (dimethyl sulfoxide, Sigma) at a concentration of $1x10^6$ cells/ml. 1 ml of suspension was aliquoted into cryovials and placed at -80 ˚C in a freezing container (Nalgene). Twenty four hours later, cells were transferred to liquid nitrogen for long term storage.

2.3.6 Neurosphere culture

Cells cultured as monolayers were harvested as described in section 2.3.3. The supernatant was discarded and the cell pellets were re-suspended in stem cell media [Serum free high glucose DMEM (4.5 g/l glucose, GIBCO), with addition of 2% B27 supplement (GIBCO), 33% Ham's F-12 solution (GIBCO), 5 ng/ml heparin (Sigma), and 1% streptomycin/penicillin (Sigma)] supplemented with 20 ng/mL basic-fibroblast growth factor (bFGF; GIBCO) and 20 ng/mL of epidermal growth factor (EGF; GIBCO). To generate secondary neurospheres, primary neurospheres were dissociated into single cells by incubating them in accutase (Sigma) for 5 minutes at 37 ˚C, followed by mechanical dispersion. These single cells were then divided into 2 flasks with freshly prepared stem cell media.

2.4 Viability assays

2.4.1 Clonogenic assay

The clonogenic assay is based on the ability of a single cell to form a colony and helps assess the response to treatments such as chemotherapy and radiotherapy in a sub-population of cells (Franken, Rodermond et al. 2006). In this study, it was used to evaluate the cytotoxic response in the CSC component of the BXD-1425EPN cell line to various drugs. The DKFZ-EP1 and EPN1 cell lines did not form colonies; so the cytotoxic response was measured by the MTT viability assay described in section 2.4.2

2.4.1.1 Cell plating

Harvested BXD-1425EPN cells were passed through a 40 µm cell strainer (Falcon) to obtain a single cell suspension. 500 cells/ 3 ml media were plated into each well of a 6-well plate and incubated for 4 hours in a standard humidified 5% CO_2-air incubator at 37 ˚C until they attached to the well. Since the principle of the experiment is based on the ability of a single cell to form a colony, treatments were begun before the cells divided.

2.4.1.2 Drug treatment

To establish dose-response curves for the chemotherapeutic drugs, cells were treated with etoposide (Sigma), vincristine (Sigma), temozolomide (TMZ, Sigma), N3-propargyl analogue of TMZ (Propargyl, Pharminox), methotrexate (25 mg/ml, GeneraMedix) and DHA (Cayman Chemical Company) at concentrations shown in Table 2.3. Duplicate plates were set up for each concentration. To assess the potentiation of response to etoposide, vincristine and methotrexate; experiments were also set up in combination with the ABCB1 inhibitors, verapamil [Vpl (20 µM), Sigma], vardenafil [Vdfl (10 µM), Toronto Pharmaceuticals], DHA (20 µM, Cayman Chemical Company) and PPAR-γ antagonist, GW9662 (15 µM, Sigma). Additional wells of cells were treated with only the drug vehicle to ensure lack of vehicle inflicted toxicity. The maximum amount of drug vehicle (DMSO) was maintained at a concentration < 0.01% v/v to prevent toxicity.

Table 2.3 Drug concentrations employed in the clonogenic assay to treat the BXD-1425EPN cell line

Cell line	Drug	Drug concentrations (μM)
BXD-1425EPN	**Methotrexate**	0.005,0.01,0.02, 0.025,0.03
	Etoposide	1,5, 10, 15,20
	Vincristine	0.005,0.01,0.02, 0.025,0.03
	TMZ	50,100, 200,300,400
	N3-propargyl analogue of TMZ	5,10,20,25,30
	DHA	5,10,20,25,30

2.4.1.3 Fixation and staining of colonies

Wells were microscopically assessed on a daily basis to assess the number of cells in a colony. When the number of control cells colonies reached 50 or more (approximately equivalent to 6 doublings), the medium was aspirated and colonies were fixed with 4% paraformaldehyde (PFA) for 20 minutes. 0.1% crystal violet was used to stain colonies for 5 minutes. Three 5 minutes PBS washes were carried out to wash out excess PFA and crystal violet. Stained colonies were counted and the average of duplicate wells over 3 experiments was analysed to produce dose-response curves.

2.4.1.4 IC_{50} estimation and analysis.

GraphPad Prism Version 6.0 was used to plot percentage of clonogenic survival against drug concentrations to establish dose-response curves. IC_{50} (half maximal inhibitory concentration of drug) values were estimated from these curves. The parametric unpaired student's t-test was used to establish any significant differences between IC_{50} values for drugs

alone or in combination with ABCB1 inhibitors, DHA GW9662 and PPAR-ϒ antagonist.

2.4.2 MTT assay

A metabolic assay was used to determine cytotoxic effect of drugs in the tumour bulk population, by employing the MTT Cell Proliferation kit (Roche). This assay is based on the principle of conversion of yellow tetrazolium MTT salt [(3-(4,5-dimethylthiazol-2-yl)-2,5-diphenyltetrazolium bromide)] to purple formazan crystals by metabolically active cells.

2.4.2.1 Plating cells

Cells were harvested as described in section 2.3.3 and counted using a haemocytometer. The number of cells plated per well for each cell line (BXD-1425EPN - 5000/well, DKFZ-EP1 - 6000/well and EPN1 - 6000/well) was established following preliminary growth curve experiments to ensure that cells were in an exponential growth phase during the assay. 100 µl of the suspension of dislodged cells in medium was pipetted into each well of a 96 well plate. The cells were allowed to attach overnight before commencing drug treatments.

2.4.2.2 Drug treatment

Cells were treated in triplicate wells at concentration ranges for each drug as described in Table 2.4. Experiments for etoposide, methotrexate and vincristine were also set up in combination with verapamil (20 µM), vardenafil (10 µM), DHA (20 µM) and PPAR- γ antagonist GW9662 (15 µM) in order to assess if there was a potentiation of response. The assay was carried out for a period of 5 days except in the case of TMZ which was carried out for 7-8 days, since activation of the mismatch repair pathway (MMR) is essential for it to induce cytotoxicity. (Discussed in detail, Chapter 1, section1,2.4.3.4)

Table 2.4 Drug concentrations employed in the MTT assay

Cell lines		BXD-1425EPN	DKFZ-EP1	EPN1
Drug concentrations (μM)	**Methotrexa-te**	0.005, 0.01,0.02,0.025, 0.03	1,2,5,10,12,15, 17,20	N/A
	Etoposide	10,20,50,70,100	10,20,50,70, 100	N/A
	Vincristine	0.005,0.01,0.02, 0.025,0.03	0.5,1,2,2.5,3	N/A
	TMZ	100,150,200, 250,300,350, 400,500	100,150,200, 250,300,350, 400,500	100,150,200, 50,300,350, 400,500
	N3-propargyl analogue	50, 100, 120,150, 200, 250	50,100, 120,150, 200, 250	50,100,120, 150, 200, 250
	DHA	5,10,20,25,30	5,10,20,25,30	5,10,20,25, 30

2.4.2.3 Detection

10 µl MTT reagent was added to each well and incubated at 37 °C for 4 hours, to allow the formation of purple formazan crystals. 100 µl of solubilisation reagent was then added to each well to dissolve the crystals whilst cells were incubated overnight at 37 ℃ to allow this to occur. The absorbance was read after 24 hours at a wavelength of 560 nm; with a reference wavelength of 650 nm using the FLUOstar plate reader (BMG labtech instruments) and the raw data from was downloaded from the Omega software (BMG labtech instruments).

2.4.2.4 IC_{50} estimation and analysis.

GraphPad Prism Version 6.0 was used to plot percentage cell survival against drug concentrations to plot dose-response curves. IC_{50} values were estimated from these curves. The parametric unpaired

student's t-test was used to establish any significant differences between IC_{50} values for drugs alone or in-combination with ABCB1 inhibitors, DHA and PPAR-ϒ antagonist GW9662.

2.4.3 Neurosphere alamar blue assay

In order to assess the effect of the BLBP inhibiting PPAR antagonists on ependymoma stem cells derived from the DKFZ-EP1 cell line, a neurosphere alamar blue assay was performed.

2.4.3.1 Plating cells and treatment

Neurospheres were dissociated into single cells as described in section 2.3.6. 5000 cells were then plated in each well of an ultra-low attachment (ULA) 96-well round bottom plate (Corning) in stem cell medium enriched with growth factors. The cells were then centrifuged at 100 g for 5 minutes and returned in to a standard incubator at 37 ºC and 5% CO_2. Once the spheroids had formed on day 3, they were treated with PPAR antagonists [FH535, GW0660, GSK9662 at 15 µM each]. Images were then obtained every 24 hours for 3 days to assess change in neurosphere diameter.

2.4.3.2 Detection

The viability was measured by using Alamar Blue® (Life Technologies). The Alamar Blue reagent was diluted in tumour media, at 1:10 dilution, and 100 µl was added to each well. The cells were incubated at 37 ˚C for 60 minutes exactly and the fluorescence was measured on the FLUOstar plate reader (BMG labtech instruments) at λ_{ex}=560nm, λ_{em}=5nm, and λ_{cutoff}=570nm.

2.4.3.3 Analysis

The percentage cell survivial was assessed for each treatment using GraphPad Prism Version 6.0 to produce a bar chart.

2.5 Wound healing assay

To investigate the effect of ABCB1 and BLBP inhibition on the migratory nature of ependymoma cells, an in vitro wound healing assay was performed (Liang, Park et al. 2007).This assay is based on making a scratch (wound) on confluent cells in a 48-well plate (Corning) and then measuring the ability of cells to migrate to close the wound. Photos were taken at fixed time intervals at 3 points, to track the migration until the wound had completely closed.

BXD-1425EPN and DKFZ-EP1 monolayers were harvested as described in section 2.3.2 and then seeded into a 48-well plate at a plating density of 30,000 and 40,000 cells per well respectively in 500 µl standard tumour medium (15% FBS in 1g/L low glucose DMEM). The plate was then incubated overnight to allow cell attachment in a standard incubator at 37 ºC and 5% CO_2. Once the cells had attached and reached 100% confluency, a scratch was made in each well using a yellow P200 tip followed by 3 washes with 500 µl HBSS to ensure that the dislodged cells did not reattach. 500 µl of tumour media was then added to each well. Cells were treated either with vehicle (DMSO), ABCB1 inhibitors [VPL (20 µM) or Vdfl (10 µM)] or PPAR antagonists [FH535, GW0660, GSK9662 at 15 µM each] or DHA (20 µM). Immediately after treating the cells, the plate was placed back into the incubator. In order to accurately identify the effect of ABCB1 and BLBP inhibition on cell migration, at least 3 independent experiments were performed each with internal triplicates.

Pictures were taken using a Cannon DS126431 camera every 4 hours for BXD-1425EPN or 8 for the DKFZ-EP1 cell line for over a 24 and 48 hour period which were their respective doubling times. This was done to ensure that the wound closure occurred as a result of migration and not proliferation. The ImageJ program was used for quantifying the cell migration response by measuring the approximate wound width at 3 random points for each image in order to determine the relative wound closure. It is designated to be zero at time zero and 100% when the wound had completely closed as a result of cell migration.

The data was exported into Microsoft Excel to calculate the percentage wound closure and GraphPad Prism Version 6.0 was used to plot the calculated percentage wound closure against time for various treatments. These response curves were then used to determine the T1/2 (time required for 50% increase in wound closure). The parametric unpaired student's t-test was used to establish any significant differences in the T1/2 values between treated and untreated (vehicle treated) conditions.

2.6 Invasion assay

In order to measure the effect of ABCB1 and BLBP inhibition on the invasive nature of ependymoma cell lines; a 3D spheroid invasion assay was performed. The assay was based on the ability of the cells to digest and invade through the basement membrane mimicking Cultrex™ basement membrane extract (BME-Trevigen) over a period of time. BME is a soluble form of basement membrane purified from Engelbreth-Holm-Swarm (EHS) tumour which gels at 37℃ when reconstituted in RPMI medium. Its major components include laminin, entactin, collagen-IV and heparin sulfate proteoglycan.

BXD-1425EPN cells were sub-cultured as in section 2.3.2 and 5,000 cells were plated in a 96-well ultra-low attachment (ULA) 96-well round bottom plates (Corning) in 100 µl tumour media. The plate was placed in a standard incubator at 37 ºC and 5% CO_2 for 3 days. On day 3, the cells were centrifuged at 100 g for 5 minutes in order for cells to come together to form spheroids by day 4.

The BME was diluted to 6 mg/ml (working stock) with cold TGA medium (1 % L-glutamine in phenol red-free RPMI-1640) and stored on ice. On day 4, the tumour medium was replaced with 2 mg/ml BME TGA medium (Sigma). This procedure was carried on a plate warmer heated to 37 ºC to facilitate BME polymerisation. Plates were transferred into a 5% CO_2 incubator (37 ºC) for approximately 1 hour before adding 50 µl of tumour medium overlay containing vehicle (DMSO), VPL (20 µM), Vdfl (10 µM), DHA (20 µM) and PPAR antagonists [FH535, GW0660, GSK9662 at

15 µM each] to wells. Immediately after treating the cells, the plate was placed into a standard incubator.

Images were taken daily for 4 days using a Cannon DS126431 camera at 40X magnification. Images were analysed using the ImageJ program. The relative wound outgrowth, (R) was calculated by taking the ratio of area of the invasive edge (A2) to the area the spheroid (A1) represented in Figure 2.1.The data were then analysed in Microsoft Excel and GraphPad Prism version 6.0 was used to plot differences in R at different time points. This method of analysis was used because R was self-normalised to decreasing area of the spheroid at each time point.

The parametric unpaired student's t-test was used to establish any significant differences in R between treated and untreated conditions.

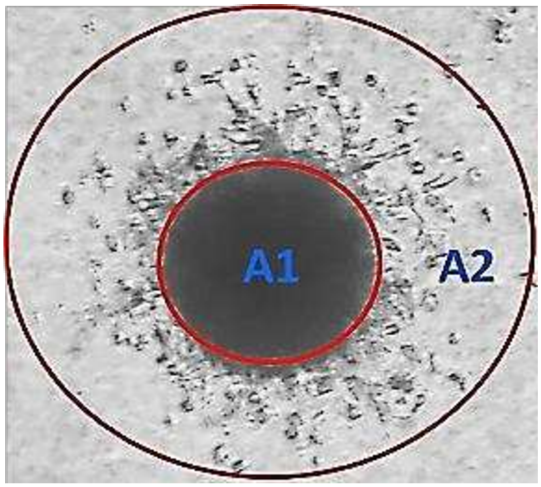


Figure 2.1 BXD-1425EPN spheroid invading through the basement membrane extract (BME) in a 3D invasion assay The relative spheroid outgrowth (R) was measured by computing the ratio of the area of the invasive edge (A2) to the area of the spheroid (A1).

Protein Based assays

2.7 Immunohistochemistry (IHC)

IHC refers to a method used to identify discrete tissue components by the interaction of target antigens with specific antibodies tagged with a visible label.

In this project, IHC was used to detect protein expression of ABCB1, BLBP and MGMT on control tissues initially to optimise each experiment and then on Tissue Micro-Arrays (TMAs) built from the two European paediatric ependymoma trial cohorts (CCLG 1992 04 / CNS9204 and SIOP Ependymoma I / CNS9904 - described in section 2.2). 5 µm thickness sections from paraffin embedded blocks of tissue or TMA were cut using a microtome and collected onto 3-aminopropyltriethixysilane (APES) coated slides. The sections were then de-paraffinised and rehydrated by immersion in decreasing concentrations of organic solvents (xylene, 100% ethanol and 95% ethanol) and then running tap water respectively. Details of various antigen retrieval techniques carried out for the different antibodies studied are provided in Table 2.5. To prevent non-specific background signal, slides were blocked with peroxidase blocking solution (Dako). The sections were then incubated with primary antibody (dilution and incubation time shown in Table 2.5) in a humidified chamber and for 1 hour with the horse radish peroxidase (HRP) tagged secondary antibody provided in the Dako kit. Slides were washed with PBS (phosphate buffered saline) in between steps, to get rid of excess antibody/ blocking solutions. The Dako Chemate Envision Antigen Detection kit (Dako, UK) was used to detect the attached primary antibody. Detection was carried out using 3,3'-diaminobenzidine (DAB) chromogen for visualisation according to the manufacturer's instructions (Dako).

Sections were counter-stained with haematoxylin and then treated with lithium carbonate until the nuclei turned blue. After a wash with water, sections were dehydrated with increasing concentrations of organic solvents (95% ethanol and 100% ethanol and xylene) before mounting with a coverslip using DPX (Distrene, Plasticiser, Xylene-Sigma).

Table 2.5 List of antibodies used for IHC

Primary antibody	Supplier	Species	Dilution	Antigen retrieval	Incubation conditions	Staining patterns	Positive control
ABCB1 (C219)	Calbiochem	Mouse	1:40	Pressure cooker	Overnight at 4℃	Membranous	Liver
BLBP (ABN14)	Millipore	Rabbit	1:500	Seamer	Room temperature, 1 hour	Nuclear and cytoplasmic	Foetal brain
MGMT (MAB16200)	Millipore	Mouse	1:50	Steamer	Overnight at 4℃	Nuclear	Tonsils

Images were obtained at a 40x magnification using the Olympus DP-25 light microscope and processed using the CellB version 2.5 Olympus Imaging Software.

2.8 Western blotting

Western blotting is a semi-quantitative method used to identify a specific amino acid sequence in proteins. It was used to detect MGMT, MLH1 and MSH6 protein expression in the cell lines. The house keeping protein glyceraldehyde 3-phosphate dehydrogenase (GAPDH) was used to check for equal loading of samples.

2.8.1 Protein lysate preparation

Protein lysates were prepared by incubating the cell pellets in 50-100 µl of lysis buffer (Appendix A1) depending on the size of the cell pellet. This was followed by incubation for 20 minutes on ice before being centrifuged for 30 minutes at 12,500 g at 4 ℃. The supernatant (protein lysate) was then transferred to a fresh eppendorf tube and stored at -80℃ for future analysis.

2.8.2 Protein quantification and sample preparation

A Bradford assay was used to determine the concentration of protein in the lysate sample by comparison to known concentrations of BSA (bovine serum albumin) determined using a spectrophotometer. BSA standards were prepared by adding 1, 5, 10, 15, 20, 30, 40 µl of a 1 µg/ml BSA stock to a 96 well plate and making each well up to 200 µl with 25 % v/v solution of the protein assay dye reagent (Coomassie Brilliant Blue G-250-Bio-Rad) in distilled water. A blank well, containing 200 µl of the dye reagent was used to correct the readings to any background signal. 2-5 µl of each lysate sample was added to separate wells and made up to 200 µl with dye. Both the standards and the samples were prepared in triplicates. The absorbance of the standards and samples was read using a FLUOstar plate reader (BMG labtech instruments) at a wavelength of 595nm and data was processed using the Omega software. The standard curve for increasing concentrations of BSA was plotted to obtain a linear equation in Microsoft

Excel. This equation (y = mx + c; m = slope, c = 0 since the line passed through the origin) was used to deduce the concentration of various lysates.

The required volumes of lysates were put into fresh eppendorf tubes with 20 % of sample buffer containing 1:20 β-mercaptoethanol. These were then heated at 95 ℃ for 5 minutes in order to break the tertiary and secondary structures of the protein and to ensure the uniform spread of negative charge across the linearised protein surface.

2.8.3 Gel electrophoresis

Gel electrophoresis was performed to separate the negatively charged proteins on the basis of size. The Mini-Protein III system (Bio-Rad) was used to prepare and run a SDS-PAGE gel. The gel cassette was prepared according to the manufacturer's instruction. After cleaning all glass plates with trigene, water and ethanol, short glass plates and larger 1.5 mm spacer plates were put into the glass plate casting frame which was clamped into the casting stand. Distilled water was added between the glass plates for 5-10 minutes to ensure lack of leakage.

4 ml of 10-15 % (depending on protein size) of lower gel (resolving gel) was prepared (Appendix A2) and immediately poured between the two glass plates to 2 cm below the top of the small glass plate. The gel was covered with a layer of 70 % ethanol to exclude any air and to ensure the gel surface was levelled and was then allowed to set for 1 hour. 2.5 ml of the upper gel (stacking gel) was prepared (Appendix A2) and added on top of the polymerised lower gel after absorbing the ethanol using a Whatmann filter paper. A 15 lane 1.5 mm comb (BioRad) was gently inserted into the stacking gel to create sample wells, and the gel was left to polymerise for 30 minutes. Once polymerised the wells were washed with electrode buffer (Appendix A1) using a syringe. The samples were loaded into the wells alongside 7.5 µl SeeBlue Plus2 marker (Novex) and were run at 140 V in a gel tank (BioRad) containing the electrode buffer for about 2 hours until the bromophenol blue dye had just run off the end.

Table 2.6 List of antibodies used in Western blotting

Primary antibody	Supplier	Species	Protein size (KDa)	Dilution	Incubation conditions
MLH1	BD Transduction Laboratories	Mouse	86	1:1000	Overnight at 4℃
MSH6	BD Transduction Laboratories	Mouse	160	1:2000	Overnight at 4℃
MGMT	Millipore	Mouse	19	1:50	Overnight at 4℃
GAPDH	Ambion	Mouse	36	1:1000	Room temperature, 1 hour

2.8.4 Transfer of proteins onto a membrane

A piece of Amersham Hybond P membrane (GE Healthcare) was cut which was the same size as the gel and was activated with methanol for 10 seconds followed by washes with water for 5 minutes, before placing in transfer buffer (Appendix 1) for 10 minutes. The upper gel was discarded and the lower gel was carefully detached from the glass plates and placed onto the membrane. Two pieces of filter paper and sponges were placed underneath and on top of the gel-membrane assembly. It was ensured that there were not any bubbles between the membrane and the gel as this would hinder the protein transfer. The whole assembly was placed into a blotting cassette, and then into a transfer tank (BioRad) filled with chilled transfer buffer and was run either overnight at 58 mA or for 2 hours at 200 mA at 10 °C.

2.8.5 Antibody treatment:

Following transfer the membrane was carefully removed from the cassette assembly and placed in 5% blocking solution [5% w/v Marvel milk powder in TBS-T (Appendix A1)] for an hour to block any non-specific antigens. After 2 X 5 minutes rinses with TBS-T, the membrane was probed with the primary antibody (details of incubation times are shown in Table 2.6) with gentle shaking on a rocker. This step was followed by 3 X 5 minutes washes with TBS-T to get rid of excess antibody and incubation for an hour in the appropriate HRP-conjugated secondary antibody (Cell Signalling), diluted 1 in 2000 in TBS-T. The excess secondary antibody was washed away with 3 X 5 minutes washes of TBS-T and 1 X 5 minutes wash of TBS (Appendix A1).

2.8.6 Enhanced chemiluminescence (ECL) detection:

The membrane was then placed on a piece of saran wrap and not allowed to dry out at any point. Equal volumes of luminol and enhancer solution (ECL kit, GE Healthcare) were mixed and immediately poured over the membrane and then left at room temperature for 5 minutes. The excess solution was dabbed off the membrane which was then wrapped in the saran wrap and placed into an x-ray cassette. In the dark room, a piece of

photographic film (Kodak bio-max) was laid over the membrane for varying exposure times depending on the intensity of the chemiluminiscent signal. The film was developed using the Ilford PQ developing solution (0.01 %v/v). The size markers were labelled on the film so as to confirm the detection of the correct protein and the membrane was saved in TBS-T at 10 ℃ for further use.

Gene based assays

2.9 RNA extraction

RNA extraction from cell pellets was performed using a mirVana kit (Ambion 1560) according to manufacturer's instructions. Cell pellets which were stored previously at -80 ˚C were suspended in the lysis/binding buffer and were vortexed so as to obtain a uniform homogenate. The miRNA Homogenate Additive was added to the cell lysates and this was then incubated on ice for 10 minutes. A 1:1 volume of acid: phenol chloroform was added to cell lysates, (this step was performed in the fume hood). After vortexing for 30-60 seconds, samples were centrifuged at 9400 g for 5 minutes to separate the solution into 3 phases; clear upper aqueous phase containing RNA, the middle protein phase and the lower phenol chloroform phase. The upper aqueous phase containing the RNA was collected into a fresh eppendorf tube without disrupting the middle or lower phases. This aqueous phase was topped up with 1.25 times its volume with 100 % ethanol in order to precipitate the RNA out of the solution. This solution was then passed through the column filter provided in the kit and centrifuged at 9400 g for 15 seconds. The eluate was discarded whilst the column which now had trapped the RNA was given several washes with 700 µl of miRNA Wash Solution 1 and 500 µl of Wash Solution 2/3 respectively. 100 µl of pre-heated (95 ˚C) RNase free water was then added to the column, centrifuged and the eluate containing the RNA was stored at -80 ˚C until further use.

2.9.1 DNase treatment

In order to reduce genomic DNA contamination, the RNA samples were treated with the DNAse enzyme. 2.4 µl RQ1 DNase (Promega), 2.8 µl RQ1 DNase buffer (Promega) and 2.8 µl depc H_2O (diethlypyrocarbonate water) were added to 20 µl of RNA solution, vortexed and incubated at 37 ˚C for 30 minutes. The DNase enzyme was then inactivated by adding 2.8 µl of RQ1 stop solution (Promega) and incubation at 65 ˚C for 10 minutes. The concentration and purity of RNA was determined using a NanoDrop 2000 spectrophotometer (Thermo Scientific).

Table 2.7 Reagents used in the first step of cDNA synthesis

Reagents	Amount added (µl)	Company
Random Primers	1	Invitrogen
Oligo dT (5 µM)	1	Eurofins, UK
dNTPs (5 mM)	1	Bioline
RNA	Equivalent to 1µg	
dH_2O	**14**	

2.10 cDNA synthesis

1 µg RNA was transferred into two PCR tubes, one labelled cDNA and one labelled nRT (no reverse transcriptase). All the contents added to both tubes in the first step of cDNA synthesis are mentioned in Table 2.7. The tubes were briefly vortexed, centrifuged and incubated at 65 ℃ for 5 minutes and on ice for 1 minute. 1 µl 0.1 M DTT (dithiothreitol, Invitrogen) and 4 µl 5 x Superscript III buffer (Invitrogen) were added to all tubes. 1 µl Superscript III (reverse transcriptase) (Invitrogen) was added to the cDNA tube and 1 µl depc dH_2O was added to the nRT tube. All tubes were heated to 25 ℃ for 5 minutes, then 42 ℃ for 45 minutes and finally 70 ℃ for 15

minutes in a thermocycler (Techne). The cDNA was then stored at -20 ºC until further analyses were carried out.

Polymerase Chain Reaction (PCR)

PCR is a method for amplifying a single or a few copies of DNA by synthesising a complementary strand to the provided template by employing the Taq DNA polymerase enzyme. The PCR process consists of 35-40 repetitions of cycles consisting of three main steps:

- The denaturation step involves heating up the samples to 95 ℃ to denature the double stranded DNA template into single strands.
- The annealing step is characterised by a reduction in temperature to 58-60 ℃ to allow the forward and reverse primers to attach to the DNA template.
- Finally during the elongation step, the Taq DNA polymerase synthesises the complementary DNA strand at 72 ℃, thus doubling the amount of DNA each time this procedure is completed.

Table 2.8 List of primers used in RT-PCR and QRT-PCR

Gene	Primers		Product size (bp)	Annealing temperature (℃)	Efficiency %	R2	Slope
ABCB1	Forward Primer (5' – 3') Reverse Primer (3' – 5')	CCCATCATTGCAATAGCAGG GTTCAAACTTCTGCTCCTGA	~150	60	91.6	0.97	3.54
BLBP	Forward Primer (5' – 3') Reverse Primer (3' – 5')	GTTGTTAGCCTGGATGGAGAC CATAGTGGCGAACAGCAAC	~150	58	99.4	0.71	3.337
C11orf95-RelA	Forward Primer (5' – 3') Reverse Primer (3' – 5')	CCTGCACCTGGACGACAT GCTGCTCAATGATCTCCACA	150-200	60	-	-	-
β-actin	Forward Primer (5' – 3') Reverse Primer (3' – 5')	TCTACAATGAGCTGCGTGTG ATCTCCTTCTGCATCCTGTC	600	60	-	-	-
GAPDH	Forward Primer (5' – 3') Reverse Primer (3' – 5')	ATGTTCGTCATGGGTGTGAA GTCTTCTGGGTGGCAGTGAT	~200	58-60	96	0.95	3.41

2.11 Reverse transcriptase-polymerase chain reaction (RT-PCR)

Standard RT-PCR was performed on cDNA prepared from all cell lines (as previously described in section 2.10) in order to investigate β-actin sequence (primer designed using the primer design tool (http://www.ensembl.org/index.html) and test for C11orf95-RELA fusion gene expression [Primers designed by Parker et al. (Parker, Mohankumar et al. 2014)]. To each tube 19 µl of master-mix was added (as described in Table 2.9). 1 µl of cDNA/nRT for each sample was added to individual tubes.

Table 2.9 RT-PCR master-mix recipe

Reagents	Amount added (µl)	Company
BioMix Red	10	Bioline,UK
Forward primer	0.4 µM	Eurofins,UK
Reverse Primer	0.4 µM	Eurofins, UK
Depc water	5	
Total	**19**	

The samples were run along with nRT (No Reverse Transcriptase control) to detect any genomic DNA contamination. A negative control containing depc water replacing cDNA (NTC- No Template Control) was used in each experiment to identify any contamination of PCR reagents. The RT-PCR reaction consisted of 40 cycles of 95 ℃ for 30 seconds (denaturation step), followed by 60 ℃ for 1 minute (annealing step) and finally then 72 ℃ for 1 minute (elongation) .

A gradient PCR reaction was performed on all newly designed primers to identify the optimal annealing temperature where a single bright band was produced when run on a 2% agarose gel by application of an

electric current as will be described in section 2.11.1. Sequences and annealing temperatures of all primers used in this project are summarised in Table 2.8.

2.11.1 PCR product analysis by agarose gel electrophoresis

This method separates negatively charged DNA molecules loaded on a 2 % agarose gel on the basis of their molecular weight by application of electric current. The amplified cDNA is then visualised under UV light using ethidium bromide that intercalates with double stranded DNA molecules. The size of the DNA molecule can be determined by comparing it to the DNA ladder run on the gel concomitantly.

4 µl of PCR product was mixed with 1 µl of loading dye (Biolabs) and loaded on a 2 % (w/v) agarose (Roche) gel containing 0.5 % (v/v) ethidium bromide (ThermoFisher Scientific). A 100 bp DNA ladder was used as the marker (Biolabs). The agarose gel was placed in a tank containing 1x TAE buffer (Tris-acetate-EDTA) and run at 150 V for 30-40 minutes. DNA bands were visualised and photographed using a GENEFLASH UV light machine (Syngene bio imaging).

The product obtained for the β-actin as well as the fusion gene PCR was sent for Sanger sequencing along with 3 µl of primer at the DNA sequencing lab at the University of Nottingham. The multi-alignment website (http://multalin.toulouse.inra.fr/multalin/cgi-bin/multalin.pl) was used to compare the gene cDNA sequence from each of the cell lines with human, mouse, and rat consensus sequences in the case of β-actin or with C11orf95 and RELA gene sequences to determine the fusion gene break point.

2.12 Quantitative reverse transcriptase-PCR (QRT-PCR)

This is based on the principle of a standard RT-PCR but also involves simultaneously quantifying the amplification of the target DNA by using non-specific double stranded DNA- binding fluorescent dyes such as SYBR green (used in this project) or specific DNA probes for the gene of interest attached to a fluorescent reporter.

2.12.1 Primer efficiency estimation

The efficiency of the primers used in this method is determined by the amount of product that is made following a given number of cycles and the rate at which the PCR reaction occurs. An efficiency of 100 % indicates that the target has doubled with each PCR cycle. Primer efficiencies between 90 and 110 % were considered satisfactory.

The ΔCt equation for quantification normalises the expression of the gene of interest with the internal control (GAPDH) used in this study. Unlike the Pfaffl equation which incorporates individual calculated primer efficiencies, the ΔCt equation assumes 100 % primer efficiency. However, in order to provide a more robust quantitative analysis, the primer efficiency was calculated to ensure it was between 90 and 110%.

To identify primer efficiency, serial dilution stocks of control cDNA (ratios 1: 0.5 : 0.25 : 0.125 : 0.625) were prepared for use. For each primer efficiency assessment, a PCR master-mix was prepared as described in Table 2.10.

Table 2.10 QRT PCR master-mix

Reagents	Amount added (µl)	Company
SYBR Green Supermix	12.5	Bio Rad, UK
Forward primer	0.4 µM (2.5 µl)	Eurofins, UK
Reverse Primer	0.4 µM (2.5 µl)	Eurofins, UK
Depc water	6.5	
Total	**24**	

24 µl of master-mix was aliquoted into wells of a 96-well PCR plate (Bio Rad). For each cDNA concentration, PCR reactions were performed in triplicate in order to minimise pipetting error. 1 µl cDNA was placed into three separate wells on the plate, with 1 µl of no reverse transcriptase (NRT) being added to another three wells as a control. In addition, 1 µl of double distilled water was added to another three wells as a no template control (NTC). The selected PCR program described in Table 2.11 incorporates each primer's optimal annealing temperature (Table 2.8) and a final melting curve reaction (Figure 2.3) for confirmation of product specificity. Each PCR reaction generated a Ct value which represents the number of cycles at which reaction fluorescence exceeds the background fluorescence threshold (Figure 2.2).

The efficiency of each primer set used in QRT-PCR was identified as shown in Table 2.8. As previously described, a primer was considered optimised if its efficiency was between 90%-110% and R^2 was greater than 0.95. Figures 2.3 and 2.4 represent an example of an melting curve and scatter plot of ABCB1 efficiency PCR.

Table 2.11 QRT- PCR program

No. of cycles	Duration	Temperature (℃)
1	5 min	95
	30 sec	95
40	1 min	Annealing temp 60
	45 sec	72
Melt Curve	Increments of 0.5 ^{o}C every 5 seconds	65 to 95

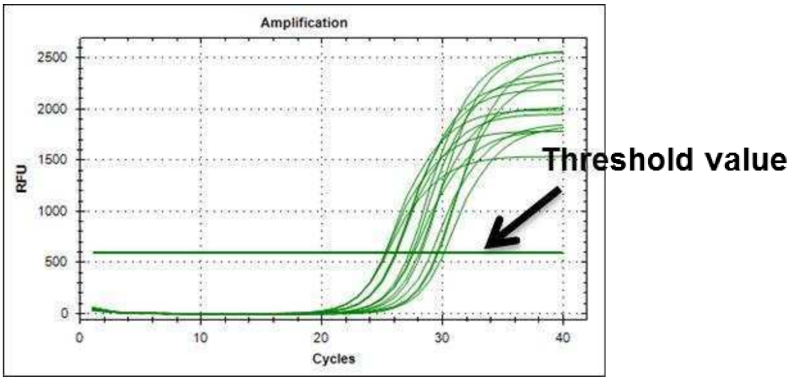


Figure 2.2 Amplification curve for ABCB1 gene generated by the CFX-96 real time system The results generated using the ABCB1 gene primer set on serial dilutions of control DNA are shown in the figure above. Each curve represents the amount of SYBR green fluorescence produced per PCR cycle for the PCR product made from each DNA concentration. The cycle threshold (Ct) value for each reaction is the value at which the SYBR fluorescence exceeds the fluorescence threshold value highlighted in the figure. RFU= relative fluorescence units

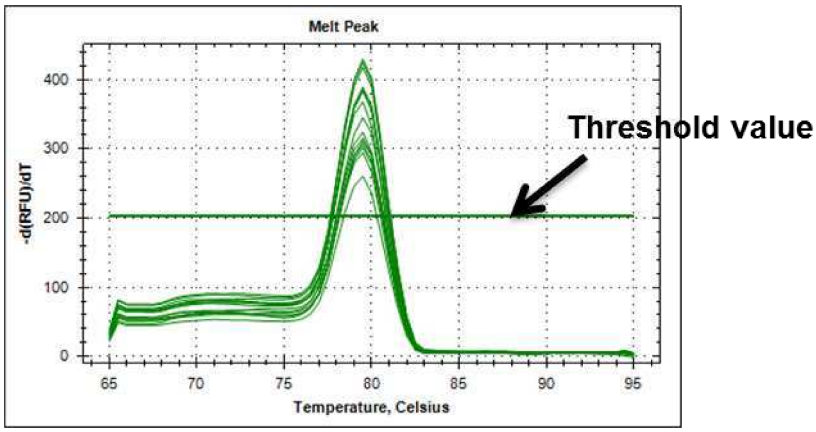


Figure 2.3 Melt curves for ABCB1 This curve is produced as a result of a reduction in the SYBR Green fluorescent signal as a result of DNA denaturation, with the gradual increase in temperature. The symmetrical curve of product peaks within short temperature range represents the ideal melting temperature at which the DNA was denatured and also shows lack of non-specific products or primer dimers. The melting curves produced from the optimisation of primer efficiency for the ABCB1 primers in the figure above depicts a major symmetrical melting temperature at ~79 ˚C, indicating a single specific ABCB1 amplicon. RFU= relative fluorescence units.

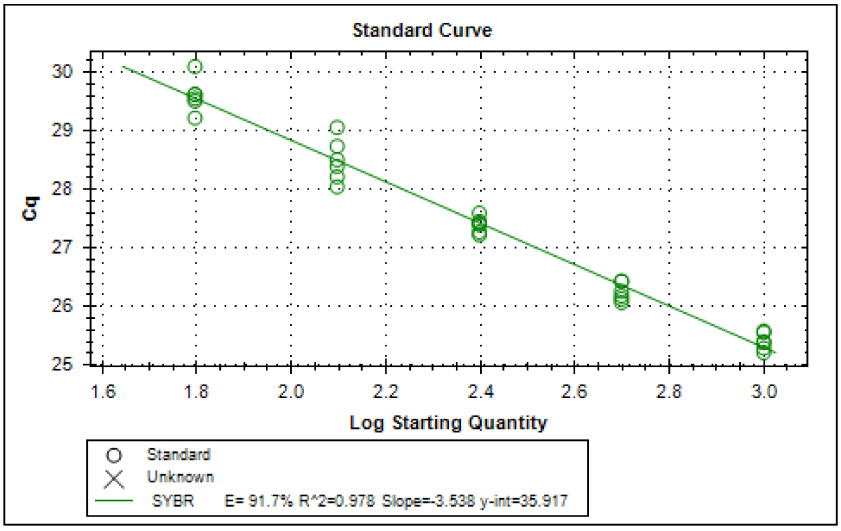


Figure 2.4 Scatter plot of the mean Ct values for the ABCB1 primers at serially diluted concentrations of DNA template The log of DNA concentration is plotted against the Ct values obtained for each reaction. Efficiency for the primers deduced from the standard curve represented above E=91.7 % and the slope recoded was -3.538. The goodness of fit measure (R^2) in this case was 0.978.

2.12.2 Quantitative reverse transcriptase PCR (QRT-PCR) for ABCB1 and BLBP

QRT-PCR was performed for target gene (ABCB1 and BLBP) and a house keeping control gene (GAPDH) on cDNA from 3 ependymoma derived cell lines. ABCB1 primers were designed and published by Valera et al., (Valera, Scrideli et al. 2004) whilst BLBP primers were designed using the primer design tool (http://www.ncbi.nlm.nih.gov/tools/primer-blast/). For the PCR, two master-mix solutions were prepared; one for the target gene and one for the housekeeping control gene (GAPDH) as previously described (Table 2.10). 24 µl/well of each master-mix was pipetted into a 96 well QRT-PCR plate (Bio-Rad). For inter-assay reproducibility three independent experiments were performed. Real time reactions were performed using the Bio Rad system with a PCR program (Table 2.11) at annealing temperature of each specific gene (Table 2.8).

2.12.3 Quantification of target gene amplification

The relative level of target gene expression (R) with respect to the GAPDH was calculated by the ΔCt method in Microsoft Excel by using equation below. These values were entered in Graphpad Prism Version 6.0 to produce column charts showing mean relative expression values along with standard errors bars.

$$\text{Relative expression level (R)} = 2^{-(Ct_{(target\ gene)} - Ct_{(GAPDH)})}$$

CHAPTER 3. CHARACTERISATION OF EPENDYMOMA CELL LINES

3.1 Introduction

Ependymomas are the 2nd most common malignant brain tumours in children and account for 9-12% cases (Ostrom, Gittleman et al. 2014). 90% of paediatric ependymomas occur intracranially with two-thirds arising from the PF and remaining one-third originating in the ST compartment (Kilday, Rahman et al. 2009). As mentioned in Chapter 1, chemoresistance (Atkinson, Shelat et al. 2011), invasion of critical structures (Godfraind, Kaczmarska et al. 2012, Phi, Wang et al. 2012) and tumour recurrence (Messahel, Ashley et al. 2009); are grave hurdles faced by clinicians in ependymoma treatment. It is hypothesised in this thesis that a sub-population of therapy resistant CSCs may contribute to this well-known aggressive behaviour of ependymoma. In order to understand the functional role played by these CSCs in ependymoma pathogenesis and progression in vitro models of the tumour, 5 ependymoma cells lines were employed in this study.

This chapter provides information regarding the doubling times, human origin, histological characteristics of the original patient tumours and expression of the aforementioned C11orf95-RELA fusion gene in all the ependymoma derived cell lines used in this study.

3.2 Results

3.2.1 Doubling times of all cell lines

To determine the growth of ependymoma cell lines when cultured as monolayers, the doubling time was determined. The average doubling times for cells cultured as monolayers for BXD-1425EPN, DKFZ-EP1, EPN1, EPN7 and EPN7R were 23 hours ± 1.23, 116.3 hours ± 9.83, 203.3 hours ± 3.33 and 205 hours ± 5 hours respectively.

The doubling time of DKFZ-EP1 cell line was found to be extremely variable in culture; therefore, all experiments on the cell line were preformed

between passages 5 to 10; when the doubling time was approximately 48 hours.

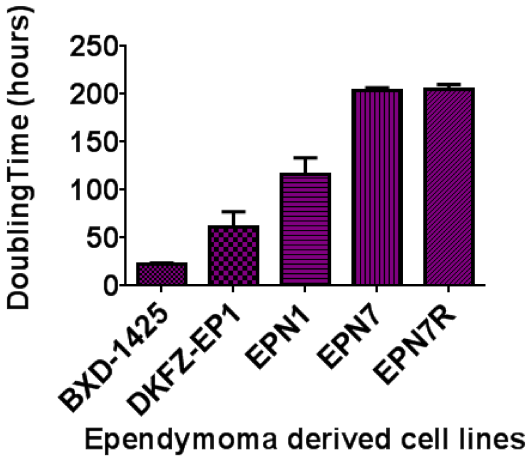


Figure 3.1 Doubling time of ependymoma cell lines The doubling time quantification was performed over ≥ 3 passages. The bar chart above shows the mean doubling times for all cell lines ± SEM.

3.2.2 All ependymoma cell lines used in this study were of human origin.

Due to several studies questioning the human origin of various established cell lines (Higgins, Steingrimsdottir et al. 2010); RT PCR followed by Sanger sequencing of the *β*-actin gene for all cell lines used in this study was performed, to confirm their human origin

The β-actin gene cDNA sequence from each of the cell lines was aligned with human, mouse, and rat consensus sequences using the multiple sequence alignment tool multalin (http://multalin.toulouse.inra.fr/multalin/cgi-bin/multalin.pl) to determine complementarity with one of the species. As depicted in Figure 3.2, sequences of the amplified *β*-actin gene matched entirely with the human sequence, confirming their human origin.

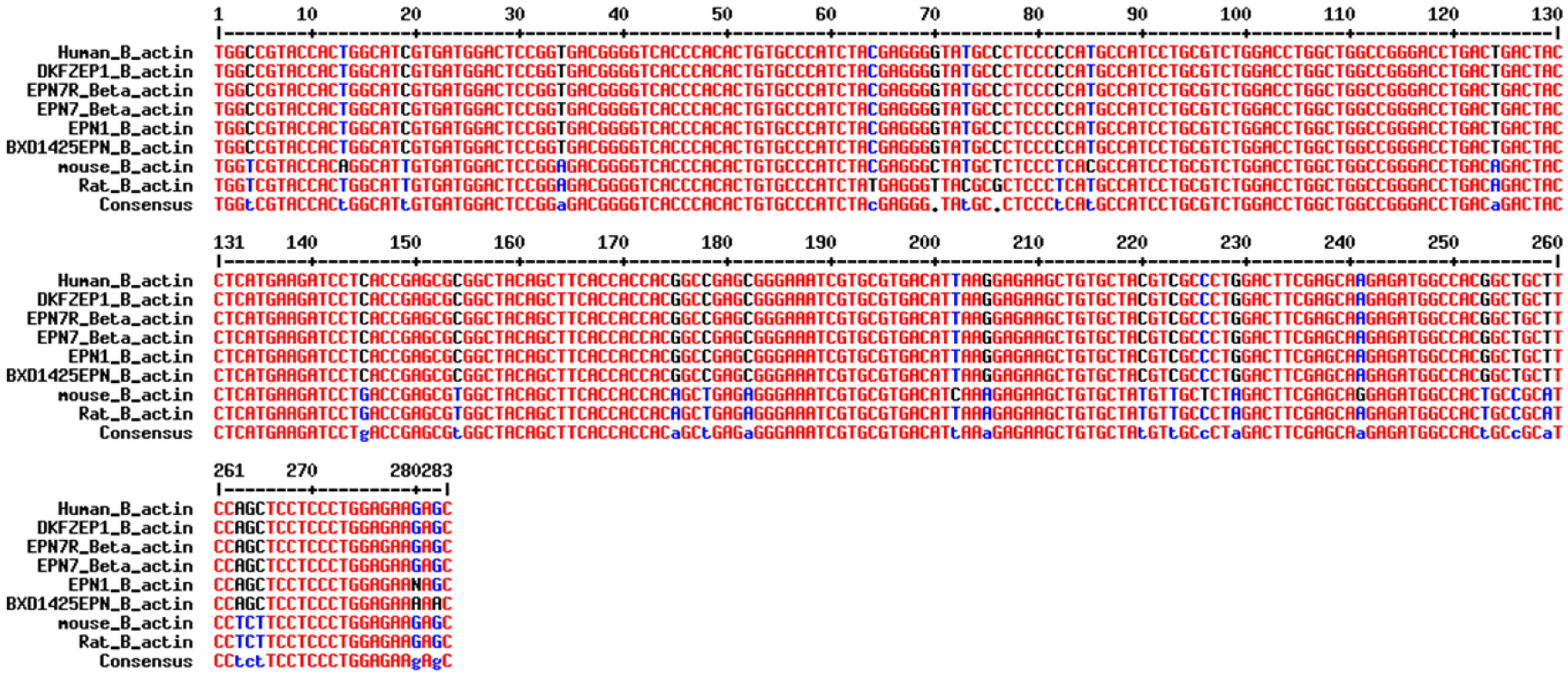


Figure 3.2 Alignment *β*-actin gene sequence for all cell lines with the human, rat and mouse sequences The β-actin gene cDNA sequence from each of the cell lines was aligned with human, mouse, and rat consensus sequences using the multiple sequence alignment tool multalin (http://multalin.toulouse.inra.fr/multalin/cgi-bin/multalin.pl) to determine complementarity with one of the species. As depicted in the figure above, β-actin gene sequence for all cell lines matched most with the human sequence, confirming their human origin.

3.2.3 Protein expression of ABCB1, BLBP and MGMT in the original patient tumours and the orthotopic tumour from which the EPN1 cell line was derived.

There have been several studies reporting the change in the expression profiles of cells maintained in culture over a period of time (Laurent, Ulitsky et al. 2011, Domcke, Sinha et al. 2013). Since the EPN1 cell line was established in-house; the protein expression of ABCB1, BLBP and MGMT was assessed in the original patient and orthotopic tumours (established from the second recurrence) from which the cell line was derived.

As depicted in Figure 3.3, ABCB1 was not expressed in the primary tumour, first and second recurrences as well the orthotopic tumour indicating the ABCB1 did not underlie chemoresistance in these tumours. However, the third recurrence expressed ABCB1 in a sub-population of cells, indicating that the powerful selection imposed by potent anti-cancer drugs resulted in overgrowth of drug-resistant clones.

In agreement with the CSC hypothesis, BLBP was expressed in a sub-population of cells in all the patient tumours as well as the orthotopic ependymoma sample. This was in support of the hypothesis that BLBP was a CSC marker in ependymomas.

Finally, due to high level of core loss, MGMT expression was only examined in the secondary patient tumour and orthotopic tumour. As depicted in Figure 3.3c, MGMT was not expressed in either section; indicating that it did not underlie chemoresistance in the EPN1 patient.

In following chapters, expression of the aforementioned markers will be assessed in the EPN1 cell line to establish its genotypic/ proteomic proximity to the patient samples from which it was derived.

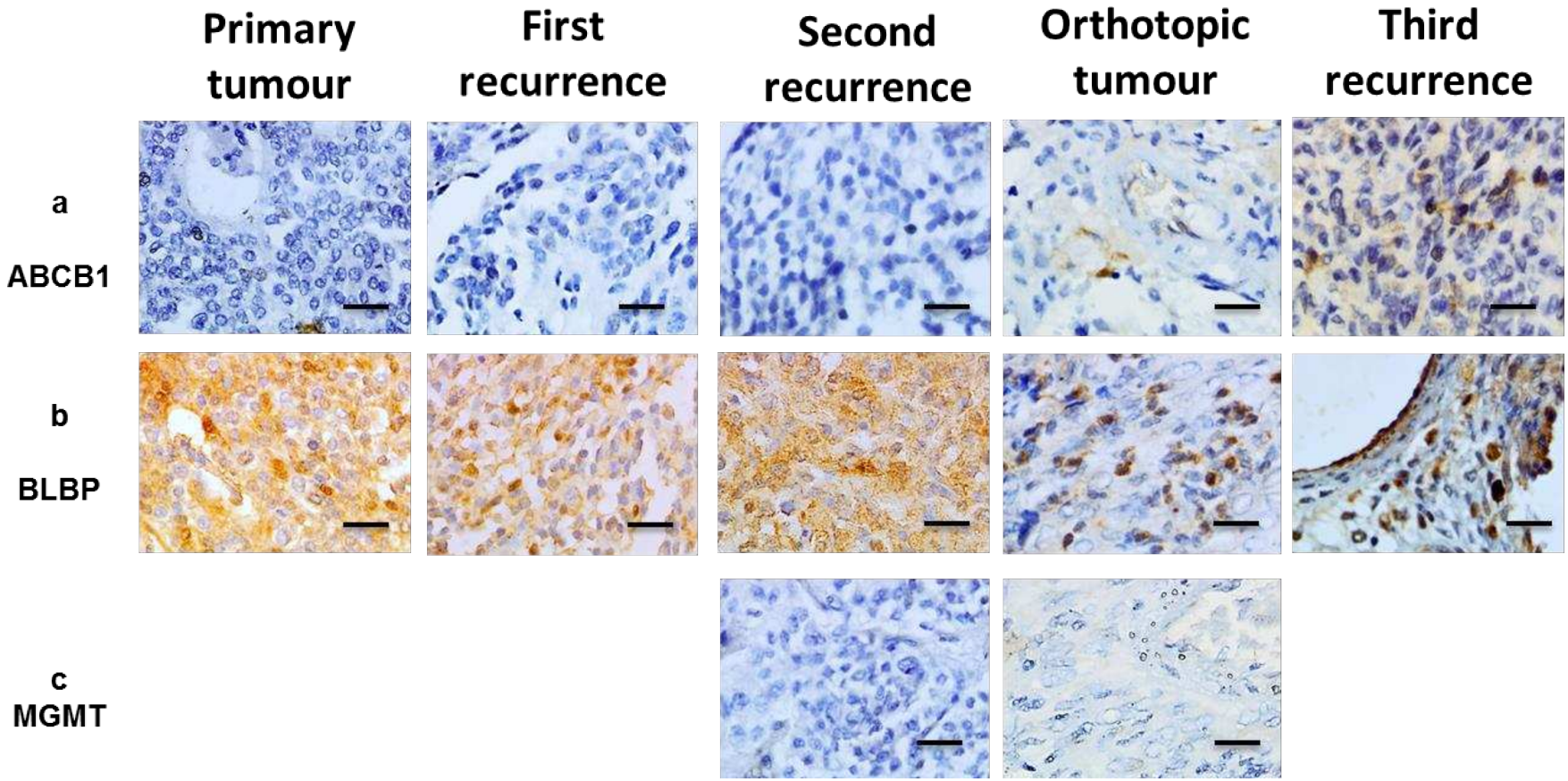


Figure 3.3 ABCB1, BLBP and MGMT expression in patient tumours and the orthotopic ependymoma from which the EPN1 cell line was derived a. ABCB1 was not expressed in the primary tumour and the first and second recurrences. The orthotopic tumour exhibited vascular staining of ABCB1 and the third recurrence showed a few ABCB1 positive cells. **b.** BLBP was expressed in a sub-population of cells in all tumour samples of the patient as well as orthotopic tumour**. c** Due to high level of TMA core loss, only the secondary and orthotopic ependymoma samples could be examined for MGMT expression. As depicted in the figures, both of them did not express MGMT. (Scale bars represent 25 µm)

3.2.4 C11orf95-RELA gene fusion was expressed in 3 out of 5 ST ependymoma derived cell lines.

After carrying out a RNA exome sequencing study, Parker et al. reported that as a result of chromothripsis involving chromosome 11q13.1, two-thirds of ST ependymomas expressed the C11orf95–RELA fusion. This gene was a fusion between C11orf95, a gene with unknown function, and v-rel avian reticuloendotheliosis viral oncogene homolog A (RELA), encoding the RELA p65 subunit of the central NF-κB complex. They also demonstrated that the fusion protein spontaneously translocated to the nucleus and was responsible for activating the NF-κB pathway in the neural stem cells; thus, transforming them and inducing tumorigenesis in mice (Parker, Mohankumar et al. 2014, Pietsch, Wohlers et al. 2014). Since all cell lines employed in this study were derived from ST ependymomas, expression of the aforementioned fusion gene was assessed.

As depicted in Figure 3.4, whilst BXD-1425EPN, DKFZ-EP1 and EPN1 expressed the fusion gene, EPN7 and EPN7R did not. Figure 3.5 depicts the sequence of the break point of the C11orf95 and RELA fusion product in the 3 aforementioned cell lines expressing the gene produced by Sanger sequencing. In spite of repeating the experiment several times, a clear sequence depicting the breakpoint for the fusion product in the EPN1 cell line was not obtained. However, since the cell line expressed the fusion protein (Appendix A4- western blot performed by Mr.Jasper Estranero); this indicated that the fusion gene was potentially retained in a sub-population of cells. This finding was consistent with the heterogeneous behaviour of EPN1 in culture.

These results indicated that owing to the expression of the fusion gene; 3/5 cell lines in this study harboured an active and oncogenic NF- κB pathway. As part of this thesis, an attempt has been made to indirectly target this pathway, in order to overcome chemoresistance and invasion in in vitro models of ependymoma.

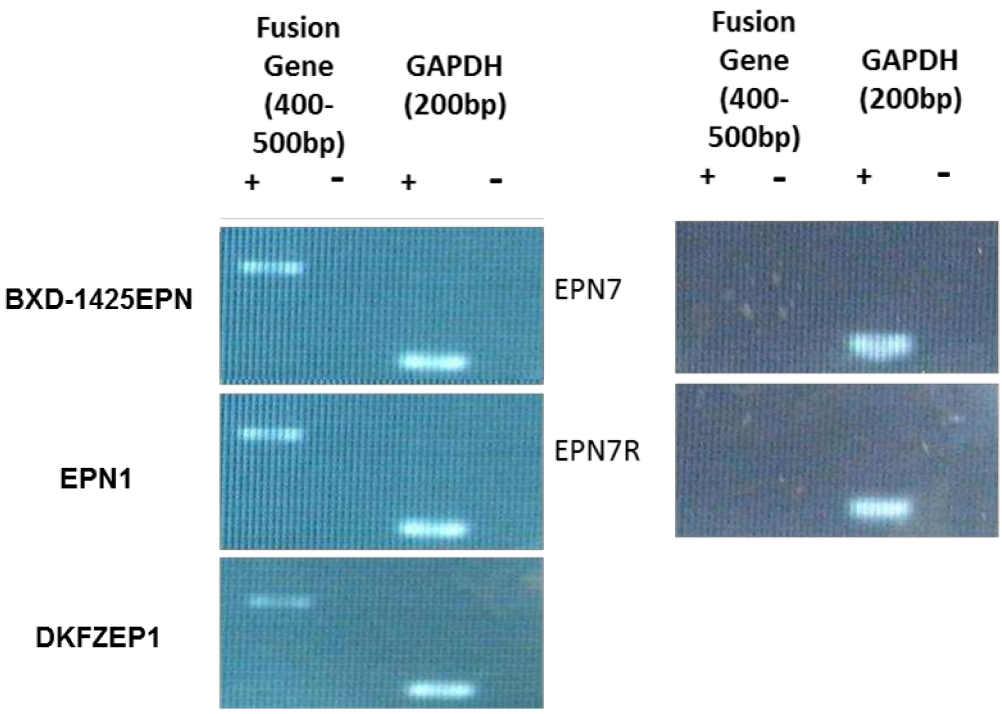


Figure 3.4 Expression of C11orf95-RELA fusion gene in ependymoma cell lines RT-PCR was performed to analyse the expression of the C11orf95-RELA fusion gene in the ependymoma cells used in this study. As depicted in the figure above showing the amplified cDNA products run on a 2 % w/v agarose gel; BXD-1425EPN, DKFZ-EP1 and EPN1 cell lines expressed the fusion gene; whilst EPN7 and EPN7R did not. Housekeeping gene GAPDH was run in parallel as an internal control whilst performing the experiment.

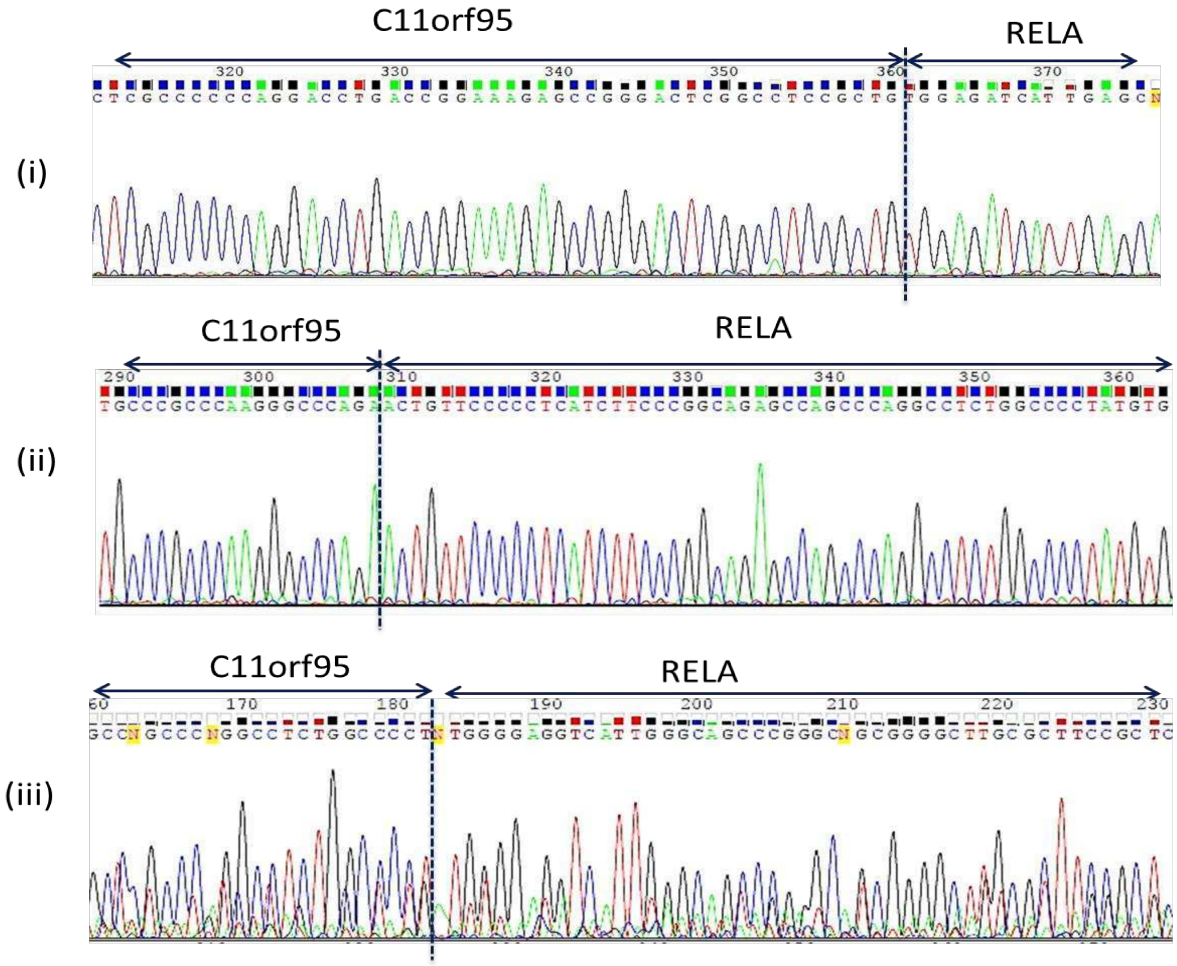


Figure 3.5 Break-points of the C11orf95-RELA fusion gene sequences in ependymoma cell lines Amplified cDNA of the fusion gene from the BXD-1425EPN, DKFZ-EP1 and EPN1 cell lines were sequenced using Sanger sequencing to produce chromatograms. **(i)** The BXD-1425EPN and **(ii)** the DKFZ-EP1 showed fusion gene break points in their cDNA sequences at nucleotides 361 and 309 respectively. **(iii)** In the EPN1 cell line, although the breakpoint was recorded at nucleotide 182, the sequence was quite complex and unclear. This potentially indicated that the fusion was retained only in a sub-population of cells.

3.3 Summary

- Paediatric ependymoma cell lines used in this study were of human origin

- BLBP was expressed in the original patient and orthotopic tumours from which the EPN1 cell line was derived. In contrast, ABCB1 was only expressed at the 3rd recurrence whilst MGMT was not expressed in either the second recurrence or the orthotopic tumour.

- 3/5 of the ST ependymoma derived cell lines used in this study expressed the C11orf95-RELA fusion gene.

CHAPTER 4. MULTIDRUG TRANSPORTER ABCB1: ITS ROLE IN PROGNOSIS, DRUG-RESISTANCE AND METASTASIS OF EPENDYMOMA

4.1 Introduction

In spite of recent advances in multimodality treatments available to ependymoma patients; 10-year survival still stands at a disappointing 64%. Conventional treatment available to patients includes gross total resection (GTR) followed by adjuvant focal radiotherapy (Merchant, Li et al. 2009). Chemotherapy is employed in a number of trial protocols as adjuvant treatment to avoid or delay radiotherapy in the case of patients less than 3 years of age. However, there is very little evidence regarding the survival benefit of chemotherapy to patients and as a result ependymomas are regarded as chemoresistant tumours (Bouffet, Perilongo et al. 1998, Geyer, Sposto et al. 2005, Merchant and Fouladi 2005, Atkinson, Shelat et al. 2011).

There is increasing evidence that a sub-population of therapy resistant cancer stem cells (CSCs) underlies the recurrent and drug-resistant nature of tumours. Brain tumour CSCs have been shown to exhibit chemoresistance (Hussein, Punjaruk et al. 2011, Milde, Kleber et al. 2011) and radioresistance (Singh, Clarke et al. 2003, Bao, Wu et al. 2006) in several studies. Previous lab data showed that when 34 patient samples from the chemotherapy led CCLG 1992 94 (CNS9204) trial (consisting of ependymoma patients less than 3 years of age) were screened for the stem cell marker CD133, 96 % tumours were found to stain positive with median percentage of positive cells per sample at 1.67 %; (range 0.33-14.67%) (Coyle, Kessler et al. 2015). Tumours which were positive for multi-drug transporter ABCB1 (0.28 % cells) frequently co-expressed CD133 (0.21 % cells); suggesting that these drug resistant cells are a subset of CSC population in ependymoma. Since four of the drugs currently used as a part of ependymoma adjuvant chemotherapeutic regimens are ABCB1 substrates (etoposide, vincristine, methotrexate and irinotecan) (Szakacs,

Paterson et al. 2006, Wright and Gajjar 2012); it was proposed in this study that ABCB1 may play a key role in the chemoresistant nature of ependymoma.

Currently, only one 3rd generation ABCB1 inhibitor, tariquidar is being tested in an on-going phase III paediatric brain tumour clinical trial, in addition to few other solid tumours in children (www.clinicaltrials.gov; NCT00020514). Issues still remain, however, regarding the therapeutic efficacy of agents in this generation (Palmeira, Sousa et al. 2012). Therefore, as part of this study, a translationally relevant ABCB1 inhibitor was employed which could easily be repurposed for treatment of paediatric ependymomas. Vardenafil (Figure 4.1) is a phosphodiesterase type-5 (PDE5) inhibitor, and is a widely used, Food and Drug Administration (FDA)-approved treatment for erectile dysfunction in men and pulmonary hypertension in children (Jing, Yu et al. 2011). It competitively inhibits cyclic guanosine monophosphate (cGMP) hydrolysis by PDE5, thereby increasing cGMP accumulation and relaxation of vascular smooth muscle (Zhu and Strada 2007). Unlike its congener sildenafil which has been demonstrated to inhibit both ABCB1 and ABCG2 (Shi, Tiwari et al. 2011); vardenafil is a specific ABCB1 inhibitor (Ding, Tiwari et al. 2011). In a study by Yin et al., it was shown to not only increase the BBB permeability but also enhance delivery of drugs such as Adriamycin to primary brain tumours (Black, Yin et al. 2008). In addition, in a recent publication by Othman et al., ABCB1 inhibition by vardenafil potentiated response to etoposide in an in vitro model of medulloblastoma (Othman, Kimishi et al. 2014). Since, it is already used in the clinic to treat children, vardenafil shows good promise in being repurposed to target chemoresistance in ependymoma in children.

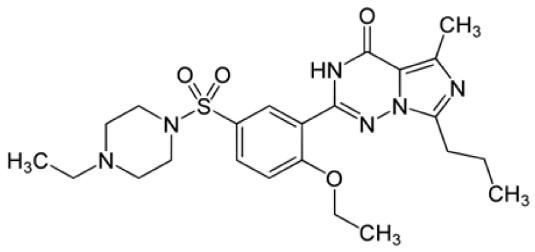


Figure 4.1 Chemical structure of vardenafil This figure was adapted from (Chrysant, 2013)

In this chapter, the expression as well as the prognostic role of ABCB1 in paediatric ependymoma patients is investigated. Furthermore, ABCB1 gene expression and its potential role in drug-resistance, migration and invasion in ependymoma derived cell lines is also examined.

4.2 Results

4.2.1 Higher ABCB1 gene expression was observed in paediatric in comparison to adult ependymomas.

Paediatric ependymomas are known to be inherently chemoresistant tumours with a paucity in the number of studies conveying the survival benefit to patients from adjuvant chemotherapy (Bouffet and Foreman 1999). It is hypothesised in this study that a sub-population of ABCB1 expressing CSCs may underlie this behaviour.

In order to assess if ABCB1 was expressed in paediatric ependymoma patients, retrospective analyses of gene expression data from 3 publicly available paediatric ependymoma datasets were performed. These were the Gilbertson dataset [Affymetrix U133 Plusv2 microarray, n=83, (Johnson, Wright et al. 2010)], the Witt dataset [Agilent two colour 4x44K Microarray, n=75, (Witt, Mack et al. 2011)] and the Mack dataset [Affymetrix Exon 1.0ST Array, n=102, (Witt, Mack et al. 2011)]. Whilst the Witt and the Mack datasets were published as part of the same study; they represent 2 independent cohorts of ependymoma patients from hospitals in Heidelberg and Toronto respectively. All this data were downloaded from the r2: Genomics Analysis and Visualization Platform (http://r2.amc.nl) and analysed using IBM, SPSS Version 2.

In the Gilbertson (Figure 4.2 a) and Witt (Figure 4.2 b) datasets, ABCB1 expression was significantly higher in paediatric patients in comparison to adults (Spearman correlation co-efficient= -0.238, P=0.03 and Spearman correlation co-efficient=-0.236, P=0.045 respectively); whilst in the Mack dataset (Figure 4.2 c), no significant association with age was recorded (Spearman correlation co-efficient=-0.139, P=0.164). Therefore,

drug efflux by ABCB1 may be one of the factors contributing to the chemoresistant behaviour of paediatric ependymoma.

.

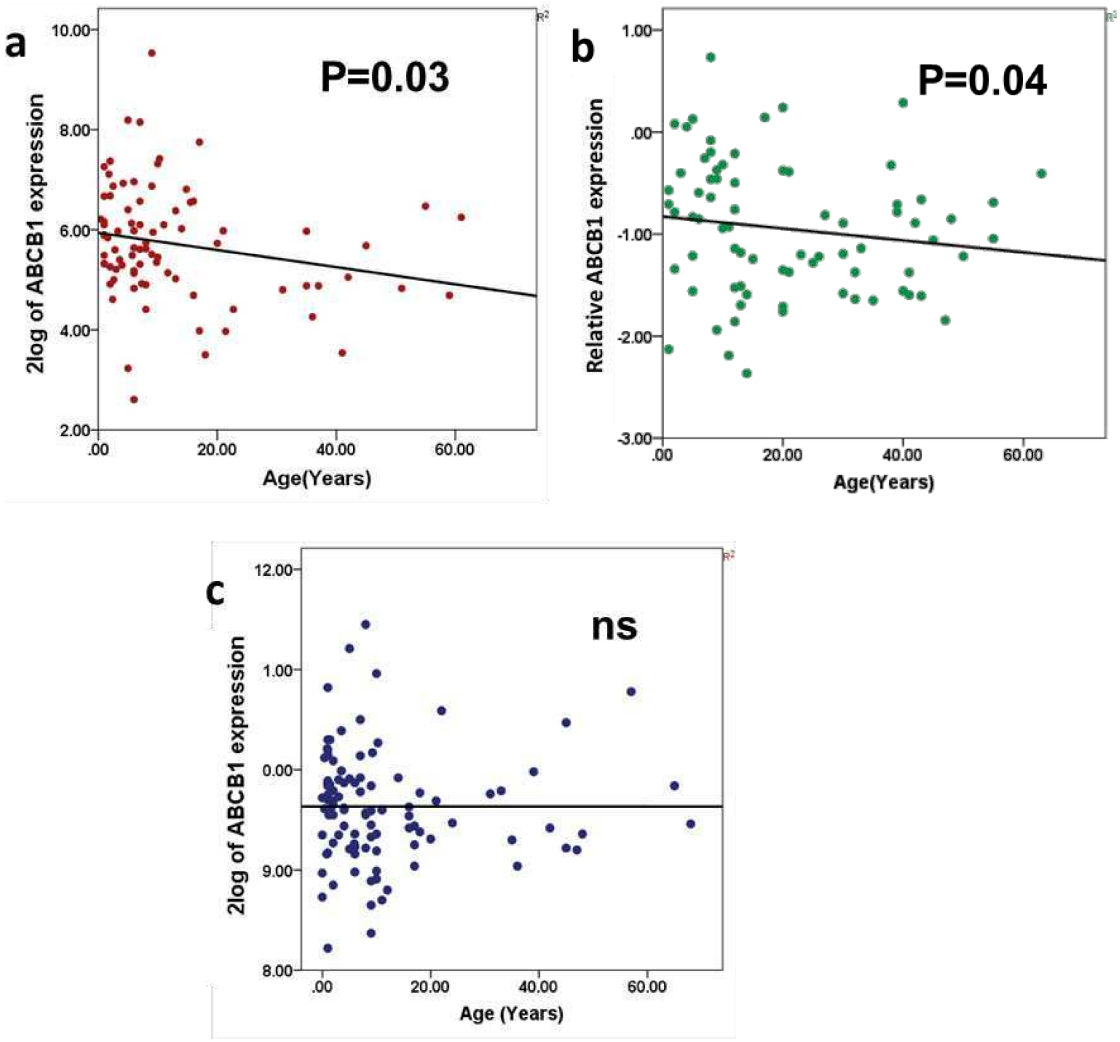


Figure 4.2 ABCB1 gene expression in ependymoma patients across 3 trial ependymoma cohorts ABCB1 expression was significantly higher in children in comparison to adults **in a.** the Gilbertson dataset (Spearman correlation co-efficient=-0.238, P=0.03) and **b.** the Witt dataset (Spearman correlation co-efficient=-0.236, P=0.045). In the **c.** Mack dataset, although ABCB1 was expressed in children; there was no significant association between its expression and patient age (Spearman correlation co-efficient=-0.139, P=0.16).

4.2.2 ABCB1 gene expression was the highest in ST ependymoma.

Several studies have demonstrated that ependymomas recapitulate location specific expression profiles (Johnson, Wright et al. 2010, Pajtler, Witt et al. 2015). It was therefore assessed in this study if ABCB1 was differentially expressed across the 3 ependymoma locations [Posterior Fossa (PF), Spinal (SP) and Supratentorial (ST)] in the aforementioned gene expression datasets.

As depicted in the box-plots in Figure 4.3, ABCB1 expression was significantly higher in ST tumours in comparison to PF and SP tumours in the Gilbertson dataset [a, ST vs. PF, Mean difference (MD) in the ABCB1 expression= 0.57 (95% Confidence Interval (95%CI) = 0.02 to 1.13) and ST vs. SP, MD = 1.27 (95% CI = 0.62 to 1.92)], the Witt dataset [b, ST vs. PF, MD = 0.63 (95%CI =- 0.33 to 0.93) and ST vs. SP, MD = 0.74 (95% CI = 0.28 to 1.19)] as well as the Mack dataset [c, ST vs. PF, MD = 0.55 (95%CI = 0.09 to 1.01) and ST vs. SP, MD = 0.71 (95% CI = 0.08 to 1.34)].

These results indicated that ABCB1 may represent a resistance mechanism mainly viable in ependymomas originating in the ST compartment which account for one-third of intracranial ependymomas in children and are correlated with a poor prognosis in a subset of patients (Kilday, Rahman et al. 2009, Parker, Mohankumar et al. 2014, Pajtler, Witt et al. 2015). Further in vitro as well as in vivo analyses are necessary to support this finding.

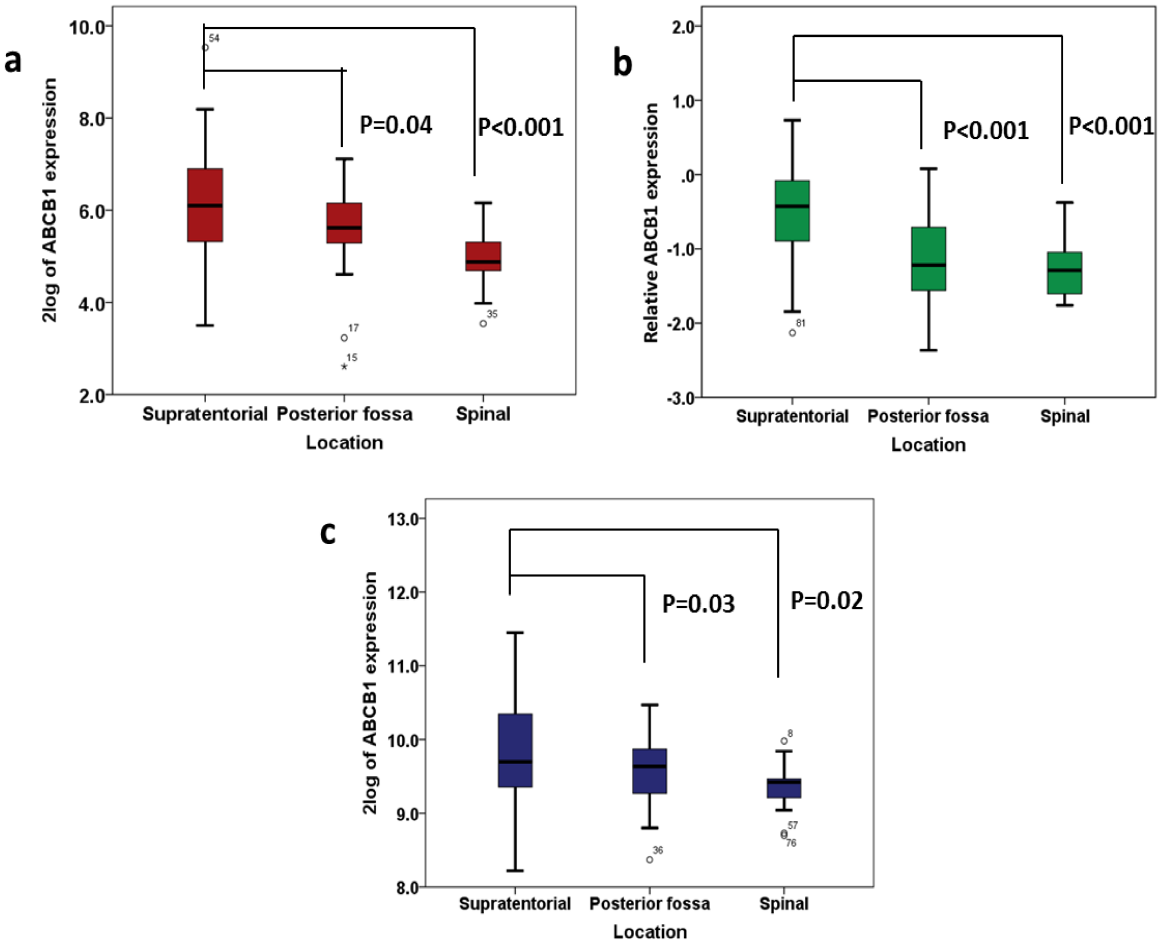


Figure 4.3 ABCB1 expression was the highest in supratentorial ependymoma ABCB1 expression was significantly higher in tumours occurring in in the ST region in comparison to PF and SP ependymomas in each of the **a.** Gilbertson, **b.** Witt and **c.** Mack datasets. The points plotted in the figures outside the box-whisker plots represented patient id numbers of outliers highlighted by the SPSS program.

4.2.3 ABCB1 protein expression was independently associated with reduced survival in the chemotherapy–led CNS9204 trial.

A number of studies so far have subdivided ependymoma on the basis of their gene expression and methylation profiles into clinically relevant groups (Witt, Mack et al. 2011, Wani, Armstrong et al. 2012, Pajtler, Witt et al. 2015). Since gene expression does not necessarily mean function, and histological techniques provide a better resolution in terms of tumour heterogeneity. Therefore, there needs to be a combination of molecular techniques along with conventional histological techniques to form a robust system of clinically stratifying ependymoma.

In this part of the study, the prognostic value of ABCB1 in the CCLG 1992 04 (CNS9204) trial cohort was investigated. This cohort consisted of paediatric ependymoma patients who received adjuvant chemotherapy following surgery in an attempt to delay/ avoid radiotherapy.

When these samples were stained for ABCB1 expression using immunohistochemistry (IHC), 28.3% (15/53) patients were found to be ABCB1 positive. Only a sub-population of cells per positive sample [always in less than 3% of cells (median 0.33%)] showed membranous ABCB1 staining (Figure 4.4 a); which is why samples were scored as a binary variable (positive or negative). This pattern of expression was consistent with the CSC hypothesis. Samples which showed only vascular ABCB1 staining were scored as negative.

When the expression was analysed in IBM SPSS, Version 21 for co-relation with survival, ABCB1 positive patients had a significantly lower event free survival (5-year EFS: 13% versus 50%, P=0.007) and overall survival (5-year OS: 33% versus 74%, p<0.009).

Since the majority of patients in this trial were diagnosed with ependymomas originating in the PF compartment, an association between ABCB1 expression and ST tumours could not be established. Patients with SP ependymomas were not a part of this study. There was no significant

correlation of ABCB1 expression with gender, resection status and histological grade of the tumour.

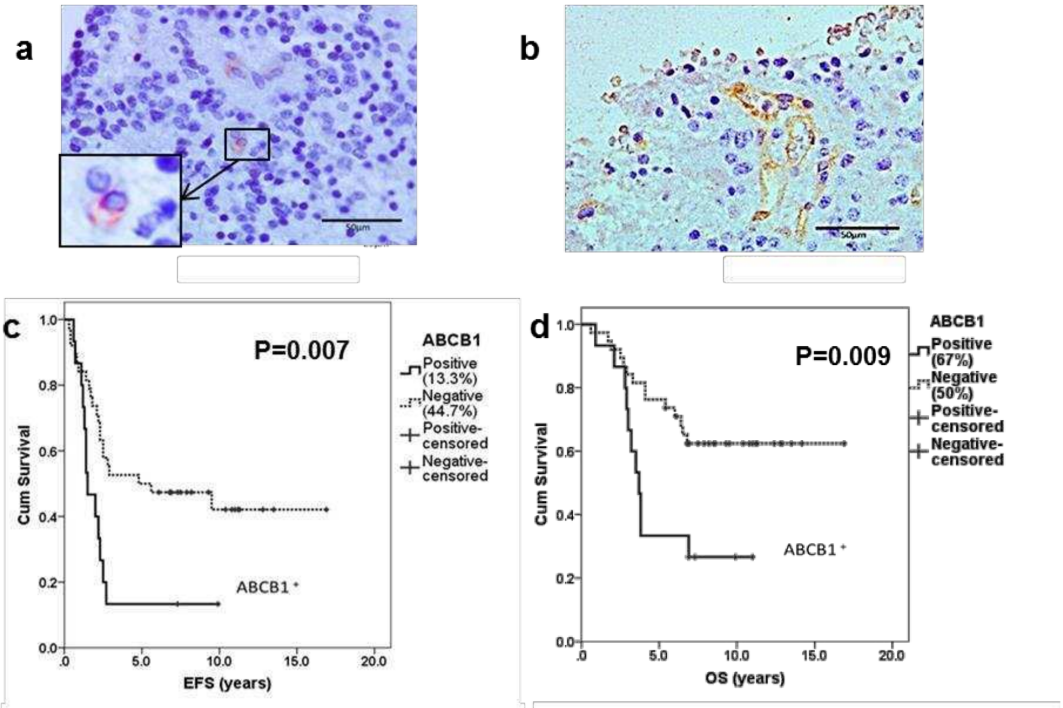


Figure 4.4 Membranous expression of ABCB1 was associated with poor survival in the chemotherapy-led CNS9204 cohort a. ABCB1 positive paediatric ependymoma samples showed membranous ABCB1 staining (boxed and magnified) whilst **b.** samples with non-specific vascular positivity were stained as ABCB1 negative. (Scale bars represent 50µm) ABCB1 positive patients from the chemotherapy-led (CNS9204) trial had a significantly reduced **c.** event-free survival (5-year EFS: 13% vs. 50%, P = 0.007) and **d.** overall survival (5-year OS: 33% vs. 74%, P = 0.009) respectively.

The feasibility of ABCB1 as an independent prognostic marker was tested using a Cox-regression multivariate model. The confounding factors included in this model were:

- Complete surgical resection, currently the most robust clinical marker of favourable prognosis in ependymoma patients (Merchant, Li et al. 2009).
- Tumour location, patients with posterior fossa tumours have the worst prognosis (Dyer, Prebble et al. 2002).
- WHO grade, although this remains a questionable marker of prognosis owing to the intra-tumoral histological heterogeneity in ependymoma (Ellison, Kocak et al. 2011).

After being corrected for the aforementioned confounding factors in the Cox-multivariate hazards ratio model, ABCB1 positive patients were almost 2.7 times more susceptible to having an event (relapse or death) (P=0.008) and 2.6 times more likely to die (P=0.021) in comparison to those who were ABCB1 negative (Table 4.1). This data implied that ABCB1 was indeed an independent histological marker of poor prognosis in the chemotherapy-led CNS9204 trial cohort.

Table 4.1 Multivariate analysis of ABCB1 expression in the chemotherapy-led CNS9204 trial

Survival	Factor	Hazard Ratio (95% CI)	P value
Event-Free Survival (EFS)	**ABCB1 expression (Positive vs. Negative)**	**2.70 (1.29-5.66)**	**0.008**
	Location (PF vs. ST)	3.37 (0.80-14.16)	0.09
	Resection (Incomplete vs. Complete)	1.32 (0.66-2.66)	0.42
	WHO Grade (Grade III Vs. Grade II)	1.23 (0.54-2.8)	0.06
Overall Survival (OS)	**ABCB1 expression (Positive vs. Negative)**	**2.57 (1.15-5.74)**	**0.02**
	Location (PF vs. ST)	5.85 (0.00-1.75E28)	0.96
	Resection (Incomplete vs. Complete)	1.11 (0.50-2.43)	0.79
	WHO Grade (Grade III vs. Grade II)	1.18 (0.58-2.44)	0.63

* 95% CI- 95% Confidence Interval

4.2.4 ABCB1 expression could not predict survival in the radiotherapy-led CNS9904 trial.

In order to assess the prognostic value of ABCB1 in older paediatric patients who received adjuvant radiotherapy following surgery; samples from the radiotherapy-led SIOP Ependymoma I (CNS9904) trial were stained for ABCB1 expression using IHC.

In this trial cohort, 37.5% (12/32) were ABCB1 positive. As depicted in the Kaplan–Meier survival curves in Figure 4.5, ABCB1 expression did not significantly correlate with reduced event-free survival (a, 5-year EFS: 54% versus 57%, P=0.57) and overall survival (b, 5-year OS: 36% versus 36.8%, P=0.86). Furthermore, there was no significant correlation of ABCB1 expression with gender, location, resection status and histological grade.

These findings indicated that ABCB1 was not of prognostic value in the radiotherapy-led CNS9904 trial. Effect of ABCB1 was only seen in the chemotherapy-led (CNS9204) trial, further supporting its role in chemoresistance in paediatric ependymomas.

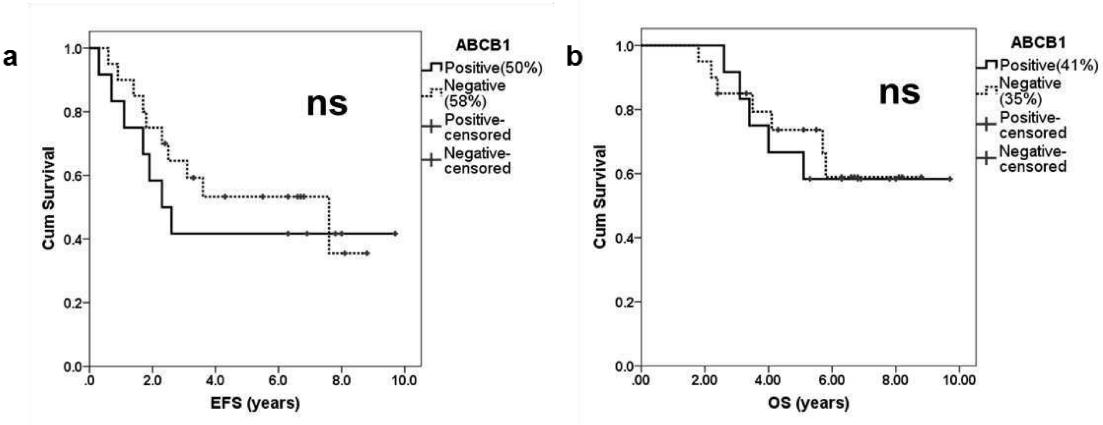


Figure 4.5 ABCB1 could not predict survival in the radiotherapy-led CNS9904 trial 37.5 % patients in the radiotherapy-led CNS9904 trial were ABCB1 positive. There was no significant association between ABCB1 expression and reduced **a.** EFS (5-year EFS: 54% versus 57%, P=0.58) as well as **b.** OS (5-year OS: 36% versus 36.8% P=0.86) in this trial.

4.2.5 ABCB1 was expressed in 4 out of 5 paediatric ependymoma derived cell lines.

To elucidate the functional role of ABCB1 in the pathogenesis and progression of ependymoma in an in vitro system, 5 paediatric ependymoma cell lines were assessed for ABCB1 expression by QRT-PCR analysis. Due to paucity of PF cell lines available, all cell lines tested in this study were of ST origin.

4 out of 5 ST paediatric ependymoma derived cell lines tested positive for ABCB1 gene expression. As demonstrated before in Chapter 3, Section 3.2.3, ABCB1 was not expressed in the original patient tumour as well as the murine orthotopic tumour from which the EPN1 cell line was derived. This status consistent with the lack of ABCB1 expression in the EPN1 cell line maintained in culture, as depicted in Figure 4.6.

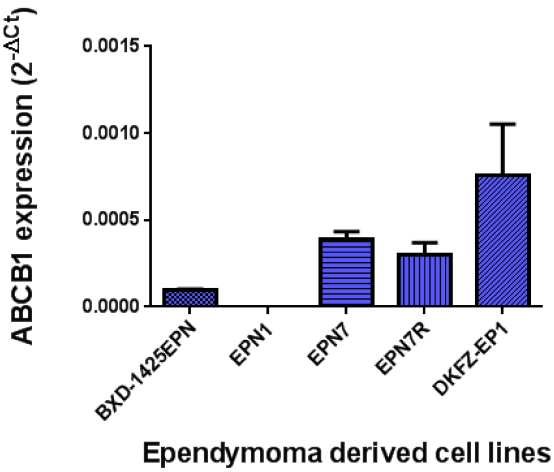


Figure 4.6 ABCB1 was expressed in 4 out of 5 ependymoma cell lines QRT-PCR was performed to assess ABCB1 expression in the ependymoma cell lines. ABCB1 gene expression in all cell lines was corrected for the expression of internal control, GAPDH by the ΔCt method. 4 out 5 paediatric ependymoma cell lines expressed varying levels of ABCB1. (n≥3)

The EPN7R cell line was derived from the recurrent tumour of the EPN7 patient. This data is consistent with the retrospective analysis of the publicly available Hoffman study which used the Affymetrix HG-U133 Plus 2 GeneChip microarrays (Affymetrix, Santa Clara, CA) to compare the transcriptomic profiles of 14 primary-recurrent ependymoma pairs (Hoffman,

Donson et al. 2014). As depicted in the Figure 4.7, ABCB1 gene expression was maintained at recurrence in 14 primary-recurrent paediatric ependymoma pairs.

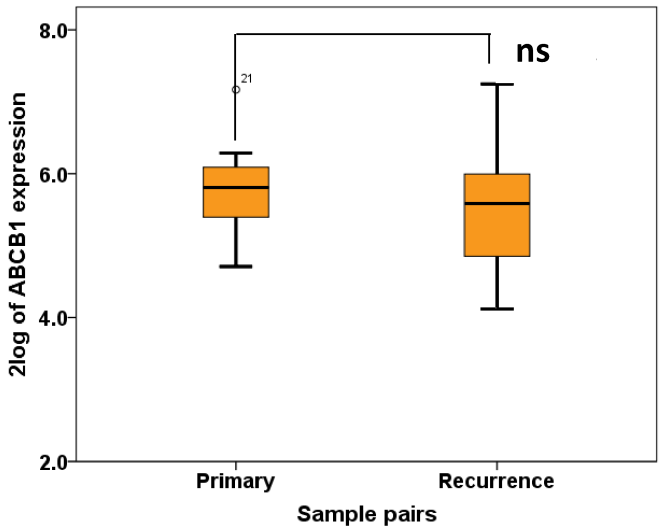


Figure 4.7 ABCB1 gene expression was maintained at recurrence in the Hoffman dataset Analysis of the publicly available Hoffman study showed that there was no significant difference in ABCB1 expression between primary and recurrent ependymoma samples [Mean difference: 0.216 (95%CI: -0.25 to 0.693), Paired t-test P=0.34].

The high ABCB1 expressing ($ABCB1^{hi}$) DKFZ-EP1 cell line and the low expressing ($ABCB1^{lo}$) BXD-1425EPN cell lines were used for further functional analyses. Since the EPN1, EPN7 and EPN7R grew very slowly in culture and were difficult to work with, they were excluded from further experiments.

4.2.6 ABCB1 expression was enriched in stem cell enriched neurospheres.

Previous lab data have shown that enriching medulloblastoma cells for stemness by growing them as neurospheres, significantly elevated corresponding ABCB1 levels (Personal communication – Dr. Beth Coyle). Since ABCB1 is one of the drug transporters which mediates classical multi-drug resistance, a hallmark of CSCs (Kroetz, Pauli-Magnus et al. 2003), it

was thus proposed that there would be an increase in ABCB1 expression when ependymoma cells were enriched for stemness.

In order to support the argument that ABCB1 was a CSC feature; the DKFZ-EP1 cell line was grown as neurospheres in stem cell media (Chapter 2, section 2.3.6) supplemented with growth factors. When assessed by QRT-PCR analysis, there was a concomitant 3 fold increase in ABCB1 expression (P=0.01) as depicted in Figure 4.8. Since the BXD-1425EPN and EPN1 cell lines could not form neurospheres, this result could not be confirmed in any other cell lines.

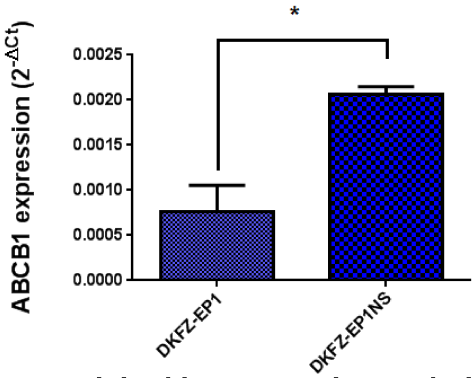


Figure 4.8 ABCB1 was enriched in neurospheres derived from the DKFZ-EP1 cell line An approximate 3 fold increase in ABCB1 expression (P=0.01) was observed when the DKFZEP1 cell line was enriched for stemness by growing it as neurospheres (DKFZ-EP1NS) in stem cell media. (n≥3)

4.2.7 ABCB1 inhibition potentiated response to chemotherapy in the ABCB1^{lo} BXD1425EPN cell line in a stem cell relevant clonogenic assay.

In order to assess the role of ABCB1 in drug resistance in paediatric ependymoma, a clonogenic assay was performed on the ABCB1^{lo} BXD-1425EPN cell line. The clonogenic assay is a CSC relevant assay since it is based on the ability of a single cell to form a colony. Single cells from the ABCB1^{lo} BXD-1425EPN cell line were treated with three chemotherapeutic drugs; methotrexate, vincristine and etoposide in combination with the specific ABCB1 inhibitor, vardenafil (10 µM) and the non-specific ABCB1 inhibitor, verapamil (20 µM) respectively.

As seen in the dose response curves depicted in Figure 4.9 a, BXD-1425EPN responded to both vincristine and methotrexate in a nano-molar range. Notably, a significant potentiation in response to both chemotherapeutics was recorded when combined with both ABCB1 inhibitors. (Figure 4.9 b and c respectively).

However, the BXD-1425EPN cell line was quite resistant to etoposide showing a response in the micro-molar range. The IC_{50} for etoposide established was 19.2 µM (SEM±0.08 µM) which is 10 fold higher than the plasma concentrations (~2 µM) achieved in patients following intravenous administration (Sonnichsen, Ribeiro et al. 1995). After combination with both verapamil and vardenafil (at non-toxic concentrations), there was a two-fold potentiation in response depicted by reduction in IC_{50} values (Figure 4.9 d) which was still 4 fold higher (by ~8 µM each) than the clinically achievable peak plasma concentration. (Independent t-test P=0.01 and P=0.006 respectively). This data confirmed that ABCB1 expression was one of the prime factors underlying chemoresistance in the BXD-1425EPN cell line.

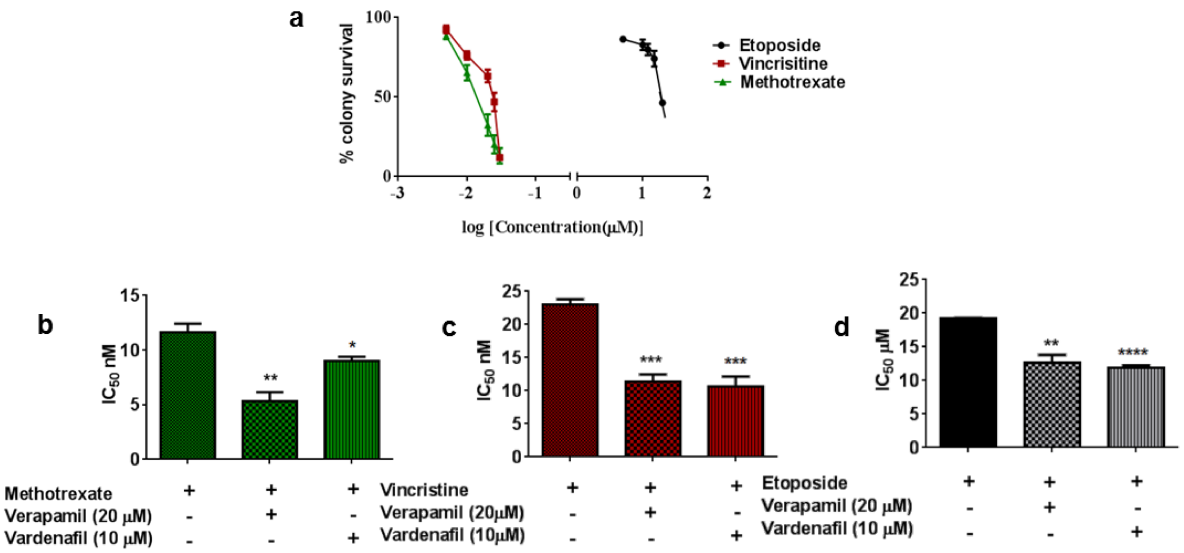


Figure 4.9 ABCB1 inhibition potentiated response to chemotherapy in ABCB1^{lo} ependymoma cell line a. Cytotoxic response of the ABCB1^{lo} BXD-1425EPN cell line to chemotherapeutic drugs methotrexate, vincristine and etoposide was assessed by the stem cell relevant clonogenic assay to produce dose response curves. There was a significant potentiation of cytotoxic response to **b.** methotrexate, **c.** vincristine and **d.** etoposide respectively; represented by reduction in the IC_{50} concentrations of drugs when combined with either, the non-specific ABCB1 inhibitor verapamil (20 µM) and specific ABCB1 inhibitor, vardenafil (10 µM).

4.2.8 ABCB1 inhibition potentiated response to chemotherapy in the ABCB1^{lo} BXD-1425EPN cell line by the MTT assay.

So far it was demonstrated in this study that ABCB1 may be one of the mechanisms underlying chemoresistance in the CSC sub-population of the BXD-1425EPN cell line. In order to assess the potentiation of response to chemotherapy in the entire cell population, an MTT viability assay was carried out. Similar to the clonogenic assay, the BXD-1425EPN cell line responded to vincristine and methotrexate in a nano-molar range, whilst the IC_{50} to etoposide was recorded at a concentration 30 times above the peak plasma levels achieved in patients (IC_{50}~60 µM-depicted in Figure 4.10 a). It was proposed that this behaviour may due to more than one resistance mechanisms to etoposide activated in these heterogeneous ependymoma cells (Discussed in detail in Chapter 1, Section 1.3.4.3.1).

Similar to the results achieved in the clonognenic assay (Section 4.2.7), there was a significant potentiation in response to all 3 drugs recorded once they were combined with both ABCB1 inhibitors depicted in Figure 4.10 b, c and d. These results further confirmed the hypothesis that ABCB1 may be one of the prime mechanisms contributing to chemoresistance in ABCB1^{lo} BXD-1425EPN cell line.

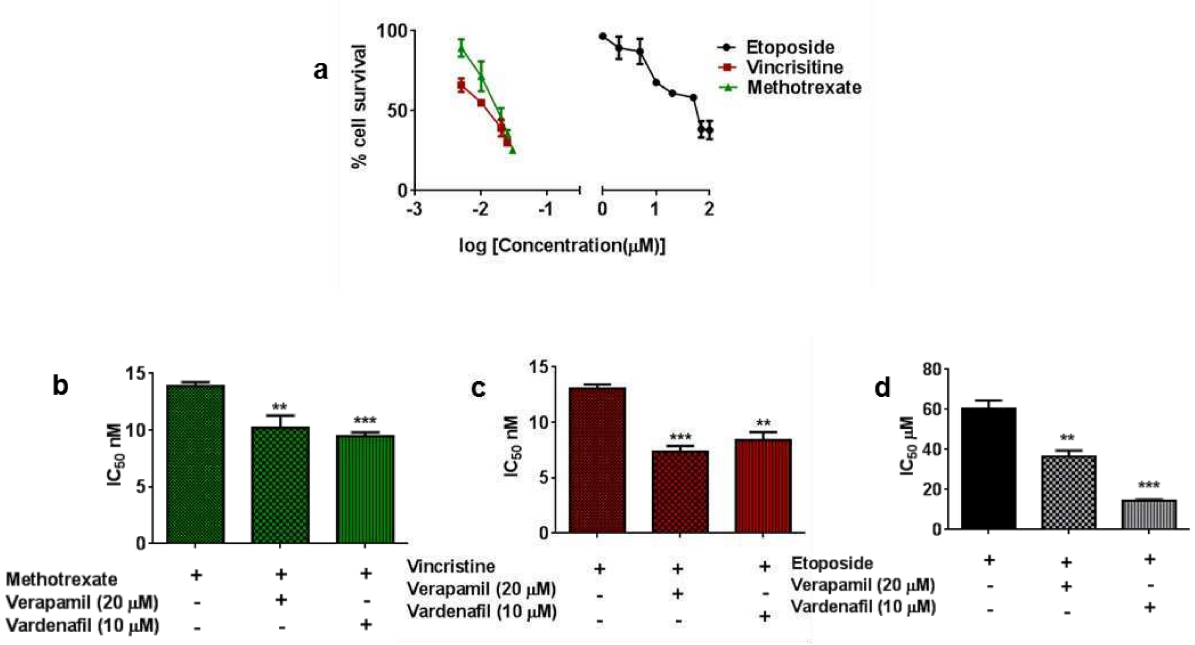


Figure 4.10 ABCB1 inhibition potentiated response to chemotherapy in ABCB1^{lo} BXD-1425EPN cell line by the MTT assay a. Cytotoxic response in the tumour bulk population of the ABCB1^{lo} BXD-1425EPN cell line to chemotherapeutic drugs methotrexate, vincristine and etoposide was measured by the MTT assay to produce the dose response curves. There was a significant potentiation of cytotoxic response depicted by reduction in the IC_{50} concentrations of **b.** methotrexate, **c.** vincristine and **d**. etoposide when combined with either, the non-specific ABCB1 inhibitor verapamil (20 μM) and specific ABCB1 inhibitor, vardenafil (10 μM). (n≥3)

4.2.9 ABCB1 inhibition could not potentiate response to chemotherapy in the ABCB1^{hi} DKFZ-EP1 cell line by the MTT assay.

Since the ABCB1^{hi} DKFZ-EP1 cell line did not form colonies, cytotoxic response to chemotherapeutic drugs was measured by the MTT assay only. It was seen that these cells were resistant to each of the three drugs over quite a wide concentration range and much above the clinically achievable peak plasma concentrations as depicted in Figure 4.11. Similar results were reported by Milde et al. who demonstrated that neurospheres derived from the DKFZ-EP1 cell line exhibited resistance to an array of conventional chemotherapeutic drugs including vincristine, temozolomide

as well as cisplatin but responded to a novel HDAC (histone deacetylase) inhibitor, vorinostat (Milde, Kleber et al. 2011).

Combination with the non-specific ABCB1 Inhibitor verapamil marginally potentiated response to methotrexate (P=0.041) at clinically unachievable concentration. However, this effect was more statistically than being biologically relevant. Combination with the specific ABCB1 inhibitor vardenafil did not potentiate response to any of the three drugs. Therefore, chemoresistance in the DKFZ-EP1 cell line may be a consequence of various other drug specific resistance mechanisms in addition to drug extrusion by ABCB1 (Discussed in detail in Chapter 1, Section 1.2.4.3).

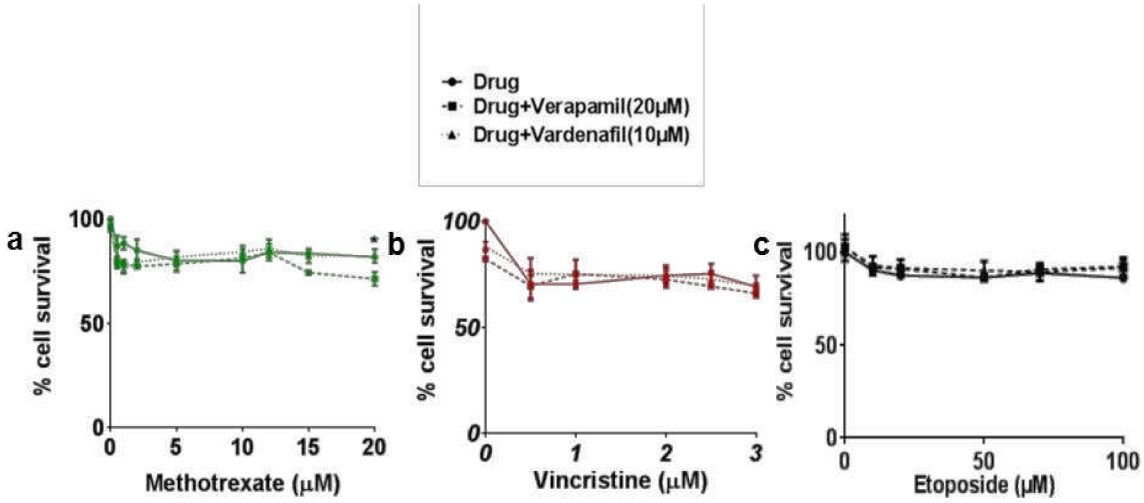


Figure 4.11 Chemoresistance in ABCB1^{hi} DKFZ-EP1 cell line Since the ABCB1^{hi} DKFZ-EP1 cell line did not form colonies; cytotoxic response to the chemotherapeutic drugs was assessed by the MTT assay. It was seen that the cell line exhibited resistance to **a.** methotrexate, **b.** vincristine and **c.** etoposide with the IC_{50} not being achieved over a wide concentration range; there was a marginal potentiation of response methotrexate (P=0.041) at clinically unachievable concentration of 20 μM when combined with verapamil (20 μM) whilst no potentiation was recorded with vardenafil (10 μM).This effect was however, more mathematically than biologically relevant. (n≥4)

4.2.10 ABCB1 inhibition reduced migration in the ependymoma cell lines.

Extra-neural metastases are rare in ependymomas accounting for only 5-10% cases; although there are several reports of these tumours spreading to the lung, liver mediastinum and muscle at recurrence z(Alzahrani, Alassiri et al. 2014, Pachella, Kamiya-Matsuoka et al. 2015, Severino, Consales et al. 2015). Ependymomas, however, tend to migrate and invade surrounding critical structures such as the brain stem, making the acquisition of complete surgical resection difficult. Ependymoma invasion has therefore been regarded as a clinical marker of poor prognosis by several studies, especially in ST ependymomas with sub-total resection (Akay, Izci et al. 2004, Godfraind, Kaczmarska et al. 2012, Phi, Wang et al. 2012). In parallel to this, several studies have also reported a possible role of ABCB1 in tumour migration and invasion in numerous cancers (Miletti-Gonzalez, Chen et al. 2005, Colone, Calcabrini et al. 2008). It was therefore assessed, if ABCB1 contributed to the invasive and migratory behaviour of ependymoma.

Both the $ABCB1^{lo}$ BXD-1425EPN and the $ABCB1^{hi}$ DKFZ-EP1 cell lines were established from aggressive WHO Grade III anaplastic ependymomas (Clinicopathological details, Chapter 2; Section 2.2). Furthermore, the DKFZ-EP1 cell line was derived from malignant ascites in the peritoneal cavity which is an indication of the ability of the cells to invade and metastasise (Milde, Kleber et al. 2011). When a 2D wound healing assay was carried out, both verapamil and vardenafil significantly reduced the rate of migration in either $ABCB1^{lo}$ BXD-1425EPN and the $ABCB1^{hi}$ DKFZ-EP1 cell lines depicted by the rightward shift in the response curves [Figure 4.12 a (ii) and b (ii) respectively] as well as reduction in the relative T1/2s (time required for the wound closure to increase by 50 %) [Figure 4.12 a (iii) and b (iii) respectively]. The assay was carried out for 24 hours and 48 hours for the BXD-1425EPN cell line (Doubling time=~24 hours) and DKFZ-EP1 cell line (Doubling time=~48 hours) respectively, to ensure that wound closed as a result of cell migration and not proliferation. It is

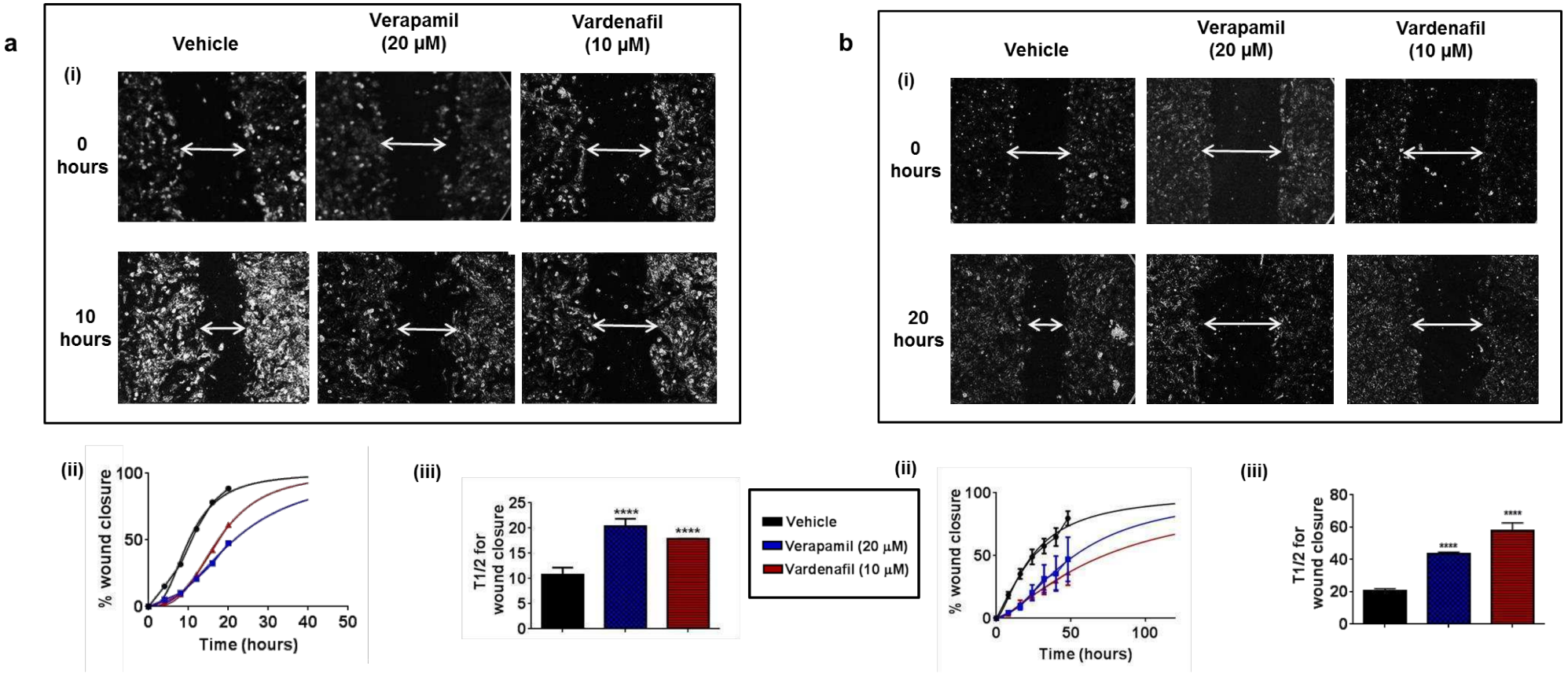


Figure 4.12 ABCB1 inhibition diminished migration in ependymoma cell lines A wound healing assay was performed to assess the effect of ABCB1 inhibition on migratory nature of ependymoma cells. When treated with non-specific ABCB1 inhibitor, verapamil (blue, 20 µM) and specific ABCB1 inhibitor vardenafil (red, 10 µM), there was a significant reduction the rate of migration in the **a (i)** ABCB1^{lo} BXD-1425EPN and **b (i)** ABCB1^{hi} DKFZ-EP1 cell line, depicted by the right ward shift in their respective response curves [**a (ii)** & **b (ii)** respectively] as well as significant reduction in their T1/2s [time required for 50% increase in wound closure, depicted **in a (iii)** and **b (iii)** respectively]. (n=3)

essential to highlight that in the ABCB1^{hi} DKFZ-EP1 cell line, the T1/2 for wound closure by vardenafil was derived from substantial extrapolation of the response curves [Figure 4.12 b (ii)]. However, to maintain consistency in the methodology used to analyse all scratch assays in this thesis; a different technique wasn't employed. These results indicated that ABCB1 expression contributed to the migratory nature of ependymomas; and both verapamil as well as vardenafil could target this behaviour at non-toxic concentrations.

4.2.11 ABCB1 inhibition reduced invasion in the ABCB1^{lo} BXD-1425EPN cell line.

As mentioned before, brain stem invasion has been regarded as a marker of poor survival in paediatric ependymoma since it prevents achieving total resection which is currently the primary treatment for ependymoma (Akay, Izci et al. 2004, Godfraind, Kaczmarska et al. 2012, Phi, Wang et al. 2012). In order to assess the role of ABCB1 in this invasive ependymoma behaviour; a 3D invasion assay was performed in which spheroids from the ABCB1^{lo} BXD-1425EPN cell line were grown in the Cultrex^{TM} Basement Membrane Extract (BME) which mimics the 3D tumour microenvironment, thus promoting cell invasion.

The spheroids displayed a distinct individual patterns of invasion, represented by single cell budding through formation of invadopodia and multicellular streaming, when introduced in the BME (Figure 4.13 a, vehicle treated condition). When this experiment was carried out in presence of ABCB1 inhibitors, verapamil and vardenafil (at non-toxic concentrations), there was a significant reduction in invasion (depicted in Figure 4.13 a), represented by a substantial reduction in the relative spheroid outgrowth (R = area of invasive edge / area of spheroid, Figure 4.13 b) at each of the 4 time points over 96 hours.

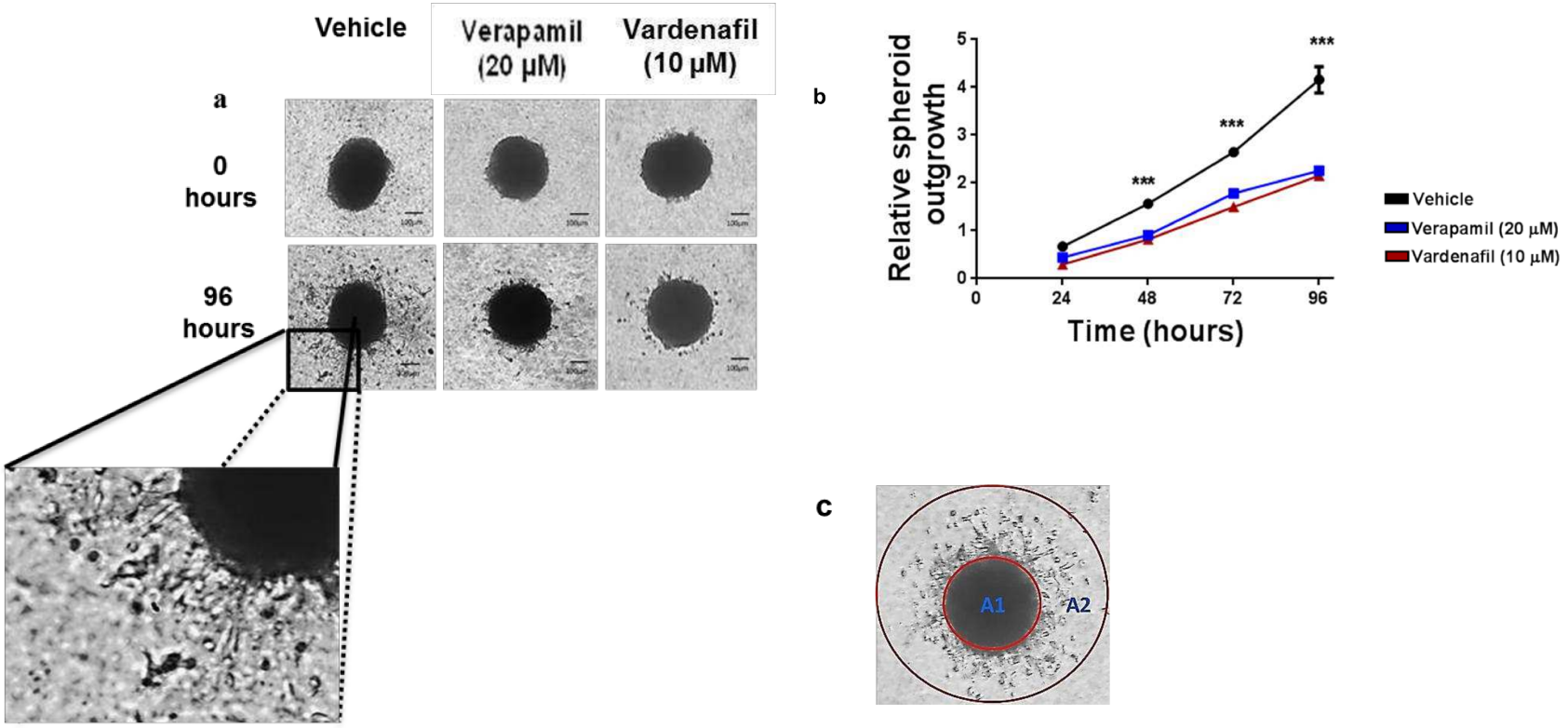


Figure 4.13 ABCB1 inhibition reduced invasion in the BXD-1425EPN cell line A 3D invasion assay was performed to assess the effect of ABCB1 inhibition on the ability of ependymoma cells to digest and invade through the Cultrex^{TM} Basement Membrane Extract (BME). Spheroids were formed from both cell lines by growing them in a 96-well ultra-low attachment (ULA) round bottom plates. The tumour media was replaced with BME on day 3 once the spheroids had formed. **a.** The BXD-1425EPN spheroids showed individual invasive pattern (boxed and magnified) which distinctly reduced over 96 hours after ABCB1 inhibition with both inhibitors (The scale bars in the images represent 100µm.) **b.** This attenuation of invasive ability was represented by a significant reduction in relative spheroid outgrowth (R), consistently over a period of 4 days when treated with both ABCB1 inhibitors. **c.** The relative spheroid outgrowth (R) was measured by computing the ratio of the area of the invasive edge (A2) to the area of the spheroid (A1). (n=3)

4.2.12 ABCB1^{hi} DKFZ-EP1 cell line did not invade in Cultrex ^{TM} BME.

Since, ABCB1 inhibition significantly attenuated ability of the ABCB1^{hi} DKFZ-EP1 cell line to migrate in the wound healing assay; a 3D invasion assay was performed in order to assess the possible role of ABCB1 in its ability to invade through the BME.

However, (as depicted in figure 4.14) when spheroids formed from the cell line were introduced in BME, they remained circumscribed and showed no signs of invasion. Since BME is derived from the basement membrane of a murine sarcoma, this system may not represent the exact ependymoma microenvironment conducive to DKFZ-EP1 invasion. A more representative in vitro system may be required to assess the effect of ABCB1 inhibition on invasion of the DKFZ-EP1 cell line. (Discussed in detail in Chapter 7, Section 7.2)

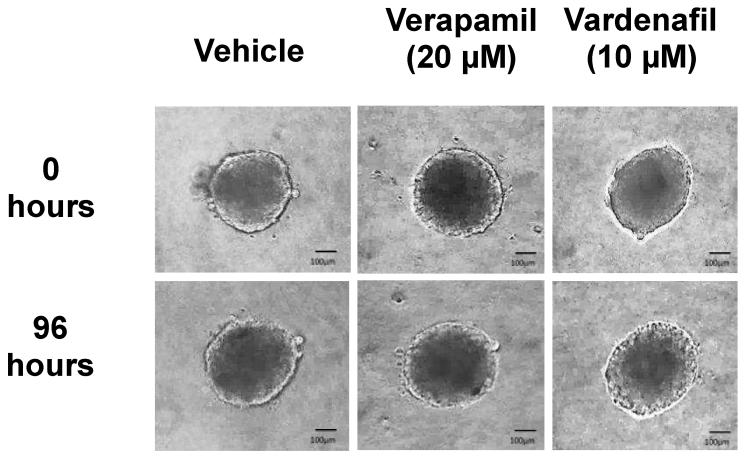


Figure 4.14 Spheroids formed from the DKFZ-EP1 cell line remained circumscribed in a 3D invasion assay Spheroids were formed by plating the DKFZ-EP1 cells in an ultra-low attachment (ULA) 96-well round bottom plate in tumour media which was replaced with BME on day 3 once the spheroids had formed. The spheroids however, remained circumscribed and showed no change in phenotype over the length of the assay (96 hours). (The scale bars in the images represent 100 µm.) (n=2)

4.3 Summary

- High ABCB1 expression in paediatric ependymoma patients supports that hypothesis that drug efflux may be one of the drug resistance mechanisms.
- ABCB1 gene expression was higher in supratentorial tumours in comparison to other locations.
- In the chemotherapy-led CNS9204 trial, ABCB1 expression was independently associated with significantly lower OS and EFS.
- ABCB1 expression did not correlate with reduced survival in the radiotherapy-led CNS9904 trial.
- ABCB1 was expressed in 4 out 5 paediatric supratentorial ependymoma derived cell lines by QRT-PCR analysis.
- ABCB1 expression showed a ~3 fold elevation when the $ABCB1^{hi}$ DKFZ-EP1 cell line was grown as neurospheres (DKFZ-EP1NS).
- ABCB1 inhibition with non-specific ABC transporter inhibitor verapamil and specific inhibitor, vardenafil potentiated response to chemotherapy in both, the stem cell relevant clonogenic assay and the MTT viability assay in the $ABCB1^{lo}$ BXD-1425EPN cell line.
- The $ABCB1^{hi}$ DKFZ-EP1 cell line was resistant to each of the 3 chemotherapeutic drugs used in this study over a wide concentration range and ABCB1 inhibition could not overcome this resistance.
- ABCB1 inhibition decreased the migratory nature of both $ABCB1^{lo}$ BXD-1425EPN and $ABCB1^{hi}$ DKFZ-EP1 cell line.
- ABCB1 inhibition reduced invasion in the BXD-1425EPN cell in a 3D invasion assay.

CHAPTER 5. FUNCTIONAL ANALYSIS OF RADIAL GLIAL STEM CELL MARKER BLBP, WHICH CORRELATES WITH POOR PROGNOSIS IN EPENDYMOMA

5.1 Introduction

Paediatric ependymomas are aggressive and clinically heterogeneous tumours which are known to be chemoresistant (Bouffet and Foreman 1999, Kilday, Rahman et al. 2009, Atkinson, Shelat et al. 2011). 50% of patients tend to relapse and these recurrent tumours are associated with dismal prognosis (Chiu, Woo et al. 1992, Messahel, Ashley et al. 2009). This study tests the hypothesis that CSCs underlie this treatment-refractory behaviour and the tendency to recur in ependymomas. A cross-species genomics study by Taylor et al. identified transformed radial glia (RG) as the stem cells of origin in ependymoma (Taylor, Poppleton et al. 2005). Since BLBP was a member of the panel of markers employed to identify these RG, it could be regarded as a CSC marker in ependymoma. Notably, the BLBP promoter was also used to establish a mouse model of ependymoma (Johnson, Wright et al. 2010). In this study the potential functional role of BLBP in the treatment refractory and invasive behaviour of ependymoma is investigated.

BLBP expression has been correlated with poor survival in a number of aggressive cancers such as glioblastoma multiforme (GBM) (Kaloshi, Mokhtari et al. 2007), and triple negative breast cancers (Tang, Umemura et al. 2010). Since it was a marker used to identify CSCs in ependymomas (Taylor, Poppleton et al. 2005, Poppleton and Gilbertson 2007); it was proposed in this study that BLBP expression could help identify high risk ependymoma patients

Although several knockdown studies so far have reported the potential functional role of BLBP in the proliferation and invasive behaviour of cancer (Kaloshi, Mokhtari et al. 2007, Slipicevic, Jørgensen et al. 2008, Tolle, Krause et al. 2011), the underlying mechanism of its action remains

unclear. Since BLBP is a chaperone for fatty acids (FA) (Manzi, Costantini et al. 2015), an essential source of energy for cancer cells in the altered tumour microenvironment; its expression may potentially be essential for their survival. Additionally, the FA chaperoned by BLBP has also shown to modulate gene expression by PPAR nuclear transcription factors (Mita, Beaulieu et al. 2010); which have also been reported to transcribe BLBP itself (De Rosa, Pellegatta et al. 2012). The nature of this FA (ω-3 or ω-6) has been shown to have a distinct effect on gene expression by the PPARs in gliomas (Mita, Beaulieu et al. 2010). Martin et al. also reported that ω-3 FA partners of BLBP such as DHA (docosahexanoic acid) modulated the transcriptional activity of PPARs to inhibit migration and proliferation in gliomas, whilst ω-6 FA arachidonic acid (AA) promoted these cancerous mechanisms (Martin, Robbins et al. 1996). In other words, the equilibrium between ω-3 and ω-6 FAs was crucial in glioma pathogenesis and progression. With reports of reduced DHA levels and unchanged AA levels in gliomas (Martin, Robbins et al. 1996); this equilibrium was likely to be disturbed, leading to transcription of pro-oncogenic genes by PPARs. Since both gliomas and ependymomas have been proposed to originate from transformed RG (Taylor, Poppleton et al. 2005, Mita, Coles et al. 2007), it is plausible that BLBP may also play similar role in ependymomas.

This chapter assesses prognostic value of BLBP in stratifying paediatric ependymoma patients into clinically relevant groups. Furthermore, it also investigates the putative functional role of BLBP in in vitro models of ependymoma by employing two strategies: firstly, by using a BLBP ligand, DHA which has been shown to inhibit proliferation and invasion in gliomas / medulloblastomas and secondly, PPAR antagonists, demonstrated to inhibit BLBP expression in gliomas.

5.2 Results

5.2.1 BLBP gene expression did not correlate with age in ependymomas.

BLBP is one of the markers for RG and its expression has been shown to be essential for RG maintenance in the rat CNS (Koirala and Corfas 2010). Since transformed RG have been proposed to be CSCs in ependymomas; it was hypothesised that the BLBP expression was maintained in all patients.

In order to assess distribution of BLBP expression across age groups of ependymoma patients, its gene expression was assessed across 3 aforementioned publicly available paediatric ependymoma datasets.

As depicted in Figure 5.1, BLBP expression positively correlated with age in the Mack dataset (Spearman correlation co-efficient=0.43, $P<0.001$) whilst there was no significant correlation between BLBP expression and age in both, the Gilbertson and Witt datasets.

These results confirmed that BLBP expression was maintained in patients; it did not significantly correlate with patient age

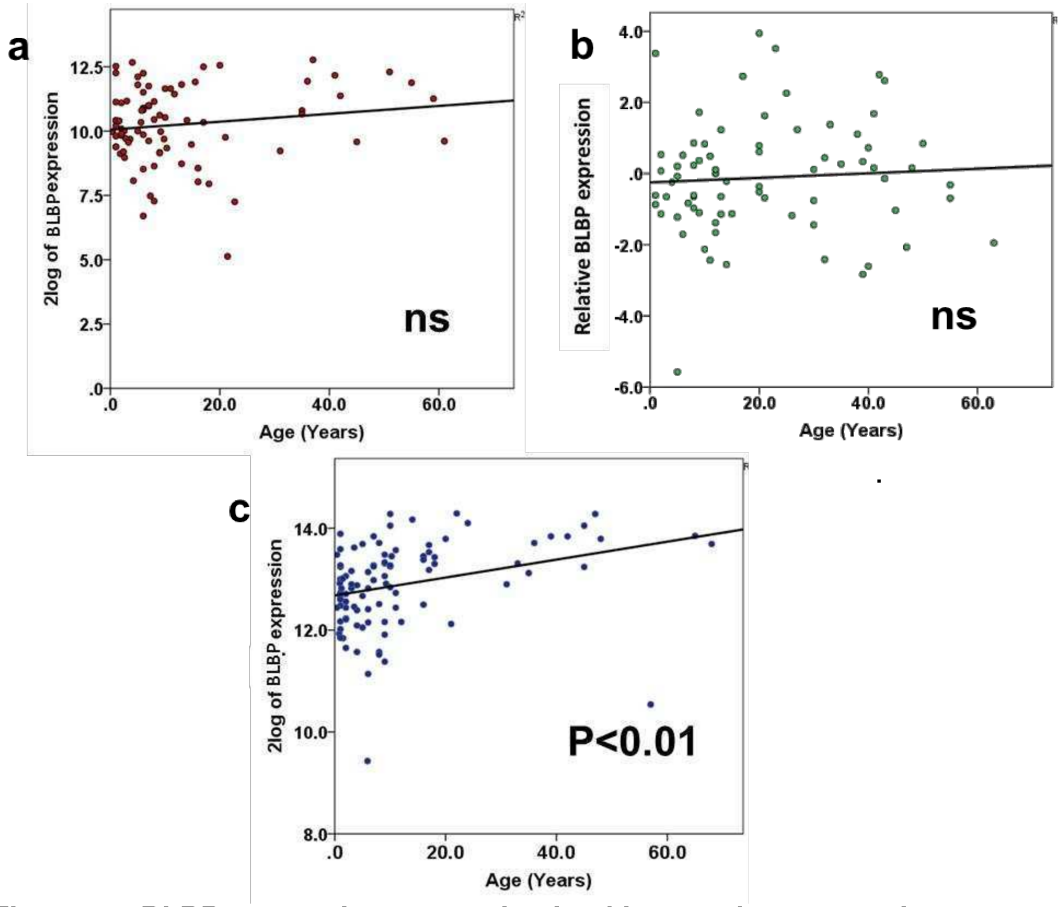


Figure 5.1 BLBP expression was maintained in ependymoma patients across all age groups There was no correlation established between age and BLBP expression in the **a.** Gilbertson dataset (Spearman correlation co-efficient=-0.082, P=0.464) and **b.** the Witt dataset (Spearman correlation co-efficient=0.11, P=0.35). However, in the **c.** Mack dataset, BLBP expression positively correlated with age (Spearman correlation co-efficient=0.43, P<0.001).

5.2.2 BLBP gene expression was higher in SP and ST ependymomas in comparison to PF ependymomas.

As described by Taylor et al., transformed RG recapitulate ependymomas originating from different locations of the CNS as a result of site specific mutations (Taylor, Poppleton et al. 2005). It was therefore assessed if there was heterogeneity in BLBP expression across different ependymoma locations.

The BLBP expression across various ependymoma locations [Posterior Fossa (PF), Spinal (SP) and Supratentorial (ST)] in the 3 aforementioned ependymoma datasets was analysed. As depicted in Figure

5.2, in the Gilbertson dataset, SP tumours expressed higher BLBP gene expression levels in comparison to PF tumours [a; SP vs. PF, MD (Mean difference)= -1.2 (95%CI (confidence interval)= -1.93 to -0.46)]. However, there was no significant difference in BLBP expression in between ST and PF tumours in this dataset. In contrast, BLBP expression was significantly higher in SP and ST ependymomas in comparison to PF ependymomas in the Witt [b; SP vs. PF, MD= -1.14 (95%CI= -1.54 to -0.73) and ST vs. PF, MD= -0.35 (95%CI= -0.71 to 0.01)] and Mack datasets [c; SP vs. PF, MD= -2.35 (95%CI= -3.18 to – 1.52) and ST vs. PF, MD= -0.70 (95%CI= -1.14 to 0.07)].

From these results, it could be inferred that although BLBP expression was maintained across all sites, its significantly higher expression in ST and SP ependymomas might indicate a possible greater role in the pathogenesis and maintenance of ependymomas arising from these specific locations. Further in vivo analyses looking at the role of BLBP in recapitulating and maintaining ependymomas originating from the ST as well as SP compartments may be necessary to confirm these results.

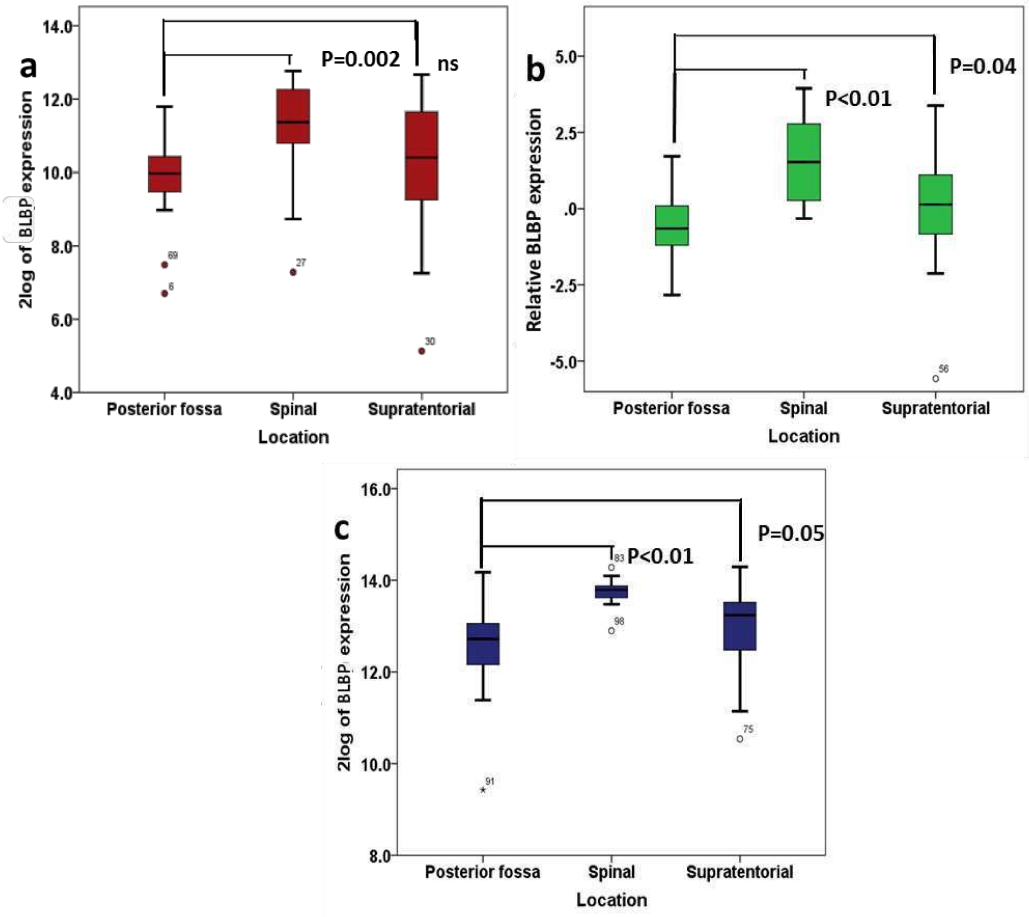


Figure 5.2 BLBP gene expression was significantly higher in SP and ST ependymomas in comparison to PF ependymomas In **a.** the Gilbertson dataset, BLBP expression was significantly higher in SP (spinal) ependymomas in comparison to PF (posterior fossa) ependymomas (P=0.002). In each of **the b.** Witt and **c.** Mack datasets; in comparison to PF tumours, BLBP expression was significantly higher in both SP ependymomas (**b,** P<0.001 and **c**, P<0.001) and ST ependymomas (**b**, P= 0.04 and **c**, P= 0.05). The points highlighted in the figures represent patient samples numbers of outliers assigned by the SPSS Version 21.

5.2.3 BLBP expression correlated with expression of other brain tumour relevant CSC markers; CD133 and SOX2.

CSCs in brain tumours have been identified by neural stem cell markers such as CD133, SOX2 and Nestin (Singh, Clarke et al. 2003, Taylor, Poppleton et al. 2005). Since BLBP is a marker of CSCs (RG) in ependymoma (Taylor, Poppleton et al. 2005); it was hypothesised that its gene expression would strongly correlate with expression of other brain tumour relevant CSC markers. To test this hypothesis, the correlation between BLBP expression and CD133, SOX2 and Nestin in the aforementioned 3 publicly available datasets was assessed.

The surface marker prominin-1 or CD133 has been utilised to characterise brain tumour CSCs (Singh, Clarke et al. 2003) and it was also one of the markers used to identify the transformed RG in ependymomas (Taylor, Poppleton et al. 2005). In the Gilbertson as well as the Mack datasets, BLBP expression strongly correlated with CD133 expression as depicted in Figure 5.3 a (i) (Spearman correlation co-efficient- 0.29, P=0.01) and c (i) (Spearman correlation co-efficient- 0.301 , P=0.002) respectively. However, there was no significant correlation between CD133 and BLBP expression in the Witt dataset (Figure 5.3 b (i) Spearman correlation co-efficient- -0.005, P=0.97).

SOX2 is a developmental pluripotency related transcription factor, routinely used to identify CSCs (Weina and Utikal 2014). It has been recently shown to induce invasion and self-renewal in glioma stem cells (Mao, Gujar et al. 2015). SOX2 expression strongly correlated with BLBP expression in all three datasets. [Gilbertson dataset (aii), Spearman correlation co-efficient-0.44, $P<0.01$; Witt dataset (bii), Spearman correlation co-efficient- 0.42, $P<0.001$ and Mack dataset (cii), Spearman correlation co-efficient- 0.23, P=0.02]

Nestin is an intermediate filament protein expressed in neural and other stem cells (Lendahl, Zimmerman et al. 1990, Milde, Hielscher et al. 2012). Similar to CD133, it was one of the markers used to identify the

transformed RG (Taylor, Poppleton et al. 2005) and its nuclear expression has also been shown to correlate with poor outcome in ependymoma by Milde et al. (Milde, Hielscher et al. 2012). There was no correlation between Nestin and BLBP expression in the Gilbertson [Gilbertson dataset (aiii), Spearman correlation co-efficient-0.007, P=0.95] and Witt datasets [(biii), Spearman correlation co-efficient-0.01, P=0.929]. In the Mack dataset however, there was heterogeneity in terms of the correlation of Nestin with BLBP. Although, there was a significant correlation of BLBP with Nestin expression for one of the probes (Spearman correlation co-efficient- 0.21, P=0.03), there was no correlation with a separate Nestin probe (Spearman correlation co-efficient- -0.23, P=0.82). There is evidence that in addition to encoding the neural stem cell marker Nestin, the Nestin gene (Nes) also encodes for the RC2 antigen which is another radial glial marker (Park, Xiang et al. 2009). Notably, RC2 was also one of the markers used to identify transformed RG in ependymomas (Taylor, Poppleton et al. 2005). Taken together, these findings indicate that the Nestin probe showing statistically significant positive correlation with BLBP might instead be the encoding RC2 antigen. Further analyses are however essential to confirm this speculation.

In addition to the ability to form self-renewing neurospheres and recapitulating orthotopic tumours in mice; expression of stem cell markers such as CD133, SOX2 and Nestin is an important characteristic of CSCs. Significant correlation between BLBP and the aforementioned 2 out of 3 CSC markers supports the proposal that BLBP is a CSC marker in ependymoma.

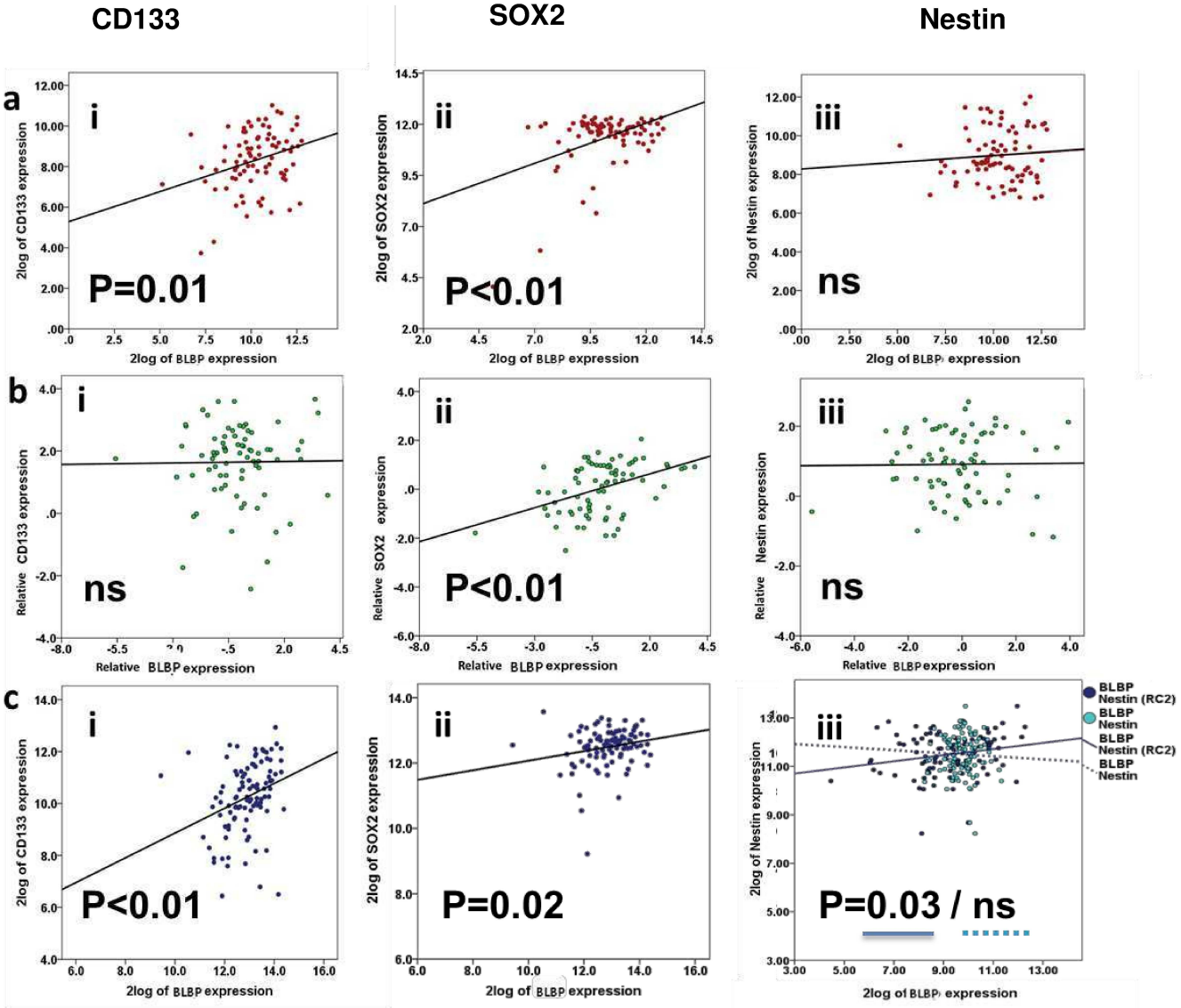


Figure 5.3 BLBP expression significantly correlated with expression of other brain tumour relevant CSC markers In the **a.** Gilbertson dataset (red), BLBP gene expression significantly correlated with expression of CD133 (i, P=0.01) and SOX2 (ii, P<0.01). In the **b.** Witt dataset (green), BLBP expression significantly correlated only with SOX2 (ii, P<0.001) expression. In the **c.** Mack dataset (blue), BLBP expression significantly correlated with expression of both, CD133 (i, P<0.01) and SOX2 (ii, P=0.02). However, there was a discrepancy in terms of correlation with Nestin (iii); although there was significantly positive correlation of BLBP with one of the Nestin probes (P=0.03), there was a weak negative correlation with a separate Nestin probe (P=0.82) established.

5.2.4 BLBP protein expression correlated with prognosis in the chemotherapy-led CNS9204 trial.

BLBP expression has been correlated with reduced prognosis in a number of aggressive cancers including triple negative breast cancer (Tang, Umemura et al. 2010) and glioblastoma (Kaloshi, Mokhtari et al. 2007). Since our data so far support the conjecture that BLBP is a marker for the CSCs in ependymoma (originally made by Taylor et al.), it was hypothesised that BLBP expression could serve as a useful tool in identifying high risk ependymoma patients.

To explore this hypothesis, the prognostic value of BLBP was assessed in the CCLG 1992 04 (CNS9204) trial cohort consisting of paediatric ependymoma patients less than 3 years of age. These patients received adjuvant chemotherapy following surgery in an attempt to delay / avoid radiotherapy (Grundy, Wilne et al. 2007, Ellison, Kocak et al. 2011).

When these samples were stained for BLBP expression using immunohistochemistry (IHC), 49% (25/53) of patients were found to be BLBP positive. Only a sub-population of cells per positive sample showed cytoplasmic and nuclear BLBP staining (Figure 5.4 b); hence, samples were scored as a binary variable (positive or negative). This pattern of expression was therefore, consistent with the CSC hypothesis.

When the expression was analysed in IBM SPSS Version 21 for correlation with survival, BLBP positive patients had a significantly lower event free survival (5-year EFS: 25% versus 56%, P=0.028) and overall survival (5-year OS: 41.6% versus 76%, p=0.01) as depicted in Kaplan-Meier curves in Figure 5.4 c and d respectively.

Since the majority of patients in this trial were diagnosed with ependymomas originating in the PF compartment, an association between BLBP and ST tumours could not be established. Patients with SP ependymomas were not a part of this study. There was no significant

correlation between BLBP expression and patient gender, resection status histological grade of tumours in this study.

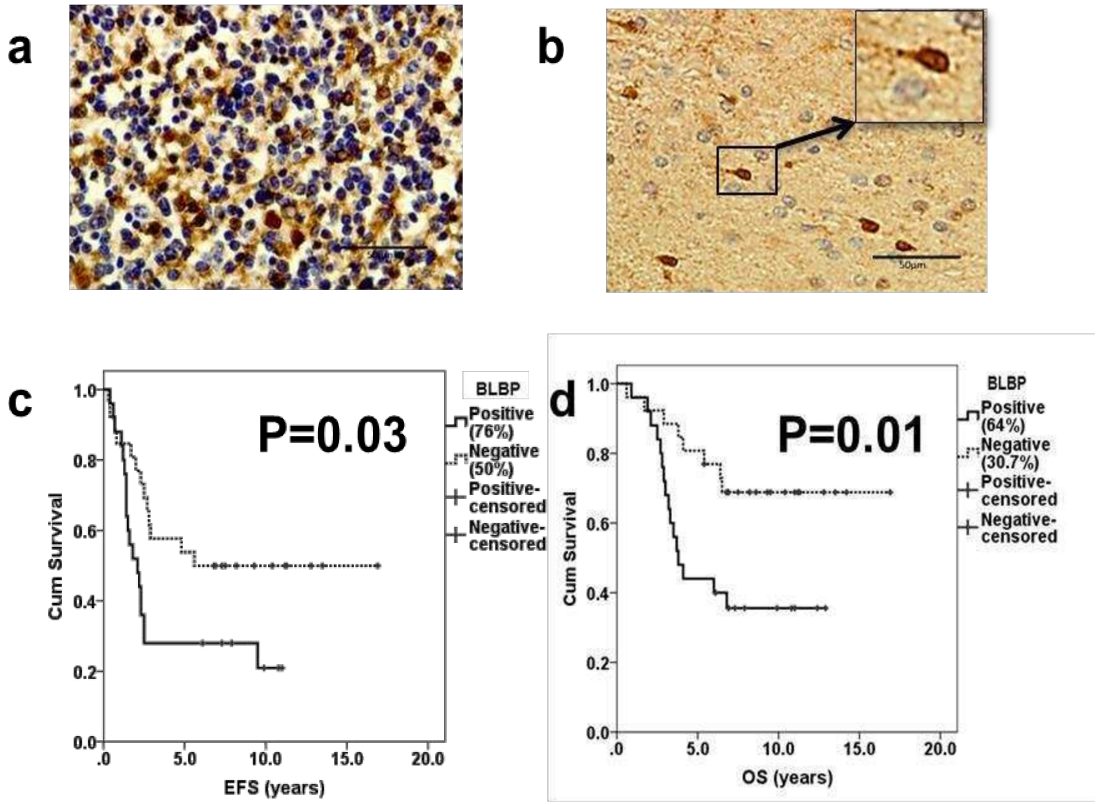


Figure 5.4 BLBP expression correlates with poor prognosis in the chemotherapy-led CNS9204 trial **a.** Since BLBP is a developmental marker, its nuclear and cytoplasmic protein expression using IHC was optimised on normal foetal brain tissue. As depicted in the image, 70-80% cells expressed BLBP. **b**. BLBP positive paediatric ependymoma samples showed nuclear and cytoplasmic staining (boxed and magnified) in a sub-population of cells. (Scale bars represent 50µm.) BLBP positive patients from the trial had a significantly reduced **c.** event-free survival (5-year EFS: 25% versus 56%, P=0.03) and **d.** overall survival (5-year OS: 41.6% versus 76%, P=0.01) respectively.

Additionally, the feasibility of BLBP as an independent prognostic marker was assessed by employing the Cox-regression multivariate model. Similar to multivariate analyses carried out in Chapter 4, surgical resection, tumour location and WHO grade were included as confounding factors included in this model. As depicted in Table 5.1, BLBP positive patients were almost twice more susceptible to having an event (relapse or death) (P=0.04) and 2.8 times more likely to die (P=0.01) in comparison to those who were BLBP negative. These results indicated that BLBP was indeed an independent histological marker of poor prognosis in the chemotherapy-led CNS9204 trial cohort.

Table 5.1 Multivariate survival analyses of BLBP expression in the chemotherapy-led CNS9204 trial

Survival	Factor	Hazard Ratio (95% CI)	P value
Event-free Survival (EFS)	**BLBP expression (Positive vs. Negative)**	**2.08 (1.01-4.26)**	**0.04**
	Location (PF vs. ST)	7.09 (0.94-53.32)	0.06
	Resection (Incomplete vs. Complete)	1.03 (0.51-2.07)	0.94
	WHO Grade (Grade III vs. Grade II)	0.81 (0.39-1.66)	0.55
Overall Survival (OS)	**BLBP expression (Positive vs. Negative)**	**2.81 (1.2-6.87)**	**0.01**
	Location (PF vs. ST)	0.00 (0.00-4.24E+295)	0.97
	Resection (Incomplete vs. Complete)	1.05 (0.47-2.34)	0.91
	WHO Grade (Grade III vs. Grade II)	1.35 (0.58-3.13)	0.97

5.2.5 BLBP expression predicted poor prognosis in the radiotherapy-led CNS9904 trial.

As demonstrated in section 5.2.1, BLBP expression was maintained in patients across all age groups; indicating that it could also be of prognostic value in older paediatric ependymoma patients. In order to assess the prognostic potential of BLBP in stratifying older paediatric ependymoma patients who received adjuvant radiotherapy following surgery, samples from the radiotherapy led SIOP Ependymoma 1 (CNS9904) trial were stained for BLBP expression using IHC.

In this trial, 31.6%, (12/38) patients expressed BLBP. As depicted in Figure 5.5, BLBP expression did not correlate with reduced EFS (5-year EFS: 18.18% versus 52%, P=0.106); however it was significantly associated with reduced OS (5-year OS: 27.27% versus 72%, P=0.002) in patients. There was no significant correlation between BLBP expression and resection status, tumour grade, location and gender in this trial.

To test the potential of BLBP expression to be an independent marker of reduced OS; multivariate analyses were performed with the confounding factors mentioned in section 5.2.4. As shown in Table 5.2, BLBP positive patients were 5.37 times more likely to die (P=0.004) in

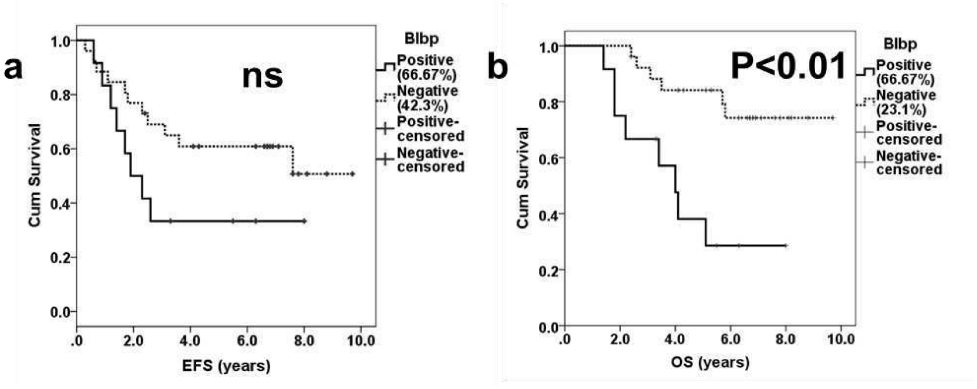


Figure 5.5 BLBP expression correlated with reduced OS in the radiotherapy-led CNS9904 trial In the radiotherapy-led CNS9904, 31.6% patients were BLBP positive. BLBP expression in a sub-population of cells did not correlate with reduced **a.** EFS (5-year EFS-18.18% versus 52%, P=0.106); however was significantly associated with reduced **b.** OS (5-year OS-27.27% versus 72%, P=0.002) in this study.

comparison to those who were BLBP negative.

From these results, it could be inferred that BLBP was a robust marker of reduced OS in the CNS9904 trial consisting of older patients who received adjuvant radiotherapy. However, due to limited sample size, these results need to be reconfirmed in an independent trial.

Table 5.2 Multivariate analysis of BLBP expression in the radiotherapy-led CNS9904 trial

Survival	Factor	Hazard Ratio (95% CI)	P value
Overall Survival (OS)	**BLBP expression (Positive Vs. Negative)**	**5.37 (1.70-16.94)**	**0.004**
	Location (PF Vs ST)	1.84 (0.52-6.47)	0.34
	Resection (Incomplete Vs. Complete)	1.08 (0.35–3.31)	0.88
	WHO Grade (Grade III Vs. Grade II)	2.32 (0.51-3.55)	0.14

5.2.6 BLBP was expressed in all paediatric ependymoma cell lines.

In order to elucidate the functional role of BLBP in ependymomas, its mRNA expression in 5 paediatric ependymoma derived cell lines; BXD-1425EPN, DKFZ-EP1, EPN1, EPN7 and EPNR was assessed. As mentioned in Chapter 4, all the aforementioned cell lines were derived from ST ependymomas.

When evaluated by QRT-PCR analysis, BLBP was expressed at varying levels in all 5 cell lines. The DKFZ-EP1 cell line expressed highest level of BLBP whilst EPN1 and BXD-1425EPN expressed low levels (as

depicted in Figure 5.6). Intermediate levels of BLBP were expressed in the EPN7 and EPN7R cell lines. As demonstrated in Chapter 3, BLBP was expressed in the original patient tumour as well as the murine orthotopic tumour from which the EPN1 cell line was derived.

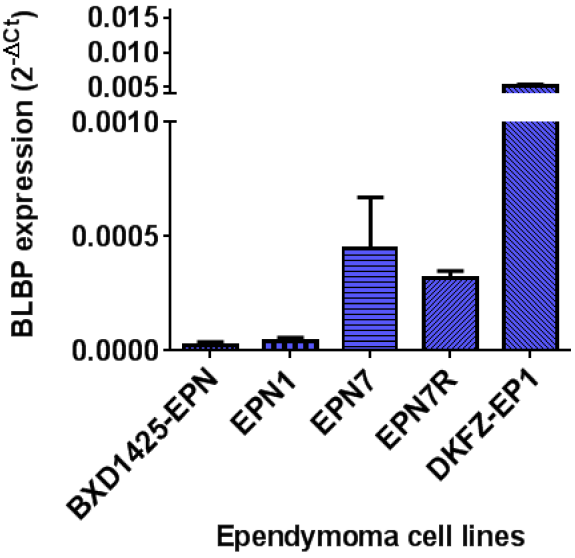


Figure 5.6 BLBP was expressed in all ependymoma cell lines QRT-PCR was perfrmed to assess BLBP mRNA expression in 5 paediatric ependymoma cell lines. BLBP gene expression in all cell lines was corrected for the internal control GAPDH, by the ΔCt method. Each of the 5 paediatric ependymoma cell lines expressed varying levels of BLBP. Bars in the figure above express the mean ± SEM of ≥ 3 experiments, each performed with internal triplicates.

The EPN7 and EPN7R cell lines were derived from the primary and recurrent tumours respectively of the same patient. This data is consistent with the results from analysis of the expression in the Hoffman study (Hoffman, Donson et al. 2014). As depicted in Figure 5.7, BLBP gene expression was maintained at recurrence in 14 primary-recurrent paediatric ependymoma pairs. This finding indicated that the BLBP expressing RG were maintained in recurrent ependymomas and may contribute to their aggressive and treatment refractory behaviour.

The high BLBP expressing ($BLBP^{hi}$) DKFZ-EP1 cell line and the low expressing ($BLBP^{lo}$) BXD-1425EPN cell line were used for further functional analyses.

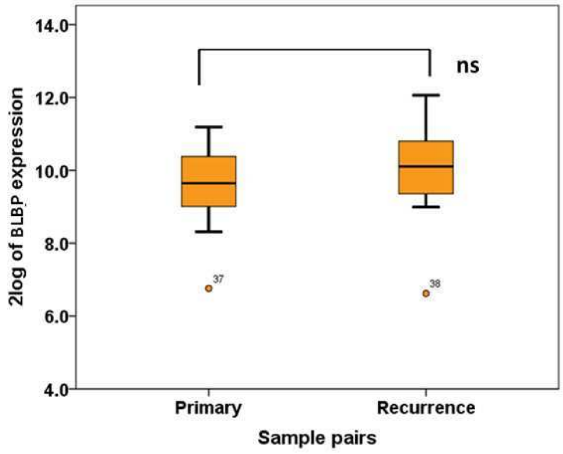


Figure 5.7 BLBP gene expression was maintained at recurrence in the Hoffman dataset Analysis of the publicly available Hoffman dataset which compared the transcriptomic profiles of 14 primary-recurrent ependymoma pairs showed that there was no significant difference in BLBP expression in between primary and recurrent ependymoma samples (Mean difference=-0.54 (95%CI= -1.55 to 0.45), Paired t-test P=0.27)

5.2.7 BLBP expression was elevated in DKFZ-EP1NS neurospheres.

Since BLBP is a marker for RG which are have been proposed to be the CSCs in ependymoma (Taylor, Poppleton et al. 2005), it was therefore proposed that there would be concomitant increase in BLBP expression levels when ependymoma derived cells were grown as neurospheres.

The DKFZ-EP1 cell line was therefore, enriched for stemness by growing it as neurospheres (DKFZ-EP1NS) in stem cell media supplemented with growth factors. When investigated by QRT-PCR analysis, there was a concomitant 5 fold increase in BLBP expression ($P<0.001$). This finding further supported the hypothesis that BLBP is a CSC marker in ependymoma. Since the other ependymoma derived cell lines could not form neurospheres, this result could not be confirmed in any other cell lines.

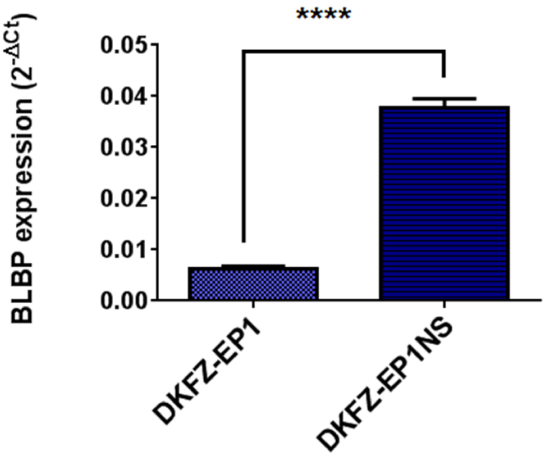


Figure 5.8 Elevation in BLBP expression in stem cell enriched neurospheres derived from the DKFZ-EP1 cell line An approximate 5 fold increase in BLBP expression (P<0.001) was observed when the DKFZEP1 cell line was grown as neurospheres (DKFZ-EP1NS) in stem cell media.

5.2.8 DHA had a differential effect on proliferation in ependymoma cell lines.

As mentioned in Section 5.1, DHA is an ω-3 fatty acid and has been shown to bind to BLBP with highest affinity (Xu, Sanchez et al. 1996). There have been studies highlighting the ability of DHA to inhibit proliferation in in vitro and in vivo models of cancer (Martin, Robbins et al. 1996, Sun, Meng et al. 2013, Zheng, Tang et al. 2014) by reducing the expression of genes such as P53, NF-κB and members of the PI3-Kinase pathway (Wang, Bhat et al. 2011). Since BLBP is essential for the intracellular transport of DHA; it was proposed that treatment with DHA would be an effective way of targeting proliferation in BLBP expressing cells.

An MTT metabolic assay was performed to measure the anti-proliferative effect of DHA on both, the $BLBP^{hi}$ DKFZ-EP1 and the $BLBP^{lo}$ BXD-1425EPN cell lines. As depicted in Figure 5.9, DHA did not have any effect on proliferation in the $BLBP^{lo}$ BXD-1425EPN cell line up to a concentration of 120 µM. In contrast, in the DKFZ-EP1 cell line; although DHA induced a steady increase in proliferation up to the concentration of 60 µM, there was a rapid reduction in proliferation thereafter, with 20% viability recorded at 120 µM. The IC_{50} was established at 103.4 µM (SEM±9.37 µM).

A similar effect of DHA has been demonstrated on in vitro models of medulloblastoma and glioma by Wang et al. (Wang, Bhat et al. 2011). These results indicated that BLBP ligand DHA had a differential effect on proliferation in the ependymoma cell lines used in this study.

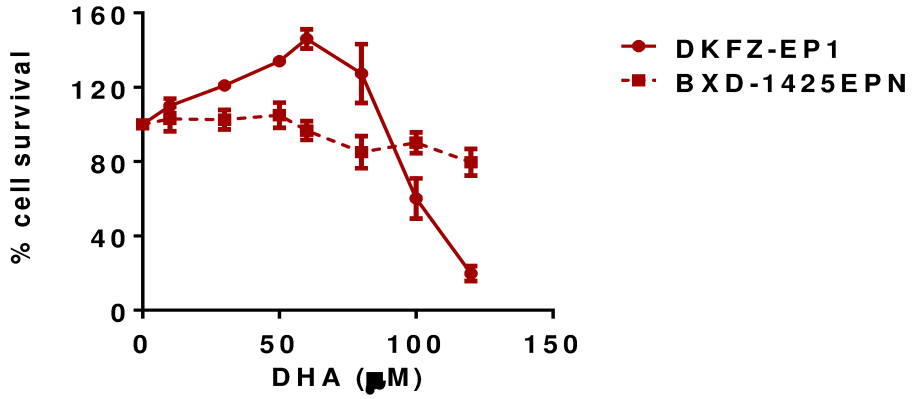


Figure 5.9 DHA had a differential effect on proliferation on ependymoma cell lines The effect of DHA on proliferation in ependymoma cell lines was measured by performing an MTT metabolic assay. DHA at concentrations up to 120 µM had no effect on proliferation in the $BLBP^{lo}$ BXD-1425EPN cell line whilst in the $BLBP^{hi}$ DKFZ-EP1 cell line, after inducing a steady increase in proliferation up to 60 µM, there was a rapid drop in proliferation recorded up to a concentration of 120 µM. The IC_{50} for DHA was established at 103.4 µM (SEM±9.37 µM) in the DKFZ-EP1 cell line. (n=3)

5.2.9 DHA induced cytotoxicity in ependymoma stem cells.

As described in the section 5.2.8, treatment with DHA inhibited proliferation in the $BLBP^{hi}$ DKFZ-EP1 cell line (at higher concentrations) but had no effect on the $BLBP^{lo}$ BXD-1425EPN cell line. Since BLBP is essential for the intracellular transport of DHA; it was assessed if DHA would have an enhanced cytotoxic effect in a clonogenic assay which selects BLBP expressing BXD-1425EPN stem cells.

It was seen that, similar to the effect on $BLBP^{hi}$ DKFZ-EP1 cell line the MTT assay in the previous section, there was an apparent modest increase in colony formation at a lower DHA concentration of 5 µM, followed by complete inhibition in viability at 50 µM. The IC_{50} for DHA was established at 25.07 µM (SEM±1.83 µM). Since it was not possible to grow

neurospheres from the BLBP^{hi} DKFZ-EP1 cell line, the effect of DHA on BLBP enriched DKFZ-EP1NS could not be assessed.

These results indicated that similar to BLBP^{hi} DKFZ-EP1 cell line, DHA had an atypical effect on proliferation in BLBP^{lo} BXD-1425EPN cells in a CSC selecting clonogenic assay.

.

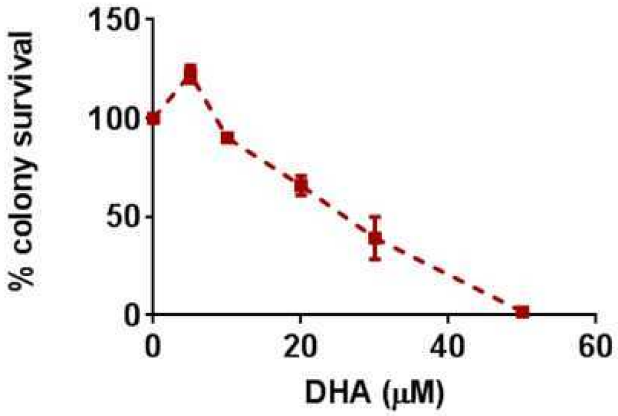


Figure 5.10 DHA inhibited colony formation in the BLBP^{lo} BXD-1425EPN cell line at high concentrations in a stem cell relevant clonogenic assay Response to DHA in a sub-population of BLBP expressing cells in the BXD-1425EPN cell line was measured by employing the stem cell relevant clonogenic assay. After an apparent increase in colony formation at 5 μM, a rapid decrease in viability was recorded up to a concentration 50 μM. The IC_{50} to DHA was established at 25.07 μM (SEM±1.83 μM). (n=3)

5.2.10 Effect of DHA on response to chemotherapy

5.2.10.1 DHA had a differential effect on response to chemotherapy in ependymoma cell lines.

There have been several reports of DHA potentiating response to chemotherapeutic drugs such etoposide, vincristine, doxorubicin and fludaribine in in vitro models of several cancers (Wang, Bhat et al. 2011, Fahrmann and Hardman 2013). This effect has been reported to be due to synergy between DNA damage caused by free radicals produced as a result of DHA peroxidation and toxic chemotherapeutics. Additionally, inhibition of genes such as p53, NF-κB and PI3-Kinase pathway has also been shown to play a role in gliomas and medulloblastomas (Wang, Bhat et

al. 2011). It was therefore assessed if DHA treatment could potentiate response to chemotherapy in ependymoma cell lines.

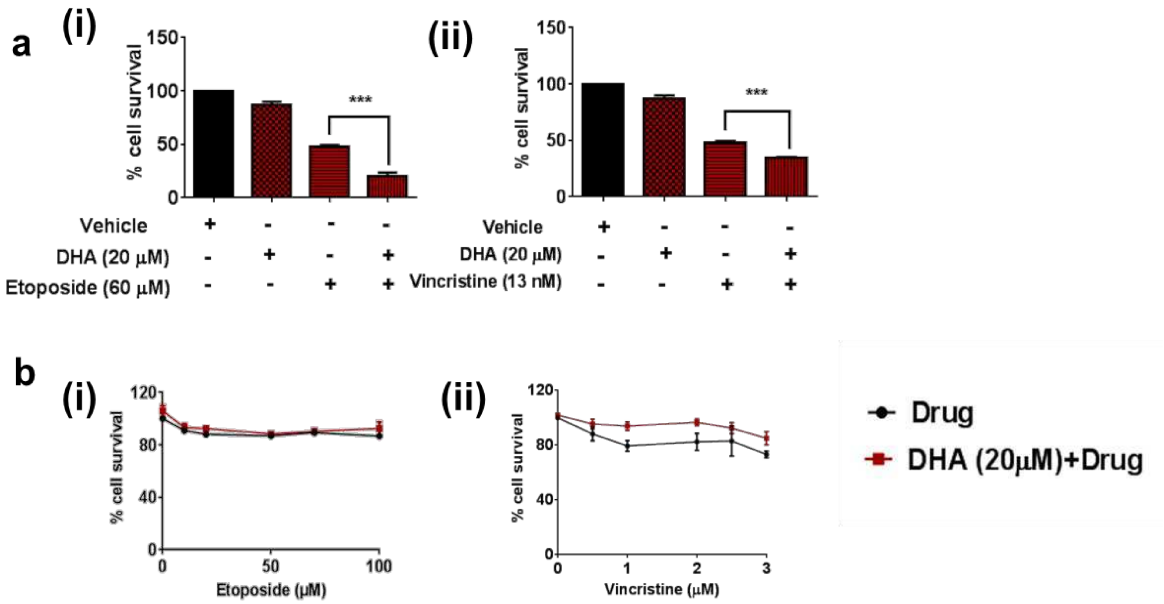


Figure 5.11 DHA had a differential effect on response to chemotherapy in the BLBP^{lo} BXD-1425EPN cell line The ability of DHA to potentiate response to chemotherapy in the total tumour population was measured by an MTT metabolic assay. **a.** In the BLBP^{lo} BXD-1425EPN cell line, the apparent increase in cytotoxicity due to DHA co-treatment seemed to be weakly synergistic in response to etoposide [(i) P<0.001]; whist the mathematically significant but additive in response to vincristine [(ii), P<0.001]. **b.** DHA could not potentiate response to either drugs in the chemoresistant BLBP ^{hi} DKFZ-EP1 cell line. (n≥3)

To investigate this effect in the tumour bulk, both the cell lines used in this study were co-treated with 20 μM DHA along with IC_{50} concentrations of conventional chemotherapeutic drugs (etoposide and vincristine) commonly used as part of chemotherapeutic regimens to treat ependymomas. The resultant cytotoxic effect was measured by means of an MTT viability assay. As depicted in Section 5.2.8, DHA monotherapy, at the concentration of 20 μM mildly inhibited proliferation in the BLBP^{lo} BXD-1425EPN cell lines. In contrast, at the same concentration, it enhanced proliferation by approximately 20% in the BLBP^{hi} DKFZ-EP1 cell line. As depicted in Figure 5.11, DHA increased the cytotoxic effect of both drugs in the BLBP^{lo} BXD-1425EPN cell line. However, this effect appeared to be synergistic in the case of etoposide [Figure 5.11 a (i) (P<0.001)] and although statistically significant seemed additive in the case of vincristine

[Figure 5. 15 a (ii) (P<0.001)]. In the BLBP^{hi} DKFZ-EP1 cell line; there was no potentiation in response recorded as shown in Figure 5.15.b (i) and (ii). These results indicated that DHA had a differential effect on response to chemotherapy in ependymoma.

5.2.10.2 DHA enhanced the cytotoxic effect of etoposide in ependymoma stem cells

Since BLBP is a marker for the transformed RG in ependymomas, the ability of DHA to potentiate response to chemotherapy in the BLBP^{lo} BXD-1425EPN stem cells was assessed by performing a stem cell relevant clonogenic assay. Due to the inherent resistance to all chemotherapeutic drugs used in this study, these experiments were not attempted on the BLBP^{hi} DKFZ-EP1 cell line. As depicted in Figure 5.12, co-treatment with DHA (20 μM) enhanced the cytotoxic effect of both chemotherapeutic drugs. This apparent increase in cytotoxicity seemed to synergistic in the case of etoposide (a, P<0.0001) and additive, although statistically significant in the case of vincristine (b, P=0.007). These results indicated that DHA was useful in enhancing the cytotoxic effect of etoposide in the sub-population of BLBP expressing ependymoma CSCs.

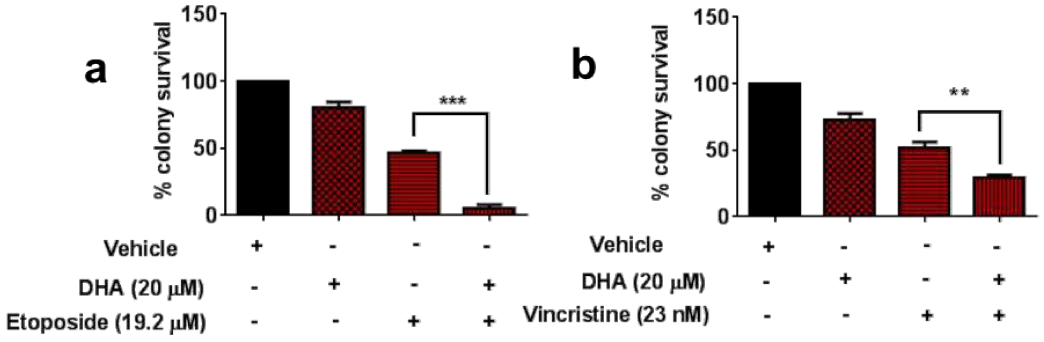


Figure 5.12 DHA enhanced the cytotoxic effect of etoposide in the BLBP^{lo} BXD-1425EPN cell line in a clonogenic assay In order to assess the effect of DHA on response to chemotherapy in BXD-1425EPN CSCs, a clonogenic assay was performed. As a result of DHA co-treatment, the apparent increase in the cytotoxic effect of **a.** etoposide (P<0.001) **and b.** vincristine (P=0.007), seemed synergistic and additive respectively. (n=3)

5.2.11 DHA inhibited the migratory capacity of ependymoma cells.

DHA has been reported to inhibit the migratory capacity of gliomas, breast and endometrial cancers (Mita, Beaulieu et al. 2010, Rahman, Veigas et al. 2013, Zheng, Tang et al. 2014). Furthermore, Wang et al. demonstrated that treatment of medulloblastoma cell lines with DHA, led to downregulation of genes such as MCAM/VCAM and CD44 (Wang, Bhat et al. 2011), all of which have been implicated in invasion and migration of cancer (Lei, Guan et al. 2015, Sacks and Barbolina 2015). In parallel, since local invasion following sub-total resection is a marker of poor prognosis in ST ependymomas (Godfraind, Kaczmarska et al. 2012), the anti-migratory capacity of DHA (20 μM) on ependymoma was assessed by implementing a 2D wound healing assay.

DHA (20 μM) significantly reduced the migratory capacity of both, the $BLBP^{lo}$ BXD-1425EPN and the $BLBP^{hi}$ DKFZ-EP1 cell lines. As depicted in section 5.2.8, DHA at the concentration of 20 μM had an insignificant effect on proliferation of the $BLBP^{lo}$ BXD-1425EPN cell lines; in contrast, at the same concentration, it enhanced proliferation by approximately 20% in the $BLBP^{hi}$ DKFZ-EP1 cell line. Therefore, since the experiment was carried out under the doubling time for each cell line, the effect of DHA in this experiment was anti-migratory, rather than anti-proliferative. This anti-migratory effect was represented by a significant rightward shift in the migratory response curves [Figure 5.13 a (ii) and b(ii)] and an increase in the T1/12 for wound closure [time required for 50% increase in wound closure - depicted in Figure 5.13a (iii) and b (iii)] in both cell lines. These T1/2 values for both cell lines were derived from substantial extrapolation of the response curves. However, to maintain consistency in the methodology used to analyse all scratch assays in this thesis; a different techniquewas not employed. These results indicated that BLBP ligand DHA was certainly useful in inhibiting the migratory capacity of ependymoma cells in a 2D scratch assay.

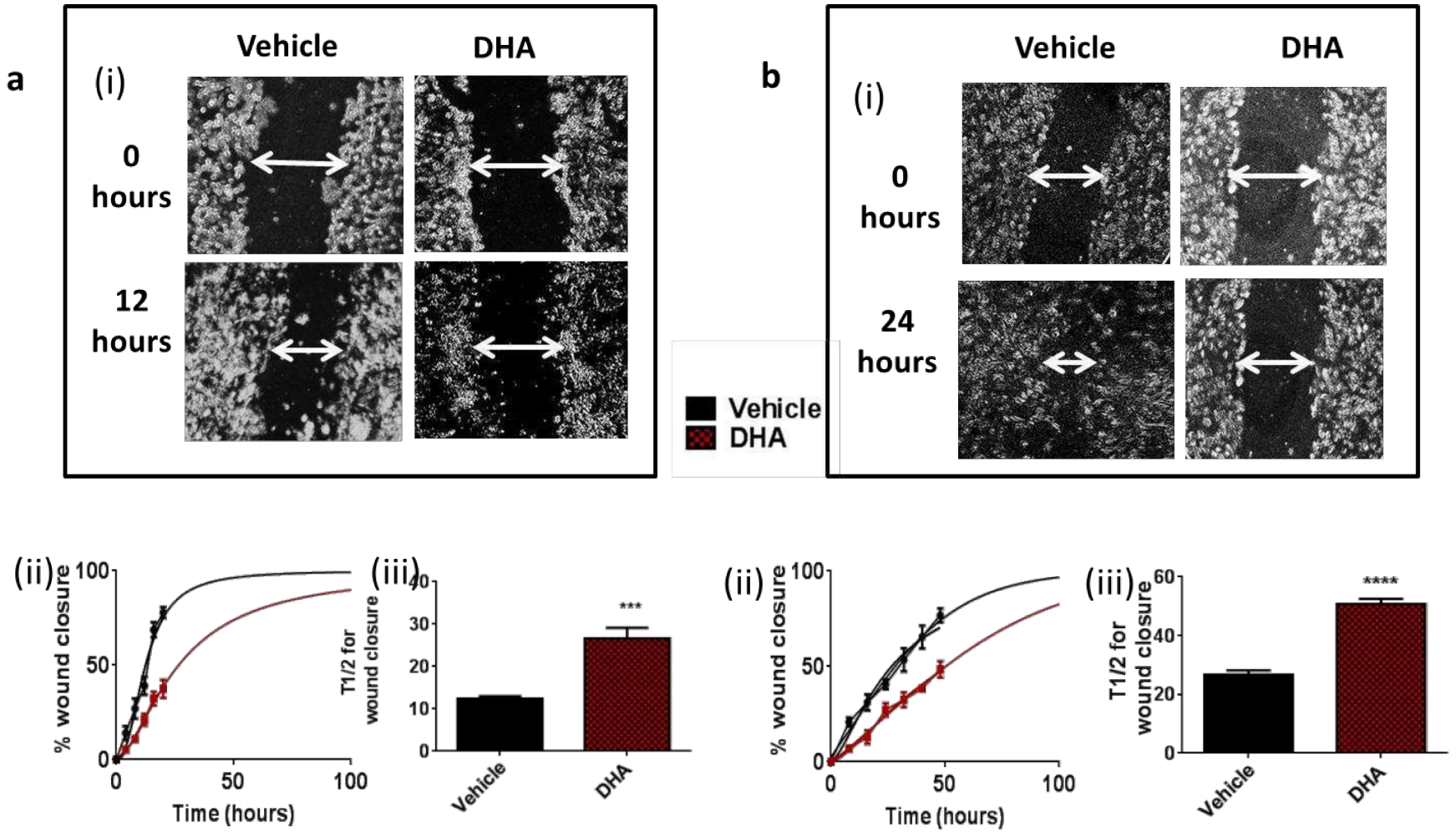


Figure 5.13 DHA diminished migration in ependymoma cell lines When treated with DHA (20 µM), there was a significant reduction the rate of migration in the **a (i)** BLBP^{lo} BXD-1425EPN and **b (i)** BLBP^{hi} DKFZ-EP1 cell line depicted by the rightward shift in their respective response curves [**a(ii)** & **b(ii)** respectively] as well as significant reduction in their T1/2s [time required for 50% increase in wound closure, depicted in **a (iii)** and **b (iii)** respectively]. The assay was carried out for 24 hours and 48 hours for the BXD-1425EPN cell line (Doubling time=~24 hours) and DKFZ-EP1 cell line (Doubling time=~48 hours) respectively to ensure that wound closed as a result of cell migration and not proliferation. (n=3)

5.2.12 DHA inhibited invasion in BLBP^{lo} BXD-1425EPN cell line.

In order to assess the ability of DHA to inhibit invasion in ependymoma cell lines, a 3D invasion assay on the BLBP^{lo} BXD-1425EPN cell line was performed. As mentioned in Chapter 4, Section 4.2.12, since the BLBP^{hi} DKFZ-EP1 cell line could not invade in the BME; this experiment was not attempted on it.

The BLBP^{lo} BXD-1425EPN cell line spheroids were grown in Cultrex^{TM} Basement Membrane Extract (BME), which mimics the 3D tumour micro-environment promoting cell invasion. The spheroids displayed a distinct individual pattern of invasion by undergoing single cell budding and multicellular streaming, when introduced in the BME (boxed and magnified in Figure 5.14 a, vehicle treated condition). Due to inter-batch variability, the cells invaded at a slower pace in this experiment; therefore instead of carrying out the assay over a period of 4 days (as was done in Chapter 4, Section 4.2.11), pictures were obtained every 48 hours over 8 days (192 hours).

When this experiment was carried out in the presence of DHA (20 μM), a gradual reduction in the ability of cells to invade was recorded (depicted in Figure 5.14a). This effect was quantified by substantial reduction in the relative spheroid outgrowth (R = area of invasive edge / area of spheroid) at 144 and 192 hours. This data indicated that DHA not only reduced the migratory capacity of ependymoma cells; it also attenuated their ability to secrete proteolytic enzymes and invade.

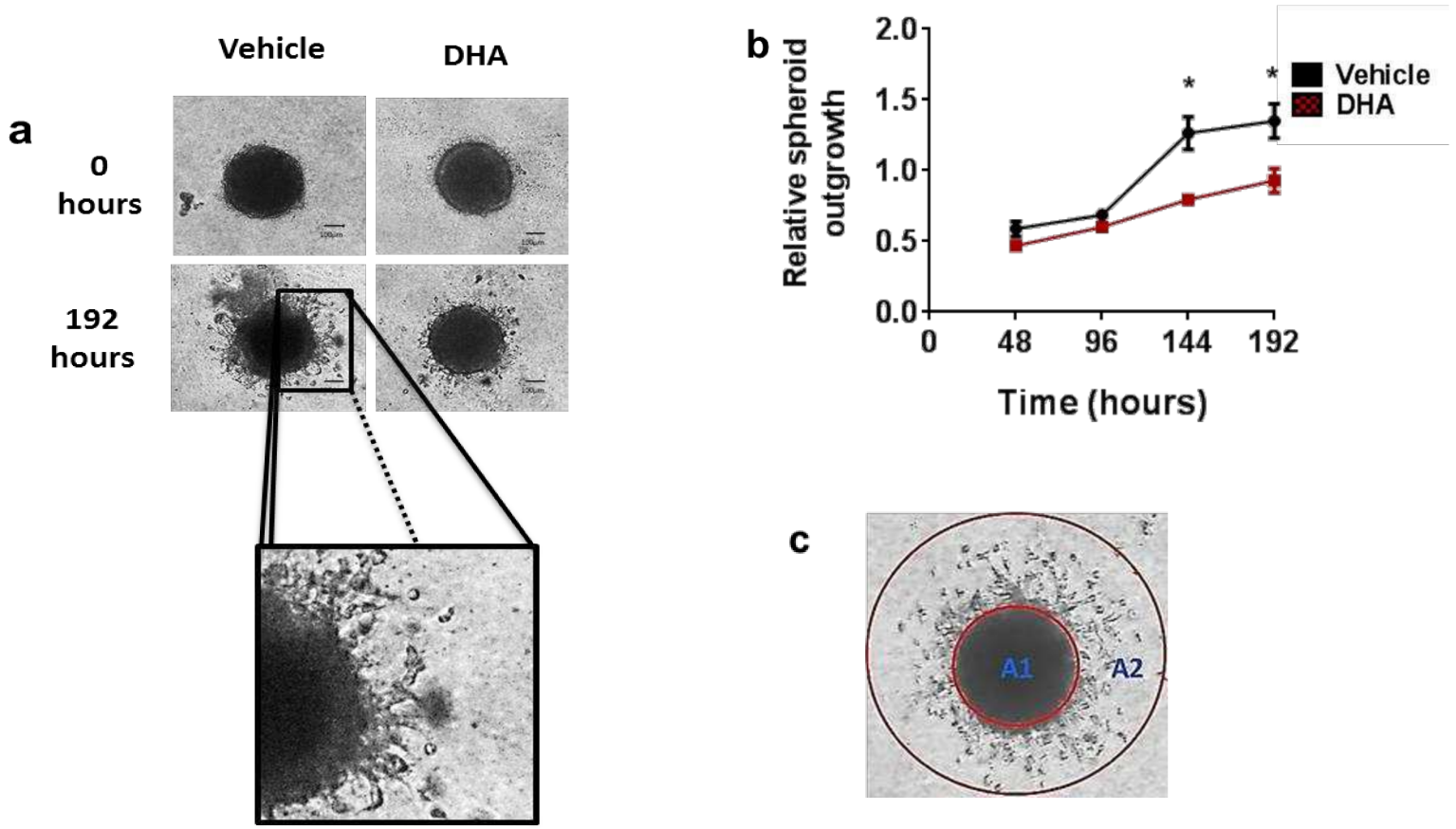


Figure 5.14 DHA inhibits invasion of the BLBP^{lo} BXD-1425EPN cell line A 3D invasion assay was performed to assess the effect of the BLBP partner DHA on the ability of ependymoma cells to digest and invade through the Cultrex^{TM} Basement Membrane Extract (BME). **a.** The BXD-1425EPN spheroids showed an individual invasive pattern through single cell budding and multicellular streaming (boxed and magnified) which gradually reduced over 192 hours after treatment with DHA. (The scale bars in the images represent 100µm.) **b.** A significant reduction in invasion, represented by lower relative spheroid outgrowth (R, ratio of the area of the invasive edge to the area of the area of spheroid), was recorded at 144 and 192 hours following DHA treatment. (n=3**) c.** The relative spheroid outgrowth (R) was measured by computing the ratio of the area of the outer invasive edge (A2) to the area of the spheroid (A1).

5.2.13 PPAR-γ and δ antagonists inhibited BLBP expression in ependymoma cell lines.

In order to elucidate the functional role of BLBP in ependymomas, its expression in in vitro models of the tumour was inhibited by employing PPAR antagonists. De Rosa et al. showed that the BLBP promoter region had a PPRE (peroxisome proliferator response element). In other words, PPARs transcribed the BLBP gene (De Rosa, Pellegatta et al. 2012). Furthermore, as mentioned in Section 5.1, the nature of FAs (ω-3 or ω-6) shuttled by BLBP modulate genes expression of PPAR transcription factors (Mita, Beaulieu et al. 2010). Due to the reported disturbed equilibrium in between ω-3 and ω-6 FAs in brain tumours such as gliomas because of reduced DHA (ω-3 FA) levels, the genes transcribed by PPARs are more likely to be pro-proliferative and pro-migratory (Martin, Robbins et al. 1996, Kokoglu, Tuter et al. 1998). Therefore, the inhibition of these PPAR transcription factors would not only inhibit the transcription of BLBP but also block expression of other oncogenic genes. De Rosa et al. also demonstrated that treatment of glioma cell lines with three PPAR antagonists; the dual PPAR-(γ/δ) antagonist FH535, the PPAR-δ antagonist GSK0660 and the PPAR-γ antagonist GW9662 resulted in a subsequent decrease in BLBP expression (De Rosa, Pellegatta et al. 2012).

Both $BLBP^{hi}$ DKFZ-EP1 and $BLBP^{lo}$ BXD-1425EPN cell lines were treated with the 3 PPAR antagonists (15 μM) [originally demonstrated by (De Rosa, Pellegatta et al. 2012)]; BLBP expression was assessed in each of them by QRT-PCR analysis at 1-3 doublings time points for each cell line. Extensive optimisation was carried out and found that the effect of PPARs on BLBP expression was most profound at each doubling. (In the case of the DKFZ-EP1 cell line, BLBP expression was measured at 48, 96 and 144 hours respectively, whilst in the BXD-1425EPN cell line, it was measured at 24,48 and 72 hours respectively).

As depicted in Figure 5.15, each of the 3 PPAR antagonists completely inhibited BLBP expression in the $BLBP^{lo}$ BXD-1425EPN cell line,

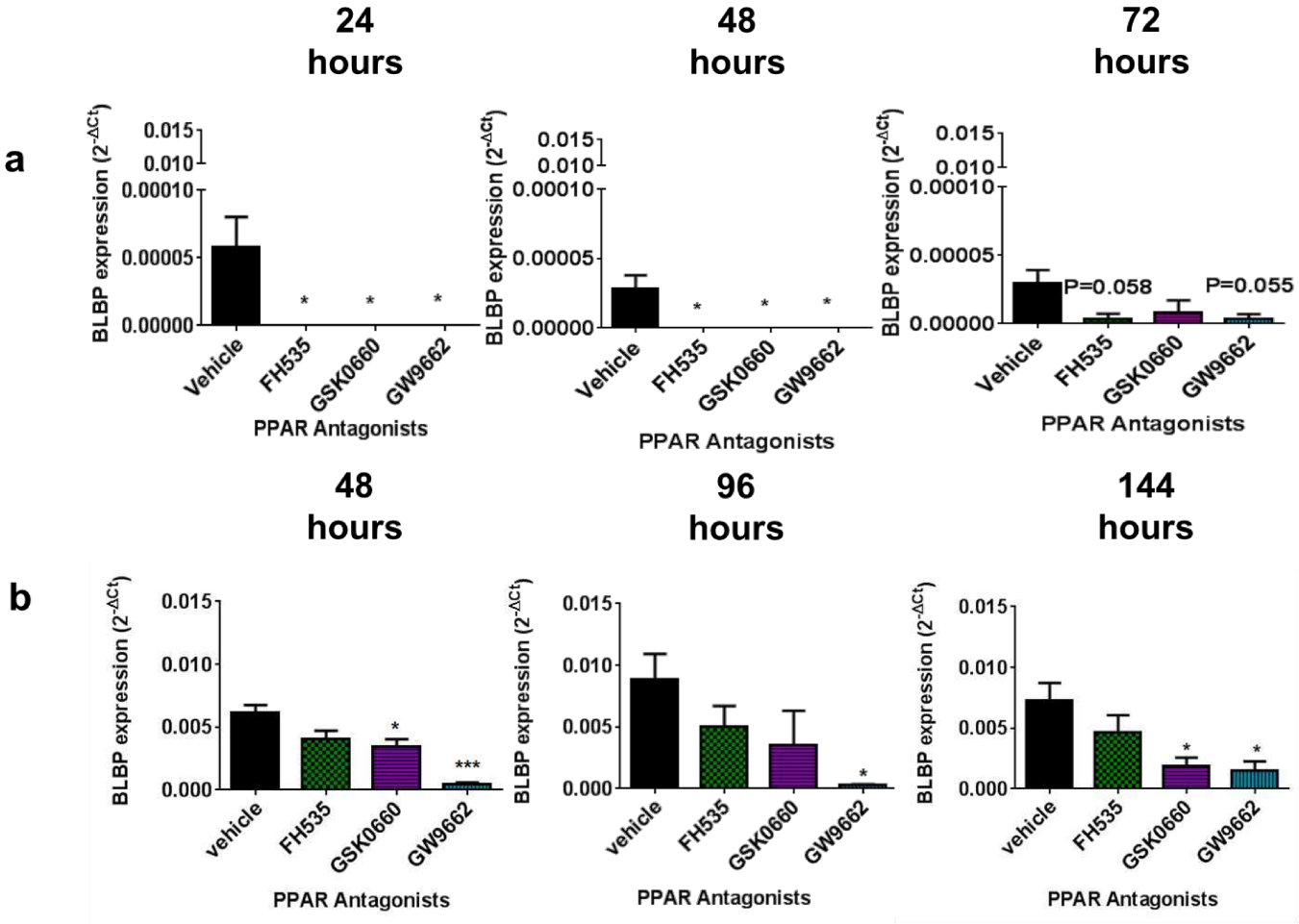


Figure 5.15 PPAR antagonists inhibited BLBP expression in ependymoma cell lines Both the ependymoma cell lines were treated with the 3 PPAR antagonists; the dual PPAR-(γ/δ) antagonist FH535, the PPAR-δ antagonist GSK0660 and the PPAR- γ antagonist GW9662. The effect on BLBP expression was measured at 3 doublings for each cell line by QRT-PCR analysis **a.** In the $BLBP^{lo}$ BXD-1425EPN cell line, BLBP expression levels significantly diminished at 24 and 48 hours respectively as a result of treatment with each of the 3 PPAR antagonists**. b.** In the $BLBP^{hi}$ DKFZ-EP1 cell line, the PPAR-γ antagonist GW9662 significantly inhibited BLBP expression at all 3 time points. Although both the PPAR-δ antagonist GSK0660 and dual PPAR-(γ/δ) antagonist FH535 inhibited BLBP expression to some extent; their effects were found to be variable and statistically insignificant respectively. (n=3)

at the 24 and 48 hour time points respectively. Due to a high level of variability, this effect did not quite reach significance at 72 hours. In the case of the BLBP^{hi} DKFZ-EP1 cell line, the PPAR- ϒ antagonist GW9662 inhibited BLBP expression at all 3 time points. The PPAR-δ antagonist GSK0660 inhibited BLBP expression at 48 and 96 hours. The effect of the dual PPAR antagonist FH535 on BLBP expression was found to be variable and therefore, statistically insignificant. This BLBP inhibitory effect of PPAR antagonists was comparable to the effect produced by sh / siRNA methods employed by several studies (Slipicevic, Jorgensen et al. 2008, Tolle, Suhail et al. 2011, De Rosa, Pellegatta et al. 2012).

These results indicated that each of the PPAR antagonists could indeed inhibit BLBP expression to some extent in both ependymoma cell lines. The effect of the PPAR- γ antagonist GW9662 was however, found to be the most consistent and statistically significant.

5.2.14 The PPAR-γ antagonist GW9662 had a weak but statistically significant anti-proliferative effect on ependymoma cell lines.

There have been contradictory reports regarding the effect of BLBP inhibition on proliferation in in vitro models of cancer (Slipicevic, Jorgensen et al. 2008, Tolle, Suhail et al. 2011, De Rosa, Pellegatta et al. 2012). It was therefore elucidated in this study if BLBP played a functional role in ependymoma proliferation.

As shown in Section 5.2.9, each of the 3 PPAR antagonists (15 μM) inhibited BLBP gene expression to some extent in both BLBP^{hi} DKFZ-EP1 and BLBP^{lo} BXD-1425EPN cell lines. Similar to the previous section, the anti-proliferative effect of the PPAR antagonists was measured at 1-3 doublings time points for each cell line (BXD-1425EPN cell line- 24, 48 & 72 hours and DKFZ-EP1 cell line- 48, 96 & 144 hours) and was quantified by performing the MTT proliferation assay (Roche). As depicted in Figure 5.16, the PPAR-γ antagonist GW9662 exclusively had a weak but statistically significant anti-proliferative effect on both cell lines, at each of the 3 time

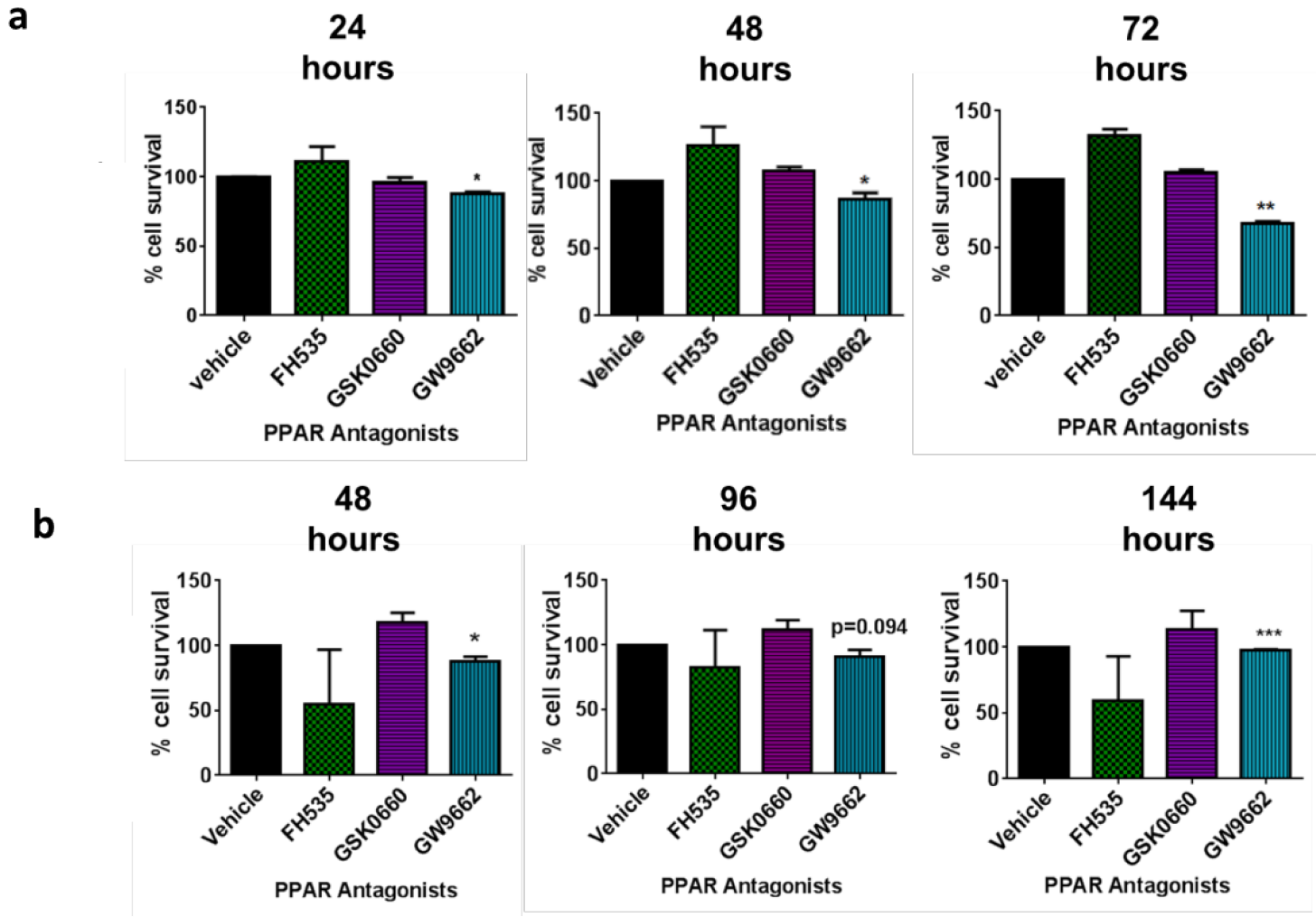


Figure 5.16 The PPAR-γ antagonist GW9662 inhibited proliferation in ependymoma cell lines The effect of BLBP inhibition caused by the 3 PPAR antagonists on proliferation of the 2 ependymoma cell lines was measured (at 3 doubling points each) by using a MTT assay. **a.** The PPAR- γ antagonist GW9662 significantly inhibited proliferation in $BLBP^{lo}$ BXD-1425EPN cell line at all three time points whilst the other 2 antagonists had no effect. **b.** Similarly, only the PPAR-ϒ antagonist, GW9662 significantly but marginally inhibited proliferation in the $BLBP^{hi}$ DKFZ-EP1 cell line. The dual PPAR-(γ/δ) antagonist, FH535 had a variable and thus, statistically insignificant effect on proliferation in this cell line. (n≥3)

points. The dual PPAR-(γ/δ) antagonist, FH535 and the PPAR-δ antagonist, GSK0660 did not have a significant effect on proliferation.

5.2.15 The dual PPAR-(γ/δ) antagonist FH535 and PPAR-γ antagonist GW9662 inhibited viability of ependymoma stem cells.

As reported by Taylor et al. and supported by the findings of this study so far, BLBP is a marker for CSCs in ependymomas. Since its expression was elevated in the stem cell enriched DKFZ-EP1NS neurospheres (section 5.2.8), this was an indication that BLBP expression was may be essential for their survival. Since the $BLBP^{lo}$ BXD-1425EPN cell line did not form neurospheres, the cytotoxic response was measured response in CSCs by carrying out a stem cell relevant clonogenic assay.

As depicted in Figure 5.17a, treatment of the BXD-1425EPN cell line with dual PPAR-(ϒ/δ) antagonist FH535 and PPAR-ϒ antagonist GW9662 significantly reduced colony survival by 42.5% (SEM± 0.88%, P<0.001) and 18 % (SEM±3.4%, P=0.006) respectively. A similar effect was seen in the case of the DKFZ-EP1NS neurospheres. When treated with dual PPAR antagonist FH535, there was a halo of dead cells formed around the neurosphere with a resultant reduction in sphere diameter. In contrast, treatment with PPAR-ϒ antagonist GW9662 only reduced the neurosphere diameter. Both these effects are depicted in Figure 5.17 b(ii) and were quantified by carrying out an alamar blue metabolic assay to produce the graph depicted in Figure 5.17 b(i). The dual PPAR-(ϒ/δ) antagonist FH535 and PPAR-ϒ antagonist, GW9662 significantly reduced percentage cell survival by 37.11% (SEM±3.36 %, P=0.005) and 18 % (SEM±2.9 %, P=0.01) respectively. The PPAR-δ antagonist GSK0660 had no effect on viability in both these stem cell relevant assays on either cell lines. Therefore, these results indicate that BLBP inhibition, by either the dual PPAR-(ϒ /δ) antagonist FH535 or the PPAR-ϒ antagonist GW9662 was useful in inducing toxicity in ependymoma CSCs.

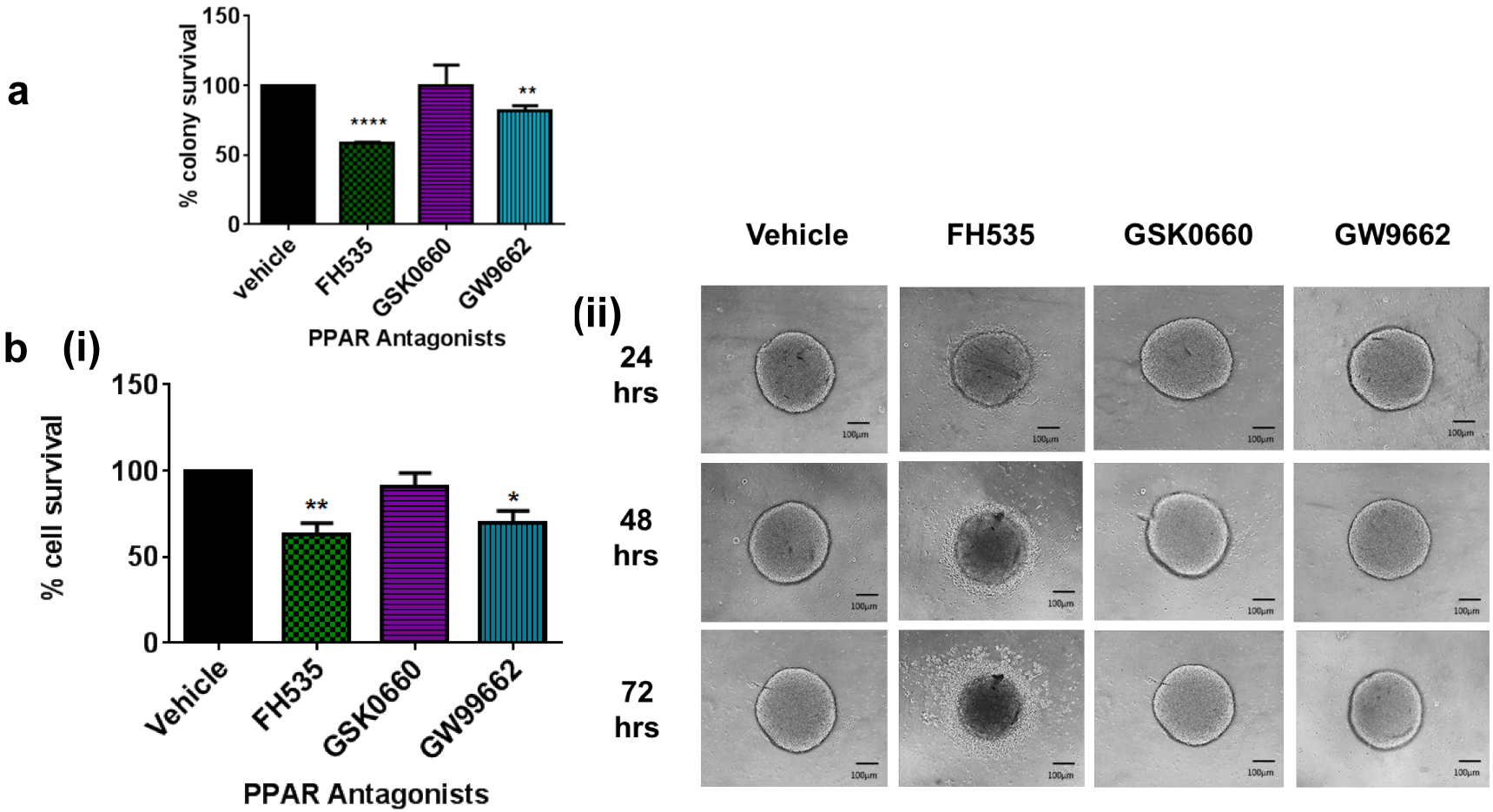


Figure 5.17 Dual PPAR- (γ/δ) antagonist FH535 and PPAR-γ antagonist GW9662 induced toxicity in ependymoma stem cells a. When the BLBP^{lo} BXD-1425EPN cell line was treated with the 3 PPAR antagonists (15 μM each) in a stem cell relevant clonogenic assay, the dual PPAR antagonist, FH535 and the PPAR-γ antagonist GW9662 significantly reduced the colony survival by 42.5% and 18% respectively. **b.** The cytotoxic effect of the PPAR antagonists on the DKFZ-EP1NS neurospheres was measured by carrying out an alamar blue assay. **(i)** FH535 and GW9662 inhibited viability by 37% and 18% respectively, 72 hours after treatment**. (ii)** These results are visually depicted by a halo of dead cells around the neurosphere treated with FH535 and a slight reduction in diameter in the GW9662 treated neurosphere. (The scale bars represent 100 μm.) (n=3)

5.2.16 Effect of BLBP inhibition on response to chemotherapy

5.2.16.1 The PPAR-γ antagonist GW9662 could not potentiate response to chemotherapy in a MTT viability assay.

As stated several times before, chemotherapy is a primary modality employed as adjuvant treatment of paediatric ependymoma patients less than 3 years of age (Grundy, Wilne et al. 2007, Ellison, Kocak et al. 2011). However, there is a paucity of studies conveying any survival benefit from it (Bouffet, Perilongo et al. 1998, Geyer, Sposto et al. 2005, Merchant and Fouladi 2005, Atkinson, Shelat et al. 2011). So far BLBP has been shown to play a role in migration, proliferation and invasion in several cancers (Slipicevic, Jorgensen et al. 2008, Tolle, Suhail et al. 2011, De Rosa, Pellegatta et al. 2012). Since it a marker for the transformed RG, it was investigated if it also played a role in chemoresistance in paediatric ependymomas. The PPAR-γ antagonist GW9662 was found to be most effective in inhibiting BLBP, reducing proliferation in monolayers and viability in stem cells derived from both cell lines; therefore its ability to overcome drug resistance in ependymomas was assessed.

The $BLBP^{lo}$ BXD-1425EPN and $BLBP^{hi}$ DKFZ-EP1 cell lines were pre-treated with PPAR-γ antagonist GW9662 for 48 hours (a significant reduction in BLBP gene expression was previously observed in both cell lines at 48 hours, as described in section 5.2.13) before treatment with conventional chemotherapy (etoposide/ vincristine). The cytotoxic effect in the tumour bulk was measured by performing an MTT metabolic assay. As depicted in Figure 5.18, there was no potentiation of response to chemotherapy recorded in either cell lines.

These results indicated that BLBP inhibition by PPAR-γ antagonist, GW9662 could not potentiate response to chemotherapy in the heterogeneous bulk tumour population of ependymomas.

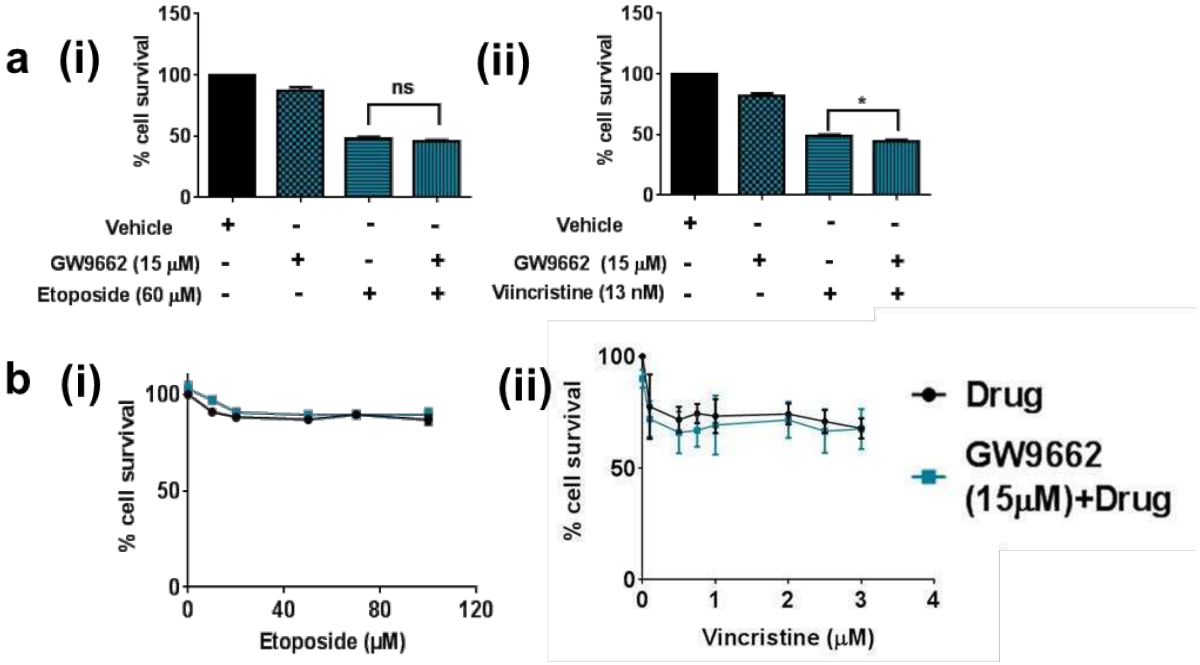


Figure 5.18 BLBP inhibition by PPAR-γ antagonist GW9662 could not potentiate response to chemotherapy The effect of BLBP inhibition on response to chemotherapy was assessed by pre-treatment of both cell lines with the PPAR-γ antagonist GW9662 for 48 hours, followed by treatment with etoposide and vincristine. The cytotoxic effect was measured by carrying out an MTT metabolic assay **a.** In the BLBP^{lo} BXD-1425EPN cell line, inhibition of BLBP by the PPAR-γ antagonist, GW9662 did not potentiate response to **(i)** etoposide. The apparent reduction in viability in the case of **(ii)** vincristine seemed more mathematically rather than biologically relevant. **b.** Similarly, in the BLBP^{hi} DKFZ-EP1 cell line, there was no potentiation in response to either etoposide or vincristine as depicted in **(i)** and **(ii)** respectively. (n=3)

5.2.16.2 The PPAR-γ antagonist GW9662 potentiated response to chemotherapy in ependymoma stem cells

As demonstrated in section 5.2.15 that the PPAR-γ antagonist reduced viability in the BLBP^{lo} BXD-1425EPN cell line by 18% in a stem cell relevant clonogenic assay. It was therefore assessed if pre-treatment with GW9662 could potentiate response etoposide and vincristine in the ependymoma CSCs. Due to inherent resistance exhibited by the BLBP^{hi} DKFZ-EP1 cell line to all chemotherapeutic drugs used in this study as a result of possible upregulation/dysregulation of a number of resistance pathways (discussed in detail in Chapter 1 section 1.3.4.3), these

experiments were not performed on stem cell enriched DKFZ-EP1NS neurospheres.

The BLBP^{lo} BXD-1425EPN cell line was pre-treated with GW9662 for 48 hours followed by treatment with etoposide and vincristine respectively in a clonogenic assay. As depicted in Figure 5.19, a potentiation in response to both etoposide and vincristine was recorded, as depicted by a significant reduction in survival at the IC_{50} values to 0% ($P<0.0001$) and 10% ($P=0.002$) respectively.

These results indicated that BLBP inhibition by the PPAR-γ antagonist GW9662 could potentiate response to chemotherapy, in BLBP^{lo} BXD-1425EPN stem cells. In other words, BLBP played a functional role chemoresistance in ependymoma stem cells.

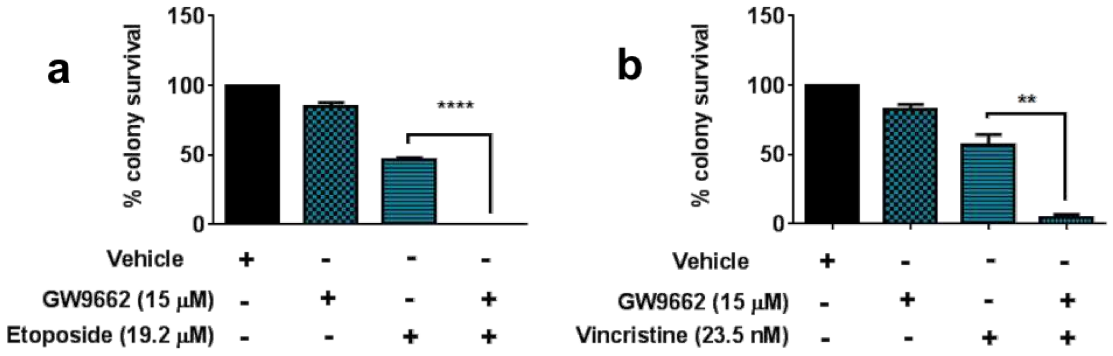


Figure 5.19 The PPAR-γ antagonist GW9662 potentiated response to chemotherapy in the BLBP^{lo} BXD-1425EPN cell line in a clonogenic assay The effect of BLBP inhibition on response to chemotherapy in the BLBP^{lo} BXD-1425EPN CSCs was assessed by pre-treatment with the PPAR-γ antagonist GW9662 for 48 hours followed by treatment with chemotherapeutic drugs, etoposide and vincristine in a stem cell relevant clonogenic assay. A potentiation in response to **a.** etoposide ($P<0.001$) and **b.** vincristine ($P=0.002$) is represented by almost complete cytotoxicity achieved at their respective IC_{50} concentrations when combined with GW9662. (n=3)

5.2.17 PPAR antagonists reduced the migratory capacity of ependymoma cells.

As described in Chapter 4, although extra-neural metastases only occur in 9-10% ependymoma patients (Alzahrani, Alassiri et al. 2014, Pachella, Kamiya-Matsuoka et al. 2015, Severino, Consales et al. 2015), local invasion of the tumour has been commonly reported and is also regarded as a marker of poor prognosis in ependymomas originating from the ST compartment (Akay, Izci et al. 2004, Godfraind, Kaczmarska et al. 2012, Phi, Wang et al. 2012). Notably, several studies also report the role of BLBP in invasion / metastasis in gliomas, melanoma and renal cancers (Slipicevic, Jørgensen et al. 2008, Mita, Beaulieu et al. 2010, Tolle, Suhail et al. 2011, De Rosa, Pellegatta et al. 2012). It was therefore assessed, if BLBP also contributed to the invasive and migratory behaviour of ependymoma. As mentioned in Chapter 4, both the $BLBP^{lo}$ BXD-1425EPN and the $BLBP^{hi}$ DKFZ-EP1 cell lines were established from aggressive WHO Grade III anaplastic ependymomas (Clinicopathological details, Chapter 2; Section 2.2). Furthermore, the DKFZ-EP1 cell line was derived from malignant ascites in the peritoneal cavity which is an indication of the ability of the cells to invade and metastasise (Milde, Kleber et al. 2011).

When a 2D scratch assay was carried out in the presence of PPAR antagonists, each of the 3 PPAR antagonists significantly reduced migration in both ependymoma cell lines as depicted in figure 5.20. However, the effect of PPAR-ϒ antagonist GW9662 was found to be the most profound, represented by a significant rightward shift in the migratory response curves [Figure 5.20 a (ii) and b(ii)] and increase in the T1/12 for wound closure [time required for 50% increase in wound closure - depicted in Figure 5.20 a (iii) and b (iii)] in both cell lines. It is essential to highlight that the assay was carried out up to 24 hours and 48 hours for the BXD-1425EPN cell line (Doubling time=~24 hours) and DKFZ-EP1 cell line (Doubling time=~48 hours) respectively to ensure that wound closed as a result of cell migration and not proliferation. These T1/2 values for treated conditions in both cell lines were derived from substantial extrapolation of the response curves.

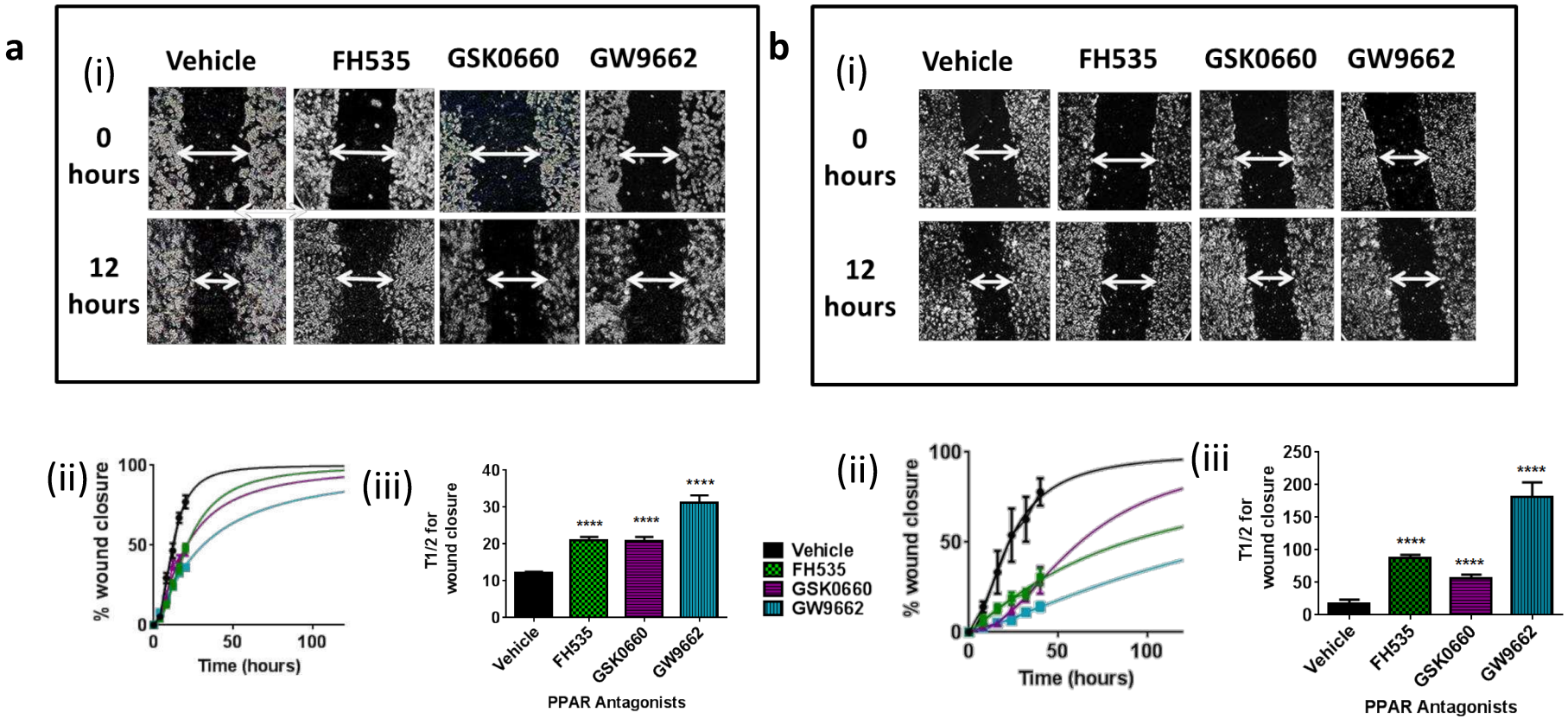


Figure 5.20 PPAR antagonists decreased migration in ependymoma cell lines A wound healing assay was performed to assess the effect of BLBP inhibition on the migratory nature of ependymoma cells. When treated with PPAR antagonists (15 µM), there was a significant reduction in the rate of migration in the **a (i)** BLBP^{lo} BXD-1425EPN and **b (i)** BLBP^{hi} DKFZ-EP1 cell line depicted by the rightward shift in their respective response curves [**a(ii)** & **b(ii)** respectively] as well as significant increase in their T1/2s [time required for 50% increase in wound closure, depicted in **a (iii)** and **b (iii)** respectively. The anti-migratory effect of PPAR-γ antagonist GW9662 was found to be the most powerful. The assay was carried out up to 24 hours and 48 hours for the BXD-1425EPN cell line (Doubling time=~24 hours) and DKFZ-EP1 cell line (Doubling time=~48 hours) respectively to ensure that wound closed as a result of cell migration and not proliferation. (n=3)

However, to maintain consistency in the methodology used to analyse all scratch assays in this thesis; a different techniques was not employed. These results indicated that PPAR antagonists, especially PPAR-γ antagonist GW9662, as a result of BLBP inhibition, significantly attenuated the migratory capacity of ependymoma cells.

5.2.18 PPAR antagonists attenuated invasion in BLBP^{lo} BXD-1425EPN cell line.

As mentioned before, brainstem invasion has been regarded as a marker of poor prognosis in ependymomas (Akay, Izci et al. 2004, Godfraind, Kaczmarska et al. 2012, Phi, Wang et al. 2012). Inhibition of BLBP has been shown to reduce tumour invasion in vitro in several cancers (Slipicevic, Jørgensen et al. 2008, Tolle, Suhail et al. 2011, De Rosa, Pellegatta et al. 2012). As shown in section 5.2.12, BLBP expression was lost in the BLBP^{lo} BXD-1425EPN cell line after treatment with PPAR antagonists; it was assessed if this reduction would affect the ability of cells to invade in a 3D-invasion assay.

In this assay, BLBP^{lo} BXD-1425EPN spheroids, grown in the Cultrex^{TM} Basement Membrane Extract (BME) were treated with the aforementioned PPAR antagonists. The spheroids displayed a distinct amoeboid pattern of invasion by undergoing single cell budding when introduced in the BME (boxed and magnified in Figure 5.21 a, untreated condition). When this experiment was carried out in the presence of PPAR antagonists, a reduction in the ability of cells to invade was recorded (depicted in Figure 5.21 a). This effect was quantified by a substantial reduction in the relative spheroid outgrowth (R = area of invasive edge / area of spheroid) at all 4 time points over 96 hours. The dual PPAR-(γ/δ) antagonist FH535 had the greatest effect, followed by the PPAR-γ antagonist, GW9662. The PPAR-δ antagonist GSK9660 significantly inhibited invasion exclusively at 72 hours. These results could not be recapitulated on the BLBP^{hi} DKFZ-EP1 cell line, since the spheroids did not

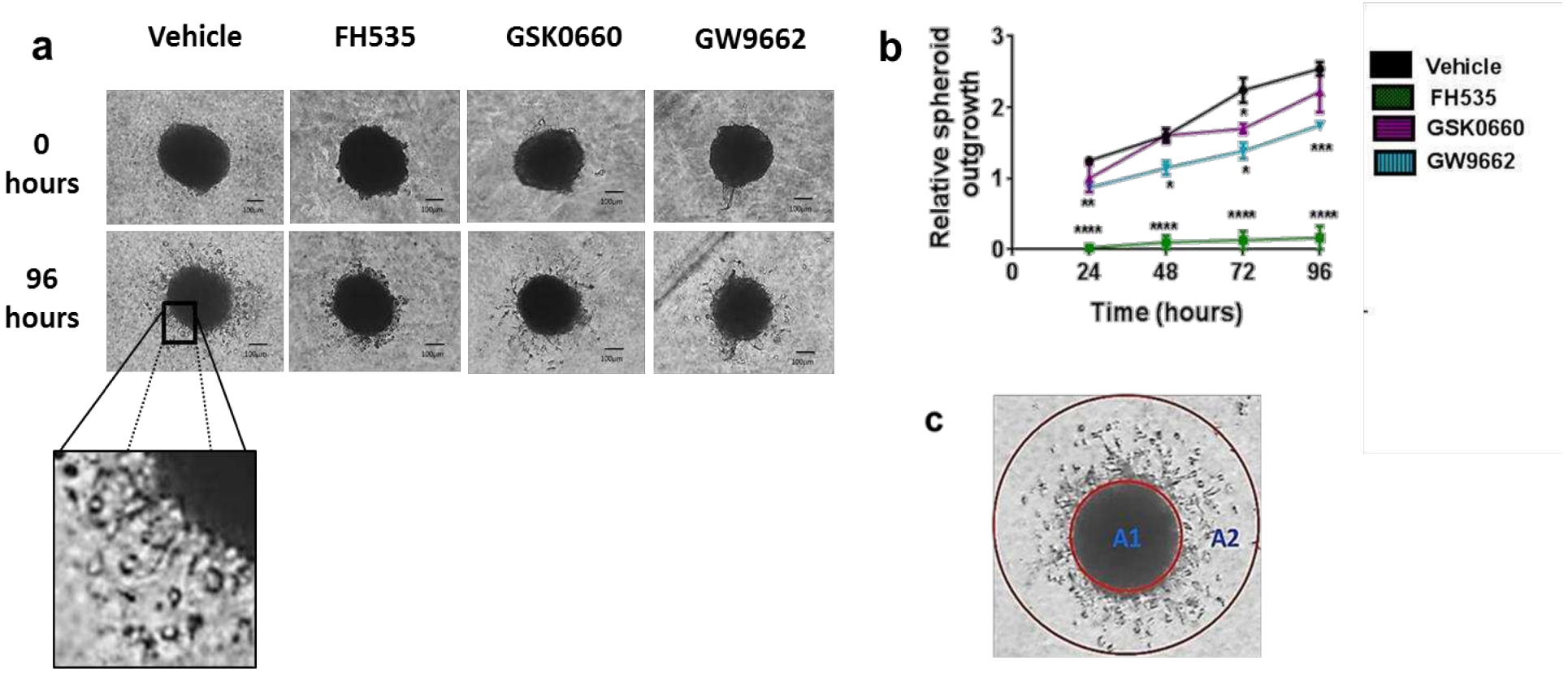


Figure 5.21 PPAR antagonists inhibited invasion in BLBP^{lo} BXD-1425EPN cell line A 3D invasion assay was performed to assess the effect of BLBP inhibition on the ability of ependymoma cells to digest and invade through Cultrex^{TM} Basement Membrane Extract (BME). **a.** The BXD-1425EPN spheroids showed an amoeboid invasion pattern through single cell budding (boxed and magnified) which distinctly reduced over 96 hours after treatment with the BLBP inhibiting dual PPAR-(γ/δ) antagonist FH535 and the PPAR-γ antagonist GW9662. The effect of PPAR-δ antagonist, GSK0660 on invasion was weak. (The scale bars in the images represent 100 µm.) **b.** A significant reduction in invasion represented by lower relative spheroid outgrowth (R, ratio of the area of the invasive edge to the area of the spheroid) was observed consistently over a period of 4 days when treated with the dual PPAR-(γ/δ) antagonist, FH535 and the PPAR- γ antagonist, GW9662.(n=3) **c.** The relative spheroid outgrowth (R) was measured by computing the ratio of the area of the invasive edge (A2) to the area of the spheroid (A1).

invade in the BME (as depicted in Chapter 4, Section 4.2.13). These results indicated that the dual PPAR-(γ/δ) antagonist FH535 and PPAR-γ antagonist GW9662 significantly decreased invasion in the $BLBP^{lo}$ BXD-1425EPN cell line.

5.3 Summary

- BLBP was expressed in paediatric ependymoma patients. This expression was significantly higher in tumours originating from the ST and SP compartment in comparison to PF ependymomas.

- BLBP expression showed a strong correlation with expression of other brain tumour relevant CSC markers; CD133 and SOX2.

- BLBP was an independent marker of reduced OS and EFS in the chemotherapy-led CNS9204 trial.

- BLBP was an independent marker of reduced OS in the radiotherapy-led CNS9904 trial.

- BLBP was expressed at variable levels in all paediatric ependymoma derived cell lines. There was a 5-fold elevation in BLBP expression in the stem cell enriched neurospheres derived from the DKFZ-EP1 cell line.

- The BLBP partner, DHA did not inhibit proliferation in $BLBP^{lo}$ BXD-1425EPN cell line. In contrast, after inducing a steady increase in proliferation at lower concentrations up to 60 µM, a rapid drop in the proliferation was recorded up to a concentration of 120 µM. The IC_{50} was established at 103.4 µM in the $BLBP^{hi}$ DKFZ-EP1 cell line.

- Similar to behaviour of the $BLBP^{hi}$ DKFZ-EP1 cell in an MTT assay, DHA induced an apparent increase in viability at a lower concentration of 5 µM, followed by completely inhibiting viability at 50 µM, in the $BLBP^{lo}$ BXD-1425EPN cell line in a stem cell

relevant clonogenic assay. The IC_{50} for DHA was established at 25.07 μM (SEM±1.83 μM).

- DHA did not potentiate response to chemotherapy in the tumour bulk of either cell lines; but, significantly enhanced cytotoxicity due to etoposide treatment in the $BLBP^{lo}$ BXD-1425EPN stem cells.

- DHA inhibited migration in both ependymoma derived cell lines used in this study.

- DHA inhibited invasion in the $BLBP^{lo}$ BXD-1425EPN cell line in a 3D invasion assay.

- In the $BLBP^{lo}$ BXD-1425EPN cell line, each of the 3 PPAR antagonists inhibited BLBP expression whilst in the $BLBP^{hi}$ DKFZ-EP1 cell line, the PPAR-γ antagonist GW9662 was found to be the most potent BLBP inhibitor.

- The PPAR-γ antagonist, GW9662 marginally, but significantly inhibited proliferation in both $BLBP^{hi}$ DKFZ-EP1 and $BLBP^{lo}$ BXD-1425EPN cell lines.

- The dual PPAR-(ϒ/δ) antagonist FH535 and PPAR-ϒ antagonist GW9662 were the most effective in inhibiting viability in ependymoma stem cells in both cell lines used in this study.

- The PPAR-γ antagonist, GW9662 enhanced the cytotoxic effect of vincristine and etoposide in the $BLBP^{lo}$ BXD-1425EPN stem cells but not in tumour bulk. It had no effect on response to chemotherapy in the $BLBP^{hi}$ DKFZ-EP1 cell line.

- The PPAR-γ antagonist, GW9662 was the most effective in attenuating migratory nature of both ependymoma derived cell lines.

- The dual PPAR-(γ/δ) antagonist, FH535 completely inhibited whilst PPAR-γ antagonist GW9662 had an intermediate inhibitory effect on invasion in the BLBP^{lo} BXD-1425EPN cell line in a 3D invasion assay.

  .

CHAPTER 6. EXPRESSION, PROMOTER METHYLATION AND CIRCUMVENTION OF MGMT IN EPENDYMOMA

6.1 Introduction

As highlighted in earlier chapters, paediatric ependymomas are regarded as chemoresistant (Grill, Pascal et al. 2003, Atkinson, Shelat et al. 2011). Despite several trials employing alkylating agents such as temozolomide (TMZ), procarbazine, decarbazine, nitrosoureas (lomustine / carmustine) and cyclophosphamide in ependymoma treatment (clinicaltrials.gov- NCT00826241, NCT00004028, NCT00005796); there is a paucity of studies confirming their therapeutic efficacy (Bouffet and Foreman 1999, Atkinson, Shelat et al. 2011). MGMT, also called O6-alkylguanine DNA alkyltransferase (AGT), repairs alkylated bases such as O6-alkylguanine induced by all the aforementioned drugs, by transferring the alkyl group from the alkylated base to its cysteine side chain within the catalytic pocket (as shown in Chapter 1, Figure 1.8). This restores the DNA structure and as a result inactivates MGMT (Pegg, Dolan et al. 1995, Xu-Welliver and Pegg 2002).

MGMT expression in several cancers has been associated with poor response to alkylating agents such as TMZ and thus, dismal prognosis (Jiang, Dong et al. 2014, Ogura, Tsukamoto et al. 2015, Walter, van Brakel et al. 2015). In ependymomas, one study on 17 patient samples reported that high MGMT protein expression correlated with an anaplastic phenotype (Buccoliero, Castiglione et al. 2008). This finding gave an indication that MGMT could be a possible contributing factor to chemoresistance exhibited by paediatric ependymomas. However, the prognostic value of MGMT expression in identifying high risk ependymoma patients still remains unelucidated.

MGMT promoter methylation has been found in 45% - 70% of high grade gliomas (Blanc, Wager et al. 2004, Stupp, Hegi et al. 2006) and has been proposed to be a common mechanism of MGMT loss. Clinical evidence suggests that patients with MGMT promoter methylation respond better to alkylating agents such as carmustine or TMZ in combination with radiotherapy (Hegi, Diserens et al. 2005, Hegi, Liu et al. 2008). So far, there have been few studies investigating MGMT promoter methylation levels in ependymomas. Studies by Buccoliero et al. and Koos et al. have reported an absence and low levels of MGMT promoter methylation in paediatric ependymomas respectively (Buccoliero, Castiglione et al. 2008, Koos, Peetz-Dienhart et al. 2010). However, the association between low MGMT promoter methylation and poor prognosis in ependymomas needs to be established.

Although MGMT has been proposed to be involved in resistance to several drugs, this chapter mainly focuses on its role in TMZ resistance. TMZ is an orally bioavailable alkylating agent employed to treat recurrent paediatric ependymoma as part of adjuvant treatment following surgery (Nicholson, Kretschmar et al. 2007, Lombardi, Pambuku et al. 2013) or salvage therapy after failure of surgery and radiotherapy (Komori, Yanagisawa et al. 2015). There is however, a lack of studies reporting any survival benefit from TMZ treatment (Chamberlain and Johnston 2009, Khoo, Kishima et al. 2013, Lombardi, Pambuku et al. 2013). Several MGMT inhibitors such as lomeguatrib (Ugur, Taspinar et al. 2014), disulfiram [clinicaltrials.gov: NCT01907165, (Paranjpe, Zhang et al. 2014)] and O6-Benzyl Guanine (06-BG) [clinicaltrials.gov: NCT00052780, (Konduri, Ticku et al. 2009)] have been employed in preclinical and clinical studies to improve response to TMZ. Preclinical studies on murine paediatric brain tumours (low grade gliomas, medulloblastomas and ependymomas) showed that 06-BG could potentiate response to TMZ and lomustine (Bobola, Silber et al. 2005). However, results from a phase-II clinical

trial employing 06-BG to treat TMZ-resistant GBM showed lack of tumour regression as well as high incidence of haematological side-effects (Quinn, Pluda et al. 2002, Quinn, Jiang et al. 2009). Several novel TMZ analogues designed to circumvent MGMT induced resistance have shown promise as alternative single agents to treat glioblastoma and medulloblastoma cell lines (Zhang, Stevens et al. 2010, Othman, Kimishi et al. 2014). However, their efficacy in ependymoma treatment needs to be determined.

This chapter assesses the expression pattern of MGMT in publicly available ependymoma datasets and its prognostic value in stratifying ependymoma patients into clinically relevant groups. Furthermore, retrospective analyses to assess MGMT promoter hyper-methylation status are performed and the prognostic value of this status in stratifying ependymoma patients is also determined. Finally, the efficacy of a MGMT circumventing new N3-propargyl analogue of TMZ in inducing cytotoxicity in in vitro models of ependymoma is assessed in this study.

6.2 Results

6.2.1 MGMT expression was higher in paediatric ependymoma patients in comparison to adults.

MGMT expression has been correlated with poor response to chemotherapy and hence, poor prognosis in several cancers (Jiang, Dong et al. 2014, Ogura, Tsukamoto et al. 2015, Walter, van Brakel et al. 2015). Its involvement in resistance to several DNA alkylating drugs employed in ependymoma adjuvant treatment (Bouffet and Foreman 1999, Wright and Gajjar 2012) indicates that MGMT expression might be one of the factors underlying its chemoresistant behaviour.

In order to assess MGMT gene expression in ependymoma patients, analysis of 3 aforementioned publicly available paediatric ependymoma datasets was performed.

As depicted in Figure 6.1, MGMT expression was significantly higher in paediatric patients in comparison to adults in the Gilbertson (a, Spearman correlation co-efficient=-0.36, P=0.001) and the Mack datasets (c, Spearman correlation co-efficient=-0.25, P=0.01) whilst in the Witt dataset, no significant association with age was recorded (b, Spearman correlation co-efficient=-0.14, P=0.23). These results therefore, suggested that MGMT expression was higher in paediatric ependymoma patients than adults and may therefore represent one of the mechanisms contributing to chemoresistance in them.

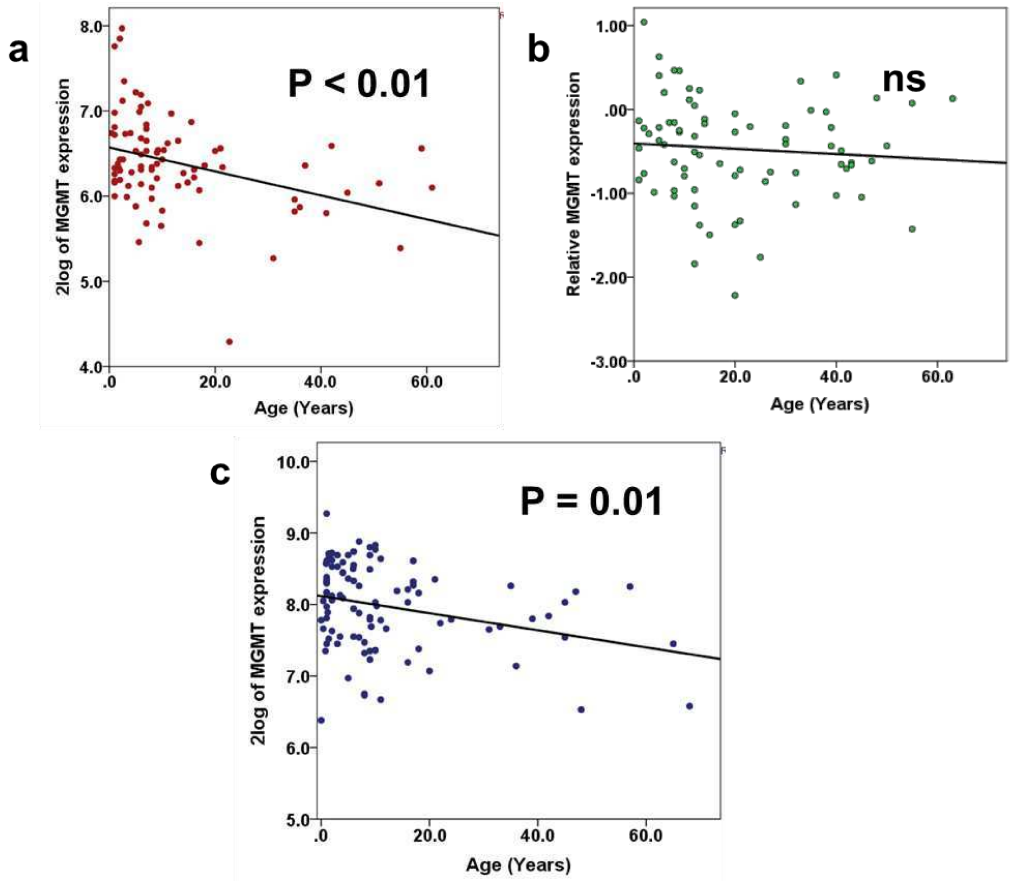


Figure 6.1 MGMT expression was higher in paediatric ependymoma patients in comparison to adults a. MGMT expression was significantly higher in children in comparison to adults in the Gilbertson dataset (Spearman correlation co-efficient=-0.36, P=0.001). **b.** Although MGMT was expressed in children in the Witt dataset; there was no significant association with patient age (Spearman correlation co-efficient=-0.14, P=0.23). **c.** In the Mack dataset, there was a negative correlation between MGMT expression and patient age (Spearman correlation co-efficient=-0.21, P=0.01).

6.2.2 MGMT gene expression was marginally higher in PF tumours in comparison to ST and SP ependymomas.

Ependymomas tend to recapitulate site specific expression profiles and were also recently classified into 3 main groups on the basis of their locations (Pajtler, Witt et al. 2015). The differential expression of MGMT across the 3 ependymoma locations [Posterior Fossa (PF), Spinal (SP) and Supratentorial (ST)] in the CNS was therefore assessed in the aforementioned publicly available datasets.

In the Gilbertson dataset (Figure 6.2 a), MGMT was highly expressed in PF tumours in comparison to SP tumours [MD=0.434 (95% CI=0.12 to 0.747)] and ST tumours [MD=0.468 (95% CI=0.01 to 0.49)]. In the Mack dataset (Figure 6.2 c), although MGMT was highly expressed in PF tumours compared to SP tumours [MD=0.58 (95% CI=0.33 to 0.82)]; there was no significant difference in MGMT expression between PF and ST tumours in this dataset. Finally in the Witt dataset (Figure 6.2 b), there was no correlation between MGMT expression and tumour location. From these results, it could not be inferred that MGMT underlies chemoresistance specifically in PF ependymomas. Similar analyses need to be performed on more independent ependymoma gene expression datasets in order to confirm association with PF tumours.

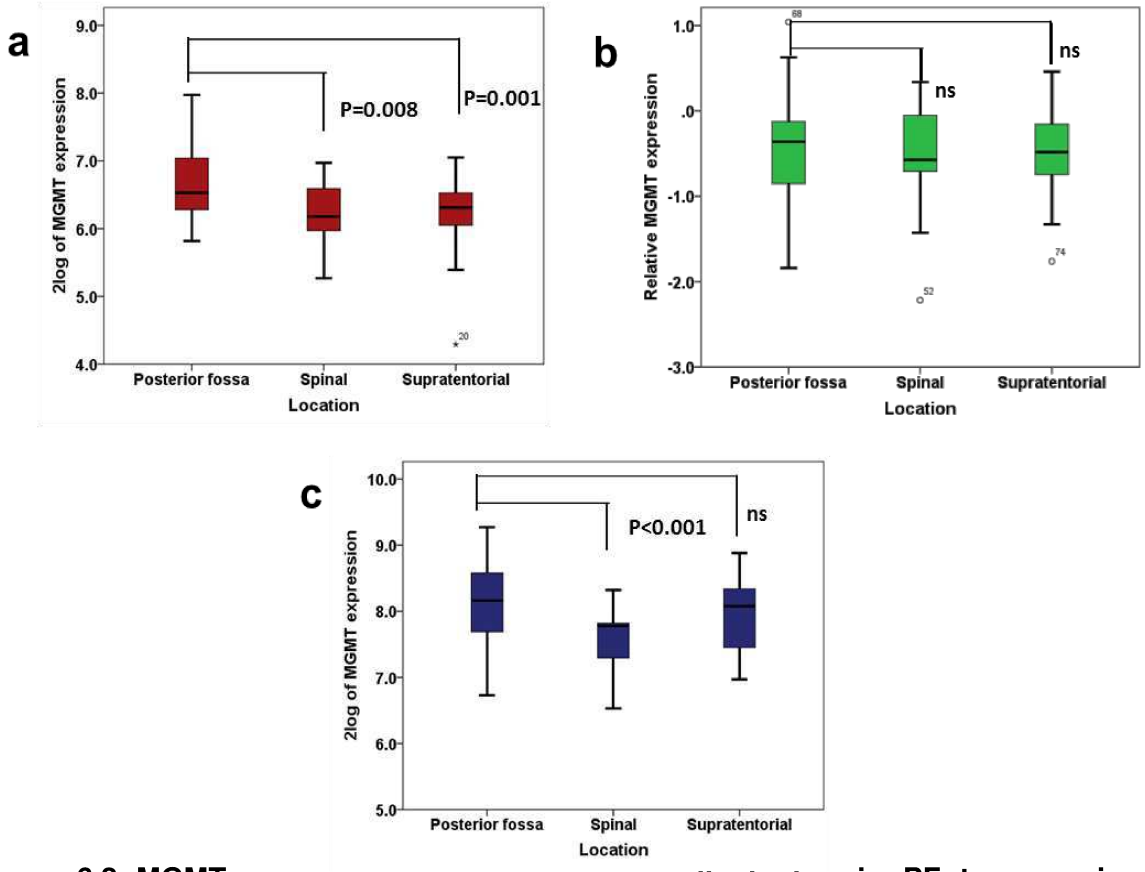


Figure 6.2 MGMT gene expression was marginally higher in PF tumours in comparison to ST and SP ependymomas a. In the Gilbertson dataset, MGMT expression was significantly higher in PF tumours in comparison to SP and ST tumours. **b.** In the Witt dataset, there was no significant association between MGMT expression and tumour location. **c.** In the Mack dataset, PF tumours expressed significantly higher MGMT levels, only in comparison to SP tumours. The points highlighted in the figures represent patient samples numbers of outliers assigned by the SPSS Version 21.

6.2.3 Paediatric ependymomas had low levels of MGMT promoter methylation.

DNA methylation refers to the covalent addition of a methyl group to the 5'-carbon of cytosine in a CpG dinucleotide; methylation of CpG islands in the promoter region of genes leads to suppression of transcription and subsequently gene expression. Aberrant methylation has been implicated in diseases such as cancer, multiple sclerosis, diabetes, and schizophrenia (Plass 2002, Poetsch and Plass 2011).

Promoter hyper-methylation is regarded as a common mechanism of MGMT loss in gliomas accounting for 45% - 70% cases (Blanc, Wager et al. 2004, Stupp, Hegi et al. 2006) and has been correlated with improved survival due to the resultant enhanced response to alkylating agents (Hegi, Diserens et al. 2005, Hegi, Liu et al. 2008). As mentioned in section 6.1, there have been very few studies which have assessed MGMT methylation levels in ependymoma. So far, most studies have either reported low or completely absent MGMT promoter methylation in ependymoma patients (Michalowski, de Fraipont et al. 2006, Buccoliero, Castiglione et al. 2008, Koos, Peetz-Dienhart et al. 2010). The findings of these studies are consistent with the results displayed in section 6.2.1 which suggest that the MGMT gene was expressed in paediatric ependymoma patients.

In order to validate the findings, retrospective analysis of global methylation data of 103 paediatric ependymoma patient samples produced by Rogers et al. using the GoldenGate Cancer Panel I assay (Illumina) was performed (Rogers, Kilday et al. 2012). This study assessed the methylation profiles of 73 primary and 25 recurrent tumours, out of which 53% were PF, 23% were ST and 15% were SP ependymomas. This cancer panel employed in this study assesses methylation status of 1,505 CpG loci of 807 genes implicated in cancer. Relative ratios of probe signals of tumour samples to normal controls

are expressed as β values. In this analysis, probes with β values ≤0.2 were considered hypo-methylated & β-values ≥0.8 were considered hyper-methylated (Rogers, Kilday et al. 2012).

For the two MGMT methylation probes MGMT_P272R & MGMT_P281_F, mean β values across the patient dataset were 0.04 (SEM±0.001) and 0.008 (SEM±0.001) respectively (depicted in Figure 6.3). In other words, the MGMT gene was hypo-methylated in this paediatric ependymoma dataset. The association between low / absent promoter methylation and MGMT gene/protein expressed has not been assessed so far. Due to the lack of corresponding MGMT gene expression data for the Rogers dataset, a correlation between MGMT methylation and gene expression results could not be made in this study. However, a few paraffin embedded ependymoma samples from 8 patients belonging to the Rogers dataset were available, allowing IHC analysis to be carried out. 6/8 available patients from this dataset exhibited nuclear expression of the MGMT protein (as depicted in Figure 6.5a). This result was consistent with the low levels of MGMT promoter methylation. Factors such as loss of chromosome 10 or post-translational modification may underlie the MGMT negative status of the 2/8 ependymoma patients.

Validation of these results, as well as correlation with MGMT gene/protein expression in a discrete methylation dataset is essential to further validate the assumption that MGMT promoter methylation is a common mechanism of MGMT loss in ependymoma.

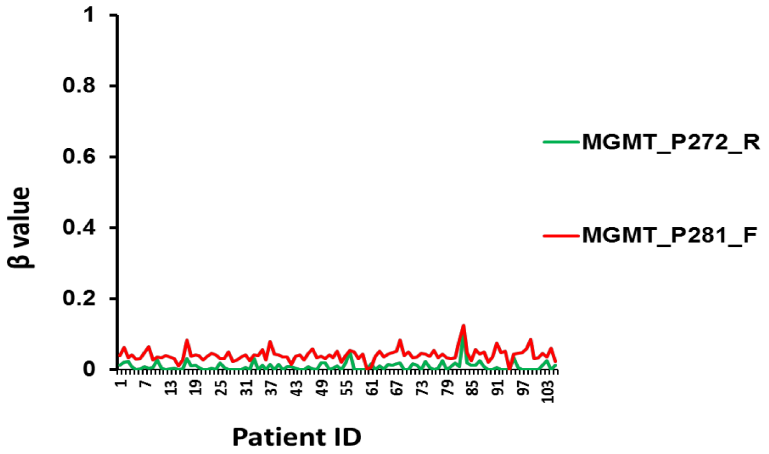


Figure 6.3 Low MGMT promoter methylation levels in ependymoma Retrospective analysis of global methylation profiling performed by Rogers et al. (Rogers, Kilday et al. 2012) using the GoldenGate Cancer Panel I assay (Illumina) showed low levels of MGMT promoter methylation as depicted in the figure above. In this analysis, probes with β values ≤0.2 were considered hypo-methylated. The mean β values for the two MGMT methylation probes (MGMT_P272R & MGMT_P281_F) were 0.04 (SEM±0.001) and 0.008 (SEM±0.001) respectively. Therefore, the MGMT gene was hypo-methylated in this paediatric ependymoma dataset

6.2.4 MGMT promoter methylation correlated with a favourable prognosis in adults with PF ependymoma.

In order to investigate the methylation status of MGMT in ependymomas in an independent dataset, global methylation data (using the Illumina Infinium 450K array) on 48 (paediatric and adult) PF ependymomas was downloaded and processed from GEO (GEO number: GSE43353) by Dr. A. Lourdasamy. This data was produced in a study by Mack et al., which utilised global methylation profiling to stratify PF ependymomas into clinically relevant subgroups (Mack, Witt et al. 2014).

As depicted in Figure 6.4, in agreement with the study by Koos et al., paediatric ependymoma patients in the Mack methylation dataset, exhibited low MGMT methylation levels; although not as low as those

recorded in the Rogers dataset (depicted in section 6.2.3). Moreover, these methylation levels were significantly lower in children in comparison to adult PF ependymomas. [MD=0.69 (95% CI=0.03-0.1), P=0.005]. This finding was consistent with the results displayed in section 6.2.1 which show that paediatric ependymomas had a significantly higher MGMT expression in comparison to adults; indicating that MGMT could be a resistance mechanism mainly viable in paediatric patients.

Furthermore, when correlated with survival, low MGMT promoter methylation was significantly associated with reduced EFS (5-year EFS: 43.5% vs. 100%, P=0.01) and OS (5-year OS: 60% vs. 100%, P=0.02) in children as depicted in Figure 6.4, b and c respectively. These results indicated that MGMT promoter methylation was of definite prognostic value in PF ependymomas. It is however, essential to highlight that out of the 48 patients with PF ependymomas in this study; the survival information was available only for 25 patients. Therefore, these findings need to be validated on a larger ependymoma methylation dataset, also consisting of tumours originating from SP and ST locations.

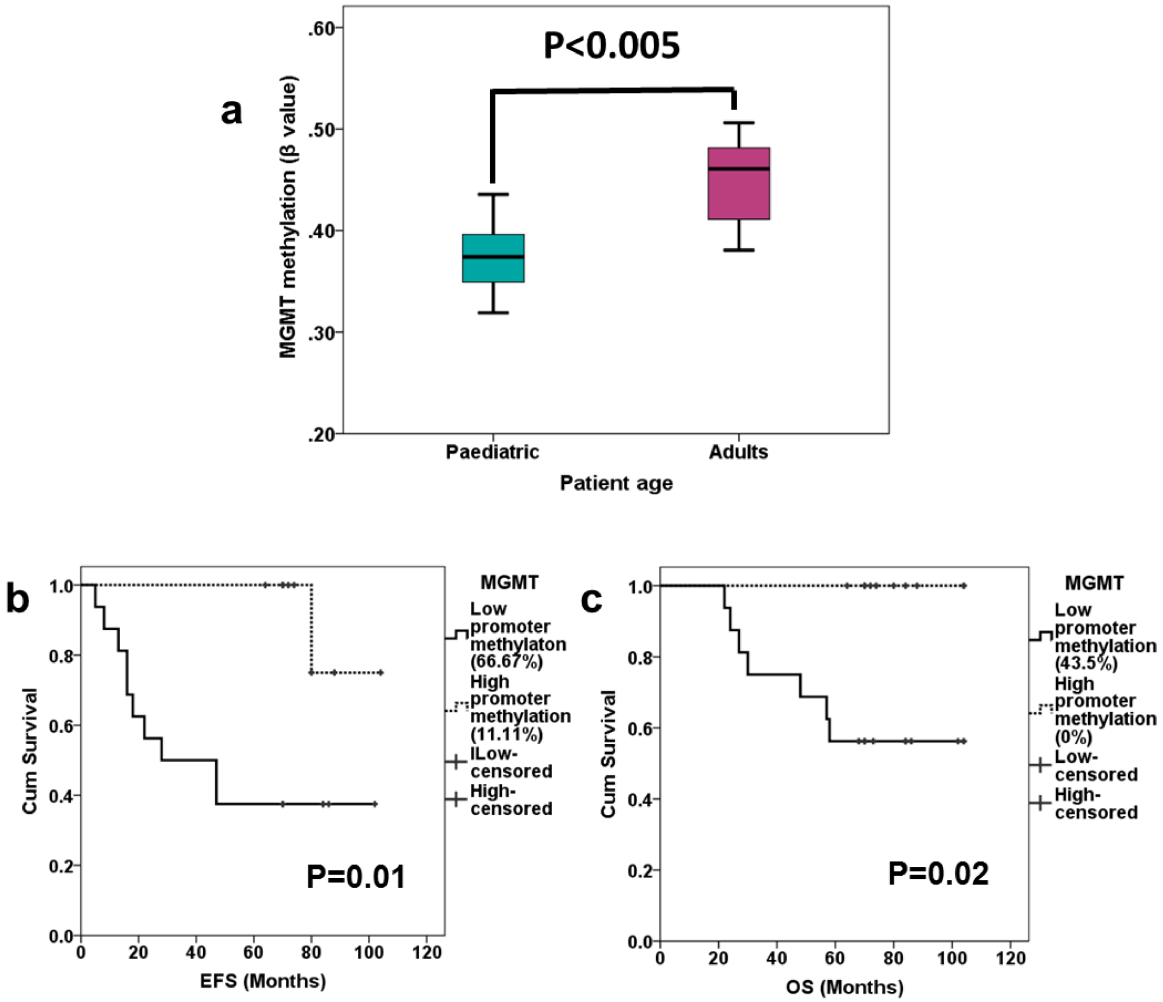


Figure 6.4 Paediatric ependymomas showed low levels of MGMT promoter methylation which was associated with poor prognosis Retrospective analysis of global methylation data of 48 ependymomas produced by Mack et al. (Mack, Witt et al. 2014), was analysed using IBM SPSS **a.** MGMT promoter methylation in paediatric patients was significantly lower in comparison to adults [MD= 0.69 (95% CI= 0.03-0.1), P=0.005]. β values were split into 'high' (above median) and 'low' (below median) to stratify patients in order to produce Kaplan-Meier survival curves. Patients with a low promoter methylation had a significantly lower **b.** EFS (5-year EFS: 43.5% vs. 100%, P= 0.01) and **c.** OS (5-year OS: 60% vs. 100%, P= 0.02) in comparison to patients with high MGMT promoter methylation

6.2.5 MGMT expression predicted poor prognosis in the chemotherapy-led CNS9204 trial by univariate analysis.

There have been several studies providing conflicting results regarding the prognostic value of MGMT protein expression in cancer (Chang, Hsu et al. 2013, Oliver, Ortiz et al. 2014, Schmitt, Pavel et al. 2014, Yang, Wang et al. 2014, Asiaf, Ahmad et al. 2015). So far it has been demonstrated in this study that MGMT could be one of the factors underlying chemoresistance in paediatric ependymomas owing to lack (section 6.2.3) / low levels (section 6.2.4) of promoter methylation and as a result, maintained MGMT gene (section 6.2.1) / protein (section 6.2.3) expression. Since the MGMT protein expression has been reported in anaplastic ependymomas (Buccoliero, Castiglione et al. 2008), its prognostic value in identifying high-risk paediatric ependymoma patients was elucidated in this study.

In order to investigate the prognostic value of MGMT protein expression in patients less than 3 years of age, TMAs from the aforementioned chemotherapy-led CCLG 1992 04 (CNS9204) trial cohort were screened.

When the patient samples were stained for MGMT expression using immunohistochemistry (IHC), 48.8% (21/43) patients were found to be MGMT positive and samples were scored as a binary variable (positive or negative). Unlike ABCB1 and BLBP wherein 53 samples were assessed; owing to core loss, only 43 samples could be analysed for MGMT protein expression in this cohort. When nuclear MGMT expression (as depicted in Figure 6.5 b) was analysed for correlation with clinical outcome, MGMT positive patients had a significantly lower overall survival (5-year OS: 45% vs. 76%, P=0.01) whilst there was no significant correlation with event-free survival (5-year EFS: 25% vs. 38%, P=0.23) in this trial cohort.

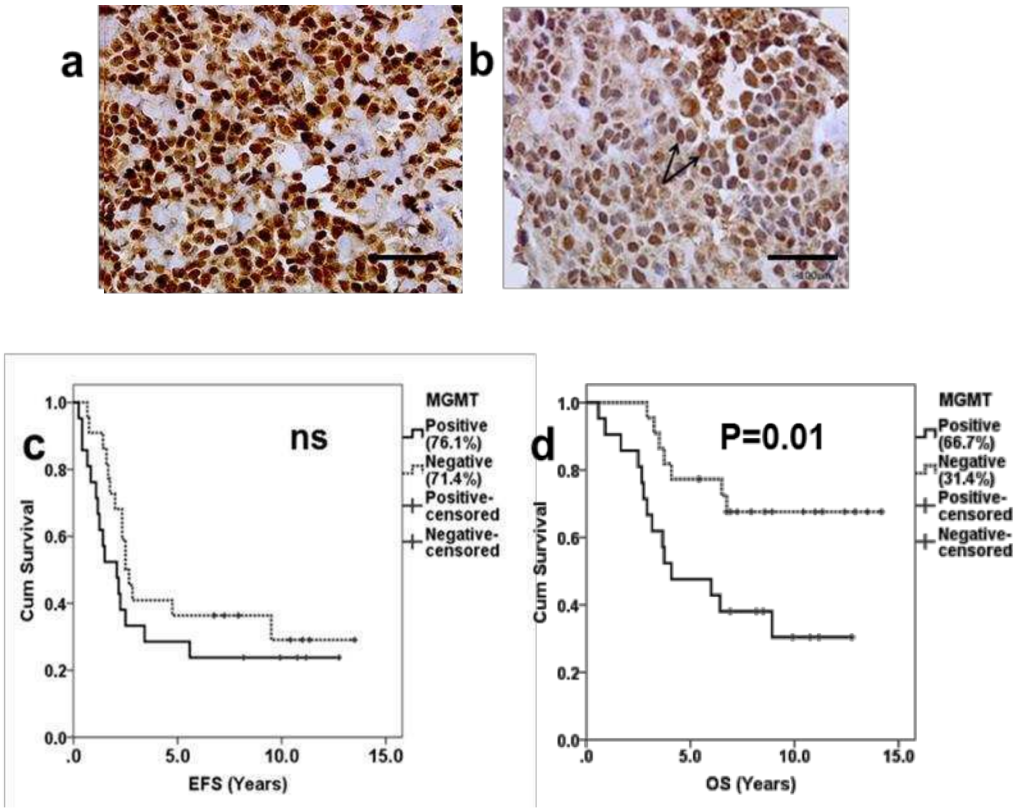


Figure 6.5 Nuclear expression of MGMT correlated with reduced survival in the chemotherapy-led CNS9204 trial a. MGMT expression was optimised using IHC on a human tonsil tissue. **b.** Nuclear expression of MGMT in ependymoma showed no correlation with **c.** event-free survival (5-year EFS: 25% vs. 38%, P = 0.23); but was associated with significantly reduced **d.** overall survival (5-year OS: 45% vs. 76%, P = 0.01). (Scale bars represent 50 µm.)

Since the majority of patients in this cohort had PF tumours; it was difficult to establish a correlation between MGMT expression and tumour location. There was no correlation between MGMT expression and resection status or gender of patients. However, a significant association with tumour grade was established (Chi-square test, P=0.04); with 68% of MGMT negative patients having Grade II or less aggressive tumours. But, due to variability in ependymoma patient outcome across and within grades (Ellison, Kocak et al. 2011), it is difficult to draw any robust conclusions from this finding.

In order to measure the feasibility of MGMT as an independent marker of reduced OS in paediatric ependymoma patients; it was introduced in a Cox-regression multivariate model with confounding

factors such as complete surgical resection, tumour location and WHO grade. As displayed in Table 6.1, after being corrected for the aforementioned confounding factors, MGMT protein expression could not independently predict OS in infants with ependymoma in the CNS9204 cohort.

Table 6.1 Multivariate analysis of MGMT expression in the CNS9204 trial

Survival	Factor	Hazard Ratio (95% CI)	P value
Overall Survival (OS)	**MGMT expression (Positive vs. Negative)**	**2.35 (0.87-6.37)**	**0.09**
	Location (PF vs ST)	1657310.538 (0.00-)	0.98
	Resection (Incomplete vs. Complete)	1.74 (0.68 – 4.45)	0.25
	WHO Grade (Grade III vs. Grade II)	2.32 (0.51-3.55)	0.53

From these results, it was deduced that MGMT was not an independent marker of reduced OS in the CNS9204 trial. Since it was possible to assess only 43 patients in this study owing to TMA core loss; these results need to be validated in other such chemotherapy-led infant ependymoma trial cohorts.

6.2.6 MGMT expression predicted poor prognosis in the radiotherapy-led CNS9904 trial.

In order to assess the prognostic value of MGMT in older paediatric patients who received adjuvant radiotherapy following surgery, samples from the radiotherapy-led SIOP Ependymoma I (CNS9904) trial were stained for MGMT expression using IHC.

In this trial cohort, 56.1% (23/41) of patients were MGMT positive. As shown in Figure 6.6, MGMT expression was associated with significantly reduced EFS (5-year EFS: 12% vs. 47%, P=0.007) and OS (5-year OS: 36.4% vs. 82.3, P<0.001). These results are consistent with recent studies which demonstrated the poor prognostic value of MGMT expression in glioma patients who exclusively received adjuvant radiotherapy following surgery (Jiang, Dong et al. 2014). There have also been recent reports which associate MGMT expression with radioresistance in in vitro models of gliomas (He, Shan et al. 2011) and breast cancer (Chen, Zhang et al. 2015); suggesting that MGMT expression is an indication of an aggressive tumour phenotype rather than exclusively a chemoresistance mechanism

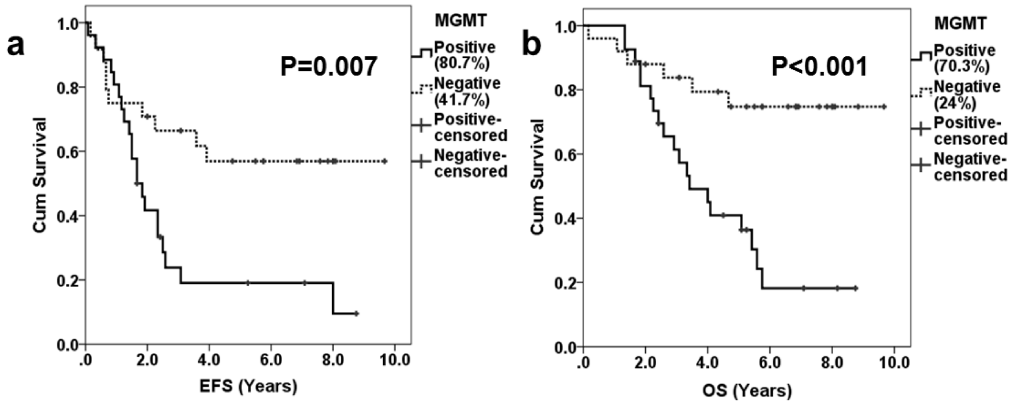


Figure 6.6 Nuclear expression of MGMT correlated with reduced survival in the radiotherapy-led CNS9904 trial Nuclear expression of MGMT in ependymoma was associated with significantly reduced **a.** event-free survival (5-year EFS: 12% vs. 47%, P=0.007) and **b.** overall survival (5-year OS: 36.4% vs. 82.3%, P<0.001).

Table 6.2 Multivariate analysis of MGMT expression in the CNS9904 trial

Survival	Factor	Hazard Ratio (95% CI)	P value
	MGMT expression (Positive vs. Negative)	**2.513 (0.97-6.48)**	**0.05**
Event-free Survival (EFS)	Location (PF vs. ST)	1.41 (0.57-3.48)	0.45
	Resection (Incomplete vs. Complete)	2.69 (1.03-6.98)	0.04
	WHO Grade (Grade III vs. Grade II)	2.71 (0.95-7.72)	0.06
	MGMT expression (Positive Vs. Negative)	**4.43 (1.19-16.4)**	**0.02**
Overall Survival (OS)	Location (PF vs. ST)	1.43 (0.50-4.04)	0.49
	Resection (Incomplete vs. Complete)	2.02 (0.68-6.05)	0.20
	WHO Grade (Grade III vs. Grade II)	3.81 (1.16-12.44)	0.02

In this trial cohort, MGMT expression did not significantly correlate with tumour grade, resection status, location or gender of patients. In order to assess the potential of MGMT as an independent prognostic marker, it was introduced in the Cox-regression multivariate hazards-ratio model. As displayed in Table 6.2, after being corrected for the same confounding factors as mentioned in section 6.2.5, MGMT positive patients were almost 2.5 times more susceptible to having an event (relapse or death) (P=0.05) and 4.43 times more likely to die (P=0.02) in comparison to those who were MGMT negative.

These results indicated that MGMT was an independent marker of reduced survival in older paediatric patients in the radiotherapy-led CNS9904 cohort, further supporting the putative role of MGMT in radioresistance

6.2.7 MGMT, MLH1 and MSH6 expression across ependymoma derived cell lines and stem cell enriched neurospheres.

So far it was demonstrated in this study that MGMT was expressed in paediatric ependymoma patients and that its expression was indeed associated with reduced patient survival times. In order to investigate its potential role in chemoresistance in in vitro models of ependymoma; western blotting analysis was performed to assess MGMT protein expression in 3 ependymoma derived cell lines (BXD-1425EPN, EPN1 and DKFZ-EP1).

As depicted in Figure 6.7, only the EPN1 cell line did not express MGMT. This was consistent with the finding of Chapter 3, section 3.2.3, which showed that MGMT was neither expressed in the original patient tumour nor in the orthotopic mouse ependymoma from which the EPN1 cell line was derived.

As mentioned before, this chapter predominantly focuses on role of MGMT in TMZ resistance. Since the response to TMZ also depends upon a proficient mismatch repair (MMR) pathway; the protein expression of 2 MMR pathway enzymes, MLH1 and MSH6 was also assessed. BXD-1425EPN and DKFZ-EP1 cell lines expressed both the aforementioned enzymes respectively whilst EPN1 did not express MLH1. On the basis of these results it could be predicted that the BXD-1425EPN and DKFZ-EP1 would be resistant to TMZ treatment owing to their positive MGMT expression status. In the case of EPN1, the TMZ induced toxic O6-MG lesion would remain due to the lack of MGMT expression. However, due to an inefficient MMR pathway; this lesion would not be recognised, subsequently leading to the acquisition of a hypermutator phenotype as demonstrated in low-grade gliomas (van Thuijl, Mazor et al. 2015), where loss of MLH1 was associated with increased possibility of developing of secondary tumours.

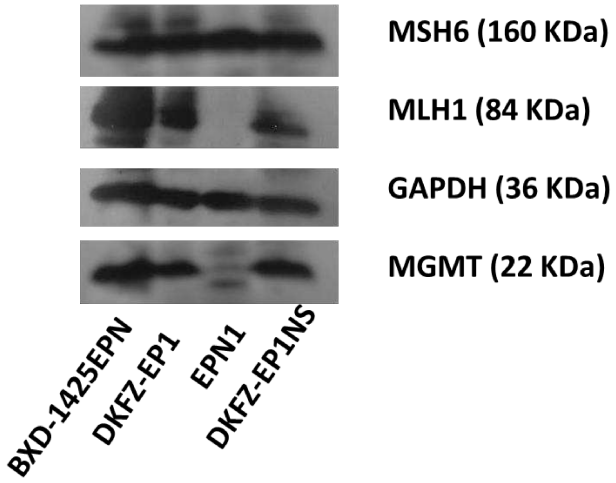


Figure 6.7 Protein expression of MGMT and MMR pathway enzymes (MLH1 and MSH6) in ependymoma cell lines and stem cell enriched neurospheres BXD-1425EPN and DKFZ-EP1 cell lines expressed MGMT as well as MMR enzymes, MLH1 and MSH6 whilst the EPN1 cell line did not express MGMT nor MLH1. The neurospheres (DKFZ-EP1NS) derived from the DKFZ-EP1 cell line maintained the MGMT and MMR enzymes expression profile of the parent cell line. (Representative blots of n=3 assays.)

The role of CSCs in chemoresistance in ependymoma was investigated in this study; the expression of each of the three aforementioned proteins in the stem cell enriched neurospheres (DKFZ-EP1NS) derived from the DKFZ-EP1 cell line was also evaluated. The MGMT and MMR pathway expression profile of DKFZ-EP1NS neurospheres was identical to the parent cell line (DKFZ-EP1) as depicted in Figure 6.7. This was consistent with MGMT staining in 70-80% of the tumour cells in a patient sample stained by IHC (Figure 6.5b), in contrast to a sub-population of cells which was witnessed in the case of BLBP and ABCB1. In other words, the MGMT resistance mechanism was maintained in both CSCs as well as differentiated tumour cells making them both TMZ refractory. Since, it was not possible to easily maintain EPN7 and EPN7R in culture, these analyses could not be performed on them. In the subsequent sections, the predictions made above regarding the response to TMZ by carrying out cytotoxicity assays on all 3 cell lines and ependymoma stem cells are validated.

6.2.8 All ependymoma derived cell lines exhibited resistance to TMZ.

In order to validate the role of MGMT and MMR pathway in response to TMZ; MTT cytotoxicity assays were carried out on BXD-1425EPN, DKFZ-EP1 and the EPN1 cell lines. As depicted in Figure 6.8, all 3 cell lines used in this study were TMZ resistant since they showed little cytotoxic response up to 500 μM of the drug. In the case of the DKFZ-EP1 cell line, the IC_{50} was established at 469 μM (SEM±20.29 μM) which is comparable to what is achieved in gliomas, known to be TMZ resistant (Zhang, Wang et al. 2015). This concentration is also 10 times the peak plasma concentration (ppc) achieved in patients (~52 μM) (Milde, Kleber et al. 2011).

As shown in section 6.2.7, BXD-1425EPN and DKFZ-EP1 cell lines both expressed MGMT protein, which was consistent with their

TMZ refractory behaviour. EPN1 on the other hand, not only lacked MGMT expression but failed to have a proficient MMR pathway which could underlie the resistance to TMZ. It is however, also essential to highlight that due to lack of a MMR proficiency, a TMZ induced toxic O6-MG lesion would induce mutagenicity and lead to acquisition of a hypermutator phenotype in the EPN1 cell line as described by Thuijl et al. in low-grade gliomas (van Thuijl, Mazor et al. 2015). Further experiments involving mass spectrometry would be necessary to confirm this proposed retention of the O6- MG lesion in the EPN1 cell line as a result of exposure to TMZ.

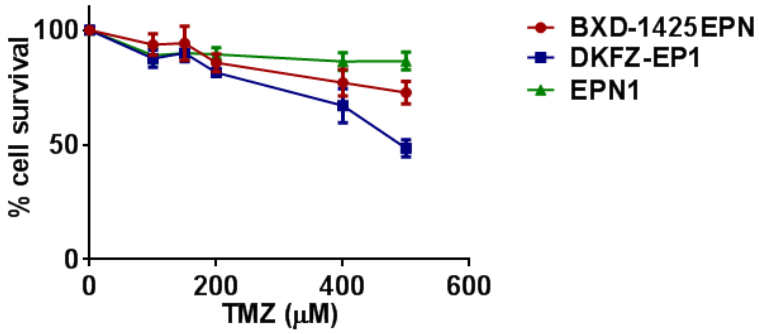


Figure 6.8 Ependymoma cell lines were TMZ resistant Cytotoxic effect of TMZ was measured by the MTT metabolic assay to produce the dose response curves displayed above. IC50 (concentration to kill 50% cells) was not achieved in the BXD-1425EPN and EPN1 cells over quite a wide concentration range (100-500 μM) of TMZ. In the DKFZ-EP1 cell line, a mean IC_{50} of 469 μM (SEM±20.29 μM) was recorded which was approximately 10 times above the ppc achieved in patients. (n=3)

These results indicated that all ependymoma cell lines employed in this study were TMZ resistant. Furthermore, it also highlighted the need to assess the MGMT as well as MMR status of a patient prior to TMZ treatment to predict response and to prevent TMZ-induced mutagenicity in ependymoma.

6.2.9 Ependymoma cell lines were sensitive to the MGMT circumventing N3-propargyl analogue of TMZ.

All 3 cell lines used in this study were TMZ resistant (section 6.2.8). Additionally, TMZ would also be expected to induce a mutagenic effect on the EPN1 cell line, due to MMR deficiency. Zhang et al. and Othman et al. demonstrated that novel analogues of TMZ could circumvent MGMT induced resistance and induce toxicity in glioblastoma and medulloblastoma cell lines respectively (Zhang, Stevens et al. 2010, Othman, Kimishi et al. 2014).

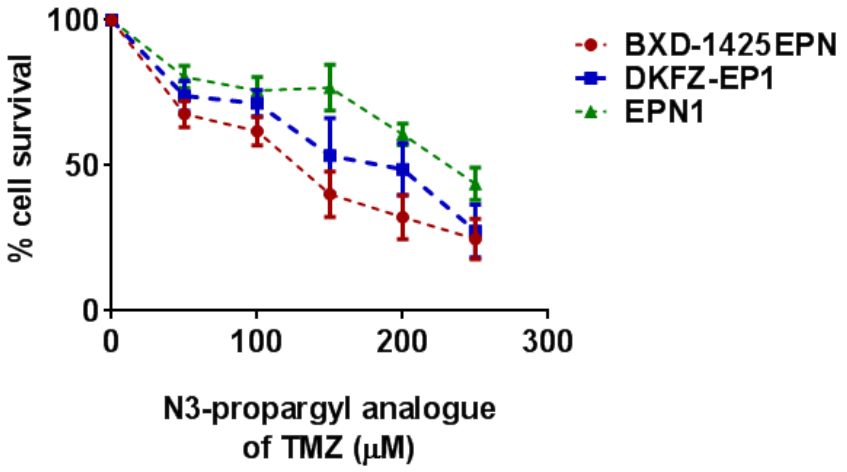


Figure 6.9 MGMT circumventing N3-propargyl analogue of TMZ induced cytotoxicity in ependymoma cell lines Cytotoxic effect of N3-propargyl analogue of TMZ was measured by the MTT metabolic assay to produce the dose response curves displayed above. IC_{50} values for BXD1425EPN, DKFZ-EP1 and EPN1 cell lines were established at 133 µM (S.E-6.021 µM), 185 µM (SEM±25.88 µM) and 223 µM (SEM±12.81 µM) respectively. (n=3)

We therefore sought to investigate if the novel N3-propargyl analogue of TMZ was able to toxicity in ependymoma cell lines by carrying out the MTT assay, to produce the dose response curves depicted in Figure 6.9. The IC_{50s} established for BXD-1425EPN, DKFZ-EP1 and EPN1 cell lines were 133 µM (SEM±6.021 µM), 185 µM (SEM±25.88 µM) and 223 (SEM±12.81 µM) respectively.

From these results it was inferred that the N3-propargyl analogue was effective at inducing toxicity in ependymoma cell lines by circumventing MGMT repair. Furthermore, since it also induced toxicity in the EPN1 cell line which was MMR deficient, it could also be concluded that the cytotoxic effect of N3-propargyl was also independent of proficient MMR repair. These findings highlighted the potential of the N3-propargyl analogue as an effective option for treatment of paediatric ependymoma patients.

6.2.10 Resistance to TMZ and sensitivity to the N3-propargyl analogue was maintained in ependymoma stem cells.

In contrast to the study by Meco et al., which demonstrated that there was a downregulation in MGMT expression in ependymoma derived neurospheres (NS), it was shown in this study that the DKFZ-EP1NS neurospheres maintained the MGMT and MMR expression profiles of the DKFZ-EP1 cell line from which they were derived, as discussed in section 6.2.7. Furthermore, Meco et al. also reported an improved sensitivity to TMZ in neurospheres due to downregulation in MGMT expression (Meco, Servidei et al. 2014).

In order to assess the response to TMZ as well as its N3-propargyl analogue in stem cells, a stem cell relevant clonogenic assay on the BXD-1425EPN cell line and a spheroid assay in the DKFZ-EP1NS neurospheres were performed. As depicted in Figure 6.10, the BXD-1425EPN cell line was resistant to TMZ whilst the IC_{50} in response to the N3-propargyl analogue was established at 26.83 µM (SEM±0.75 µM). In other words, the CSCs retained their response profile to TMZ and indeed, there was 4-fold increase in sensitivity to the N3-propargyl analogue in comparison to the tumour bulk (IC_{50}-133 µM established in an MTT assay) as discussed in sections 6.2.8 and 6.2.9 respectively. Since we could not establish neurospheres from this cell line, the MGMT and MMR enzymes expression status of the CSC component could not be determined.

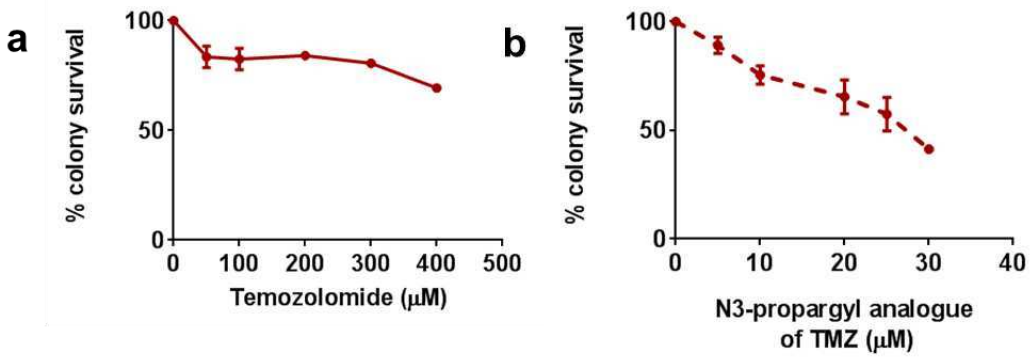


Figure 6.10 BXD-1425EPN cell line exhibited resistance to TMZ and sensitivity to the N3-propargyl analogue of TMZ in a stem cell relevant clonogenic assay In a stem cell relevant clonogenic assay, the MGMT expressing and MMR pathway proficient BXD-1425EPN cell line exhibited resistance to a. TMZ with IC_{50} not being achieved up to the concentration of 400 μM; whilst IC_{50} to the b. N3-propargyl analogue was established at 26.83 μM (SEM ±0.75 μM)

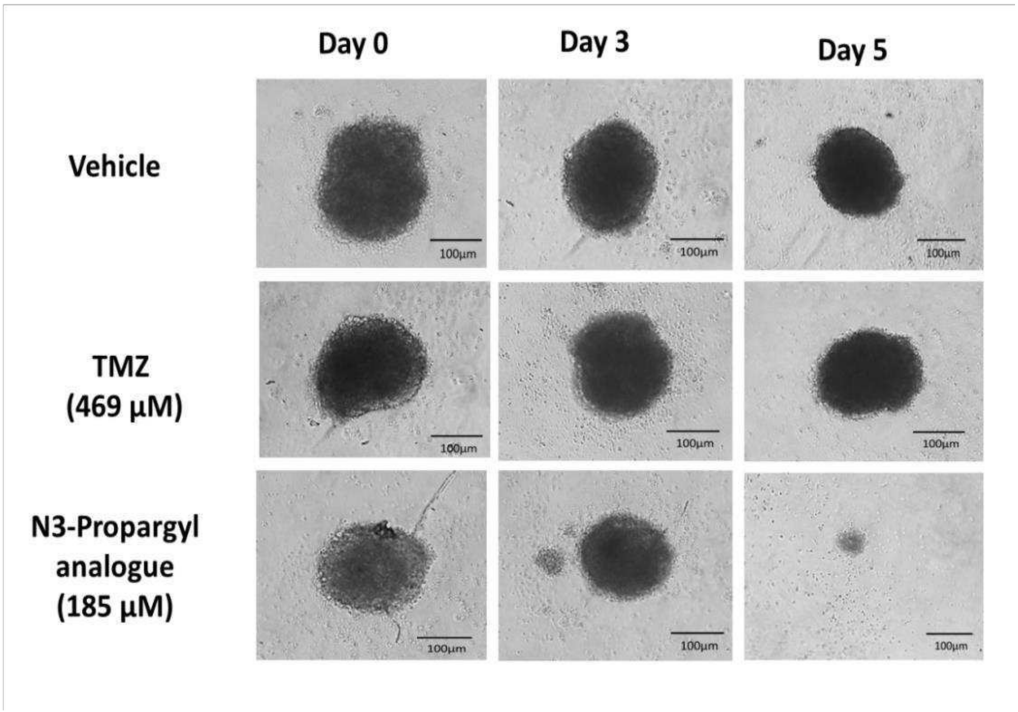


Figure 6.11 Stem cell enriched DKFZ-EP1NS are TMZ resistant but sensitive to the N3-propargyl analogue When the stem cell enriched DKFZ-EP1NS neurospheres were treated with the IC_{50} concentrations for TMZ (460 μM) and N3-propargyl analogue (170 μM) established in the MTT assay as depicted in sections 6.2.8 and 6.2.9, the TMZ treated neurosphere remained unchanged in phenotype whilst the N3-propargyl analogue disappeared.

As depicted in Figure 6.11, DKFZ-EP1NS neurospheres were treated with IC_{50} concentrations for TMZ and N3-propargyl analogue established in the DKFZ-EP1 cell line as described in sections 6.2.8 and 6.2.9 respectively. The stem cell enriched spheroids exhibited very little difference in phenotype after treatment with TMZ whilst the spheroid was completely destroyed after propargyl treatment. Since it was difficult to re-establish neurospheres at this point in this study, these results could not be repeated. But, this experiment provided us with an indication of the nature of response to TMZ and the N3-propargyl analogue in the DKFZ-EP1NS neurospheres.

These results indicated that, in contrast to results by Meco et al., ependymoma stem cells in this study maintained MGMT expression. As a result, they were TMZ resistant. However, sensitivity to MGMT circumventing N3-propargyl analogue was enhanced.

6.3 Summary

- Paediatric ependymoma patients expressed higher levels of MGMT in comparison to adults.
- MGMT expression was highest in posterior fossa ependymomas in the Gilbertson and Mack datasets.
- The MGMT gene promoter was hypo-methylated in paediatric ependymoma patients in the Rogers dataset.
- In PF ependymomas, MGMT promoter methylation was significantly lower in paediatric patients in comparison to adults. This low level of MGMT promoter methylation in paediatric patients was significantly associated with poor prognosis.

- In the chemotherapy-led CNS9204 trial, MGMT protein expression was significantly associated with reduced overall survival by univariate analysis.

- In the radiotherapy-led CNS9904 trial, MGMT protein expression was an independent marker of reduced survival.

- By western blotting analysis, paediatric ependymoma derived BXD-1425EPN and DKFZ-EP1 cell lines expressed MGMT and MMR enzymes, MLH1 and MSH6. The stem cell enriched DKFZ-EP1NS neurospheres, maintained the MGMT and MMR expression profiles of the DKFZ-EP1 cell line from which they were derived. The EPN1 cell line did not express MGMT and MLH1; therefore was both MGMT and MMR pathway deficient.

- Ependymoma derived cell lines were resistant to TMZ but exhibited sensitivity to the novel MGMT circumventing N3-propargyl analogue of TMZ in an MTT assay.

- Ependymoma stem cells remained resistant to TMZ; whilst they exhibited an elevated sensitivity to the N3-propargyl analogue in comparison to monolayers.

CHAPTER 7. DISCUSSION AND FUTURE WORK

7.1 Introduction

Ependymomas are the second most common malignant brain tumours in children (Ostrom, Gittleman et al. 2014). They are notorious for occurring throughout the neuro-axis; although 90% of cases in children occur intracranially. Two-thirds of these intracranial ependymomas occur infratentorially (in the PF) whilst the remaining one-third originate from the ST compartment (Louis, Ohgaki et al. 2007). Chemoresistance and invasion of surrounding critical structures are hallmarks of ependymomas which contribute to tumour recurrence in 50% patients (Chiu, Woo et al. 1992, Messahel, Ashley et al. 2009). This tendency to relapse is consistent with ependymomas harbouring a sub-population of therapy resistant CSCs. In spite of recent advances in paediatric neuro-oncology, current 5-year survival in infant patients stands at a disappointing 40-52% (Gajjar, Pfister et al. 2014, Gatta, Botta et al. 2014). There is therefore, a definite need to identify novel targetable prognostic markers in ependymomas which could not only facilitate early diagnosis, but also help treat and control the disease better

In this thesis, 3 novel targetable prognostic markers in ependymoma; the multi-drug transporter ABCB1, the radial glial stem cell marker BLBP and the DNA repair enzyme MGMT, have been identified. In addition, in vitro analyses to elucidate their possible role in chemoresistance and local invasion in paediatric ependymomas have also been performed.

7.2 ABCB1; drug efflux and much more – *Chapter 4*

Similar to other forms of brain tumour, conventional treatment of ependymoma consists of surgery followed by adjuvant radiotherapy/ chemotherapy (Wright and Gajjar 2012, Northcott, Pfister et al. 2015). Radiotherapy is generally avoided in children less than 3 years of age

due to long term neurological deficits associated with it (Ellison, Kocak et al. 2011, Tai, Grundy et al. 2011, Sung, Lim do et al. 2012). In spite of chemotherapy being widely employed as part of adjuvant treatment protocols to treat ependymomas; there is a paucity of studies reporting any survival benefit from it (Bouffet, Perilongo et al. 1998, Geyer, Sposto et al. 2005, Merchant and Fouladi 2005, Atkinson, Shelat et al. 2011). This has led to the assumption that ependymomas are inherently chemoresistant. It is proposed in this study that a sub-population of therapy resistant CSCs underlie this chemoresistance in ependymomas. This conjecture is supported by studies by Hussein et al. and Milde et al. which reported resistance to several chemotherapeutic drugs in CSC enriched neurospheres derived from ependymomas (Hussein, Punjaruk et al. 2011, Milde, Kleber et al. 2011)**.**

Multi-drug resistance (MDR) has been regarded as a hallmark of CSCs which gives them a survival advantage over the rest of the tumour bulk (Reya, Morrison et al. 2001, Graham, Jørgensen et al. 2002, Hirschmann-Jax, Foster et al. 2004, Clevers 2011, Ramaswamy, Remke et al. 2013). Classical MDR is mainly mediated by 3 members of the ATP-binding cassette (ABC) drug transporters super-family; ABCB1, ABCC1 and ABCG2. Efflux by these transporters prevents accumulation of chemotherapy in cells; leading to a sub-optimal response (Kroetz, Pauli-Magnus et al. 2003). Previous lab data showed that ABCB1 exclusively, was of prognostic significance in a subset of ependymoma patients from the chemotherapy-led CNS9204 trial; whilst ABCG2 and ABCC1 showed no correlation with patient survival (Personal communication with Dr. Beth Coyle). Furthermore, ependymomas which were positive for multi-drug transporter ABCB1 (0.28% cells), frequently co-expressed surface marker CD133 (0.21% cells); suggesting that these drug resistant cells were a subset of CSC population in ependymoma (Coyle, Kessler et al. 2015). This finding was consistent with the fact that a sub-population of ependymoma cells

stained positive for ABCB1 expression in patient samples by IHC analysis (Figure 4.4 a) and a 3 fold elevation of ABCB1 expression (P=0.014) in the stem cell enriched neurospheres (Section 4.2.6) derived from the DKFZ-EP1 cell line was observed.

Since 4 of the drugs currently used as part of ependymoma adjuvant chemotherapeutic regimens are ABCB1 substrates (etoposide, vincristine, methotrexate and irinotecan) (Szakacs, Paterson et al. 2006, Wright and Gajjar 2012); it is believed that ABCB1 may play a key role in the chemoresistant nature of ependymoma. This was supported by the analysis of 3 publicly available ependymoma gene expression datasets which showed that ABCB1 was expressed in ependymoma patients (Section 4.2.1) and this expression was significantly higher in ST tumours (Section 4.2.2). ST tumours account for one-third of intracranial tumours in children and a subset of them is associated with poor prognosis. Therefore, overcoming ABCB1 induced resistance in these patients could help improve the response to chemotherapy and hence, patient outcome.

Several groups have carried out gene expression studies as well as global methylation profiling to classify ependymomas into clinically relevant groups (Witt, Mack et al. 2011, Wani, Armstrong et al. 2012, Mack, Witt et al. 2014, Pajtler, Witt et al. 2015). However, gene expression does not give an indication of function and histological techniques provide a better resolution in terms of tumour heterogeneity. Therefore, it is essential to develop a panel of targetable molecular as well as histological markers to define a robust system of ependymoma classification. In this study, it was demonstrated that in the chemotherapy-led CNS9204 trial, ABCB1 expression in a sub-population of cells was an independent marker of reduced OS survival (5-year OS-33% vs. 74%, P=0.009) as well as EFS (5-year EFS-13% vs. 50%, P=0.007). In contrast, ABCB1 expression could not predict survival in the radiotherapy-led CNS9904 trial in older patients,

highlighting the role of ABCB1 in chemoresistance and hence, reduced prognosis in younger patients. However, it is essential to mention that due to a high level of core loss in the tissue microarrays from the CNS9904 cohort, we could screen only 32 samples in this study. Therefore, it would be important to validate these results in an independent cohort consisting of older paediatric ependymoma patients.

In order to elucidate the role of ABCB1 in chemoresistance in ependymomas, 5 ependymoma derived cell lines were screened for ABCB1 gene expression. Four out the five of these cell lines expressed ABCB1 (section 4.2.5). The EPN1 cell line was the only one which tested negative for ABCB1 expression. This was consistent with the lack of ABCB1 protein expression in the original patient tumours as well as the murine orthotopic tumour from which the EPN1 cell line was derived (Chapter 3, section 3.2.3). These results were in contrast to the study by Hussein et al. demonstrated that the EPN1 cell line expressed ABCB1 and could also be cultured as neurospheres (Hussein, Punjaruk et al. 2011); which could not achieve as part of this study. Similarly, studies by Yu et al. and Milde et al. reported the ability of the BXD-1425EPN and DKFZ-EP1 cell lines to form neurospheres respectively (Yu, Baxter et al. 2010, Milde, Kleber et al. 2011). As part of this study, neurospheres from the BXD-1425EPN cell line could not be derived at all, whilst the ability of the DKFZ-EP1 cell line to form neurospheres was variable and confined to a few early passages. These results therefore indicated that tumours underwent a genotypic shift as a result of culture conditions and this might lead to the loss of the sub-population of cells. Studies by Laurent et al. and Domcke et al. reported similar changes in the genomic profiles of human epithelial stem cells and several immortalised cell lines respectively, maintained in culture over a period of time and suggested thorough evaluation of cell lines by methods such as STR (short tandem repeat) profiling which is used to compare DNA microsatellite sequences between samples, to confirm

genomic proximity to parent tumour (Laurent, Ulitsky et al. 2011, Domcke, Sinha et al. 2013). Yu et al. suggested that the serial transplantation of tumours in mice was an effective method of maintaining the sub-population of cells (Yu, Baxter et al. 2010). This method however, would not only be expensive but also labour-intensive. Development of brain tumour relevant 3D in vitro systems which could recapitulate the tumour microenvironment and therefore, allow cells to maintain their genomic profiles and a sub-population of CSCs could also represent a possible cheaper solution to this issue.

As mentioned before, it is hypothesised that a sub-population of ABCB1 expressing CSCs may underlie tumour recurrence in ependymomas; thus resulting in the chemoresistant and aggressive nature of recurrent tumours. The finding that ABCB1 was maintained in the recurrent EPN7R cell line of the EPN7 patient was in support of this conjecture (section 4.2.5). Moreover, public data analysis of the Hoffman study which compared transcriptomic changes in between 16 primary-recurrent tumour pairs, showed that ABCB1 was maintained in recurrent ependymomas (section 4.2.5), further strengthening our hypothesis.

In order to investigate the role of ABCB1 in chemoresistance in in vitro models of paediatric ependymoma; a non-specific ABC transporter inhibitor, verapamil and a PDE5 inhibitor vardenafil which has been shown to specifically inhibit ABCB1 were employed. Verapamil is a first generation ABC transporter inhibitor. Despite promising results in in vitro and in vivo experiments; unacceptable side effects in patients (Ozols, Cunnion et al. 1987, Daenen, van der Holt et al. 2004), have prevented clinicians from pursuing verapamil further in cancer treatment. However, owing to its tremendous effectiveness in vitro, it was employed as a control drug to compare efficacy of vardenafil to potentiate response to chemotherapy. Ding et al. demonstrated that unlike its congener sildenafil which inhibits ABCB1

as well as ABCG2 (Shi, Tiwari et al. 2011); vardenafil could specifically inhibit ABCB1 (Ding, Tiwari et al. 2011). Several studies since, have demonstrated its efficacy in potentiating response to chemotherapy in in vitro (Othman, Kimishi et al. 2014) as well as in vivo models (Zhu and Strada 2007, Hu, Ljubimova et al. 2010) of medulloblastomas and metastatic brain tumours. Since, it is routinely used to treat pulmonary hypertension in paediatric subjects (Jing, Yu et al. 2011), vardenafil shows good promise in being repurposed to overcome ABCB1 induced chemoresistance in paediatric ependymomas. In this study, both verapamil as well as vardenafil significantly potentiated response to chemotherapy (vincristine, etoposide and methotrexate) in the tumour bulk (section 4.2.8) as well as in CSCs (section 4.2.7) in the $ABCB1^{lo}$ BXD-1425EPN cell line.

As mentioned above, chemoresistance is a common problem in paediatric ependymomas. This was consistent with the in vitro behaviour of the ependymoma derived cell lines in this study. The $ABCB1^{lo}$ BXD-1425EPN cell line was etoposide-resistant (sections 4.2.7 and 4.2.8) whilst the DKFZ-EP1 cell line exhibited resistance to all 3 chemotherapeutic drugs (etoposide, methotrexate and vincristine) used in the study (section 4.2.9). In the case of the BXD-1425EPN cell line, the IC_{50} (60 μM - tumour bulk and 20 μM - ependymoma stem cells) to etoposide was significantly higher than the clinically relevant peak plasma concentration (~2 μM); but, this was decreased when etoposide was combined with both verapamil (~2 fold -tumour bulk and ~2 fold - ependymoma stem cells) as well as vardenafil (~4 fold - tumour bulk and ~2 fold - ependymoma stem cells). This 2-4 fold reduction in IC_{50} values was not achieved in the DKFZ-EP1 cell line. These results indicated that although ABCB1 did contribute to chemoresistance in ependymomas; there are several resistance mechanisms to each respective drug which could be upregulated/dysregulated in each line (Discussed in Chapter 1, section 1.3.4.3). Notably, there have been reports of overexpression of TOPO-

IIA (resistance mechanism to etoposide) as well DHFR (dihydrofolate reductase- resistance mechanism to methotrexate) in ependymomas (Mousseau, Chauvin et al. 1993, Wani, Armstrong et al. 2012). These findings therefore indicate that chemoresistance in ependymomas is a multi-factorial process and that resistance due to ABCB1 may represent a facet of this phenomenon in the therapy resistant CSCs.

Ependymomas tend to migrate and invade surrounding critical structures such as the brain stem; making the acquisition of complete surgical resection difficult. Invasion, especially in ST ependymomas with sub-total resection has therefore been regarded as a clinical marker of poor prognosis in several studies (Akay, Izci et al. 2004, Godfraind, Kaczmarska et al. 2012, Phi, Wang et al. 2012). Previous lab data in medulloblastomas, demonstrated that ABCB1 inhibition through treatment with verapamil as well as vardenafil attenuated the migratory capacity of cells in an in vitro 2D wound healing assay (Personal communication - Dr. Beth Coyle). Notably, there are several studies proposing a role for ABCB1 in tumour migration and invasion (Miletti-Gonzalez, Chen et al. 2005, Colone, Calcabrini et al. 2008). With tumour invasion of surrounding structures being a major hurdle in achieving complete resection in ependymomas, a 2D scratch assay was performed to investigate if ABCB1 contributed to the motility of ependymoma cells. As demonstrated in section 4.2.10, verapamil and vardenafil at non-toxic concentrations and in the absence of chemotherapy, inhibited migration in both $ABCB1^{lo}$ and $ABCB1^{hi}$ ependymoma cell lines. This indicated that ABCB1 did indeed contribute to the migratory nature of ependymomas. Since tumour invasion is common in ependymomas across all age groups; ABCB1 expressing cells may also contribute towards the aggressive phenotype of ependymomas in older radiotherapy treated patients. This finding further highlights the need to confirm its prognostic value in an independent paediatric ependymoma cohort consisting of older patients (3-21 years) who received adjuvant radiotherapy following surgery.

Migration refers to the movement of cells within a tissue without causing specific damage to the host tissue and is therefore considered as one facet of the invasion process. Invasion on the other hand, refers to the ability of cells to secrete proteolytic enzymes which digest the normal cellular elements or cause cellular remodelling as the tumour cells attack the adjacent normal tissue (Bolteus, Berens et al. 2001). This behaviour is commonly witnessed in ependymomas which tend to invade critical structures such as the brain stem. Since parallel research in the laboratory was being performed in medulloblastomas to investigate an EMT-like (epithelial to mesenchymal transition) process by employing the Basement Membrane Extract (BME- a soluble form of basement membrane purified from Engelbreth-Holm-Swarm (EHS) mouse sarcoma - enriched with laminin, collagen IV, entactin, and heparan sulphate proteoglycan), it was also employed to carry out a 3D spheroid invasion assay (section 4.2.11 and 4.2.12) in both cell lines. The ABCB1^{lo} BXD-1425EPN cell line exhibited an individual cell invasion pattern; through the BME model represented by both, single cell amoeboid budding as well as multicellular streaming by formation of invasive processes or invadopodia (Figure 7.1, c and d respectively) (Friedl, Locker et al. 2012). This invasive phenotype was quite similar to that observed in the in vivo model of the original tumour from which the cell line was derived (Yu, Baxter et al. 2010).

As depicted in Figure 7.1, there were distinct similarities in the invasion patterns of the orthotopic tumour and the BXD-1425EPN spheroid invasion phenotype in the BME. This behaviour was significantly reduced after treatment with both ABCB1 inhibitors represented by the significant reduction in the relative spheroid outgrowth. This behaviour could be explained by several studies, conveying a correlation between ABCB1 and cell-surface glycoprotein CD44 expression, involved in cell adhesion and migration. ABCB1 inhibition has been reported to inhibit expression of CD44 in in vitro models of breast and ovarian cancers (Miletti-Gonzalez, Chen et al.

2005). Furthermore, ABCB1 through co-operation with CD44 has also been shown to activate expression of matrix-metalloproteinases (MMP-2 and MMP-9) (Colone, Calcabrini et al. 2008). Therefore, the attenuated ability of ependymoma cells to invade through the BME may be as a result of reduced secretion of proteolytic enzymes caused by ABCB1 inhibition. Furthermore, the brain is generally relatively sparse in ECM which is essential for tumour invasion as well as migration; since cells require a substrate to hold on to. In gliomas, it has been reported that both autocrine and paracrine growth factor stimulation of sub-populations of neoplastic glia may result in neoplastic cell-derived ECM secretion (Merzak, Koochekpour et al. 1995). In other words, tumour cells may secrete their own ECM. Assuming a similar process was involved in invasion of ependymomas in vivo; it is plausible that owing to the vast substrate specificity of ABCB1, its inhibition may also lead to attenuation of efflux of the various growth factors as well as ECM; resulting in diminished ability of cells to invade.

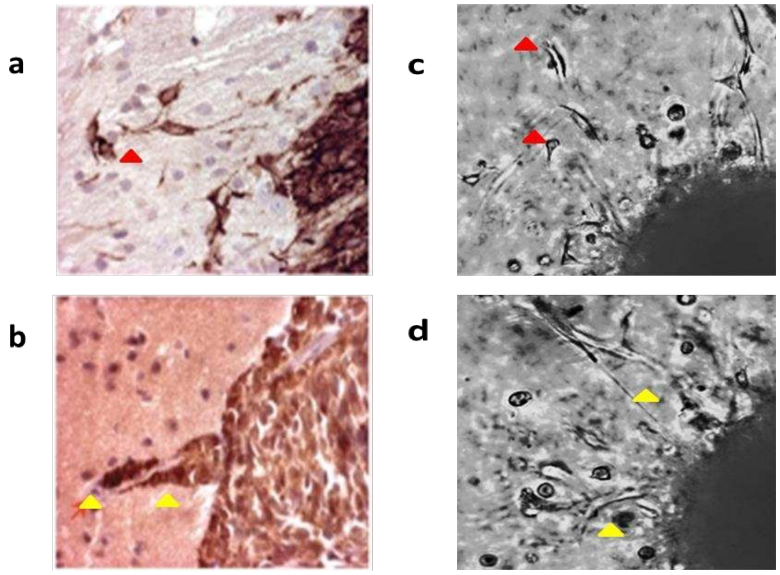


Figure 7.1 Similarity in the invasion patterns of the BXD-1425EPN orthotopic tumour and spheroid in BME BXD-1425EPN vimentin stained orthotopic tumour exhibited individual-cell invasion pattern, represented by **a.** single cell amoeboid invasion (red arrow head) and **b.** a multicellular streaming pattern by formation of invadopodia (yellow arrow head). Images obtained and modified from (Yu, Baxter et al. 2010). A similar **c.** amoeboid and **d.** multicellular streaming pattern was also observed when the BXD-1425EPN spheroid was introduced in BME.

The ABCB1^{hi} DKFZ-EP1 cell line did not invade in the BME. This behaviour might be because BME did not represent a tumour micro-environment conducive for its invasion. This cell line was established from metastatic ascites of ependymoma (Milde, Kleber et al. 2011), however, when these cells were transplanted into mice, the tumours remained circumscribed and did not invade. Additionally, it was reported that the cells changed their phenotype when grown in matrigel, forming large circular cells. A ventriculoperitoneal shunt is employed to drain excess CSF (cerebrospinal fluid) in to the peritoneal cavity post-surgery in certain patients (Wright and Gajjar 2012). Although there is no mention of the same for the DKFZ-EP1 patient; it is possible that it could be one of the reasons for development of ascites in the DKFZ-EP1 patient and their non-invasive behaviour in BME.

In summation, these results indicated that ABCB1 was certainly a robust druggable prognostic marker in ependymoma. Additionally, the PDE-5 inhibitor vardenafil, at non-toxic concentrations was useful in overcoming chemoresistance as well as targeting invasion and migration in in vitro models of ependymoma.

7.3 BLBP; not just a stem cell marker – Chapter 5

BLBP (brain lipid binding protein) is a fatty acid chaperone involved in regulating intracellular transport and metabolism of fatty acids (Anthony, Mason et al. 2005). It is a developmental marker and has been demonstrated to be a marker for radial glia (RG) which have been shown to give rise to ependymal cells, oligodendrocytes and astrocytes during neurogenesis. Similar to CSCs described in Chapter 1, Section 1.4; Taylor et al. demonstrated that ependymoma derived transformed RG expressed cell surface markers such as CD133, formed self-renewing neurospheres and recapitulated orthotopic tumours in mice. Since BLBP was one of the markers used to characterise these RG (Taylor, Poppleton et al. 2005); it was indicative of BLBP being a CSC marker in ependymomas. The results of this

study were in support of this conjecture, since BLBP was expressed in a sub-population of cells in ependymoma patient samples as depicted in Figure 5.4b and its expression was significantly elevated (5 fold, $P<0.001$) in neurospheres derived from the DKFZ-EP1 cell line (section 5.2.7). Furthermore, BLBP gene expression was maintained in patients across all age groups in the 3 publicly available ependymoma datasets (section 5.2.1) and in all cell lines used in this study (Section 5.2.6); indicating that similar to the patients, all cells lines in this study maintained a sub-population of BLBP expressing RG. Finally, BLBP gene expression also significantly correlated with expression of other brain tumour relevant CSC markers such as CD133 and SOX2 in 3 publicly available ependymoma datasets (section 5.2.4). However, its expression only correlated with one of the probes for Nestin, exclusively in the Mack dataset, which we believe codes for RC2 (also coded by the Nes gene) which is another radial glial marker (Park, Xiang et al. 2009). All these results supported the assumption that BLBP was a CSC marker in ependymomas.

Additionally, Taylor et al. demonstrated that transformed RG with site specific mutations, recapitulated ependymomas originating from those locations (Taylor, Poppleton et al. 2005). In support of this finding, it was found that the BLBP gene was expressed in ependymomas originating from different locations. Furthermore, there was a significantly higher expression of BLBP recorded in ST and SP tumours in comparison to PF tumours (section 5.2.2). This highlighted the possibility that BLBP played a greater role in their pathogenesis and progression. Further experiments need to be undertaken to confirm this assumption.

BLBP expression has been correlated with reduced survival in renal cancer (Tolle, Krause et al. 2011), adenoid cystic carcinoma of the salivary glands (Phuchareon, Overdevest et al. 2014) and aggressive triple-negative breast cancer (Tang, Umemura et al. 2010).

Since the findings of this study so far supported the hypothesis that BLBP was a CSC marker in ependymomas, it was proposed that BLBP expression could be of robust prognostic value in ependymoma. This assumption was supported by results which showed that BLBP protein expression was an independent prognostic marker in the chemotherapy-led CNS9204 trial (section 5.2.4). However, it was a marker of solely reduced OS (5-year OS- 27.27% versus 72%, P=0.002) in the radiotherapy-led CNS9904 trial consisting of older paediatric ependymoma patients (section 5.2.5). As mentioned before, since it was possible to only assess 32 patient samples for BLBP protein expression in this trial; the prognostic value of BLBP needs to be validated in independent paediatric ependymoma trials consisting of patients between 3-21 years of age.

To investigate whether BLBP played a functional role in ependymoma pathogenesis and progression, 5 ependymoma derived cell lines were analysed by QRT-PCR analysis. As mentioned before, all of the cell lines expressed BLBP at varying levels (section 5.2.6). Therefore, a BLBP expressing sub-population of cells from the patient tumour was maintained in culture and the orthotopic tumour from which the EPN1 cell line was derived (Chapter 3, Section 3.2.3). However, since neurospheres could not be derived from the EPN1 cell line, a concomitant increase in BLBP expression could not be confirmed. In further support of the speculation that transformed RG contributed to tumour recurrence in ependymomas, BLBP expression was maintained in the EPN7R cell line which was derived from the recurrent tumour of the EPN7 patient (section 5.2.6). This finding was consistent with the analysis of the Hoffman study (Hoffman, Donson et al. 2014) which showed that BLBP gene expression was maintained at relapse in ependymoma patients (section 5.2.6).

To elucidate the functional role of BLBP in ependymoma pathogenesis, further analyses were carried out on the $BLBP^{hi}$, DKFZ-EP1 cell line and the $BLBP^{lo}$ BXD-1425EPN cell lines.

Firstly, a BLBP ligand, DHA, was employed, to overcome chemoresistance and invasion in ependymomas. DHA is an ω-3 fatty acid and has been shown to bind BLBP with the highest affinity (Xu, Sanchez et al. 1996). It is a popular dietary supplement with several health benefits, including maintenance of normal brain function (Lukiw and Bazan 2008). There have been several studies which highlight the efficacy of DHA in overcoming chemoresistance (Wang, Bhat et al. 2011, Li, Qin et al. 2014, Harvey, Xu et al. 2015) and targeting proliferation as well as invasion in in vitro and in vivo models of several cancers (Rahman, Veigas et al. 2013, Li, Hou et al. 2014, Zheng, Tang et al. 2014, Blanckaert, Kerviel et al. 2015). Since BLBP is essential for the intracellular transport of DHA in order for it to induce an anti-neoplastic effect and therefore it was proposed that DHA administration would be a useful method of targeting BLBP expressing RG. As mentioned in Chapter 5, Section 5.1; the fatty acid (FA) shuttled by BLBP is essential for the PPAR transcription factors to transcribe a number of genes including BLBP itself. Furthermore, the nature of the FA shuttled by BLBP modulates the expression of genes by PPAR transcription factors (Martin, Robbins et al. 1996). This finding was consistent with the studies which demonstrated that DHA (ω-3 FA) treatment led to the reduction in survival and proliferation by inhibiting genes such as p53, NF-κB and members of PI3K pathway in medulloblastomas (Wang, Bhat et al. 2011). In contrast, arachidonic acid (AA, ω-6 FA) promoted cancer cell proliferation, survival and inflammation; although genes expressed/inhibited by PPARs as a result of AA binding have not been yet discovered (Martin, Robbins et al. 1996, Bell, Ponthan et al. 2013). Another study by Deckelbaum et al. showed that DHA inhibited proliferation in monkey kidney cell lines by inhibition of NF-κB expression in a PPAR-γ dependent manner

(Deckelbaum, Worgall et al. 2006). As shown in Chapter 3, section 3.2.4, both the cell lines used in this Chapter expressed the C11orf95-RELA fusion gene,and consequently harboured an active and oncogenic NF-κB pathway. It was therefore, proposed that DHA by means of inhibition of NF-κB expression in the ependymoma cell lines, could subsequently inhibit proliferation. However, the effect of DHA on proliferation in ependymoma cell lines was found to be atypical. As discussed in section 5.2.8, in an MTT assay to assess response in the tumour bulk, DHA had no effect on proliferation of the $BLBP^{lo}$ BXD-1425EPN cell line whereas, in the case of the $BLBP^{hi}$ DKFZ-EP1 cell line, a steady increase in proliferation was recorded up to a concentration of 60 μM. This was followed by a steep drop in proliferation to 20% viability at 120 μM. This differential behaviour of DHA was also reported by Wang et al. in glioma and medulloblastoma cell lines (Wang, Bhat et al. 2011). Similarly, in a stem cell relevant clonogenic assay on the $BLBP^{lo}$ BXD-1425EPN cell line, which selected for BLBP expressing ependymoma CSCs, DHA seemed to induce colony formation at a lower concentration of 5 μM, followed by completely inhibiting viability at 50 μM. Although DHA has been the only agent so far useful in inhibiting proliferation in the $BLBP^{hi}$ DKFZ-EP1 cell line (although at high concentrations), its pro-proliferative effect at lower concentrations, questions its potential to be employed as monotherapy in ependymoma treatment. However, titration of the optimal anti-proliferative dose of DHA in various representative in vitro models of ependymoma and further validation in in vivo models may help address this issue.

There have been several reports of DHA potentiating response to chemotherapeutic drugs such etoposide, vincristine, doxorubicin and fludaribine in in vitro models of several cancers (Wang, Bhat et al. 2011, Fahrmann and Hardman 2013). This effect has been reported to be due to synergy between DNA damage caused by free radicals produced as a result of DHA peroxidation and toxic chemotherapeutics; as well as a

result of inhibition of genes such as p53, NF-ĸB and PI3-Kinase pathway (Wang, Bhat et al. 2011). As depicted in section 5.2.10.1, in order to assess the ability of DHA to overcome chemoresistance in the tumour bulk, we carried out an MTT viability assay. DHA could not potentiate response to chemotherapy (etoposide and vincristine) in the chemoresistant $BLBP^{hi}$ DKFZ-EP1 cell line. In the $BLBP^{lo}$ BXD-1425EPN cell line, the enhanced cytotoxic effect as a result of DHA co-treatment appeared to be synergistic in the case of etoposide ($P<0.001$). In contrast to this effect on vincristine seemed additive ($P<0.001$). In a stem cell relevant clonogenic assay (section 5.2.10.2), as a result of DHA co-treatment, the apparent increase in the cytotoxic effect of etoposide ($P<0.001$) and vincristine ($P=0.007$), seemed synergistic and additive respectively. These results therefore indicated that DHA co-treatment had differential effects on response to chemotherapy in ependymomas.

DHA has been reported to control infiltration in BLBP expressing malignant glioma cells in vitro, through manipulation of the lipid environment in a PPAR-γ dependent manner (Mita, Beaulieu et al. 2010). Furthermore, DHA has been shown to inhibit pro-migratory genes such as COX-2, CD44 and adhesion molecules ICAM/VCAM in medulloblastomas (Wang, Bhat et al. 2011). In addition, as mentioned before, DHA is an essential component of biological membranes made up of phospholipids. Since it is highly prone to peroxidation; incorporation of this highly reactive peroxidised FA in the cell membrane affects its integrity, a key requirement for tumour cells to undergo EMT in order to invade or migrate (Elsherbiny, Emara et al. 2013). Notably, since tumour invasion is evidently a common issue in ependymomas and is a marker of poor prognosis, especially in tumours originating from the ST compartment (Akay, Izci et al. 2004, Godfraind, Kaczmarska et al. 2012); the ability of DHA to target this invasive behaviour of ependymomas was assessed. In agreement with several previous studies, DHA reduced the migratory capacity of cells in both

the BLBP^{lo} BXD-1425EPN ($P<0.001$) and BLBP^{hi} DKFZ-EP1 ($P<0.001$) cell lines in a 2D scratch assay (section 5.2.11). Furthermore, DHA also reduced the ability of the BLBP^{lo} BXD-1425EPN cells ($P<0.05$) to invade through BME in a 3D invasion assay (section 5.2.12). These results indicated that BLBP ligand DHA was useful in inhibiting the migratory as well as invasive behaviour of ependymomas.

In contrast to several other studies which employed shRNA or siRNA technology to inhibit BLBP in order to elucidate its function in tumour cell lines (Slipicevic, Jørgensen et al. 2008, Tolle, Suhail et al. 2011), a more translationally relevant approach to inhibit BLBP in ependymomas was adopted in this study. PPARs are transcription factors that require the FA chaperoned by BLBP to exert gene expression. As mentioned before, the nature of the FA shuttled by BLBP modulates this gene expression thereafter. ω-3 FAs such as DHA and ω-6 FA such as AA have been reported to inhibit and promote migration in glioma cell lines respectively (Martin, Robbins et al. 1996). With reports of reduced levels of DHA in glioma, the resultant genes transcribed by PPARs in these tumours are most like to be pro-oncogenic due to translocation of the abundant AA. Furthermore, evidence of a PPRE element in the promoter region of BLBP provided by De Rosa et al. indicated that in addition to expressing several pro-migratory and pro-proliferative genes, PPARs also transcribed BLBP. Therefore, three PPAR antagonists; the dual PPAR-(γ/δ) antagonist FH535, the PPAR-δ antagonist GSK0660 and the PPAR-γ antagonist GW9662 were employed in this study in the hope of not only achieving BLBP inhibition; but also attenuating expression of other pro-oncogenic genes. This approach was previously employed by De Rosa et al. who demonstrated that treatment of glioma cell lines with the aforementioned PPAR antagonists, inhibited BLBP expression (De Rosa, Pellegatta et al. 2012). Consistent with the findings of the aforementioned study, it was found that each of the 3 PPAR antagonists completely inhibited BLBP expression in the BLBP^{lo} BXD-

1425EPN cell line, at the 24 and 48 hour time points respectively. In the case of the BLBP^{hi} DKFZ-EP1 cell line, however, the effect of the PPAR-ϒ antagonist GW9662 was found to be most profound. Although the PPAR-δ antagonist GSK0660 and the dual PPAR-(γ/δ) antagonist FH535 inhibited BLBP expression; their effects on the DKFZ-EP1 cell line were found to be variable and statistically insignificant respectively (section 5.2.13).

Reports regarding the effect of BLBP inhibition on proliferation of in vitro models of cancer have been controversial (Slipicevic, Jorgensen et al. 2008, Tolle, Suhail et al. 2011, De Rosa, Pellegatta et al. 2012). In this study, GW9662 had a marginal but statistically significant effect on proliferation of both BLBP^{lo} BXD-1425EPN and BLBP^{hi} DKFZ-EP1 cell lines (section 5.2.14). These results indicated that BLBP may not play a functional role in proliferation in ependymomas. In contrast, when ependymoma CSCs were treated with the PPAR antagonists, both the dual PPAR-(γ/δ) antagonist FH535 and the PPAR-γ antagonist GW9662 inhibited viability (section 5.2.15). The effect of FH535 was found to be more potent. FH535 has been shown to be a Wnt signalling inhibitor in addition to being a dual PPAR-(γ/δ) antagonist. Wnt signalling is a proliferative pathway which has been shown to be active and enriched in CSCs (Hong, Jang et al. 2015). There have been reports of Wnt expression in ependymomas (Suarez-Merino, Hubank et al. 2005, Palm, Figarella-Branger et al. 2009) and that it is also required for maintenance of normal RG (Chen, Li et al. 2014). Assuming, that ependymoma propagating transformed RG maintained this Wnt expression; would potentially indicate that the potent effect of FH535 on ependymoma stem cell viability might have been due to synergy between the Wnt pathway and BLBP inhibition. Further experiments investigating the expression of Wnt in transformed RG and the effect of FH535 on this expression would be necessary to confirm this assumption.

It was hypothesised in this study that the transformed RG were responsible for the chemoresistant behaviour of ependymomas. Therefore, it was assessed whether the RG marker BLBP played a functional role in this treatment refractory behaviour (section 5.2.16). In the tumour bulk, BLBP inhibition by the PPAR-γ antagonist GW9662 could not potentiate response to etoposide or vincristine in either cell line. In contrast, in a stem cell relevant clonogenic assay, GW9662 significantly potentiated response to both drugs in the $BLBP^{lo}$ BXD-1425EPN cell line, indicating that BLBP played a functional role in chemoresistance in ependymoma stem cells. Since the $BLBP^{hi}$ DKFZ-EP1 cell line was resistant to all drugs employed in this study, it was not possible to support these findings in it. The BXD-1425EPN data however suggest that treatment of ependymomas with the PPAR-γ antagonist, GW9662, would be a useful strategy in targeting a sub-population of treatment refractory transformed RG.

Several studies so far have demonstrated that inhibition of BLBP, achieved by siRNA or shRNA technology, led to a decrease in the migratory and invasive behaviour of tumours (Slipicevic, Jørgensen et al. 2008, Mita, Beaulieu et al. 2010, Tolle, Suhail et al. 2011, De Rosa, Pellegatta et al. 2012). As depicted in section 5.2.17, each of the 3 PPAR antagonists inhibited migration in both the $BLBP^{hi}$ DKFZ-EP1 and $BLBP^{lo}$ BXD-1425EPN cell lines. However, the effect of the PPAR-γ antagonist GW9662 was found to be most profound. In other words, BLBP controlled migration in ependymoma cell lines mainly in a PPAR-γ dependent manner. In the 3D invasion assay, however, the effect of the dual PPAR-(γ/δ) antagonist FH535 on migration was found to be most profound, since it completely stopped the cells from invading through the BME (section 5.2.18). The PPAR-δ antagonist GSK0660 had a very mild effect whilst the PPAR-γ antagonist GW9662 had an intermediate effect on cell invasion. Currently, there are no clinical trials employing PPAR antagonists to treat cancer. However, several studies

have reported the efficacy of FH535 and GW9662 in controlling proliferation as well as migration in in vitro models of several forms of cancer (Kim, Choi et al. 2007, Lin, Hsu et al. 2014, Wu, Liang et al. 2015, Tomizawa, Shinozaki et al. 2016). There is however a need to validate the efficacy of these agents in in vivo models of ependymoma prior to their employment in clinical trials.

In conclusion, BLBP is certainly more than just a stem cell marker since its protein expression was of prognostic value in ependymoma patients. Furthermore, treatment of ependymoma cells with the PPAR-γ antagonist, GW9662, potentiated response to chemotherapy in a sub-population of cells. Finally, treatment with DHA and each of the 3 PPAR antagonists also reduced invasion and migration in in vitro models of ependymoma.

7.4 MGMT; an unexplored avenue in ependymoma treatment- Chapter 6

MGMT is a DNA alkyl transferase which is essential for repairing toxic O6- ethyl, chloroethyl, hydroxyethyl, n-propyl, n-butyl, and more bulky cyclic guanine lesions [Reviewed in (Bradshaw 2013)]. Several studies have reported a potential role of MGMT in repairing lesions induced by chemotherapeutic drugs such as temozolomide, lomustine, carmustine, decarbazine, procarbazine, cyclophosphamide and fotemustine (Lage, Christmann et al. 1999, Christmann, Pick et al. 2001, Gerson 2004, Hansen, Ludeman et al. 2007, He, Shan et al. 2011). This highlights the need to study MGMT in chemoresistant ependymomas (Bouffet and Foreman 1999, Atkinson, Shelat et al. 2011). The assessment of MGMT gene expression across 3 publicly available ependymoma datasets showed that MGMT was expressed in ependymoma patients (section 6.2.1) with higher expression recorded in aggressive PF tumours in the Gilbertson and Mack datasets (section 6.2.2). This indicated that MGMT expression could certainly be one of the factors contributing to the chemoresistant behaviour of

ependymomas. However, the weak association between MGMT expression and PF tumours needs to validated in other independent ependymoma datasets.

Promoter hyper-methylation is a common mechanism of MGMT loss recorded in 45-70% of gliomas (Blanc, Wager et al. 2004, Stupp, Hegi et al. 2006) and has been regarded as a marker of favourable prognosis in this tumour type (Hegi, Diserens et al. 2005, Hegi, Liu et al. 2008). In spite of TMZ, along with other alkylating agents, being routinely utilised to treat primary as well as recurrent ependymomas (Nicholson, Kretschmar et al. 2007, Lombardi, Pambuku et al. 2013, Komori, Yanagisawa et al. 2015, Ruda, Bosa et al. 2015), there have been very few studies investigating MGMT promoter methylation in ependymomas. So far studies have either reported low levels (Koos, Peetz-Dienhart et al. 2010) or absolute absence of MGMT promoter methylation (Buccoliero, Castiglione et al. 2008) in ependymomas. In agreement with these studies, retrospective analysis of the methylation array data produced in a study by Rogers et al. (section 6.2.3) showed very low/ almost absent MGMT promoter methylation in paediatric ependymomas (Rogers, Kilday et al. 2012). Furthermore, analysis of the publicly available CIMP study (Mack, Witt et al. 2014) dataset by Mack et al. showed that although some MGMT promoter methylation was present in paediatric ependymomas samples, these levels were significantly lower in comparison to adult ependymomas ($P<0.001$). Additionally, this low level of MGMT promoter methylation was also associated with dismal prognosis in paediatric subjects (section 6.2.4). These results indicated that not only was MGMT un-methylated or showed low levels of methylation in paediatric ependymomas; lack of its promoter methylation was also of poor prognostic value in them.

Buccoliero et al. reported that MGMT protein expression was associated with aggressive anaplastic ependymomas (Buccoliero, Castiglione et al. 2008); suggesting its possible role in an aggressive

phenotype and the associated poor outcome. In the chemotherapy-led CNS9204 trial cohort, MGMT protein expression predicted reduced OS (5-year OS 45% vs. 76%, P=0.01) exclusively in univariate analysis (Section 6.2.6). In contrast, in the radiotherapy-led CNS9904 trial cohort, MGMT expression was an independent marker of reduced OS (5-year OS-36.4% vs. 82.3%, P<0.001) as well as EFS (5-year EFS-12% vs. 47%, P=0.007). Recent studies have reported that loss of MGMT expression potentiated response to radiation in glioma (He, Shan et al. 2011) and breast cancer cell lines (Chen, Zhang et al. 2015), highlighting a potential role for MGMT in radioresistance. Additionally, MGMT has also been thought to play a role in cyclophosphamide resistance (Hansen, Ludeman et al. 2007) which was one of the agents employed as adjuvant treatment along with radiotherapy. Since, these analyses were performed on a relatively small sample-size (CNS2904-43 patients and CNS9904-41 patients) as a result of TMA core loss, it is crucial to validate the prognostic value of MGMT in independent paediatric ependymoma datasets

It is essential to highlight here that, unlike ABCB1 and BLBP; MGMT was not expressed exclusively in a sub-population of cells as depicted in Figure 6.5 a. This result was consistent with the western blotting analysis (section 6.2.7) which showed that there was no change in the MGMT protein expression of the DKFZ-EP1 cell line when it was grown as neurospheres (DKFZ-EP1NS). In other words, MGMT resistance was active in both, the tumour bulk as well as the CSCs in ependymomas. Additionally, when other ependymoma cell lines were analysed for MGMT expression; BXD-1425EPN expressed MGMT whilst EPN1 did not. Since this chapter mainly focused on response to TMZ, which depends on the lack of MGMT expression and a proficient MMR pathway; expression of MMR enzymes, MLH1 and MSH6 in the aforementioned cell lines was also analysed. Although all cell lines expressed MSH6 enzyme; MLH1 was not expressed in MGMT negative EPN1 cell line. Similar to MGMT, the expression profile of the MMR

enzymes in the DKFZ-EP1 cell line was maintained in the stem cell enriched DKFZ-EP1NS neurospheres. Since, it was not possible to easily maintain the growth of the EPN7 and EPN7R cell lines in culture, these analyses could not be carried out on them.

After carrying out viability analyses to measure the response to TMZ (section 6.2.8), it was seen that all cell lines used in this study exhibited resistance. Notably, in spite of being MGMT negative; due to lack of MMR proficiency, EPN1 was found to be the most TMZ resistant. This result indicated that, due to lack of a proficient MMR pathway, the unrepaired methyl lesion in the EPN1 cell line was retained without triggering apoptosis. This meant that TMZ potentially induced a mutation in the EPN1 cell line; preservation of which would lead to the acquisition of the hypermutator phenotype as demonstrated by Thuiji et al. in gliomas (van Thuijl, Mazor et al. 2015). It is also essential mention that the EPN1 patient received TMZ at third recurrence, which proved ineffective (Personal communication - Dr. Lisa Storer). This finding therefore, highlights the need to assess both MGMT as well as MMR status of the patient prior to TMZ administration. Finally, resistance to TMZ was maintained in the ependymoma CSCs (in both BXD-1425EPN and DKFZ-EP1 cell lines- section 6.2.10) which was in contrast to the findings by Meco et al., who reported elevated sensitivity to TMZ in ependymoma stem cells (Meco, Servidei et al. 2014).

There have been several strategies used to overcome MGMT resistance. Currently, O6-Benzyl Guanine, an MGMT inhibitor, is in clinical trials to improve the response to TMZ (NCT00275002, NCT00004072 and NCT00052780 – obtained from clinicaltrials.org). However, there have been reports of adverse haematological side effects induced by it (Konduri, Ticku et al. 2009). Zhang et al. and Othman et al. reported the efficacious effect of MGMT circumventing novel N3-propargyl analogue of TMZ in the treatment of in vitro models

of glioma (Zhang, Stevens et al. 2010) and medulloblastoma (Othman, Kimishi et al. 2014) respectively. All 3 ependymoma cell lines used in this study were N3-propargyl analogue sensitive (section 6.2.9); this response was independent of their MGMT as well as MMR status. Furthermore, there was an increased sensitivity to N3-propargyl recorded in ependymoma stem cells (Section 6.2.10). Further analyses investigating underlying factors which led to this elevated sensitivity, should be carried out. These results indicated that the N3-propargyl analogue of TMZ not only acted in a MGMT and MMR independent manner, but it was also effective in targeting the sub-population of CSCs. There have been reports following oral administration; N3-propargyl analogue was not as effective as TMZ in reducing brain tumour bulk in nude mice. This was however, proposed to be a consequence of rapid activation in the plasma and reduced delivery to brain tumour site (personal communication Dr. Beth Coyle). Therefore, development of drug delivery methods employing liposomes, nanoparticles or local delivery using biodegradable polymers need to developed to improve the stability of the drug.

In conclusion, MGMT is a viable resistance mechanism in paediatric ependymoma patients. MGMT hypo-methylation and MGMT protein expression were robust markers of poor prognosis. Finally, MGMT circumventing N3-propargyl analogue of TMZ functions has definite potential to be employed in treatment regimens for paediatric ependymoma patients.

7.5 Conclusion

In conclusion, ependymomas are extremely aggressive chemoresistant tumours which tend to recur. As a part of our study, the potential role of CSCs in imparting this vitriolic behaviour was investigated and as a result, novel and translationally relevant druggable prognostic markers in paediatric ependymoma were also identified.

7.6 Future work

7.6.1 General

In this thesis, the gene expression of all the markers in this study in 3 publicly available datasets was assessed. It was seen that ABCB1 was mainly expressed in ST tumours (Chapter 4, section 4.2.2), BLBP in SP as well as ST (Chapter 5, section 5.2.2), and finally, MGMT in PF ependymomas (Chapter 6, section 6.2.2). Analysis of similar gene expression datasets and in vitro / in vivo validation of these results would be essential to confirm results.

Furthermore, feasibility of the aforementioned proteins as independent prognostic markers in chemotherapy-led CNS9204 trial and radiotherapy-led CNS9904 trial was investigated. Therefore, it would be essential to validate their prognostic value in other independent paediatric ependymoma cohorts such as the DKFZ ependymoma cohort [(n = 379), (Milde, Hielscher et al. 2012)]. This was requested in September 2014, but so far has not been forthcoming (Personal communication-Beth Coyle).

As mentioned before, all the cell lines used in this study were derived from ST ependymomas. Since PF ependymomas account for the majority of paediatric ependymoma patients, it would be essential to also investigate the efficacy of the PPAR antagonists, DHA and the N3-propargyl analogue of temozolomide, in treating in vitro models of PF ependymomas.

Finally, the basement membrane extract derived from a murine sarcoma, used as the 3D invasion system was found to be prone to tremendous inter-experimental variability. Figure 7.2 displays the heterogeneous behaviour of the BXD-1425EPN in BME in different experiments. Novel humanised 3D systems tailored to mimic the brain tumour microenvironment employing hydrogels or alginate-chitosan

beads need to be harnessed to further confirm the efficacy of agents used in this study to inhibit cell invasion.

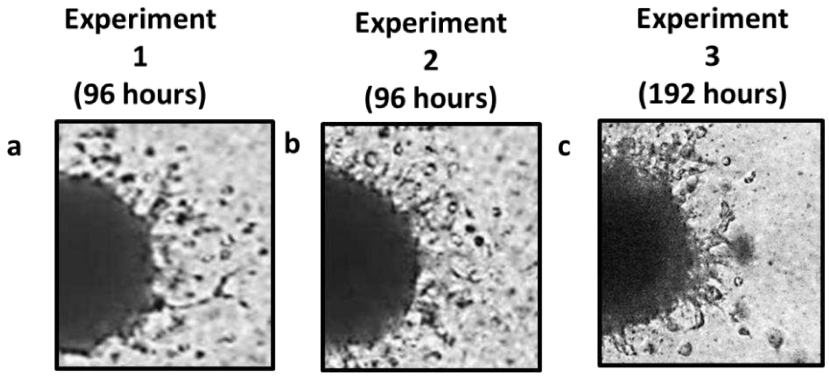


Figure 7.2 Heterogeneity in invasion behaviour of the BXD-1425EPN cell line in the BME Although the BXD-1425EPN cell line exhibited an individual cell pattern of invasion in all 3 images shown above; there was significant difference in the rate at which cells invaded through it. At 96 hours, in experiment 1 and 2 (**a** and **b**), the extent of invasion was comparable to that at 196 hours in experiment 3 (**c**)

7.6.2 ABCB1

In this study, it was demonstrated that inhibition of ABCB1 by non-specific inhibitor verapamil and specific inhibitor vardenafil, could potentiate response to chemotherapy as well as inhibit invasion and migration in in vitro models of ependymoma. Since small molecule inhibitors often have off-target effects, knock down studies using si/shRNA or knockout studies using the novel CRISPR-Cas9 system would be valuable in confirming the functional role of ABCB1 in ependymoma pathogenesis and progression.

7.6.3 BLBP

De Rosa et al. were able to demonstrate that radiation elevated BLBP expression in glioma cells (De Rosa, Pellegatta et al. 2012); indicating the possible role of BLBP in radioresistance. As part of this study, it was found that there was a positive trend in BLBP expression with an increase in dose, 24 and 48 hours after radiation (Figure 7.3). These results highlight the need to investigate the prognostic role of

BLBP in stratifying older paediatric ependymoma patients (between 3-21 years of age) who receive adjuvant radiotherapy following surgery, into clinically relevant groups. Further analysis involving repeating these experiments to confirm results (2 repeats done so far) as well as investigating the possible role of BLBP in response to radiotherapy by employing PPAR antagonists need to be undertaken.

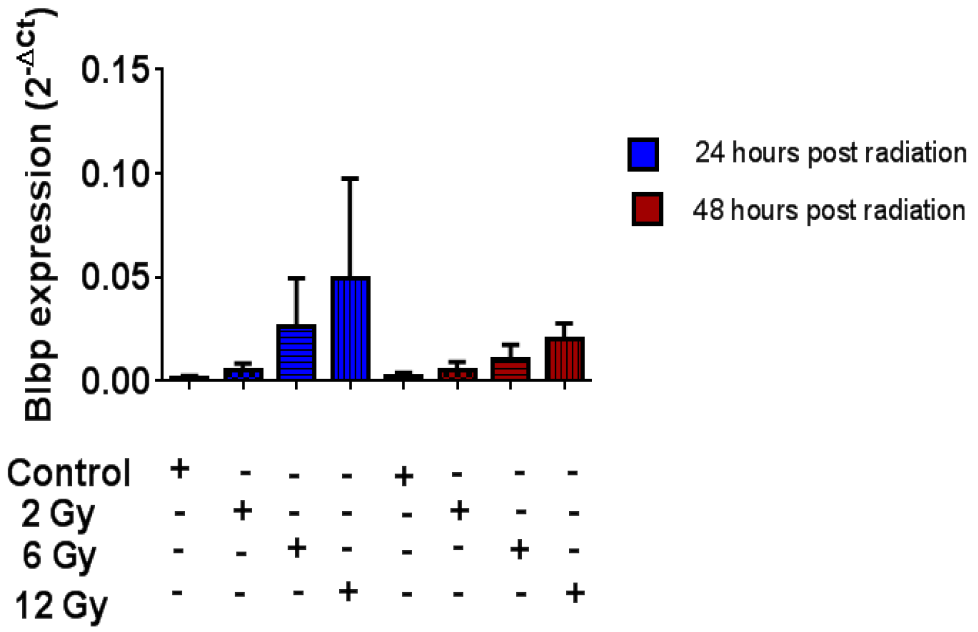


Figure 7.3 Elevation in BLBP expression after exposure to radiotherapy in the BLBP^{lo} BXD-1425EPB cell line BLBP expression was measured by qRT-PCR analysis, 24 and 48 hours after exposing BLBP^{lo} BXD-1425EPN cell line with 2, 6 and 12 Gy radiation. As depicted here, an elevation BLBP expression with an increase in dose was observed. (n=2)

7.6.4 MGMT

In this study, a correlation between MGMT promoter methylation status and patient outcome was made in a small subset of patients. It would, therefore be essential to confirm these findings in a larger methylation ependymoma dataset such as the one published by Pajtler et al. (Pajtler, Witt et al. 2015). However, this data is not currently publicly accessible.

Furthermore, in addition to TMZ, MGMT also repairs O6-guanine chloro-alkyl lesions induced by nitrosoureas such as lomustine and carmustine. All these agents are also commonly used as part of ependymoma adjuvant treatment protocols. Therefore, it would be useful to confirm the role of MGMT in resistance to these agents in in vitro models of ependymoma.

Finally, the N3-propargyl analogue is prone to rapid activation following oral administration in nude mice; resulting in a sub-optimal tumour response. Therefore, developing novel drug delivery methods employing nano-particles, liposomes as well as local delivery using bio-degradable polymers for sustained release of drug need to be tested, as they would not only increase drug stability but also mitigate non-specific side effects associated with it.

APPENDICES

APPENDIX A1 Solutions/buffers for western blotting analysis

Lysis buffer for protein extraction	150 mM of NaCl + 0.1% SDS+ 50 mM of Tris + protease inhibitor cocktail + 1% Triton X-100 in 500 ml of dH_2O
Protease cocktail inhibitor	1 tablet of complete mini protease inhibitor (~Roche) dissolved in 200 µl of dH_2O
Lower gel buffer	1.5 M of Tris + 0.4 % SDS (pH 8.8)
Upper gel buffer	0.5 M of Tris + 0.4 % of SDS solution (pH 6.7)
Electrode buffer	25mM of Tris + 193 mM of Glycine + 1% of SDS
Transfer buffer	25mM of Tris + 193 mM of Glycine + 25 % of methanol
10X Tris buffer saline (TBS)	20 mM of Tris +135 mM of NaCl (pH 7.6)
TBS-T	1 X TBS + 0.1 % tween (MERCK)
Sample buffer	0.76 % Tris + + 0.05% of bromophenol blue 6.8+ 2 % SDS + 2 % of β-mercaptoethanol+ 15 % glycerol

APPENDIX A2 preparation of lower resolving gel

	12% gel	15% gel
Lower gel buffer	1 ml	1 ml
Acrylamide	0.93 ml	1.6 ml
dH_2O	2.07 ml	0.8 ml
10% APS	25 µl	25 µl
Temed	3.3 µl	3.3 µl

APPENDIX A3 preparation of upper stacking gel

Ingredient	Volume
Upper gel buffer	625 µl
Acrylamide	312 µl
dH_2O	1500 µl
10 APS	12.5 µl
Temed	2.5 µl

APPENDIX A4

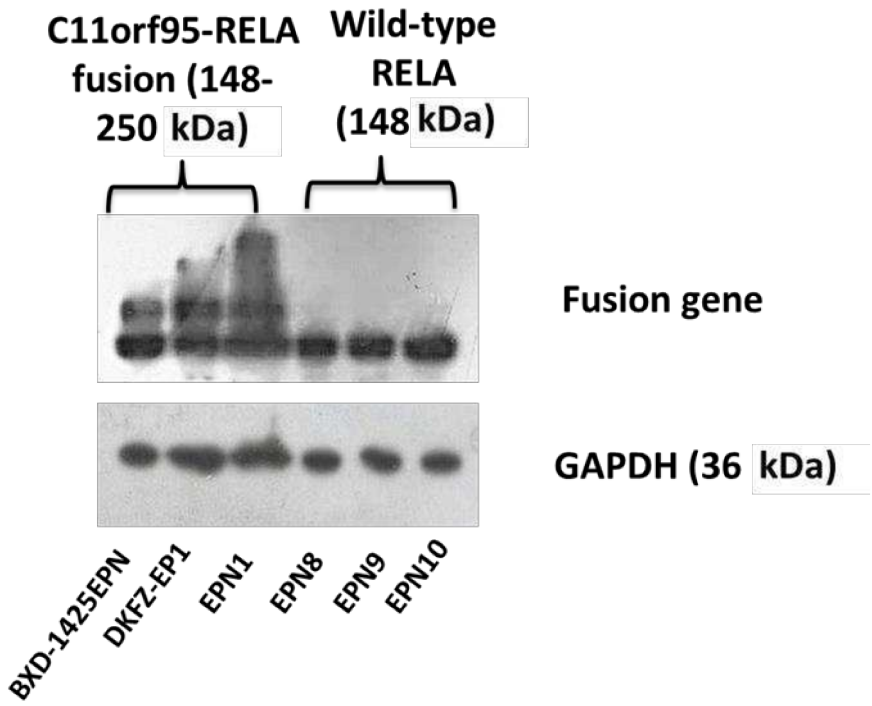


Figure 0.1 Protein expression of the C11orf95-RELA fusion in ependymoma cell lines by western blotting analysis The ST derived cell lines (BXD-1425EPN, DKFZ-EP1 and EPN1) expressed the C11orf95-RELA fusion gene whilst the newly derived (uncharacterised) PF cell lines (EPN8, EPN9 and EPN10) expressed the wild-type RELA protein. GAPDH was run as an experimental control to ensure equal loading of proteins. As the EPN7 and EPN7R cell lines did not grow well in culture, they could not be included in this analysis. (Western blot was performed by Mr. Jasper Estranero.)

REFERENCES

Aguilera, D., C. Mazewski, J. Fangusaro, T. J. MacDonald, R. Y. McNall-Knapp, L. L. Hayes, S. Kim and R. C. Castellino (2013). "Response to bevacizumab, irinotecan, and temozolomide in children with relapsed medulloblastoma: a multi-institutional experience." Child's Nervous System: 1-8.

Akay, K. M., Y. Izci, A. Baysefer, C. Atabey, E. Kismet and E. Timurkaynak (2004). "Surgical outcomes of cerebellar tumors in children." Pediatr Neurosurg **40**(5): 220-225.

Akyüz, C., H. A. Demir, A. Varan, B. Yalçın, T. Kutluk and M. Büyükpamukçu (2012). "Temozolomide in relapsed pediatric brain tumors: 14 cases from a single center." Child's Nervous System **28**(1): 111-115.

Alaoui-Jamali, M., R. Schecter, Y. Rustum, M. Centurioni, S. Lehnert and G. Batist (1993). "In vivo reversal of doxorubicin resistance by a new tiapamil analog Ro11-2933." Journal of Pharmacology and Experimental Therapeutics **264**(3): 1299-1304.

Alzahrani, A., A. Alassiri, A. Kashgari, J. Alrehaili, H. Alshaalan and R. Zakzouk (2014). "Extraneural metastasis of an ependymoma: a rare occurrence." Neuroradiol J **27**(2): 175-178.

Anthony, T. E., H. A. Mason, T. Gridley, G. Fishell and N. Heintz (2005). "Brain lipid-binding protein is a direct target of Notch signaling in radial glial cells." Genes Dev **19**(9): 1028-1033.

Armoogum, K. S. and N. Thorp (2015). "Dosimetric Comparison and Potential for Improved Clinical Outcomes of Paediatric CNS Patients Treated with Protons or IMRT." Cancers (Basel) **7**(2): 706-722.

Asiaf, A., S. T. Ahmad, A. A. Malik, S. A. Aziz, Z. Rasool, A. Masood and M. A. Zargar (2015). "Protein expression and methylation of MGMT, a DNA repair gene and their correlation with clinicopathological parameters in invasive ductal carcinoma of the breast." Tumour Biol **36**(8): 6485-6496.

Atkinson, J. M., A. A. Shelat, A. M. Carcaboso, T. A. Kranenburg, L. A. Arnold, N. Boulos, K. Wright, R. A. Johnson, H. Poppleton, K. M. Mohankumar, C. Feau, T. Phoenix, P. Gibson, L. Zhu, Y. Tong, C. Eden, D. W. Ellison, W. Priebe, D. Koul, W. K. Yung, A. Gajjar, C. F. Stewart, R. K. Guy and R. J. Gilbertson (2011). "An integrated in vitro and in vivo high-throughput screen identifies treatment leads for ependymoma." Cancer Cell **20**(3): 384-399.

Baldwin, E. L. and N. Osheroff (2005). "Etoposide, topoisomerase II and cancer." Curr Med Chem Anticancer Agents **5**(4): 363-372.

Baldwin, R. T. and S. Preston-Martin (2004). "Epidemiology of brain tumors in childhood--a review." Toxicol Appl Pharmacol **199**(2): 118-131.

Bao, S., Q. Wu, R. E. McLendon, Y. Hao, Q. Shi, A. B. Hjelmeland, M. W. Dewhirst, D. D. Bigner and J. N. Rich (2006). "Glioma stem cells promote radioresistance by preferential activation of the DNA damage response." Nature **444**(7120): 756-760.

Barvaux, V. A., P. Lorigan, M. Ranson, A. M. Gillum, R. S. McElhinney, T. B. H. McMurry and G. P. Margison (2004). "Sensitization of a human ovarian cancer cell line to temozolomide by simultaneous attenuation of the Bcl-2 antiapoptotic protein and

DNA repair by O6-alkylguanine-DNA alkyltransferase." Molecular Cancer Therapeutics **3**(10): 1215-1220.

Becker, K., C. Gregel, C. Fricke, D. Komitowski, J. Dosch and B. Kaina (2003). "DNA repair protein MGMT protects against N-methyl-N-nitrosourea-induced conversion of benign into malignant tumors." Carcinogenesis **24**(3): 541-546.

Bell, E., F. Ponthan, C. Whitworth, F. Westermann, H. Thomas and C. P. Redfern (2013). "Cell survival signalling through PPARdelta and arachidonic acid metabolites in neuroblastoma." PLoS One **8**(7): e68859.

Berger, J. and D. E. Moller (2002). "The mechanisms of action of PPARs." Annu Rev Med **53**: 409-435.

Bischoff, E. (2004). "Vardenafil preclinical trial data: potency, pharmacodynamics, pharmacokinetics, and adverse events." Int J Impot Res **16 Suppl 1**: S34-37.

Black, K. L., D. Yin, J. M. Ong, J. Hu, B. M. Konda, X. Wang, M. K. Ko, J. A. Bayan, M. R. Sacapano, A. Espinoza, D. K. Irvin and Y. Shu (2008). "PDE5 inhibitors enhance tumor permeability and efficacy of chemotherapy in a rat brain tumor model." Brain Res **1230**: 290-302.

Blanc, J., M. Wager, J. Guilhot, S. Kusy, B. Bataille, T. Chantereau, F. Lapierre, C. Larsen and L. Karayan-Tapon (2004). "Correlation of clinical features and methylation status of MGMT gene promoter in glioblastomas." Journal of neuro-oncology **68**(3): 275-283.

Blanckaert, V., V. Kerviel, A. Lepinay, V. Joubert-Durigneux, H. Hondermarck and B. Chenais (2015). "Docosahexaenoic acid inhibits the invasion of MDA-MB-231 breast cancer cells through upregulation of cytokeratin-1." Int J Oncol **46**(6): 2649-2655.

Bleau, A. M., D. Hambardzumyan, T. Ozawa, E. I. Fomchenko, J. T. Huse, C. W. Brennan and E. C. Holland (2009). "PTEN/PI3K/Akt pathway regulates the side population phenotype and ABCG2 activity in glioma tumor stem-like cells." Cell Stem Cell **4**(3): 226-235.

Bobola, M. S., J. R. Silber, R. G. Ellenbogen, J. R. Geyer, A. Blank and R. D. Goff (2005). "O6-methylguanine-DNA methyltransferase, O6-benzylguanine, and resistance to clinical alkylators in pediatric primary brain tumor cell lines." Clinical cancer research **11**(7): 2747-2755.

Boddi, V., G. Castellini, H. Casale, G. Rastrelli, L. Boni, G. Corona and M. Maggi (2015). "An integrated approach with vardenafil orodispersible tablet and cognitive behavioral sex therapy for treatment of erectile dysfunction: a randomized controlled pilot study." Andrology **3**(5): 909-918.

Boesch, D., K. Muller, A. Pourtier-Manzanedo and F. Loor (1991). "Restoration of daunomycin retention in multidrug-resistant P388 cells by submicromolar concentrations of SDZ PSC 833, a nonimmunosuppressive cyclosporin derivative." Experimental cell research **196**(1): 26-32.

Bolteus, A. J., M. E. Berens and G. J. Pilkington (2001). "Migration and invasion in brain neoplasms." Curr Neurol Neurosci Rep **1**(3): 225-232.

Bonnet, D. and J. E. Dick (1997). "Human acute myeloid leukemia is organized as a hierarchy that originates from a primitive hematopoietic cell." Nat Med **3**(7): 730-737.

Bouffet, E. and N. Foreman (1999). "Chemotherapy for intracranial ependymomas." Childs Nerv Syst **15**(10): 563-570.

Bouffet, E., G. Perilongo, A. Canete and M. Massimino (1998). "Intracranial ependymomas in children: a critical review of prognostic factors and a plea for cooperation." Med Pediatr Oncol **30**(6): 319-329; discussion 329-331.

Bradshaw, T. D. (2013). "Chemotherapeutic Allg/lating Agents in Cancer Treatment." DNA Repair and Cancer: From Bench to Clinic: 137.

Buccoliero, A. M., F. Castiglione, D. Rossi Degl'Innocenti, M. Paglierani, V. Maio, C. F. Gheri, F. Garbini, D. Moncini, A. Taddei, I. Sardi, M. Sanzo, F. Giordano, F. Mussa, L. Genitori and G. L. Taddei (2008). "O6-Methylguanine-DNA-methyltransferase in recurring anaplastic ependymomas: PCR and immunohistochemistry." J Chemother **20**(2): 263-268.

Cage, T. A., A. J. Clark, D. Aranda, N. Gupta, P. P. Sun, A. T. Parsa and K. I. Auguste (2013). "A systematic review of treatment outcomes in pediatric patients with intracranial ependymomas." J Neurosurg Pediatr **11**(6): 673-681.

Calabrese, C., H. Poppleton, M. Kocak, T. L. Hogg, C. Fuller, B. Hamner, E. Y. Oh, M. W. Gaber, D. Finklestein, M. Allen, A. Frank, I. T. Bayazitov, S. S. Zakharenko, A. Gajjar, A. Davidoff and R. J. Gilbertson (2007). "A perivascular niche for brain tumor stem cells." Cancer Cell **11**(1): 69-82.

Carter, M., J. Nicholson, F. Ross, J. Crolla, R. Allibone, V. Balaji, R. Perry, D. Walker, R. Gilbertson and D. W. Ellison (2002). "Genetic abnormalities detected in ependymomas by comparative genomic hybridisation." Br J Cancer **86**(6): 929-939.

Cejka, P., L. Stojic, N. Mojas, A. M. Russell, K. Heinimann, E. Cannavó, M. Di Pietro, G. Marra and J. Jiricny (2003). "Methylation-induced G2/M arrest requires a full complement of the mismatch repair protein hMLH1." The EMBO journal **22**(9): 2245-2254.

Chamberlain, M. C. and S. K. Johnston (2009). "Temozolomide for recurrent intracranial supratentorial platinum-refractory ependymoma." Cancer **115**(20): 4775-4782.

Chang, I. W., C. T. Hsu, J. W. Lin and C. H. Hung (2013). "The prognostic impact of MGMT expression on low-grade gangliogliomas: a clinicopathological and immunohistochemical study." Folia Neuropathol **51**(4): 275-282.

Chen, C. J., J. E. Chin, K. Ueda, D. P. Clark, I. Pastan, M. M. Gottesman and I. B. Roninson (1986). "Internal duplication and homology with bacterial transport proteins in the mdr1 (P-glycoprotein) gene from multidrug-resistant human cells." Cell **47**(3): 381-389.

Chen, C. T., J. T. Green, S. K. Orr and R. P. Bazinet (2008). "Regulation of brain polyunsaturated fatty acid uptake and turnover." Prostaglandins Leukot Essent Fatty Acids **79**(3-5): 85-91.

Chen, S., Y. Zhang and D. Zhang (2015). "Endoplasmic reticulum protein 29 (ERp29) confers radioresistance through the DNA repair gene, O(6)-methylguanine DNA-methyltransferase, in breast cancer cells." Sci Rep **5**: 14723.

Chen, X., Q. Li, H. Xu and Z. Q. Yin (2014). "Sodium iodate influences the apoptosis, proliferation and differentiation potential of radial glial cells in vitro." Cell Physiol Biochem **34**(4): 1109-1124.

Chiu, J. K., S. Y. Woo, J. Ater, J. Connelly, J. M. Bruner, M. H. Maor, J. van Eys, M. J. Oswald and R. Shallenberger (1992). "Intracranial ependymoma in children: analysis of prognostic factors." Journal of neuro-oncology **13**(3): 283-290.

Chou, P. M., M. Reyes-Mugica, N. Barquin, T. Yasuda, X. Tan and T. Tomita (1995). "Multidrug resistance gene expression in childhood medulloblastoma: correlation with clinical outcome and DNA ploidy in 29 patients." Pediatric neurosurgery **23**(6): 283-292.

Chowdhary, S., M. R. Green and M. Chamberlain (2006). "Ependymomas." Curr Treat Options Neurol **8**(4): 309-318.

Christmann, M., M. Pick, H. Lage, D. Schadendorf and K. Bernd (2001). "Acquired resistance of melanoma cells to the antineoplastic agent fotemustine is caused by reactivation of the DNA repair gene mgmt." International Journal of Cancer **92**(1): 123-129.

Clemons, M., J. Kelly, A. J. Watson, A. Howell, R. McElhinney, T. McMurry and G. P. Margison (2005). "O6-(4-bromothenyl) guanine reverses temozolomide resistance in human breast tumour MCF-7 cells and xenografts." British journal of cancer **93**(10): 1152-1156.

Clevers, H. (2011). "The cancer stem cell: premises, promises and challenges." Nature medicine: 313-319.

Colone, M., A. Calcabrini, L. Toccacieli, G. Bozzuto, A. Stringaro, M. Gentile, M. Cianfriglia, A. Ciervo, M. Caraglia, A. Budillon, G. Meo, G. Arancia and A. Molinari (2008). "The multidrug transporter P-glycoprotein: a mediator of melanoma invasion?" J Invest Dermatol **128**(4): 957-971.

Combs, S. E., C. Thilmann, J. Debus and D. Schulz-Ertner (2006). "Local radiotherapeutic management of ependymomas with fractionated stereotactic radiotherapy (FSRT)." BMC Cancer **6**: 222.

Conover, J. C. and R. L. Allen (2002). "The subventricular zone: new molecular and cellular developments." Cell Mol Life Sci **59**(12): 2128-2135.

Coyle, B., M. Kessler, D. H. Sabnis and Ian D. Kerr (2015). "ABCB1 in children's brain tumours." Biochemical Society Transactions **43**(5): 1018-1022.

D'Atri, S., L. Tentori, P. M. Lacal, G. Graziani, E. Pagani, E. Benincasa, G. Zambruno, E. Bonmassar and J. Jiricny (1998). "Involvement of the mismatch repair system in temozolomide-induced apoptosis." Molecular pharmacology **54**(2): 334-341.

Daenen, S., B. van der Holt, G. E. Verhoef, B. Löwenberg, P. W. Wijermans, P. C. Huijgens, R. van Marwijk Kooy, H. C. Schouten, M. H. Kramer and A. Ferrant (2004). "Addition of cyclosporin A to the combination of mitoxantrone and etoposide to overcome resistance to chemotherapy in refractory or relapsing acute myeloid leukaemia:: A randomised phase II trial from HOVON, the Dutch–Belgian Haemato-Oncology Working Group for adults." Leukemia research **28**(10): 1057-1067.

Dantzer, F., V. Schreiber, C. Niedergang, C. Trucco, E. Flatter, G. D. L. Rubia, J. Oliver, V. Rolli, J. Ménissier-de Murcia and G. de Murcia (1999). "Involvement of poly (ADP-ribose) polymerase in base excision repair." Biochimie **81**(1-2): 69-75.

Dantzig, A. H., R. L. Shepard, J. Cao, K. L. Law, W. J. Ehlhardt, T. M. Baughman, T. F. Bumol and J. J. Starling (1996). "Reversal of P-glycoprotein-mediated multidrug

resistance by a potent cyclopropyldibenzosuberane modulator, LY335979." Cancer Research **56**(18): 4171-4179.

Dasen, J. S., J. P. Liu and T. M. Jessell (2003). "Motor neuron columnar fate imposed by sequential phases of Hox-c activity." Nature **425**(6961): 926-933.

De Rosa, A., S. Pellegatta, M. Rossi, P. Tunici, L. Magnoni, M. C. Speranza, F. Malusa, V. Miragliotta, E. Mori, G. Finocchiaro and A. Bakker (2012). "A radial glia gene marker, fatty acid binding protein 7 (FABP7), is involved in proliferation and invasion of glioblastoma cells." PLoS One **7**(12): e52113.

Dean, M., T. Fojo and S. Bates (2005). "Tumour stem cells and drug resistance." Nature Reviews Cancer **5**(4): 275-284.

Deckelbaum, R. J., T. S. Worgall and T. Seo (2006). "n-3 fatty acids and gene expression." Am J Clin Nutr **83**(6 Suppl): 1520s-1525s.

Denny, B. J., R. T. Wheelhouse, M. F. Stevens, L. L. Tsang and J. A. Slack (1994). "NMR and molecular modeling investigation of the mechanism of activation of the antitumor drug temozolomide and its interaction with DNA." Biochemistry **33**(31): 9045-9051.

Ding, P. R., A. K. Tiwari, S. Ohnuma, J. W. Lee, X. An, C. L. Dai, Q. S. Lu, S. Singh, D. H. Yang, T. T. Talele, S. V. Ambudkar and Z. S. Chen (2011). "The phosphodiesterase-5 inhibitor vardenafil is a potent inhibitor of ABCB1/P-glycoprotein transporter." PLoS One **6**(4): e19329.

Dolan, M. E., R. C. Moschel and A. E. Pegg (1990). "Depletion of mammalian O6-alkylguanine-DNA alkyltransferase activity by O6-benzylguanine provides a means to evaluate the role of this protein in protection against carcinogenic and therapeutic alkylating agents." Proceedings of the National Academy of Sciences **87**(14): 5368-5372.

Domcke, S., R. Sinha, D. A. Levine, C. Sander and N. Schultz (2013). "Evaluating cell lines as tumour models by comparison of genomic profiles." Nat Commun **4**.

Duffner, P. K., M. E. Cohen, M. H. Myers and H. W. Heise (1986). "Survival of children with brain tumors: SEER Program, 1973-1980." Neurology **36**(5): 597-601.

Duncan, J. A. (1995). "Intracranial ependymomas." Brain Tumors **124**(3).

Dyer, S., E. Prebble, V. Davison, P. Davies, P. Ramani, D. Ellison and R. Grundy (2002). "Genomic imbalances in pediatric intracranial ependymomas define clinically relevant groups." Am J Pathol **161**(6): 2133-2141.

Eckford, P. D. and F. J. Sharom (2006). "P-glycoprotein (ABCB1) interacts directly with lipid-based anti-cancer drugs and platelet-activating factors." Biochem Cell Biol **84**(6): 1022-1033.

Ellison, D. W., M. Kocak, D. Figarella-Branger, G. Felice, G. Catherine, T. Pietsch, D. Frappaz, M. Massimino, J. Grill, J. M. Boyett and R. G. Grundy (2011). "Histopathological grading of pediatric ependymoma: reproducibility and clinical relevance in European trial cohorts." J Negat Results Biomed **10**: 7.

Elsherbiny, M. E., M. Emara and R. Godbout (2013). "Interaction of brain fatty acid-binding protein with the polyunsaturated fatty acid environment as a potential determinant of poor prognosis in malignant glioma." Prog Lipid Res **52**(4): 562-570.

Endicott, J. A. and V. Ling (1989). "The biochemistry of P-glycoprotein-mediated multidrug resistance." Annu Rev Biochem **58**: 137-171.

Fahrmann, J. F. and W. E. Hardman (2013). "Omega 3 fatty acids increase the chemo-sensitivity of B-CLL-derived cell lines EHEB and MEC-2 and of B-PLL-derived cell line JVM-2 to anti-cancer drugs doxorubicin, vincristine and fludarabine." Lipids Health Dis **12**: 36.

Feng, L., M. E. Hatten and N. Heintz (1994). "Brain lipid-binding protein (BLBP): a novel signaling system in the developing mammalian CNS." Neuron **12**(4): 895-908.

Filipski, E., E. Berland, N. Ozturk, C. Guettier, G. T. van der Horst, F. Levi and A. Okyar (2014). "Optimization of irinotecan chronotherapy with P-glycoprotein inhibition." Toxicol Appl Pharmacol **274**(3): 471-479.

Fishell, G. and A. R. Kriegstein (2003). "Neurons from radial glia: the consequences of asymmetric inheritance." Curr Opin Neurobiol **13**(1): 34-41.

Ford, J. M. and W. N. Hait (1993). "Pharmacologic circumvention of multidrug resistance." Cytotechnology **12**(1-3): 171-212.

Franken, N. A., H. M. Rodermond, J. Stap, J. Haveman and C. van Bree (2006). "Clonogenic assay of cells in vitro." Nat Protoc **1**(5): 2315-2319.

Friedl, P., J. Locker, E. Sahai and J. E. Segall (2012). "Classifying collective cancer cell invasion." Nat Cell Biol **14**(8): 777-783.

Friedman, H. S., J. Pluda, J. A. Quinn, R. B. Ewesuedo, L. Long, A. H. Friedman, I. Cokgor, O. M. Colvin, M. M. Haglund and D. M. Ashley (2000). "Phase I trial of carmustine plus O6-benzylguanine for patients with recurrent or progressive malignant glioma." Journal of clinical oncology **18**(20): 3522-3528.

Friedmann-Morvinski, D., E. A. Bushong, E. Ke, Y. Soda, T. Marumoto, O. Singer, M. H. Ellisman and I. M. Verma (2012). "Dedifferentiation of neurons and astrocytes by oncogenes can induce gliomas in mice." Science **338**(6110): 1080-1084.

Gajjar, A., S. M. Pfister, M. D. Taylor and R. J. Gilbertson (2014). "Molecular insights into pediatric brain tumors have the potential to transform therapy." Clin Cancer Res **20**(22): 5630-5640.

Gatta, G., L. Botta, S. Rossi, T. Aareleid, M. Bielska-Lasota, J. Clavel, N. Dimitrova, Z. Jakab, P. Kaatsch, B. Lacour, S. Mallone, R. Marcos-Gragera, P. Minicozzi, M. J. Sanchez-Perez, M. Sant, M. Santaquilani, C. Stiller, A. Tavilla, A. Trama, O. Visser and R. Peris-Bonet (2014). "Childhood cancer survival in Europe 1999-2007: results of EUROCARE-5--a population-based study." Lancet Oncol **15**(1): 35-47.

Gerson, S. L. (2004). "MGMT: its role in cancer aetiology and cancer therapeutics." Nat Rev Cancer **4**(4): 296-307.

Geyer, J. R., R. Sposto, M. Jennings, J. M. Boyett, R. A. Axtell, D. Breiger, E. Broxson, B. Donahue, J. L. Finlay, J. W. Goldwein, L. A. Heier, D. Johnson, C. Mazewski, D. C. Miller, R. Packer, D. Puccetti, J. Radcliffe, M. L. Tao and T. Shiminski-Maher (2005). "Multiagent chemotherapy and deferred radiotherapy in infants with malignant brain tumors: a report from the Children's Cancer Group." J Clin Oncol **23**(30): 7621-7631.

Godfraind, C., J. M. Kaczmarska, M. Kocak, J. Dalton, K. D. Wright, R. A. Sanford, F. A. Boop, A. Gajjar, T. E. Merchant and D. W. Ellison (2012). "Distinct disease-risk

groups in pediatric supratentorial and posterior fossa ependymomas." Acta Neuropathol **124**(2): 247-257.

Goldman, B. (2003). "Multidrug resistance: can new drugs help chemotherapy score against cancer?" Journal of the National Cancer Institute **95**(4): 255-257.

Goldstein, L. J., H. Galski, A. Fojo, M. Willingham, S.-L. Lai, A. Gazdar, R. Pirker, A. Green, W. Crist and G. M. Brodeur (1989). "Expression of multidrug resistance gene in human cancers." Journal of the National Cancer Institute **81**(2): 116-124.

Goodman, L. S., A. G. Gilman and A. Gilman (1980). Pharmacological Basis of Therapeutics. Edited by Alfred Goodman Gilman, Louis S Goodman [and] Alfred Gilman, Macmillan.

Goto, Y., Y. Matsuzaki, S. Kurihara, A. Shimizu, T. Okada, K. Yamamoto, H. Murata, M. Takata, H. Aburatani, D. S. Hoon, T. Saida and Y. Kawakami (2006). "A new melanoma antigen fatty acid-binding protein 7, involved in proliferation and invasion, is a potential target for immunotherapy and molecular target therapy." Cancer Res **66**(8): 4443-4449.

Gottesman, M. M. and S. V. Ambudkar (2001). "Overview: ABC transporters and human disease." Journal of bioenergetics and biomembranes **33**(6): 453-458.

Gotz, M. and W. B. Huttner (2005). "The cell biology of neurogenesis." Nat Rev Mol Cell Biol **6**(10): 777-788.

Graham, S. M., H. G. Jørgensen, E. Allan, C. Pearson, M. J. Alcorn, L. Richmond and T. L. Holyoake (2002). "Primitive, quiescent, Philadelphia-positive stem cells from patients with chronic myeloid leukemia are insensitive to STI571 in vitro." Blood **99**(1): 319-325.

Granzow, M., S. Popp, S. Weber, B. Schoell, H. Holtgreve-Grez, L. Senf, D. Hager, J. Boschert, W. Scheurlen and A. Jauch (2001). "Isochromosome 1q as an early genetic event in a child with intracranial ependymoma characterized by molecular cytogenetics." Cancer Genet Cytogenet **130**(1): 79-83.

Grill, J., M. C. Le Deley, D. Gambarelli, M. A. Raquin, D. Couanet, A. Pierre-Kahn, J. L. Habrand, F. Doz, D. Frappaz, J. C. Gentet, C. Edan, P. Chastagner and C. Kalifa (2001). "Postoperative chemotherapy without irradiation for ependymoma in children under 5 years of age: a multicenter trial of the French Society of Pediatric Oncology." J Clin Oncol **19**(5): 1288-1296.

Grill, J., C. Pascal and K. Chantal (2003). "Childhood ependymoma: a systematic review of treatment options and strategies." Paediatr Drugs **5**(8): 533-543.

Grosflam, J. and M. E. Weinblatt (1991). "Methotrexate: mechanism of action, pharmacokinetics, clinical indications, and toxicity." Current opinion in rheumatology **3**(3): 363-368.

Grundy, R. G., S. A. Wilne, C. L. Weston, K. Robinson, L. S. Lashford, J. Ironside, T. Cox, W. K. Chong, R. H. Campbell, C. C. Bailey, R. Gattamaneni, S. Picton, N. Thorpe, C. Mallucci, M. W. English, J. A. Punt, D. A. Walker, D. W. Ellison and D. Machin (2007). "Primary postoperative chemotherapy without radiotherapy for intracranial ependymoma in children: the UKCCSG/SIOP prospective study." Lancet Oncol **8**(8): 696-705.

Guns, E. S., T. Denyssevych, R. Dixon, M. B. Bally and L. Mayer (2002). "Drug interaction studies between paclitaxel (Taxol) and OC144-093—a new modulator of

MDR in cancer chemotherapy." European journal of drug metabolism and pharmacokinetics **27**(2): 119-126.

Gupta, R. K., M. C. Sharma, V. Suri, A. Kakkar, M. Singh and C. Sarkar (2014). "Study of chromosome 9q gain, Notch pathway regulators and Tenascin-C in ependymomas." J Neurooncol **116**(2): 267-274.

Hadnagy, A., L. Gaboury, R. Beaulieu and D. Balicki (2006). "SP analysis may be used to identify cancer stem cell populations." Experimental cell research **312**(19): 3701-3710.

Hande, K. R. (1998). "Etoposide: four decades of development of a topoisomerase II inhibitor." Eur J Cancer **34**(10): 1514-1521.

Hansen, R. J., S. M. Ludeman, S. J. Paikoff, A. E. Pegg and M. E. Dolan (2007). "Role of MGMT in protecting against cyclophosphamide-induced toxicity in cells and animals." DNA Repair (Amst) **6**(8): 1145-1154.

Harvey, K. A., Z. Xu, M. R. Saaddatzadeh, H. Wang, K. Pollok, A. A. Cohen-Gadol and R. A. Siddiqui (2015). "Enhanced anticancer properties of lomustine in conjunction with docosahexaenoic acid in glioblastoma cell lines." J Neurosurg **122**(3): 547-556.

He, J., Z. Shan, L. Li, F. Liu, Z. Liu, M. Song and H. Zhu (2011). "Expression of glioma stem cell marker CD133 and O6-methylguanine-DNA methyltransferase is associated with resistance to radiotherapy in gliomas." Oncology reports **26**(5): 1305-1313.

Hegi, M. E., A.-C. Diserens, T. Gorlia, M.-F. Hamou, N. de Tribolet, M. Weller, J. M. Kros, J. A. Hainfellner, W. Mason and L. Mariani (2005). "MGMT gene silencing and benefit from temozolomide in glioblastoma." New England Journal of Medicine **352**(10): 997-1003.

Hegi, M. E., L. Liu, J. G. Herman, R. Stupp, W. Wick, M. Weller, M. P. Mehta and M. R. Gilbert (2008). "Correlation of O6-methylguanine methyltransferase (MGMT) promoter methylation with clinical outcomes in glioblastoma and clinical strategies to modulate MGMT activity." Journal of clinical oncology **26**(25): 4189-4199.

Higgins, S. C., H. Steingrimsdottir and G. J. Pilkington (2010). "Human, mouse or rat? Species authentication of glioma-derived cell cultures." Journal of neuroscience methods **194**(1): 139-143.

Hirschmann-Jax, C., A. E. Foster, G. G. Wulf, J. G. Nuchtern, T. W. Jax, U. Gobel, M. A. Goodell and M. K. Brenner (2004). "A distinct side population of cells with high drug efflux capacity in human tumor cells." Proceedings of the National Academy of Sciences of the United States of America **101**(39): 14228.

Hoffman, K. E. and T. I. Yock (2009). "Radiation therapy for pediatric central nervous system tumors." J Child Neurol **24**(11): 1387-1396.

Hoffman, L. M., A. M. Donson, I. Nakachi, A. M. Griesinger, D. K. Birks, V. Amani, M. S. Hemenway, A. K. Liu, M. Wang, T. C. Hankinson, M. H. Handler and N. K. Foreman (2014). "Molecular sub-group-specific immunophenotypic changes are associated with outcome in recurrent posterior fossa ependymoma." Acta Neuropathol **127**(5): 731-745.

Hong, I. S., G. B. Jang, H. Y. Lee and J. S. Nam (2015). "Targeting cancer stem cells by using the nanoparticles." Int J Nanomedicine **10**(Spec Iss): 251-260.

Horton, J. K. and S. H. Wilson (2007). "Hypersensitivity phenotypes associated with genetic and synthetic inhibitor-induced base excision repair deficiency." DNA repair **6**(4): 530.

Hu, J., J. Y. Ljubimova, S. Inoue, B. Konda, R. Patil, H. Ding, A. Espinoza, K. A. Wawrowsky, C. Patil, A. V. Ljubimov and K. L. Black (2010). "Phosphodiesterase type 5 inhibitors increase Herceptin transport and treatment efficacy in mouse metastatic brain tumor models." PLoS One **5**(4): e10108.

Hussein, D., W. Punjaruk, L. C. Storer, L. Shaw, R. Othman, A. Peet, S. Miller, G. Bandopadhyay, R. Heath, R. Kumari, K. J. Bowman, P. Braker, R. Rahman, G. D. Jones, S. Watson, J. Lowe, I. D. Kerr, R. G. Grundy and B. Coyle (2011). "Pediatric brain tumor cancer stem cells: cell cycle dynamics, DNA repair, and etoposide extrusion." Neuro Oncol **13**(1): 70-83.

Jamroziak, K. and T. Robak (2004). "Pharmacogenomics of MDR1/ABCB1 gene: the influence on risk and clinical outcome of haematological malignancies." Hematology **9**(2): 91-105.

Jiang, M., X. Dong, J. Li, J. Li and J. Qi (2014). "[IDH1 mutation and MGMT expression in astrocytoma and the relationship with prognosis after radiotherapy]." Zhonghua Bing Li Xue Za Zhi **43**(10): 668-672.

Jing, Z. C., Z. X. Yu, J. Y. Shen, B. X. Wu, K. F. Xu, X. Y. Zhu, L. Pan, Z. L. Zhang, X. Q. Liu, Y. S. Zhang, X. Jiang and N. Galie (2011). "Vardenafil in pulmonary arterial hypertension: a randomized, double-blind, placebo-controlled study." Am J Respir Crit Care Med **183**(12): 1723-1729.

Johnson, K. J., J. Cullen, J. S. Barnholtz-Sloan, Q. T. Ostrom, C. E. Langer, M. C. Turner, R. McKean-Cowdin, J. L. Fisher, P. J. Lupo, S. Partap, J. A. Schwartzbaum and M. E. Scheurer (2014). "Childhood brain tumor epidemiology: a brain tumor epidemiology consortium review." Cancer Epidemiol Biomarkers Prev **23**(12): 2716-2736.

Johnson, R. A., K. D. Wright, H. Poppleton, K. M. Mohankumar, D. Finkelstein, S. B. Pounds, V. Rand, S. E. Leary, E. White, C. Eden, T. Hogg, P. Northcott, S. Mack, G. Neale, Y. D. Wang, B. Coyle, J. Atkinson, M. DeWire, T. A. Kranenburg, Y. Gillespie, J. C. Allen, T. Merchant, F. A. Boop, R. A. Sanford, A. Gajjar, D. W. Ellison, M. D. Taylor, R. G. Grundy and R. J. Gilbertson (2010). "Cross-species genomics matches driver mutations and cell compartments to model ependymoma." Nature **466**(7306): 632-636.

Johnstone, R. W., A. A. Ruefli and M. J. Smyth (2000). "Multiple physiological functions for multidrug transporter P-glycoprotein?" Trends in biochemical sciences **25**(1): 1-6.

Jordan, M. A. (2002). "Mechanism of action of antitumor drugs that interact with microtubules and tubulin." Curr Med Chem Anticancer Agents **2**(1): 1-17.

Jun, G.-J., J.-Y. Ro, M. H. Kim, P. Gil-Hong, W. K. Paik, P. N. Magee and K. Sangduk (1986). "Studies on the distribution of< i> O</i>< sup> 6</sup>-methylguanine-dna methyltransferase in rat." Biochemical pharmacology **35**(3): 377-384.

Kaloshi, G., K. Mokhtari, C. Carpentier, S. Taillibert, J. Lejeune, Y. Marie, J. Y. Delattre, R. Godbout and M. Sanson (2007). "FABP7 expression in glioblastomas: relation to prognosis, invasion and EGFR status." J Neurooncol **84**(3): 245-248.

Kennedy, R. D. and A. D. D'Andrea (2006). "DNA repair pathways in clinical practice: lessons from pediatric cancer susceptibility syndromes." Journal of clinical oncology **24**(23): 3799-3808.

Khan, O., M. Ranson, M. Michael, I. Olver, N. Levitt, P. Mortimer, A. J. Watson, G. P. Margison, R. Midgley and M. R. Middleton (2008). "A phase II trial of lomeguatrib and temozolomide in metastatic colorectal cancer." British journal of cancer **98**(10): 1614-1618.

Khatua, S., Z. S. Sadighi, M. L. Pearlman, S. Bochare and T. S. Vats (2012). "Brain tumors in children--current therapies and newer directions." Indian J Pediatr **79**(7): 922-927.

Khoo, H. M., H. Kishima, M. Kinoshita, Y. Goto, N. Kagawa, N. Hashimoto, M. Maruno and T. Yoshimine (2013). "Radiation-induced anaplastic ependymoma with a remarkable clinical response to temozolomide: a case report." Br J Neurosurg **27**(2): 259-261.

Kilday, J. P., B. Mitra, C. Domerg, J. Ward, F. Andreiuolo, T. Osteso-Ibanez, A. Mauguen, P. Varlet, M. C. Le Deley, J. Lowe, D. W. Ellison, R. J. Gilbertson, B. Coyle, J. Grill and R. G. Grundy (2012). "Copy number gain of 1q25 predicts poor progression-free survival for pediatric intracranial ependymomas and enables patient risk stratification: a prospective European clinical trial cohort analysis on behalf of the Children's Cancer Leukaemia Group (CCLG), Societe Francaise d'Oncologie Pediatrique (SFOP), and International Society for Pediatric Oncology (SIOP)." Clin Cancer Res **18**(7): 2001-2011.

Kilday, J. P., R. Rahman, S. Dyer, L. Ridley, J. Lowe, B. Coyle and R. Grundy (2009). "Pediatric ependymoma: biological perspectives." Mol Cancer Res **7**(6): 765-786.

Kim, K. R., H. N. Choi, H. J. Lee, H. A. Baek, H. S. Park, K. Y. Jang, M. J. Chung and W. S. Moon (2007). "A peroxisome proliferator-activated receptor gamma antagonist induces vimentin cleavage and inhibits invasion in high-grade hepatocellular carcinoma." Oncol Rep **18**(4): 825-832.

Koirala, S. and G. Corfas (2010). "Identification of Novel Glial Genes by Single-Cell Transcriptional Profiling of Bergmann Glial Cells from Mouse Cerebellum." PLoS ONE **5**(2): e9198.

Kokoglu, E., Y. Tuter, K. S. Sandikci, Z. Yazici, E. Z. Ulakoglu, H. Sonmez and E. Ozyurt (1998). "Prostaglandin E2 levels in human brain tumor tissues and arachidonic acid levels in the plasma membrane of human brain tumors." Cancer Lett **132**(1-2): 17-21.

Kolitz, J. E., S. L. George, R. K. Dodge, D. D. Hurd, B. L. Powell, S. L. Allen, E. Velez-Garcia, J. O. Moore, T. C. Shea and E. Hoke (2004). "Dose escalation studies of cytarabine, daunorubicin, and etoposide with and without multidrug resistance modulation with PSC-833 in untreated adults with acute myeloid leukemia younger than 60 years: final induction results of Cancer and Leukemia Group B Study 9621." Journal of clinical oncology **22**(21): 4290-4301.

Komori, K., R. Yanagisawa, Y. Miyairi, K. Sakashita, M. Shiohara, I. Fujihara, D. Morita, T. Nakamura, Y. Ogiso, K. Sano, M. Shirahata, K. Fukuoka, K. Ichimura and H. Shigeta (2015). "Temozolomide treatment for pediatric refractory anaplastic ependymoma with low MGMT protein expression." Pediatr Blood Cancer.

Komori, K., R. Yanagisawa, Y. Miyairi, K. Sakashita, M. Shiohara, I. Fujihara, D. Morita, T. Nakamura, Y. Ogiso, K. Sano, M. Shirahata, K. Fukuoka, K. Ichimura and

H. Shigeta (2016). "Temozolomide Treatment for Pediatric Refractory Anaplastic Ependymoma with Low MGMT Protein Expression." Pediatr Blood Cancer **63**(1): 152-155.

Konduri, S. D., J. Ticku, G. C. Bobustuc, R. M. Sutphin, J. Colon, B. Isley, K. K. Bhakat, K. S. Srivenugopal and C. H. Baker (2009). "Blockade of MGMT expression by O6 benzyl guanine leads to inhibition of pancreatic cancer growth and induction of apoptosis." Clin Cancer Res **15**(19): 6087-6095.

Koos, B., S. Bender, H. Witt, S. Mertsch, J. Felsberg, R. Beschorner, A. Korshunov, B. Riesmeier, S. Pfister, W. Paulus and M. Hasselblatt (2011). "The transcription factor evi-1 is overexpressed, promotes proliferation, and is prognostically unfavorable in infratentorial ependymomas." Clin Cancer Res **17**(11): 3631-3637.

Koos, B., S. Peetz-Dienhart, B. Riesmeier, M. C. Fruhwald and M. Hasselblatt (2010). "O(6)-methylguanine-DNA methyltransferase (MGMT) promoter methylation is significantly less frequent in ependymal tumours as compared to malignant astrocytic gliomas." Neuropathol Appl Neurobiol **36**(4): 356-358.

Kowalsky, L., G. D. Nieminen, R. H. Braxtan and M. L. Mathis (2004). System and method to effect mitral valve annulus of a heart, Google Patents.

Kramer, D. L., A. H. Parmiter, L. B. Rorke, L. N. Sutton and J. A. Biegel (1998). "Molecular cytogenetic studies of pediatric ependymomas." J Neurooncol **37**(1): 25-33.

Krishna, R., G. De Jong and L. Mayer (1997). "Pulsed exposure of SDZ PSC 833 to multidrug resistant P388/ADR and MCF7/ADR cells in the absence of anticancer drugs can fully restore sensitivity to doxorubicin." Anticancer research **17**(5A): 3329-3334.

Krishna, R. and L. D. Mayer (2000). "Multidrug resistance (MDR) in cancer: mechanisms, reversal using modulators of MDR and the role of MDR modulators in influencing the pharmacokinetics of anticancer drugs." European Journal of Pharmaceutical Sciences **11**(4): 265-283.

Kroetz, D. L., C. Pauli-Magnus, L. M. Hodges, C. C. Huang, M. Kawamoto, S. J. Johns, D. Stryke, T. E. Ferrin, J. DeYoung, T. Taylor, E. J. Carlson, I. Herskowitz, K. M. Giacomini, A. G. Clark and I. Pharmacogenetics of Membrane Transporters (2003). "Sequence diversity and haplotype structure in the human ABCB1 (MDR1, multidrug resistance transporter) gene." Pharmacogenetics **13**(8): 481-494.

Kuhn, M. and A. Von Wartbung (1967). "Podophyllum-Lignane: Struktur und Absolutkonfiguration von Podorhizol-β-D-glucosid (= Lignan F). 19. Mitt. über mitosehemmende Naturstoffe [1]." Helvetica Chimica Acta **50**(6): 1546-1565.

Laberge, M. (2002). "http://www.healthline.com/galecontent/ependymoma#diagnosis." heathline.

Lage, H., M. Christmann, M. A. Kern, M. Dietel, M. Pick, B. Kaina and D. Schadendorf (1999). "Expression of DNA repair proteins hMSH2, hMSH6, hMLH1, O6-methylguanine-DNA methyltransferase and N-methylpurine-DNA glycosylase in melanoma cells with acquired drug resistance." Int J Cancer **80**(5): 744-750.

Laurent, L. C., I. Ulitsky, I. Slavin, H. Tran, A. Schork, R. Morey, C. Lynch, J. V. Harness, S. Lee and M. J. Barrero (2011). "Dynamic changes in the copy number of pluripotency and cell proliferation genes in human ESCs and iPSCs during reprogramming and time in culture." Cell stem cell **8**(1): 106-118.

Lee, A., J. D. Kessler, T. A. Read, C. Kaiser, D. Corbeil, W. B. Huttner, J. E. Johnson and R. J. Wechsler-Reya (2005). "Isolation of neural stem cells from the postnatal cerebellum." Nature neuroscience **8**(6): 723.

Lee, C. T., S. D. Bilton, R. M. Famiglietti, B. A. Riley, A. Mahajan, E. L. Chang, M. H. Maor, S. Y. Woo, J. D. Cox and A. R. Smith (2005). "Treatment planning with protons for pediatric retinoblastoma, medulloblastoma, and pelvic sarcoma: how do protons compare with other conformal techniques?" Int J Radiat Oncol Biol Phys **63**(2): 362-372.

Lei, X., C. W. Guan, Y. Song and H. Wang (2015). "The multifaceted role of CD146/MCAM in the promotion of melanoma progression." Cancer Cell Int **15**(1): 3.

Leighton Jr, J. C. and L. J. Goldstein (1995). "P-glycoprotein in adult solid tumors. Expression and prognostic significance." Hematology/oncology clinics of North America **9**(2): 251.

Lendahl, U., L. B. Zimmerman and R. D. McKay (1990). "CNS stem cells express a new class of intermediate filament protein." Cell **60**(4): 585-595.

Li, A. M., C. Dunham, U. Tabori, A. S. Carret, P. D. McNeely, D. Johnston, L. Lafay-Cousin, B. Wilson, D. D. Eisenstat, N. Jabado, S. Zelcer, M. Silva, K. Scheinemann, C. Fryer, G. Hendson, A. Fotovati, C. Hawkins, S. Yip, S. E. Dunn and J. Hukin (2015). "EZH2 expression is a prognostic factor in childhood intracranial ependymoma: a Canadian Pediatric Brain Tumor Consortium study." Cancer **121**(9): 1499-1507.

Li, C. C., Y. C. Hou, C. L. Yeh and S. L. Yeh (2014). "Effects of eicosapentaenoic acid and docosahexaenoic acid on prostate cancer cell migration and invasion induced by tumor-associated macrophages." PLoS One **9**(6): e99630.

Li, S., J. Qin, C. Tian, J. Cao, G. Fida, Z. Wang, H. Chen, Z. Qian, W. R. Chen and Y. Gu (2014). "The targeting mechanism of DHA ligand and its conjugate with Gemcitabine for the enhanced tumor therapy." Oncotarget **5**(11): 3622-3635.

Liang, C.-C., A. Y. Park and J.-L. Guan (2007). "In vitro scratch assay: a convenient and inexpensive method for analysis of cell migration in vitro." Nat. Protocols **2**(2): 329-333.

Liang, Y., A. W. Bollen, K. D. Aldape and N. Gupta (2006). "Nuclear FABP7 immunoreactivity is preferentially expressed in infiltrative glioma and is associated with poor prognosis in EGFR-overexpressing glioblastoma." BMC Cancer **6**: 97.

Lim, A. and B. F. Li (1996). "The nuclear targeting and nuclear retention properties of a human DNA repair protein O6-methylguanine-DNA methyltransferase are both required for its nuclear localization: the possible implications." EMBO J **15**(15): 4050-4060.

Lin, L. C., S. L. Hsu, C. L. Wu and C. M. Hsueh (2014). "TGFbeta can stimulate the p(38)/beta-catenin/PPARgamma signaling pathway to promote the EMT, invasion and migration of non-small cell lung cancer (H460 cells)." Clin Exp Metastasis **31**(8): 881-895.

Lombardi, G., A. Pambuku, L. Bellu, A. Della Puppa, L. Rumano, M. P. Gardiman, F. Pomerri and V. Zagonel (2013). "Cisplatin and temozolomide combination in the treatment of supratentorial anaplastic ependymoma." Chemotherapy **59**(3): 176-180.

Louis, D. N., H. Ohgaki, O. D. Wiestler, W. K. Cavenee, P. C. Burger, A. Jouvet, B. W. Scheithauer and P. Kleihues (2007). "The 2007 WHO classification of tumours of the central nervous system." Acta Neuropathol **114**(2): 97-109.

Lukiw, W. J. and N. G. Bazan (2008). "Docosahexaenoic acid and the aging brain." J Nutr **138**(12): 2510-2514.

MacDonald, S. M., S. Safai, A. Trofimov, J. Wolfgang, B. Fullerton, B. Y. Yeap, T. Bortfeld, N. J. Tarbell and T. Yock (2008). "Proton radiotherapy for childhood ependymoma: initial clinical outcomes and dose comparisons." Int J Radiat Oncol Biol Phys **71**(4): 979-986.

Mack, S. C., H. Witt, R. M. Piro, L. Gu, S. Zuyderduyn, A. M. Stutz, X. Wang, M. Gallo, L. Garzia, K. Zayne, X. Zhang, V. Ramaswamy, N. Jager, D. T. Jones, M. Sill, T. J. Pugh, M. Ryzhova, K. M. Wani, D. J. Shih, R. Head, M. Remke, S. D. Bailey, T. Zichner, C. C. Faria, M. Barszczyk, S. Stark, H. Seker-Cin, S. Hutter, P. Johann, S. Bender, V. Hovestadt, T. Tzaridis, A. M. Dubuc, P. A. Northcott, J. Peacock, K. C. Bertrand, S. Agnihotri, F. M. Cavalli, I. Clarke, K. Nethery-Brokx, C. L. Creasy, S. K. Verma, J. Koster, X. Wu, Y. Yao, T. Milde, P. Sin-Chan, J. Zuccaro, L. Lau, S. Pereira, P. Castelo-Branco, M. Hirst, M. A. Marra, S. S. Roberts, D. Fults, L. Massimi, Y. J. Cho, T. Van Meter, W. Grajkowska, B. Lach, A. E. Kulozik, A. von Deimling, O. Witt, S. W. Scherer, X. Fan, K. M. Muraszko, M. Kool, S. L. Pomeroy, N. Gupta, J. Phillips, A. Huang, U. Tabori, C. Hawkins, D. Malkin, P. N. Kongkham, W. A. Weiss, N. Jabado, J. T. Rutka, E. Bouffet, J. O. Korbel, M. Lupien, K. D. Aldape, G. D. Bader, R. Eils, P. Lichter, P. B. Dirks, S. M. Pfister, A. Korshunov and M. D. Taylor (2014). "Epigenomic alterations define lethal CIMP-positive ependymomas of infancy." Nature **506**(7489): 445-450.

Manzi, L., L. Costantini, R. Molinari and N. Merendino (2015). "Effect of Dietary omega-3 Polyunsaturated Fatty Acid DHA on Glycolytic Enzymes and Warburg Phenotypes in Cancer." Biomed Res Int **2015**: 137097.

Mao, D. D., A. D. Gujar, T. Mahlokozera, I. Chen, Y. Pan, J. Luo, T. Brost, E. A. Thompson, A. Turski, E. C. Leuthardt, G. P. Dunn, M. R. Chicoine, K. M. Rich, J. L. Dowling, G. J. Zipfel, R. G. Dacey, S. Achilefu, D. D. Tran, H. Yano and A. H. Kim (2015). "A CDC20-APC/SOX2 Signaling Axis Regulates Human Glioblastoma Stem-like Cells." Cell Rep **11**(11): 1809-1821.

Margison, G. P. and M. F. Santibáñez-Koref (2002). "O6-alkylguanine-DNA alkyltransferase: Role in carcinogenesis and chemotherapy." Bioessays **24**(3): 255-266.

Martin, D. D., M. E. Robbins, A. A. Spector, B. C. Wen and D. H. Hussey (1996). "The fatty acid composition of human gliomas differs from that found in nonmalignant brain tissue." Lipids **31**(12): 1283-1288.

Massimino, M., L. Gandola, F. Giangaspero, A. Sandri, P. Valagussa, G. Perilongo, M. L. Garre, U. Ricardi, M. Forni, L. Genitori, G. Scarzello, F. Spreafico, S. Barra, M. Mascarin, B. Pollo, M. Gardiman, A. Cama, P. Navarria, M. Brisigotti, P. Collini, R. Balter, P. Fidani, M. Stefanelli, R. Burnelli, P. Potepan, M. Podda, G. Sotti and E. Madon (2004). "Hyperfractionated radiotherapy and chemotherapy for childhood ependymoma: final results of the first prospective AIEOP (Associazione Italiana di Ematologia-Oncologia Pediatrica) study." Int J Radiat Oncol Biol Phys **58**(5): 1336-1345.

Meco, D., T. Servidei, G. Lamorte, E. Binda, V. Arena and R. Riccardi (2014). "Ependymoma stem cells are highly sensitive to temozolomide in vitro and in orthotopic models." Neuro Oncol **16**(8): 1067-1077.

Mendrzyk, F., A. Korshunov, A. Benner, G. Toedt, S. Pfister, B. Radlwimmer and P. Lichter (2006). "Identification of gains on 1q and epidermal growth factor receptor overexpression as independent prognostic markers in intracranial ependymoma." Clin Cancer Res **12**(7 Pt 1): 2070-2079.

Merchant, T. E. and M. Fouladi (2005). "Ependymoma: new therapeutic approaches including radiation and chemotherapy." J Neurooncol **75**(3): 287-299.

Merchant, T. E., C. H. Hua, H. Shukla, X. Ying, S. Nill and U. Oelfke (2008). "Proton versus photon radiotherapy for common pediatric brain tumors: comparison of models of dose characteristics and their relationship to cognitive function." Pediatr Blood Cancer **51**(1): 110-117.

Merchant, T. E., C. Li, X. Xiong, L. E. Kun, F. A. Boop and R. A. Sanford (2009). "Conformal radiotherapy after surgery for paediatric ependymoma: a prospective study." Lancet Oncol **10**(3): 258-266.

Merchant, T. E., Y. Zhu, S. J. Thompson, M. R. Sontag, R. L. Heideman and L. E. Kun (2002). "Preliminary results from a Phase II trail of conformal radiation therapy for pediatric patients with localised low-grade astrocytoma and ependymoma." Int J Radiat Oncol Biol Phys **52**(2): 325-332.

Merzak, A., S. Koochekpour, F. Dkhissi, S. Raynal, D. Lawrence and G. Pilkington (1995). "Synergism between growth-factors in the control of glioma cell-proliferation, migration and invasion in-vitro." Int J Oncol **6**(5): 1079-1085.

Messahel, B., S. Ashley, F. Saran, D. Ellison, J. Ironside, K. Phipps, T. Cox, W. K. Chong, K. Robinson, S. Picton, C. R. Pinkerton, C. Mallucci, D. Macarthur, T. Jaspan, A. Michalski and R. G. Grundy (2009). "Relapsed intracranial ependymoma in children in the UK: patterns of relapse, survival and therapeutic outcome." Eur J Cancer **45**(10): 1815-1823.

Michalowski, M. B., F. de Fraipont, S. Michelland, N. Entz-Werle, J. Grill, B. Pasquier, M. C. Favrot and D. Plantaz (2006). "Methylation of RASSF1A and TRAIL pathway-related genes is frequent in childhood intracranial ependymomas and benign choroid plexus papilloma." Cancer Genet Cytogenet **166**(1): 74-81.

Middleton, M. R., J. Kelly, N. Thatcher, D. J. Donnelly, R. S. McElhinney, T. B. H. McMurry, J. E. McCormick and G. P. Margison (2000). "O6-(4-bromothenyl) guanine improves the therapeutic index of temozolomide against A375M melanoma xenografts." International journal of cancer **85**(2): 248-252.

Mikkelsen, T. S., C. F. Thorn, J. J. Yang, C. M. Ulrich, D. French, G. Zaza, H. M. Dunnenberger, S. Marsh, H. L. McLeod, K. Giacomini, M. L. Becker, R. Gaedigk, J. S. Leeder, L. Kager, M. V. Relling, W. Evans, T. E. Klein and R. B. Altman (2011). "PharmGKB summary: methotrexate pathway." Pharmacogenet Genomics **21**(10): 679-686.

Milde, T., T. Hielscher, H. Witt, M. Kool, S. C. Mack, H. E. Deubzer, I. Oehme, M. Lodrini, A. Benner, M. D. Taylor, A. von Deimling, A. E. Kulozik, S. M. Pfister, O. Witt and A. Korshunov (2012). "Nestin expression identifies ependymoma patients with poor outcome." Brain Pathol **22**(6): 848-860.

Milde, T., S. Kleber, A. Korshunov, H. Witt, T. Hielscher, P. Koch, H. G. Kopp, M. Jugold, H. E. Deubzer, I. Oehme, M. Lodrini, H. J. Grone, A. Benner, O. Brustle, R. J. Gilbertson, A. von Deimling, A. E. Kulozik, S. M. Pfister, A. Martin-Villalba and O. Witt (2011). "A novel human high-risk ependymoma stem cell model reveals the

differentiation-inducing potential of the histone deacetylase inhibitor Vorinostat." Acta Neuropathol **122**(5): 637-650.

Miletti-Gonzalez, K. E., S. Chen, N. Muthukumaran, G. N. Saglimbeni, X. Wu, J. Yang, K. Apolito, W. J. Shih, W. N. Hait and L. Rodriguez-Rodriguez (2005). "The CD44 receptor interacts with P-glycoprotein to promote cell migration and invasion in cancer." Cancer Res **65**(15): 6660-6667.

Mita, R., M. J. Beaulieu, C. Field and R. Godbout (2010). "Brain fatty acid-binding protein and omega-3/omega-6 fatty acids: mechanistic insight into malignant glioma cell migration." J Biol Chem **285**(47): 37005-37015.

Mita, R., J. E. Coles, D. D. Glubrecht, R. Sung, X. Sun and R. Godbout (2007). "B-FABP-expressing radial glial cells: the malignant glioma cell of origin?" Neoplasia **9**(9): 734-744.

Modena, P., E. Lualdi, F. Facchinetti, J. Veltman, J. F. Reid, S. Minardi, I. Janssen, F. Giangaspero, M. Forni, G. Finocchiaro, L. Genitori, F. Giordano, R. Riccardi, E. F. Schoenmakers, M. Massimino and G. Sozzi (2006). "Identification of tumor-specific molecular signatures in intracranial ependymoma and association with clinical characteristics." J Clin Oncol **24**(33): 5223-5233.

Moitra, K., H. Lou and M. Dean (2011). "Multidrug Efflux Pumps and Cancer Stem Cells: Insights Into Multidrug Resistance and Therapeutic Development." Clinical Pharmacology & Therapeutics **89**(4): 491-502.

Mousseau, M., C. Chauvin, M. F. Nissou, M. Chaffanet, D. Plantaz, B. Pasquier, R. Schaerer and A. Benabid (1993). "A study of the expression of four chemoresistance-related genes in human primary and metastatic brain tumours." Eur J Cancer **29a**(5): 753-759.

Mouthon, M. A., P. Fouchet, C. Mathieu, K. Sii-Felice, O. Etienne, C. S. Lages and F. D. Boussin (2006). "Neural stem cells from mouse forebrain are contained in a population distinct from the 'side population'." J Neurochem **99**(3): 807-817.

Nakatsuru, Y., S. Matsukuma, N. Nemoto, H. Sugano, M. Sekiguchi and T. Ishikawa (1993). "O6-methylguanine-DNA methyltransferase protects against nitrosamine-induced hepatocarcinogenesis." Proceedings of the National Academy of Sciences **90**(14): 6468-6472.

Newlands, E., G. Blackledge, J. Slack, G. Rustin, D. Smith, N. Stuart, C. Quarterman, R. Hoffman, M. Stevens and M. Brampton (1992). "Phase I trial of temozolomide (CCRG 81045: M&B 39831: NSC 362856)." British journal of cancer **65**(2): 287.

Nicholson, H. S., C. S. Kretschmar, M. Krailo, M. Bernstein, R. Kadota, D. Fort, H. Friedman, M. B. Harris, N. Tedeschi-Blok, C. Mazewski, J. Sato and G. H. Reaman (2007). "Phase 2 study of temozolomide in children and adolescents with recurrent central nervous system tumors: a report from the Children's Oncology Group." Cancer **110**(7): 1542-1550.

Northcott, P. A., S. M. Pfister and D. T. Jones (2015). "Next-generation (epi)genetic drivers of childhood brain tumours and the outlook for targeted therapies." Lancet Oncol **16**(6): e293-302.

Novik, A., T. Ionova, G. Gorodokin, A. Smoljaninov and B. Afanasyev (2009). "The maximow 1909 centenary: a reappraisal." Cellular Therapy and Transplantation **1**(3): 31-34.

O'Connor, M. L., D. Xiang, S. Shigdar, J. Macdonald, Y. Li, T. Wang, C. Pu, Z. Wang, L. Qiao and W. Duan (2014). "Cancer stem cells: A contentious hypothesis now moving forward." Cancer Lett **344**(2): 180-187.

O'Reilly, S., E. Newlands, M. Brampton, M. Glaser, J. Rice-Edwards, R. Illingworth, P. Richards, C. Kennard, I. Colquhoun and P. Lewis (1993). "Temozolomide: a new oral cytotoxic chemotherapeutic agent with promising activity against primary brain tumours." European Journal of Cancer **29**(7): 940-942.

Ogura, R., Y. Tsukamoto, M. Natsumeda, M. Isogawa, H. Aoki, T. Kobayashi, S. Yoshida, K. Okamoto, H. Takahashi, Y. Fujii and A. Kakita (2015). "Immunohistochemical profiles of IDH1, MGMT and P53: practical significance for prognostication of patients with diffuse gliomas." Neuropathology **35**(4): 324-335.

Oliver, J. A., R. Ortiz, C. Melguizo, P. J. Alvarez, J. Gomez-Millan and J. Prados (2014). "Prognostic impact of MGMT promoter methylation and MGMT and CD133 expression in colorectal adenocarcinoma." BMC Cancer **14**: 511.

Ostrom, Q. T., H. Gittleman, P. Liao, C. Rouse, Y. Chen, J. Dowling, Y. Wolinsky, C. Kruchko and J. Barnholtz-Sloan (2014). "CBTRUS statistical report: primary brain and central nervous system tumors diagnosed in the United States in 2007-2011." Neuro Oncol **16 Suppl 4**: iv1-63.

Othman, R. T., I. Kimishi, T. D. Bradshaw, L. C. Storer, A. Korshunov, S. M. Pfister, R. G. Grundy, I. D. Kerr and B. Coyle (2014). "Overcoming multiple drug resistance mechanisms in medulloblastoma." Acta Neuropathol Commun **2**: 57.

Ozols, R. F., R. E. Cunnion, R. Klecker, T. C. Hamilton, Y. Ostchega, J. E. Parrillo and R. C. Young (1987). "Verapamil and adriamycin in the treatment of drug-resistant ovarian cancer patients." Journal of clinical oncology **5**(4): 641-647.

Pachella, L. A., C. Kamiya-Matsuoka, E. L. Lee, A. Olar and W. K. Yung (2015). "Supratentorial extraventricular anaplastic ependymoma with extracranial metastasis." J Clin Neurosci **22**(3): 605-607.

Padovani, L., N. Andre, J. C. Gentet, D. Figarella Branger, D. Scavarda, A. Verschuur, O. Chinot, D. Cowen and X. Muracciole (2011). "Reirradiation and concomitant metronomic temozolomide: an efficient combination for local control in medulloblastoma disease?" Journal of Pediatric Hematology/Oncology **33**(8): 600.

Pajtler, K. W., S. M. Pfister and M. Kool (2015). "Molecular dissection of ependymomas." Oncoscience **2**(10): 827-828.

Pajtler, K. W., H. Witt, M. Sill, D. T. Jones, V. Hovestadt, F. Kratochwil, K. Wani, R. Tatevossian, C. Punchihewa, P. Johann, J. Reimand, H. J. Warnatz, M. Ryzhova, S. Mack, V. Ramaswamy, D. Capper, L. Schweizer, L. Sieber, A. Wittmann, Z. Huang, P. van Sluis, R. Volckmann, J. Koster, R. Versteeg, D. Fults, H. Toledano, S. Avigad, L. M. Hoffman, A. M. Donson, N. Foreman, E. Hewer, K. Zitterbart, M. Gilbert, T. S. Armstrong, N. Gupta, J. C. Allen, M. A. Karajannis, D. Zagzag, M. Hasselblatt, A. E. Kulozik, O. Witt, V. P. Collins, K. von Hoff, S. Rutkowski, T. Pietsch, G. Bader, M. L. Yaspo, A. von Deimling, P. Lichter, M. D. Taylor, R. Gilbertson, D. W. Ellison, K. Aldape, A. Korshunov, M. Kool and S. M. Pfister (2015). "Molecular Classification of Ependymal Tumors across All CNS Compartments, Histopathological Grades, and Age Groups." Cancer Cell **27**(5): 728-743.

Palm, T., D. Figarella-Branger, F. Chapon, C. Lacroix, F. Gray, F. Scaravilli, D. W. Ellison, I. Salmon, M. Vikkula and C. Godfraind (2009). "Expression profiling of

ependymomas unravels localization and tumor grade-specific tumorigenesis." Cancer **115**(17): 3955-3968.

Palmeira, A., E. Sousa, M. H. Vasconcelos and M. M. Pinto (2012). "Three decades of P-gp inhibitors: skimming through several generations and scaffolds." Curr Med Chem **19**(13): 1946-2025.

Pan, B.-F., A. Dutt and J. A. Nelson (1994). "Enhanced transepithelial flux of cimetidine by Madin-Darby canine kidney cells overexpressing human P-glycoprotein." Journal of Pharmacology and Experimental Therapeutics **270**(1): 1-7.

Paranjpe, A., R. Zhang, F. Ali-Osman, G. C. Bobustuc and K. S. Srivenugopal (2014). "Disulfiram is a direct and potent inhibitor of human O6-methylguanine-DNA methyltransferase (MGMT) in brain tumor cells and mouse brain and markedly increases the alkylating DNA damage." Carcinogenesis **35**(3): 692-702.

Park, D., A. P. Xiang, L. Zhang, F. F. Mao, N. M. Walton, S. S. Choi and B. T. Lahn (2009). "The radial glia antibody RC2 recognizes a protein encoded by Nestin." Biochem Biophys Res Commun **382**(3): 588-592.

Parker, M., K. M. Mohankumar, C. Punchihewa, R. Weinlich, J. D. Dalton, Y. Li, R. Lee, R. G. Tatevossian, T. N. Phoenix, R. Thiruvenkatam, E. White, B. Tang, W. Orisme, K. Gupta, M. Rusch, X. Chen, Y. Li, P. Nagahawhatte, E. Hedlund, D. Finkelstein, G. Wu, S. Shurtleff, J. Easton, K. Boggs, D. Yergeau, B. Vadodaria, H. L. Mulder, J. Becksford, P. Gupta, R. Huether, J. Ma, G. Song, A. Gajjar, T. Merchant, F. Boop, A. A. Smith, L. Ding, C. Lu, K. Ochoa, D. Zhao, R. S. Fulton, L. L. Fulton, E. R. Mardis, R. K. Wilson, J. R. Downing, D. R. Green, J. Zhang, D. W. Ellison and R. J. Gilbertson (2014). "C11orf95-RELA fusions drive oncogenic NF-[kgr]B signalling in ependymoma." Nature **506**(7489): 451-455.

Parker, M., K. M. Mohankumar, C. Punchihewa, R. Weinlich, J. D. Dalton, Y. Li, R. Lee, R. G. Tatevossian, T. N. Phoenix, R. Thiruvenkatam, E. White, B. Tang, W. Orisme, K. Gupta, M. Rusch, X. Chen, Y. Li, P. Nagahawhatte, E. Hedlund, D. Finkelstein, G. Wu, S. Shurtleff, J. Easton, K. Boggs, D. Yergeau, B. Vadodaria, H. L. Mulder, J. Becksfort, P. Gupta, R. Huether, J. Ma, G. Song, A. Gajjar, T. Merchant, F. Boop, A. A. Smith, L. Ding, C. Lu, K. Ochoa, D. Zhao, R. S. Fulton, L. L. Fulton, E. R. Mardis, R. K. Wilson, J. R. Downing, D. R. Green, J. Zhang, D. W. Ellison and R. J. Gilbertson (2014). "C11orf95-RELA fusions drive oncogenic NF-kappaB signalling in ependymoma." Nature **506**(7489): 451-455.

Peck, R. A., J. Hewett, M. W. Harding, Y.-M. Wang, P. R. Chaturvedi, A. Bhatnagar, H. Ziessman, F. Atkins and M. J. Hawkins (2001). "Phase I and pharmacokinetic study of the novel MDR1 and MRP1 inhibitor biricodar administered alone and in combination with doxorubicin." Journal of clinical oncology **19**(12): 3130-3141.

Pegg, A. E., M. E. Dolan and R. C. Moschel (1995). "Structure, Function, and Inhibition of O< sup> 6</sup>-Alkylguanine-DNA Alkyltransferase." Progress in nucleic acid research and molecular biology **51**: 167-223.

Phi, J. H., K. C. Wang, S. H. Park, I. H. Kim, I. O. Kim, K. D. Park, H. S. Ahn, J. Y. Lee, Y. J. Son and S. K. Kim (2012). "Pediatric infratentorial ependymoma: prognostic significance of anaplastic histology." J Neurooncol **106**(3): 619-626.

Phuchareon, J., J. B. Overdevest, F. McCormick, D. W. Eisele, A. van Zante and O. Tetsu (2014). "Fatty Acid binding protein 7 is a molecular marker in adenoid cystic carcinoma of the salivary glands: implications for clinical significance." Transl Oncol **7**(6): 780-787.

Pietsch, T., I. Wohlers, T. Goschzik, V. Dreschmann, D. Denkhaus, E. Dorner, S. Rahmann and L. Klein-Hitpass (2014). "Supratentorial ependymomas of childhood carry C11orf95-RELA fusions leading to pathological activation of the NF-kappaB signaling pathway." Acta Neuropathol **127**(4): 609-611.

Plass, C. (2002). "Cancer epigenomics." Hum Mol Genet **11**(20): 2479-2488.

Poetsch, A. R. and C. Plass (2011). "Transcriptional regulation by DNA methylation." Cancer Treat Rev **37 Suppl 1**: S8-12.

Pollack, I. F. (1999). "Pediatric brain tumors." Semin Surg Oncol **16**(2): 73-90.

Pollack, I. F., P. C. Gerszten, A. J. Martinez, K. H. Lo, B. Shultz, A. L. Albright, J. Janosky and M. Deutsch (1995). "Intracranial ependymomas of childhood: long-term outcome and prognostic factors." Neurosurgery **37**(4): 655-666; discussion 666-657.

Poppleton, H. and R. J. Gilbertson (2007). "Stem cells of ependymoma." Br J Cancer **96**(1): 6-10.

Quinn, J. A., S. X. Jiang, D. A. Reardon, A. Desjardins, J. J. Vredenburgh, J. N. Rich, S. Gururangan, A. H. Friedman, D. D. Bigner and J. H. Sampson (2009). "Phase II trial of temozolomide plus o6-benzylguanine in adults with recurrent, temozolomide-resistant malignant glioma." Journal of clinical oncology **27**(8): 1262-1267.

Quinn, J. A., J. Pluda, M. E. Dolan, S. Delaney, R. Kaplan, J. N. Rich, A. H. Friedman, D. A. Reardon, J. H. Sampson and O. M. Colvin (2002). "Phase II trial of carmustine plus O6-benzylguanine for patients with nitrosourea-resistant recurrent or progressive malignant glioma." Journal of clinical oncology **20**(9): 2277-2283.

Radice, P., P. Bunn Jr and D. Ihde (1979). "Therapeutic trials with VP-16-213 and VM-26: active agents in small cell lung cancer, non-Hodgkin's lymphomas, and other malignancies." Cancer treatment reports **63**(8): 1231.

Rahman, M. M., J. M. Veigas, P. J. Williams and G. Fernandes (2013). "DHA is a more potent inhibitor of breast cancer metastasis to bone and related osteolysis than EPA." Breast Cancer Res Treat **141**(3): 341-352.

Rakha, E. A., D. Soria, A. R. Green, C. Lemetre, D. G. Powe, C. C. Nolan, J. M. Garibaldi, G. Ball and I. O. Ellis (2014). "Nottingham Prognostic Index Plus (NPI+): a modern clinical decision making tool in breast cancer." Br J Cancer **110**(7): 1688-1697.

Ramaswamy, V., M. Remke, E. Bouffet, C. C. Faria, S. Perreault, Y. J. Cho, D. J. Shih, B. Luu, A. M. Dubuc, P. A. Northcott, U. Schuller, S. Gururangan, R. McLendon, D. Bigner, M. Fouladi, K. L. Ligon, S. L. Pomeroy, S. Dunn, J. Triscott, N. Jabado, A. Fontebasso, D. T. Jones, M. Kool, M. A. Karajannis, S. L. Gardner, D. Zagzag, S. Nunes, J. Pimentel, J. Mora, E. Lipp, A. W. Walter, M. Ryzhova, O. Zheludkova, E. Kumirova, J. Alshami, S. E. Croul, J. T. Rutka, C. Hawkins, U. Tabori, K. E. Codispoti, R. J. Packer, S. M. Pfister, A. Korshunov and M. D. Taylor (2013). "Recurrence patterns across medulloblastoma subgroups: an integrated clinical and molecular analysis." Lancet Oncol **14**(12): 1200-1207.

Rand, V., E. Prebble, L. Ridley, M. Howard, W. Wei, M. A. Brundler, B. E. Fee, G. J. Riggins, B. Coyle and R. G. Grundy (2008). "Investigation of chromosome 1q reveals differential expression of members of the S100 family in clinical subgroups of intracranial paediatric ependymoma." Br J Cancer **99**(7): 1136-1143.

Reya, T., S. J. Morrison, M. F. Clarke and I. L. Weissman (2001). "Stem cells, cancer, and cancer stem cells." Nature **414**(6859): 105-111.

Rogers, H. A., J. P. Kilday, C. Mayne, J. Ward, M. Adamowicz-Brice, E. C. Schwalbe, S. C. Clifford, B. Coyle and R. G. Grundy (2012). "Supratentorial and spinal pediatric ependymomas display a hypermethylated phenotype which includes the loss of tumor suppressor genes involved in the control of cell growth and death." Acta Neuropathol **123**(5): 711-725.

Rogers, H. A., C. Mayne, R. J. Chapman, J. P. Kilday, B. Coyle and R. G. Grundy (2013). "PI3K pathway activation provides a novel therapeutic target for pediatric ependymoma and is an independent marker of progression-free survival." Clin Cancer Res **19**(23): 6450-6460.

Rolhion, C., F. Penault-Llorca, J. L. Kemeny, F. Kwiatkowski, J. J. Lemaire, P. Chollet, F. Finat-Duclos and P. Verrelle (1999). "O6-methylguanine-DNA methyltransferase gene (MGMT) expression in human glioblastomas in relation to patient characteristics and p53 accumulation." International journal of cancer **84**(4): 416-420.

Rorke, L. B. (1985). "Classification and grading of childhood brain tumors. Overview and statement of the problem." Cancer **56**(7 Suppl): 1848-1849.

Rottenberg, D., J. Ginos, K. Kearfott, L. Junck and D. Bigner (1984). "In vivo measurement of regional brain tissue pH using positron emission tomography." Annals of neurology **15**(S1): 98-102.

Ruda, R., C. Bosa, M. Magistrello, F. Franchino, A. Pellerino, V. Fiano, M. Trevisan, P. Cassoni and R. Soffietti (2015). "Temozolomide as salvage treatment for recurrent intracranial ependymomas of the adult: a retrospective study." Neuro Oncol **18**(2): 261-268.

Ruth, A. C. and I. B. Roninson (2000). "Effects of the multidrug transporter P-glycoprotein on cellular responses to ionizing radiation." Cancer research **60**(10): 2576-2578.

Sacks, J. D. and M. V. Barbolina (2015). "Expression and Function of CD44 in Epithelial Ovarian Carcinoma." Biomolecules **5**(4): 3051-3066.

Sazakcs, G., J. K. Paterson, J. A. Ludwig, C. Booth-Genthe and M. M. Gottesman (2006). "Targeting multidrug resistance in cancer." Nature Reviews Drug Discovery **5**(3): 219-234.

Schiffer, D., A. Chio, H. Cravioto, M. T. Giordana, A. Migheli, R. Soffietti and M. C. Vigliani (1991). "Ependymoma: internal correlations among pathological signs: the anaplastic variant." Neurosurgery **29**(2): 206-210.

Schmitt, A. M., M. Pavel, T. Rudolph, H. Dawson, A. Blank, P. Komminoth, E. Vassella and A. Perren (2014). "Prognostic and predictive roles of MGMT protein expression and promoter methylation in sporadic pancreatic neuroendocrine neoplasms." Neuroendocrinology **100**(1): 35-44.

Segal, R., M. Yaron and B. Tartakovsky (1990). Methotrexate: mechanism of action in rheumatoid arthritis. Seminars in arthritis and rheumatism, Elsevier.

Severino, M., A. Consales, M. Doglio, D. Tortora, G. Morana, S. Barra, P. Nozza and M. L. Garre (2015). "Intradural Extramedullary Ependymoma with Leptomeningeal Dissemination: The First Case Report in a Child and Literature Review." World Neurosurg **84**(3): 865 e813-869.

Shi, Z., A. K. Tiwari, S. Shukla, R. W. Robey, S. Singh, I. W. Kim, S. E. Bates, X. Peng, I. Abraham, S. V. Ambudkar, T. T. Talele, L. W. Fu and Z. S. Chen (2011). "Sildenafil reverses ABCB1- and ABCG2-mediated chemotherapeutic drug resistance." Cancer Res **71**(8): 3029-3041.

Silber, J. R., A. Blank, M. S. Bobola, B. A. Mueller, D. D. Kolstoe, G. A. Ojemann and M. S. Berger (1996). "Lack of the DNA repair protein O6-methylguanine-DNA methyltransferase in histologically normal brain adjacent to primary human brain tumors." Proceedings of the National Academy of Sciences **93**(14): 6941-6946.

Singh, S. K., I. D. Clarke, T. Hide and P. B. Dirks (2004). "Cancer stem cells in nervous system tumors." Oncogene **23**(43): 7267-7273.

Singh, S. K., I. D. Clarke, M. Terasaki, V. E. Bonn, C. Hawkins, J. Squire and P. B. Dirks (2003). "Identification of a cancer stem cell in human brain tumors." Cancer Res **63**(18): 5821-5828.

Slipicevic, A., K. Jorgensen, M. Skrede, A. K. Rosnes, G. Troen, B. Davidson and V. A. Florenes (2008). "The fatty acid binding protein 7 (FABP7) is involved in proliferation and invasion of melanoma cells." BMC Cancer **8**: 276.

Slipicevic, A., K. Jørgensen, M. Skrede, A. K. R. Rosnes, G. Trøen, B. Davidson and V. A. Flørenes (2008). "The fatty acid binding protein 7 (FABP7) is involved in proliferation and invasion of melanoma cells." BMC Cancer **8**: 276-276.

Sonnichsen, D. S., R. C. Ribeiro, X. Luo, P. Mathew and M. V. Relling (1995). "Pharmacokinetics and pharmacodynamics of 21-day continuous oral etoposide in pediatric patients with solid tumors." Clin Pharmacol Ther **58**(1): 99-107.

Struski, S., M. Doco-Fenzy and P. Cornillet-Lefebvre (2002). "Compilation of published comparative genomic hybridization studies." Cancer Genet Cytogenet **135**(1): 63-90.

Stupp, R., M. E. Hegi, M. J. van den Bent, W. P. Mason, M. Weller, R. O. Mirimanoff and J. G. Cairncross (2006). "Changing paradigms—an update on the multidisciplinary management of malignant glioma." The Oncologist **11**(2): 165-180.

Stupp, R., W. P. Mason, M. J. Van Den Bent, M. Weller, B. Fisher, M. J. Taphoorn, K. Belanger, A. A. Brandes, C. Marosi and U. Bogdahn (2005). "Radiotherapy plus concomitant and adjuvant temozolomide for glioblastoma." New England Journal of Medicine **352**(10): 987-996.

Suarez-Merino, B., M. Hubank, T. Revesz, W. Harkness, R. Hayward, D. Thompson, J. L. Darling, D. G. Thomas and T. J. Warr (2005). "Microarray analysis of pediatric ependymoma identifies a cluster of 112 candidate genes including four transcripts at 22q12.1-q13.3." Neuro Oncol **7**(1): 20-31.

Sun, H., X. Meng, J. Han, Z. Zhang, B. Wang, X. Bai and X. Zhang (2013). "Anti-cancer activity of DHA on gastric cancer--an in vitro and in vivo study." Tumour Biol **34**(6): 3791-3800.

Sung, K. W., H. Lim do, S. H. Lee, K. H. Yoo, H. H. Koo, J. H. Kim, Y. L. Suh, Y. S. Joung and H. J. Shin (2012). "Tandem high-dose chemotherapy and autologous stem cell transplantation for anaplastic ependymoma in children younger than 3 years of age." J Neurooncol **107**(2): 335-342.

Szakacs, G., J. K. Paterson, J. A. Ludwig, C. Booth-Genthe and M. M. Gottesman (2006). "Targeting multidrug resistance in cancer." Nat Rev Drug Discov **5**(3): 219-234.

Tai, B. C., R. Grundy and D. Machin (2011). "On the importance of accounting for competing risks in pediatric brain cancer: II. Regression modeling and sample size." Int J Radiat Oncol Biol Phys **79**(4): 1139-1146.

Tainton, K., M. Smyth, J. Jackson, J. Tanner, L. Cerruti, S. Jane, P. Darcy and R. Johnstone (2004). "Mutational analysis of P-glycoprotein: suppression of caspase activation in the absence of ATP-dependent drug efflux." Cell Death & Differentiation **11**(9): 1028-1037.

Takara, K., M. Matsubara, K. Yamamoto, T. Minegaki, S. Takegami, M. Takahashi, T. Yokoyama and K. Okumura (2012). "Differential effects of calcium antagonists on ABCG2/BCRP-mediated drug resistance and transport in SN-38-resistant HeLa cells." Molecular medicine reports **5**(3): 603-609.

Tang, X. Y., S. Umemura, H. Tsukamoto, N. Kumaki, Y. Tokuda and R. Y. Osamura (2010). "Overexpression of fatty acid binding protein-7 correlates with basal-like subtype of breast cancer." Pathol Res Pract **206**(2): 98-101.

Tawbi, H., L. Villaruz, A. Tarhini, S. Moschos, M. Sulecki, F. Viverette, J. Shipe-Spotloe, R. Radkowski and J. Kirkwood (2011). "Inhibition of DNA repair with MGMT pseudosubstrates: phase I study of lomeguatrib in combination with dacarbazine in patients with advanced melanoma and other solid tumours." British journal of cancer **105**(6): 773-777.

Taylor, M. D., H. Poppleton, C. Fuller, X. Su, Y. Liu, P. Jensen, S. Magdaleno, J. Dalton, C. Calabrese, J. Board, T. Macdonald, J. Rutka, A. Guha, A. Gajjar, T. Curran and R. J. Gilbertson (2005). "Radial glia cells are candidate stem cells of ependymoma." Cancer Cell **8**(4): 323-335.

Tisdale, M. J. (1987). "Antitumour imidazotetrazines—XV: Role of guanine O6 alkylation in the mechanism of cytotoxicity of imidazotetrazinones." Biochemical pharmacology **36**(4): 457-462.

Tolle, A., H. Krause, K. Miller, K. Jung and C. Stephan (2011). "Importance of braintype fatty acid binding protein for cell-biological processes in human renal carcinoma cells." Oncol Rep **25**(5): 1307-1312.

Tolle, A., S. Suhail, M. Jung, K. Jung and C. Stephan (2011). "Fatty acid binding proteins (FABPs) in prostate, bladder and kidney cancer cell lines and the use of IL-FABP as survival predictor in patients with renal cell carcinoma." BMC Cancer **11**: 302.

Tomizawa, M., F. Shinozaki, Y. Motoyoshi, T. Sugiyama, S. Yamamoto and N. Ishige (2016). "FH535 suppresses the proliferation and motility of hepatocellular carcinoma cells." Int J Oncol **48**(1): 110-114.

Tumours/Childhood, N. R. o. C. and C. R. G. http://www.ccrg.ox.ac.uk.

Ugur, H. C., M. Taspinar, S. Ilgaz, F. Sert, H. Canpinar, J. A. Rey, J. S. Castresana and A. Sunguroglu (2014). "Chemotherapeutic resistance in anaplastic astrocytoma cell lines treated with a temozolomide-lomeguatrib combination." Mol Biol Rep **41**(2): 697-703.

Valera, E. T., C. A. Scrideli, R. Queiroz, B. Mori and L. G. Tone (2004). "Multiple drug resistance protein (MDR-1), multidrug resistance-related protein (MRP) and lung resistance protein (LRP) gene expression in childhood acute lymphoblastic leukemia." Sao Paulo Med J **122**(4): 166-171.

van Thuijl, H. F., T. Mazor, B. E. Johnson, S. D. Fouse, K. Aihara, C. Hong, A. Malmstrom, M. Hallbeck, J. J. Heimans, J. J. Kloezeman, M. Stenmark-Askmalm, M. L. Lamfers, N. Saito, H. Aburatani, A. Mukasa, M. S. Berger, P. Soderkvist, B. S. Taylor, A. M. Molinaro, P. Wesseling, J. C. Reijneveld, S. M. Chang, B. Ylstra and J. F. Costello (2015). "Evolution of DNA repair defects during malignant progression of low-grade gliomas after temozolomide treatment." Acta Neuropathol **129**(4): 597-607.

von Bossanyi, P., S. Diete, K. Dietzmann, M. Warich-Kirches and E. Kirches (1997). "Immunohistochemical expression of P-glycoprotein and glutathione S-transferases in cerebral gliomas and response to chemotherapy." Acta neuropathologica **94**(6): 605-611.

Walter, T., B. van Brakel, C. Vercherat, V. Hervieu, J. Forestier, J. A. Chayvialle, Y. Molin, C. Lombard-Bohas, M. O. Joly and J. Y. Scoazec (2015). "O6-Methylguanine-DNA methyltransferase status in neuroendocrine tumours: prognostic relevance and association with response to alkylating agents." Br J Cancer **112**(3): 523-531.

Wang, C.-H., T.-R. Hsu, T.-T. Wong and K.-P. Chang (2009). "Efficacy of temozolomide for recurrent embryonal brain tumors in children." Child's Nervous System **25**(5): 535-541.

Wang, F., K. Bhat, M. Doucette, S. Zhou, Y. Gu, B. Law, X. Liu, E. T. Wong, J. X. Kang, T. C. Hsieh, S. Y. Qian and E. Wu (2011). "Docosahexaenoic acid (DHA) sensitizes brain tumor cells to etoposide-induced apoptosis." Curr Mol Med **11**(6): 503-511.

Wang, S. W., J. Monagle, C. McNulty, D. Putnam and H. Chen (2004). "Determination of P-glycoprotein inhibition by excipients and their combinations using an integrated high-throughput process." Journal of pharmaceutical sciences **93**(11): 2755-2767.

Wani, K., T. S. Armstrong, E. Vera-Bolanos, A. Raghunathan, D. Ellison, R. Gilbertson, B. Vaillant, S. Goldman, R. J. Packer, M. Fouladi, I. Pollack, T. Mikkelsen, M. Prados, A. Omuro, R. Soffietti, A. Ledoux, C. Wilson, L. Long, M. R. Gilbert and K. Aldape (2012). "A prognostic gene expression signature in infratentorial ependymoma." Acta Neuropathol **123**(5): 727-738.

Wani, K., T. S. Armstrong, E. Vera-Bolanos, A. Raghunathan, D. Ellison, R. Gilbertson, B. Vaillant, S. Goldman, R. J. Packer, M. Fouladi, I. Pollack, T. Mikkelsen, M. Prados, A. Omuro, R. Soffietti, A. Ledoux, C. Wilson, L. Long, M. R. Gilbert, K. Aldape and N. Collaborative Ependymoma Research (2012). "A prognostic gene expression signature in infratentorial ependymoma." Acta Neuropathol **123**(5): 727-738.

Wedge, S. and E. Newlands (1996). "O6-benzylguanine enhances the sensitivity of a glioma xenograft with low O6-alkylguanine-DNA alkyltransferase activity to temozolomide and BCNU." British journal of cancer **73**(9): 1049.

Wedge, S., J. Porteous and E. Newlands (1996). "3-aminobenzamide and/or O6-benzylguanine evaluated as an adjuvant to temozolomide or BCNU treatment in cell lines of variable mismatch repair status and O6-alkylguanine-DNA alkyltransferase activity." British journal of cancer **74**(7): 1030.

Weina, K. and J. Utikal (2014). "SOX2 and cancer: current research and its implications in the clinic." Clin Transl Med **3**: 19.

Witt, H., S. C. Mack, M. Ryzhova, S. Bender, M. Sill, R. Isserlin, A. Benner, T. Hielscher, T. Milde, M. Remke, D. T. Jones, P. A. Northcott, L. Garzia, K. C. Bertrand, A. Wittmann, Y. Yao, S. S. Roberts, L. Massimi, T. Van Meter, W. A. Weiss, N. Gupta,

W. Grajkowska, B. Lach, Y. J. Cho, A. von Deimling, A. E. Kulozik, O. Witt, G. D. Bader, C. E. Hawkins, U. Tabori, A. Guha, J. T. Rutka, P. Lichter, A. Korshunov, M. D. Taylor and S. M. Pfister (2011). "Delineation of two clinically and molecularly distinct subgroups of posterior fossa ependymoma." Cancer Cell **20**(2): 143-157.

Wright, K. D. and A. Gajjar (2012). "Current treatment options for pediatric and adult patients with ependymoma." Curr Treat Options Oncol **13**(4): 465-477.

Wu, C.-Y., L. Z. Benet, M. F. Hebert, S. K. Gupta, M. Rowland, D. Y. Gomez and V. J. Wacher (1995). "Differentiation of absorption and first-pass gut and hepatic metabolism in humans: Studies with cyclosporine&ast." Clinical Pharmacology & Therapeutics **58**(5): 492-497.

Wu, M. Y., R. R. Liang, K. Chen, M. Shen, Y. L. Tian, D. M. Li, W. M. Duan, Q. Gui, F. R. Gong, L. Lian, W. Li and M. Tao (2015). "FH535 inhibited metastasis and growth of pancreatic cancer cells." Onco Targets Ther **8**: 1651-1670.

Wu, X., G. Daniels, P. Lee and M. E. Monaco (2014). "Lipid metabolism in prostate cancer." Am J Clin Exp Urol **2**(2): 111-120.

www.clinicaltrials.gov.

Xu-Welliver, M. and A. E. Pegg (2002). "Degradation of the alkylated form of the DNA repair protein, O6-alkylguanine-DNA alkyltransferase." Carcinogenesis **23**(5): 823-830.

Xu, L. Z., R. Sanchez, A. Sali and N. Heintz (1996). "Ligand specificity of brain lipid-binding protein." J Biol Chem **271**(40): 24711-24719.

Yang, Q. C., Y. H. Wang, Y. Lin, L. Xue, Y. J. Chen, M. H. Chen and J. Chen (2014). "Expression of O(6)-methylguanine DNA methyltransferase (MGMT) and its clinical significance in gastroenteropancreatic neuroendocrine neoplasm." Int J Clin Exp Pathol **7**(7): 4204-4212.

Yoshida, G. J. (2015). "Metabolic reprogramming: the emerging concept and associated therapeutic strategies." J Exp Clin Cancer Res **34**(1): 111.

Yu, L., P. A. Baxter, H. Voicu, S. Gurusiddappa, Y. Zhao, A. Adesina, T. K. Man, Q. Shu, Y. J. Zhang, X. M. Zhao, J. M. Su, L. Perlaky, R. Dauser, M. Chintagumpala, C. C. Lau, S. M. Blaney, P. H. Rao, H. E. Leung and X. N. Li (2010). "A clinically relevant orthotopic xenograft model of ependymoma that maintains the genomic signature of the primary tumor and preserves cancer stem cells in vivo." Neuro Oncol **12**(6): 580-594.

Zacharoulis, S., S. Ashley, L. Moreno, J. C. Gentet, M. Massimino and D. Frappaz (2010). "Treatment and outcome of children with relapsed ependymoma: a multi-institutional retrospective analysis." Childs Nerv Syst **26**(7): 905-911.

Zacharoulis, S., L. Ji, I. F. Pollack, P. Duffner, R. Geyer, J. Grill, S. Schild, T. H. Jaing, M. Massimino, J. Finlay and R. Sposto (2008). "Metastatic ependymoma: a multi-institutional retrospective analysis of prognostic factors." Pediatr Blood Cancer **50**(2): 231-235.

Zacharoulis, S., A. Levy, S. N. Chi, S. Gardner, M. Rosenblum, D. C. Miller, I. Dunkel, B. Diez, R. Sposto, L. Ji, S. Asgharzadeh, J. Hukin, J. Belasco, R. Dubowy, S. Kellie, A. Termuhlen and J. Finlay (2007). "Outcome for young children newly diagnosed with ependymoma, treated with intensive induction chemotherapy followed by

myeloablative chemotherapy and autologous stem cell rescue." Pediatr Blood Cancer **49**(1): 34-40.

Zacharoulis, S. and L. Moreno (2009). "Ependymoma: an update." J Child Neurol **24**(11): 1431-1438.

Zagon, I. S. and P. J. McLaughlin (1981). "Nucleic acids and protein in brains and cerebella of rats transplacentally exposed to ethylnitrosourea." Brain Research Bulletin **6**(4): 355-360.

Zhang, J., M. Stevens and T. Bradshaw (2012). "Temozolomide: mechanisms of action, repair and resistance." Current molecular pharmacology **5**(1): 102.

Zhang, J., M. F. Stevens and T. D. Bradshaw (2012). "Temozolomide: mechanisms of action, repair and resistance." Curr Mol Pharmacol **5**(1): 102-114.

Zhang, J., M. F. G. Stevens, C. A. Laughton, S. Madhusudan and T. D. Bradshaw (2010). "Acquired resistance to temozolomide in glioma cell lines: molecular mechanisms and potential translational applications." Oncology **78**(2): 103-114.

Zhang, Z. S., J. Wang, Y. B. Shen, C. C. Guo, K. E. Sai, F. R. Chen, X. Mei, F. U. Han and Z. P. Chen (2015). "Dihydroartemisinin increases temozolomide efficacy in glioma cells by inducing autophagy." Oncol Lett **10**(1): 379-383.

Zheng, H., H. Tang, M. Liu, M. He, P. Lai, H. Dong, J. Lin, C. Jia, M. Zhong, Y. Dai, X. Bai and L. Wang (2014). "Inhibition of endometrial cancer by n-3 polyunsaturated fatty acids in preclinical models." Cancer Prev Res (Phila) **7**(8): 824-834.

Zhu, B. and S. J. Strada (2007). "The novel functions of cGMP-specific phosphodiesterase 5 and its inhibitors in carcinoma cells and pulmonary/cardiovascular vessels." Curr Top Med Chem **7**(4): 437-454.